

Characterization of a *Plasmodium falciparum* protein kinase

Sasha Roets

**A dissertation submitted to the Faculty of Science, University of the Witwatersrand,
in fulfilment of the requirements for the degree of Master of Science.**

Johannesburg, April 2013

DECLARATION

I declare that this dissertation is my own, unaided work. It is being submitted for the Degree of Master of Science in the University of the Witwatersrand, Johannesburg. It has not been submitted before for any degree or examination in any other university.

A handwritten signature in black ink, appearing to read 'Roets'.

SASHA ROETS

2nd day of April 2013

ABSTRACT

Malaria is caused by *Plasmodium* parasites and is the world's most devastating tropical infectious disease. The need for identifying novel drug targets is fuelled by an increased resistance of these parasites against available drugs. The human host red cell membrane plays an important role during invasion and subsequent development of the parasite within the red cell and undergoes several structural, functional and biochemical changes triggered by various protein-protein interactions between the parasite and the host cells. These interactions form a fundamental part of malaria research, since the parasite spends the pathogenic stage of its life cycle in the human erythrocyte. The *Plasmodium* kinome is complex and the exact role of protein phosphorylation in malaria parasites is not yet fully understood. This study aims to characterise the kinase domain of *Plasmodium falciparum* (3D7) Protein Kinase 8 (*Pf*PK8), described as a putative protein on the *Plasmodium falciparum* database. *Pf*PK8 is encoded by the *Pf*B0150c gene (recently renamed as PF3D7_0203100) situated on chromosome 2 of the parasite genome. A 1 507bp section of the *Pf*B0150c gene, containing a 822bp centrally located kinase domain was cloned into a pTriEx-3 expression vector. A soluble recombinant octa-histidine-tagged *Pf*PK8 was expressed in *Escherichia coli* Rosetta 2 (DE3) cells, but with relatively low yield and purity. To improve the expression, a recombinant *Pf*B0150c-baculovirus infected *Spodoptera frugiperda* (*Sf*9) insect cell system was attempted, but without success. A different tag was employed and glutathione-S-transferase-*Pf*PK8 was successfully expressed in *Escherichia coli* Rosetta 2 (DE3) cells, with a higher yield and purity. Recombinant GST-*Pf*PK8 was used in non-radioactive coupled spectrophotometric kinase assays in the presence of known kinase substrates casein, MBP and H1 to determine kinetic parameters of the enzyme. It phosphorylated all three substrates at a temperature of 37°C and pH of 7.4. Recombinant GST-*Pf*PK8 was inactive at a pH below 6 and most active at pH 7.4. The relative activity of the enzyme was highest at a temperature synonymous to a fever spike in a *Plasmodium falciparum* infected individual. Secondary structural analysis of *Pf*PK8 revealed the position of a conserved substrate binding domain containing an ATP-binding site and binding loop within the kinase domain. The

kinase domain of rPfPK8 was modelled using available crystal structures of its identified homologues. The gene is expressed throughout the intraerythrocytic stages of the parasite life cycle, as well as in gametocytes. Protein-protein binding studies revealed that host-parasite protein-protein interactions exist between rPfPK8 and erythrocyte membrane protein, band 3. *Plasmodium falciparum* PK8 could therefore play a role during invasion of host erythrocytes and during the intraerythrocytic development of the parasite, by phosphorylating red blood cell membrane proteins. This study provides the groundwork for future X-ray crystallographic studies to elucidate the structure of the enzyme, and for additional gene manipulation experiments to ascertain whether it is essential for parasite survival in all the intraerythrocytic stages and therefore a potential new drug target candidate.

DEDICATION

*Thank you God for the health and energy that You
have given me to reach my goals.*

*I dedicate this dissertation to my amazing parents,
Kallie and Sarah, and my loving husband Frederick
who accompanied me through this MSc journey.
Your encouraging words and unconditional love kept
me working when I wanted to give up.*

ACKNOWLEDGEMENTS

I would like to acknowledge:

- My supervisor, Professor Theresa L. Coetzer for her support and guidance throughout this study.
- My laboratory colleagues of the *Plasmodium* Molecular Research Unit and the Department of Molecular Medicine and Haematology for their motivational support.
- Brigit Karen Smit for providing me with the pGEX-4T-2-*Pf*B0150c construct.
- The National Research Foundation and the University of the Witwatersrand Medical Faculty Research Endowment fund for providing project funding.
- Thank you to the Pay It Forward Trust Fund for a postgraduate bursary.

RESEARCH OUTPUTS

Sasha Roets and Theresa L. Coetzer: “Analysis of the catalytic domain of *Pf*PK8, a *Plasmodium falciparum* protein kinase”

Poster presentations at:

- SASBMB 2010, 22ND Congress of the South African Society for Biochemistry and Molecular Biology, Bloemfontein, South Africa
- Molecular Biosciences Research Thrust annual meeting, December 2010 and December 2011 at the University of the Witwatersrand, Johannesburg, South Africa.

ETHICS CLEARANCE

Ethics clearance for this study was granted by the University of the Witwatersrand Committee (Ethics Clearance Number: M03-11-06).

TABLE OF CONTENTS

DECLARATION	2
ABSTRACT	3
DEDICATION	5
ACKNOWLEDGEMENTS	6
TABLE OF CONTENTS	9
ABBREVIATIONS	15
LIST OF FIGURES	22
LIST OF TABLES	25
1 INTRODUCTION	27
1.1 The developing world's struggle with malaria	27
1.2 Anti-malarial drugs and drug resistance of <i>Plasmodium sp.</i>	29
1.3 Anti-malarial vaccines	30
1.4 The life cycle of the parasite	31
1.4.1 Asexual stage of development	32
1.4.2 Sexual stage of development	33
1.5 The human host erythrocyte	34
1.5.1 Erythrocyte membrane structure	34
1.5.2 Morphological and structural changes of the erythrocyte during <i>Plasmodium falciparum</i> invasion and intra-erythrocytic development	39
1.6 Protein kinases	42
1.6.1 <i>Plasmodium falciparum</i> protein kinases	42
1.6.2 Phosphorylation during malaria parasite invasion and intraerythrocytic development	48
1.6.3 Kinases as novel drug targets	49
1.7 Expression of <i>Plasmodium falciparum</i> recombinant proteins	52
PROJECT OBJECTIVES	54
2 MATERIALS AND METHODS	55
2.1 <i>Plasmodium falciparum</i> culturing techniques	55

2.1.1	Parasite culture preparation from a frozen stock.....	55
2.1.2	Heat inactivation of plasma.....	55
2.1.3	Erythrocyte preparation.....	56
2.1.4	Preparation of smears and calculating parasitaemia	56
2.1.5	Culture maintenance.....	57
2.1.6	Dividing the culture.....	57
2.1.7	Culture synchronisation	57
2.1.8	Preparation of parasite stock suspension for long term storage	58
2.2	Cloning	58
2.2.1	<i>Plasmodium falciparum</i> DNA extraction	58
2.2.2	Determination of DNA concentration, purity and integrity	60
2.2.3	The polymerase chain reaction (PCR)	61
2.2.4	Cloning of <i>Pf</i> B0150c into the pTriEx-3 expression vector.....	65
2.2.5	Recombinant <i>Pf</i> B0150c-pTriEx-3 plasmid DNA sequencing	71
2.2.6	Retransformation of Rosetta 2 (DE3) cells with recombinant pGEX-4T-2 plasmid	72
2.3	Prokaryotic protein expression system.....	73
2.3.1	Recombinant <i>Pf</i> PK8 protein expression in <i>Escherichia coli</i> Rosetta 2 (DE3) cells	73
2.3.2	Recombinant protein extraction	75
2.3.3	Recombinant GST- <i>Pf</i> PK8 purification using MagneGST™ beads	76
2.3.4	r <i>Pf</i> PK8-His purification using MagneHis™ beads.....	78
2.3.5	Laemmli sodium dodecyl sulphate-polyacrylamide gel electrophoresis (SDS-PAGE)	81
2.3.6	Immunoblotting of GST-tagged recombinant proteins	82
2.3.7	Immunoblotting of His-tagged recombinant proteins	84
2.4	Eukaryotic protein expression system	85
2.4.1	<i>Sf</i> 9 insect cell culturing techniques	85
2.4.2	Production of recombinant baculovirus	89

2.4.3	Recombinant <i>Pf</i> PK8-His expression analysis in <i>Sf9</i> insect cells	94
2.5	Non-radio-active coupled protein kinase assay	96
2.5.1	Kinetic analysis of rGST- <i>Pf</i> PK8	96
2.5.2	Effect of temperature on the enzyme activity of rGST- <i>Pf</i> PK8	100
2.5.3	Effect of pH on enzyme activity of rGST- <i>Pf</i> PK8	101
2.5.4	rGST- <i>Pf</i> PK8 enzyme stability	102
2.6	Protein-protein interactions between RBCM proteins and rGST- <i>Pf</i> PK8...	102
2.6.1	Red blood cell membrane (RBCM) protein preparation	102
2.6.2	Red blood cell membrane protein (RBCM) quantitation	103
2.6.3	Red blood cell membrane blot overlays	104
2.7	Bio-informatic analysis of <i>Pf</i> PK8	106
2.7.1	Sequence alignment of <i>Pf</i> PK8 with other protein kinases	106
2.7.2	Structure prediction of recombinant <i>Pf</i> PK8	106
2.7.3	<i>Pf</i> PK8 protein parameter prediction	107
3	RESULTS	108
3.1	<i>Plasmodium falciparum</i> culturing	108
3.2	<i>Plasmodium falciparum</i> DNA extraction	108
3.3	Amplification of the kinase domain of <i>Pf</i> B0150c	110
3.4	Cloning	113
3.4.1	Plasmid preparation	113
3.4.2	Restriction endonuclease digestion and ligation	115
3.4.3	Transformation of <i>Escherichia coli</i> DH5 α cells with <i>Pf</i> B0150c- pTriEx-3	116
3.4.4	Sequence analysis of recombinant <i>Pf</i> B0150c-pTriEx-3	118
3.4.5	Transformation of <i>Escherichia coli</i> Rosetta 2 (DE3) cells with <i>Pf</i> B0150c-pTriEx-3	120
3.5	Expression of recombinant r <i>Pf</i> PK8-His protein	121
3.5.1	Prokaryotic protein expression of r <i>Pf</i> PK8-His	122

3.5.2	Eukaryotic protein expression of r <i>Pf</i> PK8-His.....	125
3.5.3	Protein expression and purification of r <i>Pf</i> PK8-His	129
3.6	Expression of recombinant rGST- <i>Pf</i> PK8 protein.....	132
3.7	Non-radioactive coupled protein kinase assays.....	138
3.7.1	Stability of rGST- <i>Pf</i> PK8	139
3.7.2	Substrate specificity of rGST- <i>Pf</i> PK8	140
3.7.3	Kinetic analysis of rGST- <i>Pf</i> PK8.....	143
3.7.4	Effect of temperature on rGST- <i>Pf</i> PK8 activity.....	148
3.7.5	Effect of pH on rGST- <i>Pf</i> PK8 activity	149
3.8	Recombinant GST- <i>Pf</i> PK8 and red blood cell membrane protein-protein interactions	151
3.8.1	Red blood cell membrane protein quantitation	151
3.8.2	Binding studies.....	152
3.9	Bioinformatic analysis of <i>Pf</i> PK8.....	156
3.9.1	Identification of <i>Pf</i> PK8 homologues and functional regions using BLAST	156
3.9.2	Secondary structure prediction of <i>Pf</i> PK8.....	162
3.9.3	Three dimensional structure prediction of <i>Pf</i> PK8.....	163
3.9.4	Predicted protein parameters of recombinant <i>Pf</i> PK8.....	168
4	DISCUSSION.....	169
4.1	Expression of r <i>Pf</i> PK8 in heterologous hosts	169
4.1.1	Expression of r <i>Pf</i> PK8-His in <i>Escherichia coli</i>	170
4.1.2	Expression of r <i>Pf</i> PK8-His in <i>Spodoptera frugiperda</i> insect cells	173
4.1.3	Expression rGST- <i>Pf</i> PK8 in <i>Escherichia coli</i>	174
4.2	<i>Pf</i> B0150c mRNA and protein expression	175
4.3	Recombinant <i>Pf</i> PK8 is an active protein kinase	177
4.4	Structural aspects of r <i>Pf</i> PK8	181
4.4.1	Homologues of r <i>Pf</i> PK8	181
4.4.2	Secondary structure of r <i>Pf</i> PK8	181

4.4.3	Three dimensional structure of r <i>Pf</i> PK8.....	182
4.5	Host-parasite protein-protein interactions and a possible function for <i>Pf</i> PK8	184
5	CONCLUSION.....	186
6	REFERENCE LIST	187
7	APPENDIX.....	205
7.1	Reagents	205
7.1.1	<i>Plasmodium falciparum</i> culturing.....	205
7.1.2	Cloning.....	207
7.1.3	<i>Escherichia coli</i> cell growth reagents	209
7.1.4	Recombinant protein extraction reagents.....	210
7.1.5	Laemmli SDS-PAGE reagents	211
7.1.6	Fairbanks SDS-PAGE reagents.....	213
7.1.7	Immunoblot analysis reagents for GST-tagged recombinant proteins	214
7.1.8	Immunoblot analysis reagents for Histidine-tagged recombinant proteins	215
7.1.9	Reagents for recombinant baculovirus (BacVirus- <i>Pf</i> B0150c) production	215
7.1.10	Non-radioactive kinase assay reagents.....	216
7.1.11	Protein-protein interactions.....	218
7.2	Equipment and reagent suppliers list.....	219
7.3	Sequence data	225
7.3.1	<i>Pf</i> B0150c DNA sequence (PlasmoDB version 8.1, 2011).....	225
7.3.2	<i>Pf</i> B0150c predicted protein sequence (PlasmoDB version 8.1, 2011)	229
7.3.3	Recombinant GST- <i>Pf</i> PK8 protein sequence (PlasmoDB version 8.1, 2011)	231
7.3.4	pGEX-4T-2- <i>Pf</i> B0150c DNA sequence.....	232
7.3.5	<i>Pf</i> B0150c-pTriEx-3 DNA sequence	236
7.3.6	Expression vector maps.....	240

7.3.7	<i>Pf</i> B0150c-pTriEx-3 sequence chromatograms	242
7.3.8	<i>Pf</i> B0150c-pTriEx-3 construct 2 DNA sequence alignment.....	244
7.4	BLAST data of <i>Pf</i> PK8 protein sequence.....	250
7.4.1	Sequences with significant alignments to the target sequence.....	250

ABBREVIATIONS

A

aa:	Amino acids
ACD:	Acid citrate dextrose
ACTs:	Artemisinin-combination therapies
AMA:	Apical membrane antigen
APS:	Ammonium persulphate
ASKA:	Analogue-sensitive kinase allele
ATP:	Adenosine triphosphate

B

BAC:	Bacterial artificial chromosome
β-gal:	β-galactosidase
BKI:	Bumped kinase inhibitor
BLAST:	Basic local alignment search tool

C

CADD:	Computer-assisted drug design
CaMK:	Calmodulin dependent kinase
cAMP:	Adenosine 3',5'-cyclic monophosphate
cdb3:	Cytoplasmic domain 3
CDK:	Cyclin/casein dependent protein kinase
CDPK:	Calcium/calmodulin-dependent kinase
cGAK:	Cyclin G associated kinase
Cgmp:	Cyclic guanosine monophosphate
CK1:	Casein kinase 1
CLK:	Casein dependent-like kinase

CMV: Cytomegalovirus

D

D: Aspartate

DMSO: Dimethyl sulphoxide

DNA: Deoxyribonucleic acid

dNTP: Deoxyribonucleotide

DRM: Detergent-resistant membrane

E

E: Glutamate

EBA: Erythrocyte binding antigens

E. coli: *Escherichia coli*

EDTA: Ethylenediaminetetraacetic acid

ePKs: Eukaryotic protein kinases

F

F-actin: Filamentous actin

FEST: Falciparum exported serine/threonine kinases

FIKK: Phenylalanine-isoleucine-lysine-lysine enzyme group

G

G3PD: Glyceraldehyde 3-phosphate dehydrogenase

GAP45: Glideosome associated protein 45

GK: Glycerol kinase

gp64: Glycoprotein 64

GPA: Glycophorin A

GPC: Glycophorin C

GPI:	Glycosylphosphatidylinositol
GSK:	Glycogen synthase kinase
GSK3:	Glycogen synthase kinase 3
GST:	Glutathione-S-transferase
GTP:	Guanosine-5-triphosphate

H

H1:	Histone protein 1
HRP:	Horse radish peroxidase

I

IgG:	Immunoglobulin G
------	------------------

K

K:	Lysine
kDa:	Kilodalton
KHARP:	Knob-associated histidine-rich proteins

L

<i>lac</i> promoter:	Lactose gene promoter
LB medium:	Luria-Bertani medium
LDH:	Lactate dehydrogenase
LW:	Landsteiner and Wiedner blood antigen

M

MAPK:	Mitogen activated kinase
MBP:	Myelin basic protein
MCV:	Multiple cloning site

MESA:	Mature parasite-infected erythrocyte surface antigen
MOI:	Multiplicity of infection
Mr:	Molecular weight
MSP1:	Merozoite surface protein 1
MST1:	Mammalian sterile-20 like kinase 1
MST3:	Mammalian sterile-20 like kinase 3
MW:	Molecular weight

N

N:	Asparagine
NADH:	Nicotinamide adenine dinucleotide
NBT:	Nitroblue tetrazolium
Nek:	NIMA related kinases
NIMA:	Never-in-mitosis in <i>Aspergillus nidulans</i>

O

OPKs:	Orphan protein kinases
ORF:	Open reading frame

P

PAGE:	Polyacrylamide gel electrophoresis
PBS:	Phosphate buffered saline
PCR:	Polymerase chain reaction
PEP:	Phosphoenolpyruvate
PEXEL:	<i>Plasmodium</i> Export Element
<i>Pf</i> :	<i>Plasmodium falciparum</i> 3D7
<i>P. falciparum</i> :	<i>Plasmodium falciparum</i>
<i>Pf</i> CK1:	<i>Plasmodium falciparum</i> casein kinase 1

<i>PfEMP1</i> :	<i>Plasmodium falciparum</i> erythrocyte membrane protein 1
<i>PfEMP3</i> :	<i>Plasmodium falciparum</i> erythrocyte membrane protein 3
<i>PfSBP1</i> :	<i>Plasmodium falciparum</i> skeleton binding protein 1
Pfu:	Plaque forming units
Phyre:	Protein-homology/analogy recognition engine
pI:	Protein isoelectric point
PIP2:	Phosphatidyl-4-5-bisphosphate
PK8:	Protein kinase 8
PKA:	Protein kinase A
PKC:	Protein kinase C
PKc_STEs:	Catalytic domain of protein kinases from the STE kinase family
PKG:	Protein kinase G
PlasmoDB:	<i>Plasmodium falciparum</i> Data Base
pRBCs:	Parasitised red blood cells
PS:	Phosphatidylserine
PVM:	Parasitophorous vacuolar membrane
PyrK:	Pyruvate kinase

R

R:	Arginine
RBCM:	Red blood cell membrane
RBCs:	Red blood cells
RESA:	Ring-infected surface antigen
Rf :	Retardation factor
rGST:	Recombinant glutathione-S-transferase
Rh:	Rhesus blood group
RNA:	Ribonucleic acid

RNase A: Pancreatic ribonuclease A

S

SDS: Sodium dodecyl sulphate

SDS-PAGE: Sodium dodecyl sulphate polyacrylamide gel electrophoresis

Sf9: *Spodoptera frugiperda*

STE20: Sterile-20 like kinase

STKs: Serine/threonine kinases

STKcs: Catalytic domain of serine/threonine kinases

T

TAE: Tris-Acetate-EDTA

TBST: Tris buffered saline with Tween

TE: Tris-EDTA

TEMED: Tetramethylethylenediamine

TKL: Tyrosine-kinase like

T_m: Melting temperature

TVN: Tubulovesicular network

TyrK: Tyrosine kinase

U

UV: Ultra violet

V

V_t: Total volume

X

X-Gal: 5-bromo-4-chloro-3-indoyl- β -D-galactopyranoside

XK: Kell blood group precursor.

LIST OF FIGURES

Figure 1: Global map showing countries with ongoing malaria transmission (WHO, 2012).....	28
Figure 2: Diagrammatic representation of the asexual and sexual life cycle stages of <i>Plasmodium falciparum</i> (www.proteinlounge.com).	32
Figure 3: A schematic representation of the major proteins in the human erythrocyte membrane (Adapted from Mohandas and Gallagher, 2008).	35
Figure 4: Characteristic structure of the catalytic domain of eukaryotic protein kinases (ePKs) (adapted from Doerig et al., 2008).	43
Figure 5: Protein sequence of the cloned region of <i>Pf</i> PK8 (PlasmoDB version 8.1, 2011).	106
Figure 6: Photograph of the ring and trophozoite intra-erythrocytic stages of <i>Plasmodium falciparum</i>	108
Figure 7: <i>Plasmodium falciparum</i> 3D7 genomic DNA resolved on a 0.8% agarose gel.....	109
Figure 8: RNase A-treated <i>Plasmodium falciparum</i> 3D7 genomic DNA resolved on a 0.8% agarose gel.....	110
Figure 9: A section of chromosome 2 of the <i>Plasmodium falciparum</i> genome (PlasmoDB version 8.1, 2011).	111
Figure 10: Diagrammatic representation of <i>Pf</i> B0150c and the sections of interest.	111
Figure 11: Region of <i>Pf</i> B0150c used for subcloning.....	112
Figure 12: <i>Pf</i> B0150c amplicons resolved on a 0.8% agarose gel.	113
Figure 13: Recombinant pGEX-4T-2- <i>Pf</i> B0150c and pGEX-4T-2 plasmid DNA.	114
Figure 14: Agarose gel of DNA samples used for cloning the <i>Pf</i> B0150c amplicon into the pTri-Ex-3 expression vector.	115
Figure 15: Digested <i>Pf</i> B0150c amplicon and pTriEx-3 expression vector resolved on a 0.8% agarose gel.....	116
Figure 16: Positive colony selection PCR of <i>Escherichia coli</i> DH5 α cells transformed with recombinant <i>Pf</i> B0150c-pTriEx-3 resolved on a 0.8% agarose gel.....	117
Figure 17: Restriction endonuclease digestion of plasmid DNA extracted from DH5 α cells transformed with recombinant <i>Pf</i> B0150c-pTriEx-3.	118

Figure 18: A section of the sequence chromatogram of recombinant <i>Pf</i> B0150c-Tri-Ex-3 construct 2 sequenced with a forward vector-specific primer.	119
Figure 19: A section of the sequence chromatogram of recombinant <i>Pf</i> B0150c-Tri-Ex-3 construct 2 sequenced with a reverse vector-specific primer.....	119
Figure 20: A section of the sequence alignment of the r <i>Pf</i> B0150c-pTriEx-3 construct 2 sequence.	120
Figure 21: Digested recombinant plasmids (<i>Pf</i> B0150c-pTriEx-3) extracted from transformed <i>Escherichia coli</i> Rosetta 2 (DE3) cells.	121
Figure 22: Protein sequence of the translated r <i>Pf</i> PK8-His protein.	122
Figure 23: Coomassie stained 12% Laemmli gel of purified r <i>Pf</i> PK8-His from a 20ml <i>Escherichia coli</i> Rosetta 2 (DE3) culture.	123
Figure 24: Immunoblot of r <i>Pf</i> PK8-His proteins.	124
Figure 25: Photograph of a healthy <i>Spodoptera frugiperda</i> (<i>Sf</i> 9) cell culture stained with Trypan Blue dye solution as seen under a phase contrast inverted microscope with a 40x magnification.	125
Figure 26: <i>Spodoptera frugiperda</i> (<i>Sf</i> 9) insect cells pre- and post infection with BacVirus- <i>Pf</i> B0150c.	126
Figure 27: Growth curves of <i>Spodoptera frugiperda</i> (<i>Sf</i> 9) insect cell suspension cultures infected with recombinant BacVirus- <i>Pf</i> B0150c.....	127
Figure 28: Recombinant baculovirus-infected <i>Spodoptera frugiperda</i> (<i>Sf</i> 9) cells 24 hours post infection visualized with the FastPlax™ Titer kit.	129
Figure 29: Coomassie Blue stained 12% Laemmli gel analysis of r <i>Pf</i> PK8-His expression in recombinant BacVirus- <i>Pf</i> B0150c infected <i>Sf</i> 9 insect cells.	131
Figure 30: Immunoblot of r <i>Pf</i> PK8-His proteins expressed in <i>Sf</i> 9 insect cells infected with recombinant BacVirus- <i>Pf</i> B0150c.	132
Figure 31: Protein sequence of rGST- <i>Pf</i> PK8.....	133
Figure 32: Coomassie stained 12% Laemmli gel of purified rGST- <i>Pf</i> PK8 from a 250ml <i>Escherichia coli</i> Rosetta 2 (DE3) culture.	134
Figure 33: Immunoblot of rGST- <i>Pf</i> PK8 proteins probed with anti-GST-HRP conjugated antibody.	135
Figure 34: Densitometric analysis of a Coomassie stained 12% Laemmli gel. .	136
Figure 35: Densitometric scan of the first elution fraction of rGST- <i>Pf</i> PK8.	137
Figure 36: Stability of rGST- <i>Pf</i> PK8.	140

Figure 37: Spectrophotometric data of the non-radioactive coupled enzyme assay showing the decrease of NADH due to the kinase activity of recombinant rGST- <i>Pf</i> PK8 in the presence of exogenous substrates.	142
Figure 38: Michaelis-Menten plots for rGST- <i>Pf</i> PK8 in the presence of three exogenous substrates and ATP.	145
Figure 39: Lineweaver-Burk plots for rGST- <i>Pf</i> PK8 in the presence of three exogenous substrates and ATP.	147
Figure 40: Effect of temperature on rGST- <i>Pf</i> PK8 enzyme activity.....	149
Figure 41: Effect of pH on rGST- <i>Pf</i> PK8 enzyme activity.....	150
Figure 42: BSA standard curve.	152
Figure 43: Dot blots of immobilised red blood cell membrane proteins overlaid with rGST- <i>Pf</i> PK8.....	153
Figure 44: Amido black stained nitrocellulose membrane used in the binding study of rGST- <i>Pf</i> PK8 with RBCM proteins.	154
Figure 45: Immunoblots of RBCM – rGST- <i>Pf</i> PK8 overlays using anti-GST HRP-conjugated antibody.	155
Figure 46: An alignment of the kinase domain of <i>rPf</i> PK8 with its closest serine/threonine-like kinase homologues.....	158
Figure 47: Areas of identity between the cloned region of <i>Pf</i> PK8, PKc_STEs and S_TKcs.....	159
Figure 48: Conserved ATP-binding pocket residues of the <i>rPf</i> PK8 kinase domain	160
Figure 49: Conserved substrate binding site residues of the <i>rPf</i> PK8 kinase domain.....	161
Figure 50: Secondary structure and disorder prediction of the cloned region of <i>Pf</i> PK8.....	163
Figure 51: Predicted 3D structure of the cloned region of <i>Pf</i> PK8.....	164
Figure 52: Predicted 3D structure of the kinase domain of <i>Pf</i> PK8.....	164
Figure 53: Template information of homologues used to predict the 3D structure of the kinase domain of <i>Pf</i> PK8.	166
Figure 54: Predicted 3D structure of <i>Pf</i> PK8.	167
Figure 55: mRNA expression levels of <i>Pf</i> B0150c during the asexual stages of development in the human host erythrocyte.	176
Figure 56: Expression of <i>Pf</i> B0150c in <i>Plasmodium falciparum</i> 3D7 parasites.	177

LIST OF TABLES

Table 1: Classification of eukaryotic protein kinases (ePKs) (Hanks, 2003).	44
Table 2: PCR reaction mixture using the GoTaq® Green Master Mix PCR system.....	62
Table 3: Preparation of the PCR reaction mixture using the Expand High Fidelity PLUS PCR system.	64
Table 4: Preparation of a 30µl Fermentas Fast Digest® restriction enzyme mixture utilizing <i>Bam</i> HI and <i>Xho</i> I endonucleases.....	65
Table 5: Preparation of a 60µl Fermentas Fast Digest® restriction enzyme mixture utilizing <i>Bam</i> HI and <i>Xho</i> I endonucleases to digest pTriEx-3 plasmid DNA.	67
Table 6: Ligation reaction mixtures.	68
Table 7: PCR reaction mixture for screening <i>Escherichia coli</i> colonies.	70
Table 8: Preparation of the BigDye® terminator sequencing reaction mixtures.	72
Table 9: Protein samples (100µl) collected during extraction and purification of rGST- <i>Pf</i> PK8.....	78
Table 10: Protein samples (100µl) collected during extraction and purification of r <i>Pf</i> PK8-His.....	80
Table 11: Laemmli SDS-PAGE gel solutions.....	81
Table 12: Preparation of insect cell transfection mixtures.....	90
Table 13: Protein kinase assay control and blank reaction mixture (1ml) preparations.....	99
Table 14: Protein kinase assay sample reaction mixture (1ml) preparations.....	100
Table 15: Reaction mixture preparation used to determine the effect of temperature on rGST- <i>Pf</i> PK8 enzyme activity.	101

Table 16: Reaction mixture preparation to study the effect of pH on rGST- <i>Pf</i> PK8 activity.....	101
Table 17: Fairbanks SDS-PAGE gel solutions.	104
Table 18: Spectrophotometric data of <i>Plasmodium falciparum</i> 3D7 genomic DNA.	109
Table 19: Spectrophotometric data of pooled <i>Plasmodium falciparum</i> 3D7 genomic DNA after RNase A treatment.	110
Table 20: Spectrophotometric data of the purified <i>Pf</i> B0150c amplicons.	113
Table 21: Spectrophotometric data of extracted plasmid DNA.	114
Table 22: Plasmids from <i>Escherichia coli</i> DH5 α colonies transformed with <i>Pf</i> B0150c-pTriEx-3.....	117
Table 23: <i>Sf</i> 9 plaques formed by BacVirus- <i>Pf</i> B0150c.	129
Table 24: Densitometric analysis data of rGST- <i>Pf</i> PK8 Elution 1.	137
Table 25: Approximate K_m and V_{max} values for rGST- <i>Pf</i> PK8 for three exogenous substrates and ATP.	148
Table 26: Absorbance values of the Coomassie protein determination assay of BSA standards and red blood cell membrane protein sample.....	151

1 INTRODUCTION

1.1 The developing world's struggle with malaria

Malaria is known today as the world's most lethal parasitic disease and kills more people than any other communicable disease except tuberculosis. Charles Alphonse Louis Laveran described a single celled Apicomplexan as the causative agent of malaria in 1880 (Haas, 1999). Malaria in humans is caused by five protozoan species, *Plasmodium falciparum* (*P. falciparum*), *Plasmodium vivax*, *Plasmodium malariae*, *Plasmodium knowlesi* (Singh *et al.*, 2004) and *Plasmodium ovale* (Persidis, 2000). *Plasmodium falciparum* causes cerebral malaria and is the most lethal of the five parasite species (Rinaldi, 2004).

Approximately half of the world's population (3.3 billion) are at risk of malaria. An estimated 219 million (range 154-289 million) cases of malaria and 660 000 (range 610 000 – 971 000) deaths due to this disease were reported in 2010 (WHO Malaria Report 2012). The disease is a problem in 104 countries (Figure 1), affecting mostly the developing world and the tropics.

The World Health Organisation (WHO) estimated that malaria-burdened countries lose 1.3% of their annual gross domestic product due to this tropical disease. The African region accounts for 85% of malaria cases and 90% of all deaths caused by malaria (WHO, 2012). Families in Africa spend an average of 25% of their income on malaria treatment and disease prevention. Immunity reduces the risk of infection causing severe disease and is developed over years of exposure. For this reason, most deaths in Africa occur in young children under the age of 5 years. Malaria claims the life of an African child every minute (WHO Malaria Report 2012) and is the cause of 7.4% of all childhood deaths (Liu *et al.*, 2012).

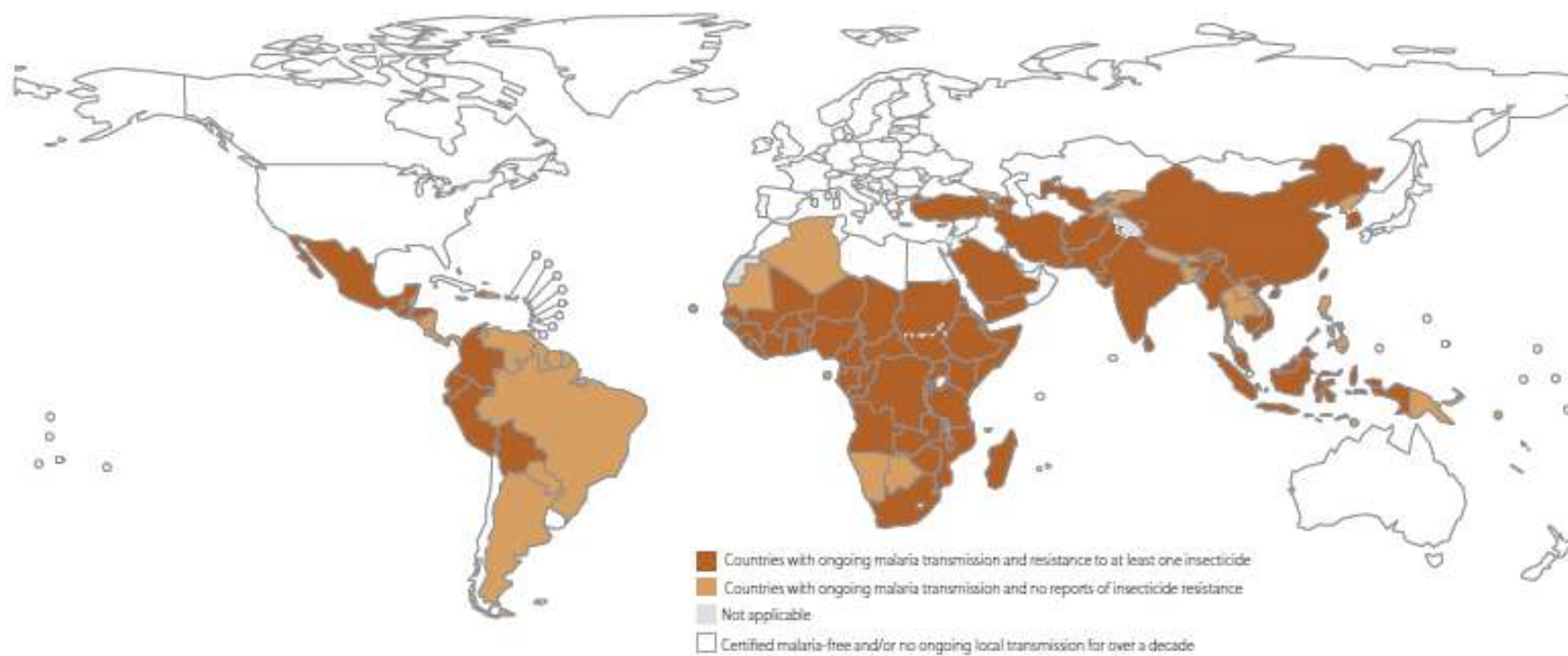


Figure 1: Global map showing countries with ongoing malaria transmission (WHO, 2012).

The increase in drug resistant parasites makes the fight against the disease more difficult especially for countries in the developing world. These countries are not able to tackle the problem effectively due to their poor economic status and low infrastructure. The WHO Malaria Report 2012 (WHO, 2012) highlights a decrease in the burden of malaria due to the widespread use of bednets and increased vector control measures. It is of the utmost importance that a regulated treatment plan using a combination drug and effective vector control measures is implemented in affected countries worldwide.

1.2 Anti-malarial drugs and drug resistance of *Plasmodium sp.*

Artemisinin is the most recent and widely used anti-malarial drug with a good safety-profile (White, 2008). This plant-derived peroxide was first described in the 1970's and WHO announced the use of artemisinin-combination therapies (ACTs) as first line defence against *P. falciparum* in 2005 (Liao, 2009). ACTs is defined by the WHO as an anti-malarial combination therapy with one component being an artemisinin-derivative. The reasoning behind using ACTs is because the premature discontinuation of a monotherapy based on artemisinin as soon as the symptoms of malaria disappear may lead to incomplete treatment of the disease. Persistent parasites may still be present in the blood and without a second drug to kill these resistant parasites; they may be passed onto a mosquito which would lead to continued infection and the possibility of artemisinin-resistant parasites in the long term (WHO, 2012). ACTs are used to exploit the additive and synergistic potential of individual drugs to improve efficacy. Drug resistance depends essentially on mutation and if the constituent drugs of the combination have different modes of action and follow independent pathways, the probability of mutations leading to the resistance of the drugs making up the combination therapy, is less likely to occur (White, 2008).

Drug resistance in *Plasmodium sp.* and its origins are the most important factors to consider in the fight against this disease and it increases the need to find novel drug targets. Reports of resistance against newer drugs developed in the last 20 years such as atovaquone, malarone, halofantrine, mefloquine, proguanil, and the

more classical drugs chloroquine and sulphadoxine-pyrimethamine have been documented (WHO Malaria Report 2012, 2012). Signs of chloroquine resistance were described as early as 1964 in South East Asia and South America with resistant parasites spreading to Africa in the 1980's (Ridley, 1998). The chloroquine anti-malarial drug failure rate at the beginning of the nineties was considered to be 100% (Andrade, 1992). The spread of chloroquine resistant strains of the parasite lead to the use of sulphadoxine-pyrimethamine as an anti-malarial drug, however, sulphadoxine-pyrimethamine resistant parasites surfaced in the eighties (Souza, 1992). Recently, a delay in the clearance of *P. falciparum* following artemisinin treatment has been reported in four countries in South East Asia, including Myanmar, Thailand, Cambodia and Vietnam (Dondorp *et al.*, 2009, WHO, 2012). The increase in the spread of drug-resistant parasites in developing countries is mostly due to either the continued use of out-dated drugs, such as chloroquine, or else artemisinin monotherapy.

1.3 Anti-malarial vaccines

There are three main ideas for targeting the parasite by means of vaccines. These include: sporozoite-vaccines to prevent infection, transmission blocking-vaccines which may reduce the spread of the disease by arresting parasite development within the vector itself and vaccines targeting the asexual-stage of the parasite to reduce the manifestation of severe symptoms of the disease (Persidis, 2000).

A malaria vaccine candidate called RTS,S targets the pre-erythrocytic stages of *Plasmodium falciparum*. This vaccine candidate has been shown to prevent malaria infection and clinical disease in Phase 2b field trials in some infants, children and adults and more recently in a Phase 3 trial in Africa (The RTS SCTP, 2011). In these trials, vaccination with vaccine RTS,S induced high levels of antibodies and CD4⁺ T cells specific for the circumsporozoite protein.

According to White *et al.* (2013) sporozoites inoculated into the skin via a mosquito bite can be immobilised by vaccine-induced anti-CSP antibodies as they

migrate through tissue. Sporozoites that reach the liver will invade hepatocytes where they undergo hepatic development. Hepatocyte invasion could potentially be prevented by anti-CSP antibodies and intracellular *Plasmodium* parasites can be targeted by vaccine-induced CSP-specific CD4⁺ T cells leading to killing of the infected hepatocyte. It is suggested that the RTS,S vaccine acts through the induction of high levels of both anti-CSP antibodies and CSP specific CD4⁺ T cells, with the antibody response playing a greater role (White *et al.*, 2013). The most recent results of the Phase 3 trial indicated a vaccine efficacy of only approximately 30% (The RTS,S Clinical Trials Partnership, 2012). Until a commercial, effective vaccine becomes available to prevent malaria, drug development remains an important priority.

1.4 The life cycle of the parasite

Plasmodium falciparum has a complex life cycle (Figure 2) alternating between two hosts and is characterised by developmental stages with different morphological forms. Some of these stages undergo continuous cell proliferation whereas in others the cell cycle is arrested.

The parasite is transmitted by the *Anopheles sp.* mosquito. Mosquito species found in Africa have a long life span and adds to the reason why more than 90% of all malaria deaths occur in Africa (WHO, 2012). Sexual reproduction occurs in the mosquito and the parasite multiplies asexually in erythrocytes and hepatocytes within its human host.

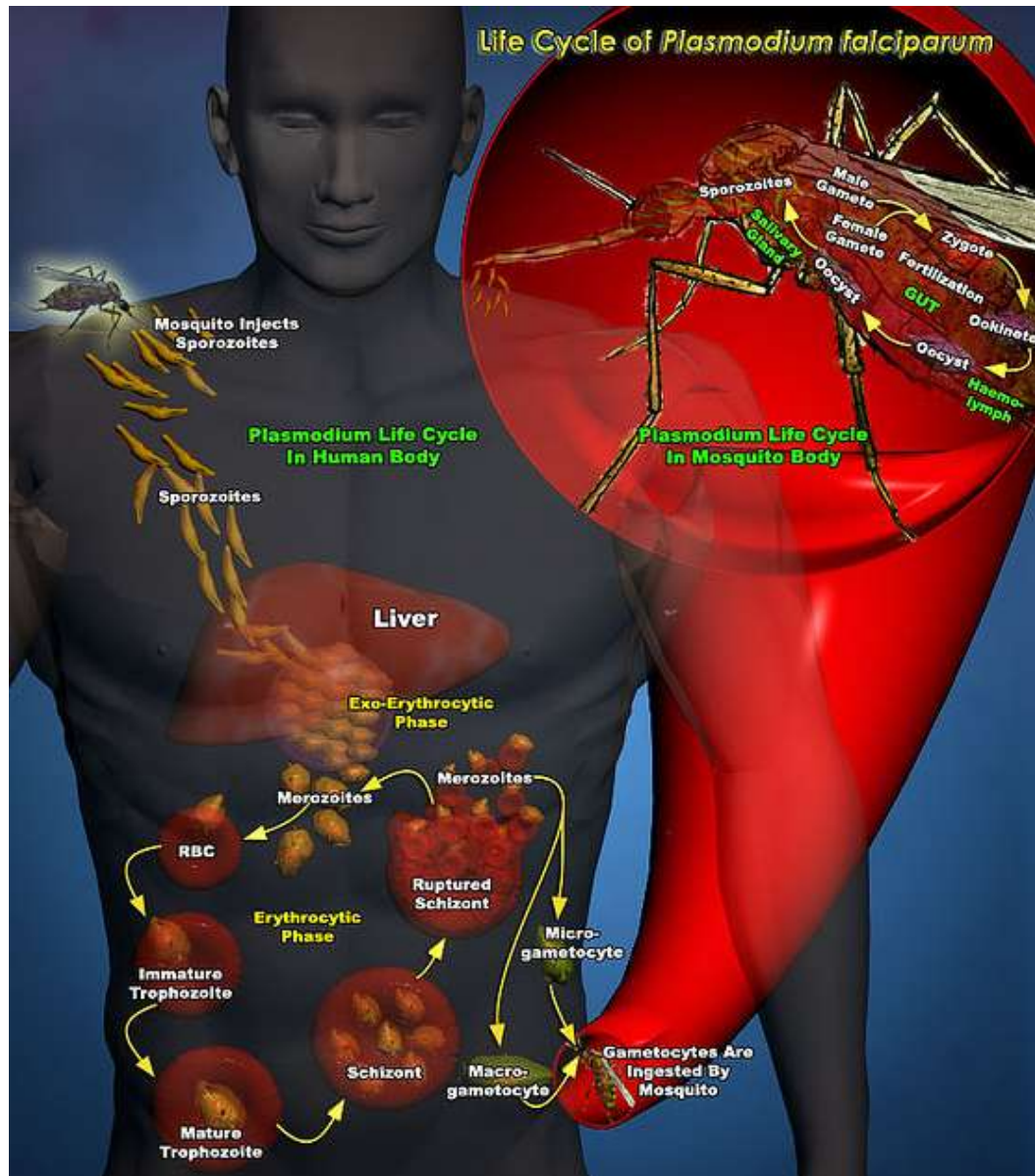


Figure 2: Diagrammatic representation of the asexual and sexual life cycle stages of *Plasmodium falciparum* (www.proteinlounge.com).

1.4.1 Asexual stage of development

When an infected female *Anopheles* mosquito takes a blood meal from a human host, saliva is injected into the host's bloodstream containing an anti-coagulant along with approximately 20 tiny, elongated haploid sporozoites. The sporozoites are injected into its host's subcutaneous tissue or directly into the blood stream and then travel to the liver. These enter hepatocytes and a series of asexual reproductions (schizogony) is initiated producing approximately 30 to 50

thousand merozoites within a period of 5 to 7 days. Mature merozoites are subsequently released from the hepatocytes into the bloodstream, where they attach and penetrate erythrocytes and enter the erythrocytic stage of their life cycle (Schmidt and Roberts, 2005).

Upon entry into an erythrocyte, a second round of asexual multiplication takes place, generating new merozoites in the infected erythrocyte. The parasite begins to enlarge as a uni-nucleate ring form which is apparent immediately after erythrocyte invasion. This ring-form later transforms into a young feeding trophozoite. Trophozoites divide asexually and rapidly develop into schizonts that have 12 to 32 nuclei (Schmidt and Roberts, 2005). The schizonts undergo segmentation once nuclear division is complete, forming 8 to 32 mono-nucleated merozoites. The infected cells rupture releasing the merozoites and metabolic waste into the host's bloodstream. Newly released merozoites attach to new erythrocytes and subsequently invade them. These erythrocytic events cause the characteristic chills and fever associated with malaria (Fujioka and Aikawa, 1999). This cyclic erythrocytic stage repeats itself approximately every 48 hours in a *P. falciparum* infected human host.

1.4.2 Sexual stage of development

Some merozoites differentiate into female macrogametocytes and male microgametocytes which is the onset of the sexual stage of reproduction. Upon ingestion by a female *Anopheles sp.* mosquito when taking a blood meal from an infected human, the gametocytes will develop into male and female gametes. The male gametocyte exits its cell cycle arrest and undergoes cell division to form eight microgametes. The gametes exit the erythrocyte once in the mosquito's midgut. The microgametes penetrate the macrogamete and these fuse to form a diploid zygote. Zygotes develop into motile ookinetes which penetrate the mosquito's gut wall to form immobile oocysts on its outer surface. The oocyst undergoes asexual multiplication and forms thousands of sporozoites that migrate to the mosquito's salivary glands (Schmidt and Roberts, 2005), which completes the parasite life cycle.

1.5 The human host erythrocyte

The erythrocyte plays an important role in the asexual life cycle of *P. falciparum*. It is a major component of blood and is an 8µm biconcave disk enclosed by a plasma membrane. The distinct biconcave shape of the erythrocyte evolves from a reticulocyte after 48 hours of maturation in the bone marrow followed by further maturation while circulating within the capillaries (Mohandas and Gallagher, 2008).

The erythrocyte is in circulation for 120 days supplying oxygen from the lungs to all the tissues in the human body and carries carbon dioxide from the tissues back to the lungs. The ability of the erythrocyte to squeeze through capillaries as narrow as 5µm is made possible by its remarkable architecture. The erythrocyte membrane is extremely elastic and has been described as being stronger than steel considering its structural resistance (Mohandas and Gallagher, 2008).

1.5.1 Erythrocyte membrane structure

The erythrocyte cell membrane consists of a lipid bilayer with an interacting group of peripheral and integral membrane proteins which not only supports and reinforces the lipid bilayer but have recognition, transport and enzyme activities (Mohandas and Gallagher, 2008). Erythrocyte membrane protein complexes involved in the maintenance of the membrane's structural integrity are an ankyrin-based and a protein 4.1-based macromolecular complex (Figure 3). This protein meshwork is essential for the survival of the cells within the vascular system of the body.

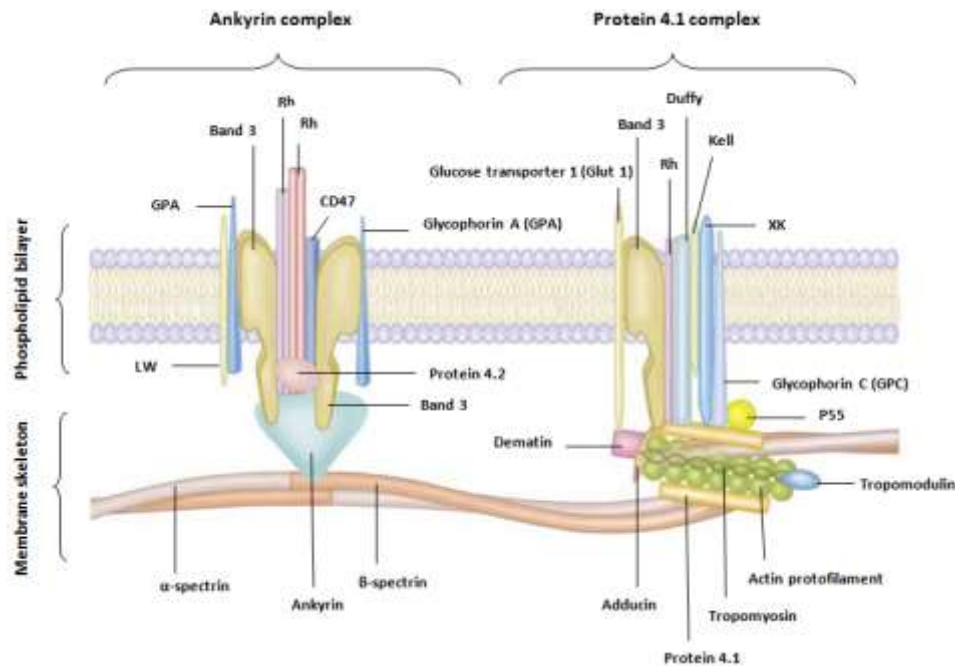


Figure 3: A schematic representation of the major proteins in the human erythrocyte membrane (Adapted from Mohandas and Gallagher, 2008).

The following blood group antigens are shown in the figure Rhesus antigen (Rh), Landsteiner and Wiener antigen (LW), XK (Kell blood group precursor) and the Kell antigen. Dematin is also referred to as protein 4.9.

The lipid bilayer is composed of phospholipids and cholesterol in even proportions by weight. The four phospholipids are asymmetrically dispersed between the outer and inner leaflet of the lipid bilayer. The outer monolayer contains mostly sphingomyelin and phosphatidylcholine while all of the phosphatidylserine (PS) and most phosphatidylethanolamine are confined to the inner monolayer (Mohandas and Gallagher, 2008). PS and phosphatidyl-4-5-bisphosphate (PIP2) regulate the mechanical functioning of the membrane. A study conducted by Manno *et al.* (2002) proved that the interaction between spectrin and PS improves the mechanical stability of the erythrocyte membrane. The binding of protein 4.1 to glycophorin C (GPC) is enhanced by PIP2, but PIP2 decreases the interaction between protein 4.1 and band 3. These synergies regulate the linkage of the lipid bilayer to the membrane skeleton (An *et al.*, 2006).

Spectrin, actin, protein 4.1, adducin and ankyrin are peripheral erythrocyte membrane proteins whereas band 3, glycophorin A (GPA) and glycophorin C,

protein 4.2 and protein 4.9 are classified as integral membrane proteins. The cell membrane embodies a 2-dimensional spectrin-based skeletal network attached to the phospholipid bilayer. The main proteins of the skeletal network are α -spectrin, β -spectrin, actin, protein 4.1, adducin, dematin, tropomyosin and tropomodulin. The skeletal network connection is not fixed and can undergo remodelling when the cell experiences a change due to a shift in the biochemical environment. Calcium and adenosine triphosphate (ATP) concentrations have been shown to regulate cytoskeleton remodelling (Manno *et al.*, 2004).

Spectrin is the major protein of the erythrocyte membrane skeleton making up 25% - 30% of the total membrane proteins and has two subunits with a molecular weight of 260kDa (α -spectrin) and 225kDa (β -spectrin), respectively (Bennett, 1988). Multiple tandem spectrin-type repeats are characteristics of the spectrin superfamily. In human spectrin, these domains consist of approximately 106 amino acids and have a triple helical fold (Ipsaro *et al.*, 2010). Adjacent repeats are connected by α -helical linkers. The subunits are arranged to form heterodimers in an antiparallel side-to-side manner. α -Spectrin and β -spectrin dimers associate in a head-to-head fashion to form a spectrin heterotetramer (Ipsaro *et al.*, 2010). The other end of the spectrin dimer interacts with protein 4.1, filamentous actin (F-actin) and actin binding proteins (dematin, adducin, tropomyosin and tropomodulin) to form a junctional complex (An *et al.*, 2005).

Actin filaments interact with the carboxy terminus of the α -subunit and the amino terminus of the β -subunit of spectrin. The tight junction at this end of the spectrin tetramer is essential for the stable association with actin filaments (Bennett, 1988). The ends of actin filaments are capped with adducin at one end and tropomodulin at the other (Mohandas and Gallagher, 2008).

Protein 4.1 is the major protein associated with spectrin and actin in erythrocyte membranes and is encoded by a gene located on chromosome 1 of the human genome. Protein 4.1 constitutes approximately 6% of the total erythrocyte membrane proteins and exists in two isoforms. These isoforms separate into two clear bands on a PAGE (polyacrylamide gel electrophoresis) gel with molecular weights of 80kDa (protein 4.1a) and 78kDa (protein 4.1b), respectively

(Takakuwa, 2000) . Protein 4.1 binds to phospholipids phosphatidylserine (PS) and phosphatidyl-4-5-bisphosphate (PIP2) and to transmembrane proteins glycophorin C (GPC) and band 3 (Baines *et al.*, 2009). Protein 4.1, actin and spectrin are associated with each other to form a ternary complex (Tyler *et al.*, 1979). The ternary complex connects the junctional complex to the membrane and plays an essential role in regulating cell membrane deformation and fragmentation by mechanically stabilising the membrane (Mohandas and Gallagher, 2008).

Ankyrin (band 2.1) is a hydrophobic bipolar protein which interacts with the β -subunit of spectrin and the cytoplasmic domain of the transmembrane anion-channel protein, band 3 (Pinder *et al.*, 1989). This interaction is the primary attachment of the spectrin-based cytoskeleton to the erythrocyte membrane bilayer. Ankyrin makes up 5% of the total red blood cell membrane proteins with an approximate molecular weight of 210kDa. The major structural and functional domains of ankyrin are the 90kDa band 3 binding region domain and a phosphorylated 72kDa domain containing the spectrin binding site (32kDa) (Lambert *et al.*, 1990).

The red blood cell membrane is rich in band 3, comprising approximately 25% of the total membrane proteins. Band 3 consists of a 55kDa membrane domain and a 43kDa cytoplasmic domain (cdb3) (Steck, 1978). The function of the 55kDa domain is to catalyse the exchange of $\text{Cl}^-/\text{HCO}_3^-$ across the phospholipid bilayer. The 43kDa domain serves as an anchor for ankyrin, protein 4.1, protein 4.2, haemoglobin and various glycolytic enzymes. This smaller domain of band 3 binds to adducin and plays an important role in the vertical linking-bridge formations between the spectrin-based membrane skeleton and the phospholipid bilayer (Mohandas and Gallagher, 2008, Anong *et al.*, 2009).

Protein 4.2 is a 72kDa protein which constitutes approximately 5% of the total erythrocyte membrane proteins. It has been demonstrated that protein 4.2 associates with the major membrane proteins ankyrin, the 43kDa cytoplasmic domain of band 3 (Korsgren and Cohen, 1988) and to a 30kDa N-terminal binding domain of spectrin (Mandal *et al.*, 2002).

Adducin is a 200kDa α - β -heterotetramer connecting the ternary complex and the junctional complex to band 3 (Franco and Low, 2010). Adducin acts as a capping protein of actin filaments to prevent extensive elongation of these protofilaments. Dematin (previously known as protein 4.9) is a 100kDa trimer (Khanna *et al.*, 2002) known to bind to F-actin and cause bundling of these actin filaments (Chishti *et al.*, 1988). Dematin interacts with glucose transporter-1 thereby anchoring the membrane skeleton to the phospholipid bilayer (Khan *et al.*, 2008) and regulates the mechanical stability of the erythrocyte membrane by promoting spectrin-actin interactions (Koshino *et al.*, 2012). Tropomyosin is a 56kDa dimer with two polypeptide chains of similar molecular weight (Fowler and Bennett, 1984). Tropomyosin is an actin binding protein and forms part of the junctional complex that regulates the stability of the erythrocyte membrane (An *et al.*, 2007).

Glycoproteins are rich in sialic acid and account for approximately 60% of the red blood cell's negative surface charge. For this reason, glycophorins play an important role in erythrocyte-erythrocyte interactions and also interactions involving erythrocytes and other cells while in circulation. The negative charge on the erythrocyte surface produces electrostatic repulsive energy and thereby prevents the aggregation of erythrocytes (Chien and Sung, 1987). According to Chasis and Mohandas (1992) the cytoplasmic domain of glycophorin A (GPA) interacts with the skeletal network. When a ligand specific for GPA binds to it, it causes a change in the conformation of the cytoplasmic domain of this protein which results in an increased interaction with the underlying membrane skeleton. This in turn causes a decrease in the lateral mobility and therefore a decrease in membrane deformability. Ligand specific binding for other erythrocyte surface proteins such as band 3 and blood antigens (A, B, Rh and Kell) are not known to change the properties of the membrane. GPA is therefore considered as the only erythrocyte surface protein involved in the abovementioned type of ligand-induced signal transductions.

p55 is a 55kDa highly palmitoylated human erythrocyte peripheral membrane protein (Metzenberg and Gitscheir, 1992). A study using naturally mutated erythrocytes showed that p55 is absent in cells devoid of either protein 4.1 or

GPC. Protein 4.1 interacts with the cytoplasmic domain of GPC thereby anchoring p55 in the phospholipid bilayer (Reid *et al.*, 1990).

A study conducted by Pasini *et al.* (2006) identified more than 300 erythrocyte proteins of which 105 were integral membrane proteins. Current erythrocyte membrane structural organisation models accounts on average for only 15% of the membrane proteins identified by Pasini *et al.* (2006). This leaves room for extensive progress regarding our understanding of the erythrocyte membrane structure.

1.5.2 Morphological and structural changes of the erythrocyte during *Plasmodium falciparum* invasion and intra-erythrocytic development

The asexual life cycle of *Plasmodium sp.* within the erythrocyte is responsible for the pathogenesis associated with malaria. A mature erythrocyte is haemoglobin rich and lacks organelles needed to transcribe new proteins or lipids; trafficking mechanisms to transport proteins within the cell are absent and nutrients or other proteins cannot cross the erythrocyte plasma membrane by means of endocytosis (Haldar and Mohandas, 2007). *Plasmodium* parasites therefore need to change the permeability of the parasitized erythrocyte membrane to make nutrient uptake (Martin and Kirk, 2007) and the removal of waste products possible. The parasite activates new protein trafficking pathways to transport proteins across their own plasma membrane and the erythrocyte membrane, thus ensuring its survival within the host cell (Haldar and Mohandas, 2007).

The critical invasion process of the malaria parasite into the host cell is complex. More than 400 parasite proteins are involved in erythrocyte remodelling during invasion and intraerythrocytic development of the parasite (Haldar and Mohandas, 2007). After schizont rupture, mature merozoites are released into the bloodstream of the host. The first interactions between the merozoite and the erythrocyte involve parasite surface proteins which recognise host cell ligands. These proteins are intensely studied as possible vaccine candidates. Proteins involved in the invasion process are linked via glycosylphosphatidylinositol (GPI) anchor proteins to the merozoite surface or found within specialised merozoite secretory organelles called rhoptries, micronemes and dense granules (Cowman

and Crabb, 2006). The merozoite orientates itself in such a manner that the anterior apical end housing the secretory organelles faces the targeted site of invasion.

A cascade of erythrocyte membrane deformation events is triggered upon contact of the merozoite with the host cell membrane (Haldar and Mohandas, 2007). Proteins secreted by the micronemes bind irreversibly to host surface sialic acid residues which are present in abundance on erythrocyte glycophorin A (Cowman and Crabb, 2006). A definite parasite-erythrocyte mobile junction is formed between the two cells (Aikawa *et al.*, 1978). Biochemical evidence gathered by Baum *et al.* (2006) suggests that this junction is connected to a merozoite plasma membrane molecule which is associated with a myosin-actin complex and is considered as the driving force behind the invasion process. The secretory organelles release their contents onto the erythrocyte surface and cause an invagination of the erythrocyte lipid bilayer at the junction site (Haldar and Mohandas, 2007). This leads to a restructuring of the erythrocyte membrane cytoskeleton. The host cell also plays a role in the invasion process and the erythrocyte membrane is changed by parasite-induced post-translational modifications during merozoite invasion (Zuccala and Baum, 2011).

The structural changes of the erythrocyte membrane skeleton make it possible for the merozoite to be engulfed by the host cell. The erythrocyte membrane closes behind the merozoite at the site of invasion and echinocytosis follows. Echinocytosis is the process whereby the flow of chloride and potassium ions causes a change in the shape of the cell. The erythrocyte membrane returns to its normal morphology within approximately 10 minutes post-invasion and post-echinocytosis (Cowman *et al.*, 2012). The merozoite is now enclosed by a membrane called the parasitophorous vacuolar membrane (PVM). The rhoptries are the driving force behind the formation of the PVM (Haldar and Mohandas, 2007). This early stage in the parasite's intraerythrocytic life cycle is sometimes referred to as the ring-stage, characteristic of the intracellular ring-like appearance of the PVM (Bannister *et al.*, 2000).

During the ring stage of the parasite, finger-like extensions protrude from the parasitophorous vacuole as viewed by electron microscopy. These extensions stay connected to the parasitophorous vacuole to form the tubulovesicular networks (TVNs) (Spycher *et al.*, 2006). The parasite secretes proteins not only during the process of invasion but continuously while maturing within the erythrocyte. Transport of parasite proteins occurs mainly during the trophozoite and schizont stages of the parasite's life cycle. The transport of proteins within the erythrocyte cytoplasm is made possible by TVNs and Maurer's clefts (Maier *et al.*, 2008). The Maurer's clefts originate from the PVM or are subdomains of the TVN (Wickert and Krohne, 2007). Some proteins predestined to the erythrocyte surface reside in the Maurer's clefts situated at the periphery of the host cell.

Exported parasite proteins have a profound effect on the infected erythrocyte and promote morphological, structural and biological changes. Up to 10 000 electron-dense protrusions, called knobs, develop on the surface of the erythrocyte approximately 16 hours post-invasion (An and Mohandas, 2010). These knobs are involved in cytoadherence of parasitized erythrocytes to the vascular epithelium, thereby evading the spleen which is part of the host's immune defence. Remodelling of the membrane is triggered by the export of parasite proteins to the erythrocyte cytoplasm. Some of these proteins are trafficked to the erythrocyte membrane, via the PVM or via lipid rafts present in the parasitophorous vacuole (Crabb *et al.*, 2010). These erythrocyte detergent-resistant membrane (DRM) lipid rafts contain approximately 12 host cell membrane proteins (Murphy *et al.*, 2004).

Parasite proteins and virulence antigens (for example, STEVOR and RIFIN proteins) (Cheng *et al.*, 1998) destined for transport across and beyond the boundaries of the PVM have a *Plasmodium* export element (PEXEL) consisting of an 11 amino acid signal sequence that directs export to the parasitophorous vacuole (Marti *et al.*, 2004, Hiller *et al.*, 2004). *Plasmodium falciparum* erythrocyte membrane protein 1 (*PfEMP1*), *P. falciparum* erythrocyte membrane protein 3 (*PfEMP3*), knob associated histidine rich protein (KHARP), ring-

infected erythrocyte surface antigen (RESA) and mature parasite-infected erythrocyte surface antigen (MESA) are well known erythrocyte membrane associated parasite proteins containing an export element. *PfEMP1* and *KHARP* are found in higher numbers beneath knobs whereas *PfEMP3* and *RESA* are distributed around the erythrocyte membrane (An and Mohandas, 2010). These proteins and virulence antigens are classified as part of the host-targeting secretome of the parasite.

1.6 Protein kinases

1.6.1 *Plasmodium falciparum* protein kinases

The *Plasmodium* and human kinomes share similarities with regards to extremely diverse and large gene families. However, major structural and functional differences exist between the kinases of *Plasmodium* parasites and their vertebrate hosts. The large phylogenetic distance between these kinases (Ward *et al.*, 2004b) are exploited for the development of anti-malarial drug therapies (Doerig *et al.*, 2005).

Protein kinases are important in all cellular processes of eukaryotes. The human genome codes for more than 500 protein kinases (Manning *et al.*, 2002) and 65 typical eukaryotic protein kinases (ePKs) have been identified in the *P. falciparum* genome (Ward *et al.*, 2004b). The ePKs have multiple conserved amino acid sequences and a characteristic structural fold (Figure 4).

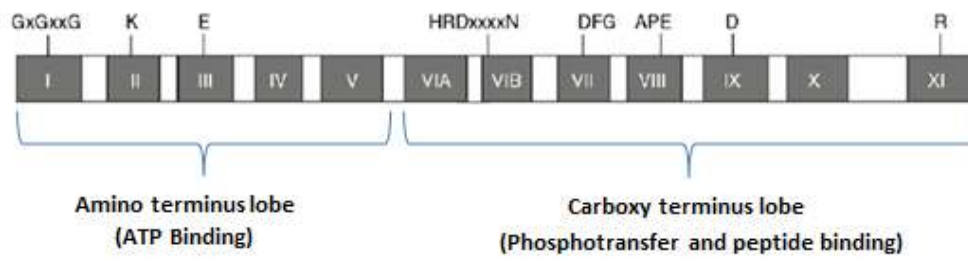


Figure 4: Characteristic structure of the catalytic domain of eukaryotic protein kinases (ePKs) (adapted from Doerig et al., 2008).

Eukaryotic protein kinases contain 11 subdomains with conserved amino acid sequences. Subdomains I to V are known as the amino terminus lobe responsible for the binding of ATP and subdomains VI to XI form the carboxy terminus lobe where peptide binding and phosphotransfer takes place. Subdomain I has three glycine residues (GxGxxG) which forms a hairpin that surrounds part of the ATP molecule. Subdomain II has a lysine (K) residue which orientates ATP through the contact with phosphate molecules. A salt bridge is formed by glutamate (E) in subdomain III and the lysine in subdomain II. The HRDXXXXN motif of subdomain VIB has an aspartate (D) and asparagine (N) residue. The aspartate of subdomain VIB is thought to be the catalytic residue which acts as a base acceptor. Aspartate in the DFG motif of subdomain VII binds to Mg^{2+} or Mn^{2+} linked with ATP. Glutamate of subdomain VIII forms a salt bridge with arginine (R) of subdomain XI. This C-terminal lobe of the kinase is structurally stabilised by this salt bridge. Aspartate in subdomain IX forms a hydrogen bond with the backbone thereby stabilising the catalytic loop of subdomain VI. The letter “x” denotes any amino acid.

There is limited knowledge of the phosphorylation cascades and the role of kinases in the life cycle of *Plasmodium species*. Two kinome studies of the *P. falciparum* genome identified 86 genes (Ward et al., 2004b; Anamika et al., 2005) coding for putative protein kinases. Sixty five of these kinases are related to the ePK family. The ePKs are divided into seven main kinase families (Table 1). The majority of the putative *P. falciparum* ePKs (*PfePKs*) are grouped into the well-known AGC, CK, CMGC, tyrosine-kinase like and CaMK groups of human kinases (Doerig et al., 2008). Solyakov et al. (2011) performed a study where kinome-wide gene knockout and reverse genetics approaches in combination with global phospho-proteomics identified the importance of phosphorylation in the asexual life cycle of *P. falciparum*. Their research showed that approximately half of the 65 *PfePKs* are essential for the intraerythrocytic survival of the parasites. These kinases are involved in the invasion process, various metabolic pathways, transcription and DNA replication. It was noted in this study that tyrosine phosphorylation does take place within the parasites even though a classic tyrosine kinase family in *P. falciparum* has not yet been identified.

Plasmodium falciparum has only one member of casein kinase 1 (CK1) with unknown function and it has been described as being one of the most primitive *P. falciparum* kinases. *In vitro* studies of the enzyme by Barik *et al.*, (1997) revealed that it is a polypeptide of approximately 37kDa with 324 amino acids. The protein was expressed in bacteria and shared characteristic properties with other known CK1 isoforms. *PfCK1* was able to phosphorylate a specific peptide substrate and exhibited a preference for ATP over GTP. The enzyme was most active in the trophozoite stages of the parasite's development.

Table 1: Classification of eukaryotic protein kinases (ePKs) (Hanks, 2003).

Kinase family	Kinase sub-family
Casein kinase 1 (CK1)	
CMGC	<ul style="list-style-type: none"> • Cyclin dependent protein kinase (CDK) • Glycogen synthase kinase 3 (GSK3) • CLKs (CDK-like kinases, tyrosine-kinase like (TKL))
AGC	<ul style="list-style-type: none"> • Protein kinase A (PKA) (cAMP-dependent protein kinase) • Protein kinase G (PKG) • Protein kinase C (PKC)
Calcium/calmodulin-dependent kinase (CDPK)	
STE kinase	<ul style="list-style-type: none"> • Protein kinases acting as regulators of mitogen activated protein kinases (MAPKs) and serine/threonine kinases (STKs)
Tyrosine kinase (TyrK)	
Orphan protein kinase (OPKs)	<ul style="list-style-type: none"> • ePKs not fitting into any of the other kinase families

The *P. falciparum* CMGC kinase family is divided into four subfamilies: casein dependent kinases (CDKs), mitogen-activated protein kinases (MAPKs), glycogen synthase kinase 3 (GSK3) and casein dependent-like kinases (CLKs).

Several CDKs are coded for by the *P. falciparum* genome with at least three of these being regulated by their interaction with cyclins (*PfPK5*, *Pfmrk* and *Pfcrk3*) (Doerig *et al.*, 2002; Halbert *et al.*, 2010). CDKs play a regulatory role in the cell-cycle. Mammalian and *Saccharomyces sp.* CDKs are regulated by phosphorylation but this type of regulation has not yet been elucidated for *PfCDKs*. *PfCDKs* are however autophosphorylated *in vitro* (Doerig *et al.*, 2002). MAPKs are signal transduction molecules that transfer intracellular and extracellular signals to various effectors to regulate cellular functions like transcription (Doerig *et al.*, 2008). *Pfmap-1* and *Pfmap-2* are two *P. falciparum* MAPK homologues. Deletion of the *Pfmap-1* gene does not result in a different sporozoite or schizont phenotype since the role of *Pfmap-1* is taken over by *Pfmap-2* in the absence of *Pfmap-1*. This is indicative that *Pfmap-1* fulfils an important function in wild-type parasites. The presence of *Pfmap-2* is crucial to complete the asexual life cycle of *P. falciparum* (Dorin-Semblat *et al.*, 2007). *PfMAPK* regulation is not yet fully understood but a study by Dorin *et al.* (2001) suggested that the never-in-mitosis A (NIMA) –related kinase, *Pfnek-1*, may play a role. Members of the GSK3 kinase family regulate cellular proliferation (Doerig *et al.*, 2008). Three *P. falciparum* GSK3 sequences are known but only one of these has been characterised. *PfGSK3* is a 53kDa protein with a conserved catalytic domain encoded by 452 amino acids. The enzyme is localised to the Maurer's clefts and is exported to the erythrocyte. *PfGSK3* is primarily expressed in the early trophozoites (Droucheau *et al.*, 2004). CLKs are crucial to RNA metabolism. There are four identified *P. falciparum* sequences that cluster with CLKs (Doerig *et al.*, 2008). Agarwal *et al.* (2011) demonstrated that the Lammer kinase homolog *PfCLK1* and *PfCLK-2* play important roles in gene regulation through post-transcriptional modification of mRNA. Western blot analysis, immunofluorescence and electron microscopy revealed that both *PfCLK-1* and *PfCLK-2* were predominantly localised in the parasite nucleus and *PfCLK-2* was also found in the cytoplasm.

Plasmodium falciparum has thirteen kinases that belong to the calcium/calmodulin dependent kinase (CDPK) family (Ward *et al.*, 2004b). CDPKs require calcium ions as second messengers to regulate their activity

(Zhang and Choi, 2001). Gene knockout studies performed in *Plasmodium berghei* showed that CDPKs exhibited definite functions in the motility of ookinetes (Siden-Kiamos *et al.*, 2006), the formation of microgametes (Bilker *et al.*, 2004) and hepatocyte invasion by sporozoites during its asexual life cycle stages (Coppi, 2007). *Pf*CDPK1 plays a crucial role in the asexual life cycle of the *Plasmodium* parasite. CDPK1 inhibition studies demonstrated that merozoite egress was blocked by the inactivation of this enzyme (Kato *et al.*, 2008).

Signalling pathways dependent upon cyclic adenosine monophosphate (cAMP) and cyclic guanosine monophosphate (cGMP) have important functions in all stages of the parasite's life cycle. *Pf*PKA, *Pf*PKB and *Pf*PKG are protein kinases belonging to this AGC kinase family. The inhibition of the cAMP effector *Pf*PKA results in *in vitro* growth arrest of *P. falciparum* parasites (Syn *et al.*, 2001). It was demonstrated in *Plasmodium berghei* sporozoites lacking adenyl cyclase α , that cAMP- and calcium-dependent signalling pathways modulate the release of the microneme contents (Ono *et al.*, 2008). *Pf*PKA has been proven to regulate an anion channel of the erythrocyte (Merckx *et al.*, 2008b) and intracellular calcium levels in the erythrocytic stages of *P. falciparum* (Beraldo *et al.*, 2005). PKG plays an important role in microneme secretion, gliding motility, tachozoite attachment to host cells, and invasion of host cells of the *Toxoplasma gondii* parasite (Wiersma *et al.*, 2004). It was demonstrated by McRobert *et al.* (2008) that *Pf*PKG plays a key role in the activation of *P. falciparum* gametocytes. *Pf*PKB is activated by calmodulin and calcium and plays a role in the signalling pathway which involves phospholipase C as an upstream regulator (Vaid *et al.*, 2008). An essential protein of the *P. falciparum* glideosome complex is glideosome associated protein 45 (*Pf*GAP45). The glideosome houses the actomyosin motor complex needed for the gliding motility of the parasite's migrant forms and for the invasion process of its host cells. *Pf*GAP45 plays a role in anchoring the parasite to its host cell and the optimal functioning of the actomyosin motor complex. *Pf*GAP45 is phosphorylated by *Pf*PKB and *Pf*CDPK1 (Thomas *et al.*, 2012).

The *P. falciparum* genome has five known sequences possibly belonging to the tyrosine kinase-like (TKL) kinase family (Doerig *et al.*, 2008). Abdi *et al.* (2010) characterised *P. falciparum* TKL 3 (*PfTKL3*), an enzyme encoded by the gene *Pf13-0288*. *PfTKL3* plays an essential role in parasite proliferation in erythrocytes and may represent a novel drug target. *PfTKL3* co-localised with cytoskeletal microtubules in gametocytes and was also expressed in the asexual life cycle stages of the parasite. *In vitro* studies of recombinant *PfTKL3* revealed that the enzyme phosphorylated exogenous substrates and exhibited autophosphorylation activity (Abdi *et al.*, 2010).

The OPK family is a group of enzymes that does not cluster with any of the other ePK families. The NIMA (never-in-mitosis A) related kinases (Nek) belong to the OPK family. Nek kinases are serine/threonine related kinases involved in cell cycle regulation. Four of these enzymes have been identified in *P. falciparum* (Doerig *et al.*, 2008). *PfNeks* are expressed in both the sexual and asexual blood stages (*Pfnek-1*) and in the gametocytes (*Pfnek-2*, *Pfnek-3* and *Pfnek-4*) (Le Roch *et al.*, 2003). *PfPK7* is an orphan kinase displaying the highest percentage homology with MAPK (Dorin-Semblat *et al.*, 2005). An *in vitro* study by Dorin-Semblat *et al.* (2007) showed that schizonts of parasites devoid of *PfPK7* had fewer daughter merozoites which lead to a slower growth rate. *PfPK9* has the ability to phosphorylate exogenous substrates and autophosphorylates *in vitro* (Philip and Haystead, 2007). Another group of OPKs are the FIKK kinases. FIKK kinases are named after a shared amino acid motif of phenylalanine-isoleucine-lysine-lysine in the amino terminal domain of the enzyme. Some FIKK kinase family members are transported via the Maurer's clefts to the host cell membrane (Nunes *et al.*, 2007). *Plasmodium falciparum* has twenty FIKK-related members scattered across eleven of the fourteen parasite chromosomes (Ward *et al.*, 2004b). The majority of the *P. falciparum* FIKK enzymes have an export element or host targeting motif essential for trafficking to the erythrocyte membrane across the parasitophorous vacuole (Marti *et al.*, 2004).

1.6.2 Phosphorylation during malaria parasite invasion and intraerythrocytic development

Changes in the structure of the erythrocyte membrane are important to facilitate erythrocyte invasion and the intraerythrocytic survival of the parasite. An extensive study of the parasite's proteome showed that a large number of plasmodial proteins contribute to these changes of the parasitized erythrocyte (Maier *et al.*, 2008). Phosphorylation plays a key role in remodelling the erythrocyte membrane. However, little is known about the phosphorylation of proteins at the erythrocyte membrane and what effect the binding of *Plasmodium* proteins to skeletal membrane proteins has on the ability of kinases to efficiently phosphorylate their target molecules.

A controlled and transient disruption of the erythrocyte membrane is induced by the binding of merozoites to ligands on the surface of the erythrocyte. The invasion of the merozoite into its host cell has been linked to the phosphorylation of membrane skeleton proteins, such as β -spectrin, protein 4.1 and band 3, which destabilises the membrane skeleton. The permeability of the infected erythrocyte membrane is modified shortly after invasion by parasite-induced permeation pathways to ensure the parasite's survival within the host cell. This increase in solute permeability has been linked to phosphorylation (Decherf *et al.*, 2004).

Plasmodial kinases and phosphatases are trafficked to the host cell membrane and signify that post-translational modification plays a role in the intracellular development of the parasite. FIKK kinases (Nunes *et al.*, 2007), falciparum exported serine/threonine kinases (FEST) (Kun *et al.*, 1997), CDPKs (Moskes *et al.*, 2004) and a protein phosphatase (Blisnick *et al.*, 2006) are parasite enzymes trafficked to the host cell membrane. These enzymes can alter the phosphorylation state of other parasite proteins that are exported to the erythrocyte membrane, thereby controlling their function. The incorporation of parasite phosphoproteins such as *P. falciparum* skeleton binding protein 1 (*Pf*SBP1), RESA and MESA into the host cell membrane will lead to organisational changes of erythrocyte membrane proteins (Maier *et al.*, 2009).

RESA is stored in dense granules of the merozoite and is one of the first proteins trafficked to the erythrocyte membrane where it interacts with β -spectrin (Pei *et al.*, 2007). RESA is found in all strains of *Plasmodium* and is thought to be essential for parasite survival in its host cell (Maier *et al.*, 2009). MESA interacts with a 51-amino acid sequence of protein 4.1 which interferes with its binding to p55 and glycophorin C thereby disrupting the formation of the ternary complex (Waller *et al.*, 2003). MESA has also been documented to interact with band 3 and the Rh protein.

KHARP binds to α -spectrin and to the cytoplasmic domain of *Pf*EMP1 (An and Mohandas, 2010). The binding affinity between *Pf*EMP1 and KHARP is enhanced by the phosphorylation of the cytoplasmic domain of *Pf*EMP1 by erythrocyte casein kinase II (Hora *et al.*, 2009). Phosphoproteins such as *Pf*EMP1 are inserted into the host cell membrane skeleton and this is facilitated by *Pf*SBP1, which is a protein associated with the Maurer's clefts. (Cooke *et al.*, 2006, Maier *et al.*, 2009). *Pf*EMP3 forms an interaction with the C-terminal domain of α -spectrin. This interaction leads to destabilisation of the spectrin-actin-protein 4.1 junctional complex and decreases the stability of the erythrocyte membrane skeleton thereby enabling the release of merozoites from infected erythrocytes (Maier *et al.*, 2009).

An increase in the extent of phosphorylation of protein 4.1 has been documented in parasitized erythrocytes. Phosphorylation of protein 4.1, presumably by a plasmodial casein kinase (Chishti *et al.*, 1994) resulted in a decrease in rigidity of the erythrocyte membrane skeletal network due to changes in skeletal protein-protein interactions. *Pf*EMP1 interacts with protein 4.1 and disturbs the binding of protein 4.1 to spectrin and actin (Maier *et al.*, 2009), which contributes to the altered mechanical stability and structure of the parasitized erythrocyte membrane.

1.6.3 Kinases as novel drug targets

Cohen (2002) described kinases as the most attractive drug targets of the twenty-first century. One of the reasons for this is that the structure and catalytic mechanism of protein kinases are conserved and small inhibitory molecules can

easily bind to their catalytic core (Gray *et al.*, 1999). The other is that phosphorylation is considered to be one of the most important regulatory mechanisms of cell proliferation, differentiation, migration and homeostasis in all biological systems, including *Plasmodium* parasites (Leroy and Doerig, 2008).

Drug resistance in *P. falciparum* parasites is emerging and greatly hinders the possibility of eradicating malaria. The main focus of many malaria research groups is to identify and characterise novel drug targets that can be used to develop new chemotherapeutic agents. The parasite's pathogenic phase, erythrocytic schizogony, is the primary target phase for these drugs. One of the chemotherapeutic strategies considered by research groups is to interfere with the host-parasite phospho-signalling pathways. The malaria parasite is dependent on its host cell to survive and disrupting the signalling between the intraerythrocytic parasite and its host cell will lead to the death of the parasite (Doerig *et al.*, 2005). Divergence between host cell protein kinases and their signalling pathways and those of the *Plasmodium* parasite has been exploited to design lead compounds that may be used to develop anti-malarial drugs targeting major signalling pathways used by the parasite without influencing host cells (Holten *et al.*, 2003; Merckx *et al.*, 2008a).

The launch of the *P. falciparum* Data Base (PlasmoDB) (Kissinger *et al.*, 2001) and publication of the *P. falciparum* genome in 2002 by Gardner *et al.* made the identification and analysis of possible drug targets easier by providing sufficient *in silico* molecular biology tools to research teams. New approaches for novel drug target discovery against *Plasmodium* parasites include computer-assisted drug design (CADD) and virtual screening (Leroy and Doerig, 2008). Crystallographic data of numerous identified *P. falciparum* protein kinases are not yet available, but *in silico* methods can be carried out to create three dimensional (3D) models of the target molecule using crystal data from a related protein kinase. Quinolines and oxindoles have been identified as inhibitory molecules of *Pfmrk* using this CADD approach and *in silico* virtual screening (Bhattacharjee *et al.*, 2004). The availability of the 3D structure of kinases inferred using 3D-based computerized modelling or experimental X-ray crystallography in conjunction

with enzyme kinetics leads to prompt structure-activity relationship (SAR)-based progression and identification of possible novel drug targets and enzyme inhibitory molecules (Leroy and Doerig, 2008). The potency of these compounds on the protein kinase of interest is tested in *in vitro* assays of enzyme activity and also in live animals infected with viable parasites. The target molecules will then enter clinical trials depending on the outcome of these *in vivo* studies.

The possibility to study protein kinases and their activity *in vitro* has made medium and high-throughput screening for drug targets uncomplicated and easily accessible. A good understanding of the biochemistry of the target candidate is a vital key when choosing and optimising the molecular assay to be used for screening. Conventional drug target screening of protein kinases involves the evaluation of the enzyme's fundamental role in the parasite's asexual life cycle stages (curative drug targets) or in the sexual life cycle stages (transmission-blocking drug targets) (Leroy and Doerig, 2008). Target validation can be achieved by gene knock-out studies where the genomic locus of the protein kinase of interest is removed from the *Plasmodium* genome or inactivated to ascertain whether the enzyme is essential for parasite survival (Balu and Adams, 2007).

The analogue-sensitive kinase allele (ASKA) approach is another strategy used for the *in vivo* validation of protein kinases as possible novel drug targets (Specht and Shokat, 2002). ASKA has also been described as a chemical genetics approach based on biochemically engineering an ATP-binding pocket in the kinase of interest which will allow for the selective binding of a variety of inhibitory molecules without having any effect on the wild type protein kinase. The gatekeeper amino acid with a large side chain is replaced by a smaller residue to create a novel ATP-binding pocket for the binding of large inhibitory molecules which would not be accommodated by the native catalytic binding cleft. The ASKA approach has been used in the investigation of a calcium-dependent kinase 1 inhibitor in *Toxoplasma gondii* (Ojo *et al.*, 2010) and has recently been used to investigate the effects of bumped kinase inhibitors (BKIs) on a recombinant *P. falciparum* kinase (Ojo *et al.*, 2012). BKIs inhibit a protein that is essential for the parasite to transform from gametocytes to sporozoites. Ojo *et al.* (2012)

proved that this BKI protein in *P. falciparum* is calcium-dependent kinase 4 and that it prevents microgametocyte exflagellation.

1.7 Expression of *Plasmodium falciparum* recombinant proteins

The devastating impact of malaria on affected countries fuels the need for new vaccines and drugs. The production of high quality recombinant proteins in vast quantities is important for the essential characterization of malaria proteins used in vaccine and drug development. Various organisms have been used as expression vectors for *Plasmodium* proteins including *Escherichia coli* (Flick *et al.*, 2004; reviewed in Birkholtz *et al.*, 2008), *Saccharomyces cerevisiae* (Miles *et al.*, 2002; reviewed in Birkholtz *et al.*, 2008), baculovirus (Pang *et al.*, 2002; reviewed in Birkholtz *et al.*, 2008), *Dictyostelium discodium* (Van Bemmelen *et al.*, 2000; reviewed in Birkholtz *et al.*, 2008) and *Tetrahymena thermophile* (Peterson *et al.*, 2002). The *Escherichia coli* expression system is most commonly used in *P. falciparum* recombinant protein expression due to the fast and cost effective production of large amounts of recombinant proteins. *Escherichia coli* cells are easily transformed and a vast amount of bacterial expression vectors and host strains are available. The quality of the expressed proteins is however not always of a high standard. Truncated forms of the protein are often expressed or it is expressed as insoluble aggregates in the bacterial cells. It is possible to refold the proteins produced in these inclusion bodies (Singh *et al.*, 2003), but the success rate of refolding all proteins is low.

Major studies conducted by Mehlin *et al.* (2006) and Vedadi *et al.* (2007) tested the expression of >1000 *P. falciparum* genes in bacterial cells. Three hundred thirty seven of these proteins were expressed as insoluble and only 63 proteins were successfully expressed as soluble (Mehlin *et al.* 2006). Eukaryotic expression systems are known to be more successful than prokaryotic expression systems for parasite proteins. Seventeen genes which expressed as insoluble proteins in prokaryotic *Escherichia coli* were expressed in the eukaryotic Baculovirus Sf-21 system, but only seven were soluble (Mehlin *et al.*, 2006).

There is a closer phylogenetic relationship between the host insect cell and the parasite and crucial post-translational modifications including glycosylation and acetylation, proteolytic activity, sub-cellular arrangement, the potential to form disulfide bonds and secretion pathways are active in insect cells (Makrides, 1996). Recombinant proteins expressed using the baculovirus system may be folded correctly but not all proteins are successfully expressed since some may have a toxic effect on the insect cells. Heterologous expression of *P. falciparum* proteins is challenging due to various factors ranging from the AT-rich genome where the genes have lengthy stretches of adenosines and thymidines; different codon usage; unique glycosylation patterns (Gowda and Davidson, 1999) and larger proteins compared to homologues in other parasite species (Arawind *et al.*, 2003) and other eukaryotes. The *Plasmodium falciparum* genome also codes for recurrent lysine-arginine repeats which have been proposed to cause early translation termination resulting in difficult protein expression in bacterial cells (Flick *et al.*, 2004). Some of the methods that have been explored to overcome these challenges include the use of plasmids or bacterial host cells equipped with tRNA that will identify rare codons (Baca and Hol, 2000). Despite current approaches to increase the success rate, the *P. falciparum* proteins remain difficult to express (Fernandez-Robledo and Vasta, 2010).

PROJECT OBJECTIVES

The aim of this project is to analyse the biochemical properties of *Plasmodium falciparum* PfB0150c. In the latest version of PlasmoDB (version 9.3, 11 March 2013) the gene has been renamed as PF3D7_0203100, but for the purpose of this study the original nomenclature will be used. The gene is situated on chromosome 2 of the malaria parasite and codes for a protein kinase, denoted PfPK8. Characterization of this enzyme will be achieved by:

- * culturing *P. falciparum* 3D7 strain parasites,
- * extracting genomic DNA from the parasites,
- * amplifying PfB0150c using PCR,
- * cloning of PfB0150c into a pTri-Ex-3 expression vector,
- * transforming *Escherichia coli* cells with the recombinant PfB0150c-pTriEx-3 plasmid,
- * retransforming *Escherichia coli* cells with a recombinant pGEX-4T-2-PfB0150c plasmid,
- * expressing the recombinant PfPK8 in *Escherichia coli* cells,
- * create recombinant baculovirus-particles with the PfB0150c-pTriEx-3 plasmid and baculovirus DNA,
- * co-transfect Sf9 insect cells with baculovirus recombinants and induce these cells to express the recombinant PfPK8,
- * purifying and analysing the recombinant PfPK8 protein,
- * performing enzyme assays using the purified protein, and
- * extracting red blood cell membrane proteins (RBCM proteins) from whole blood samples to investigate protein-protein interactions of PfPK8 with RBC membrane proteins.

2 MATERIALS AND METHODS

All *P. falciparum* 3D7 and *Spodoptera frugiperda* (Sf9) cell culturing procedures were performed under sterile conditions in a laminar flow hood. Solutions used in this study are listed in the Appendix and were prepared with Milli-Q water from the Milli-QTM Water System (Millipore Corporation, Bedford, USA) and autoclaved where necessary.

2.1 *Plasmodium falciparum* culturing techniques

Parasite culture preparation from a frozen stock

Plasmodium falciparum 3D7 strain parasites were cultured according to the method described by Trager and Jensen (1976). The cryo-preserved parasite suspension was thawed at 37°C and transferred to sterile 15ml Falcon tubes (Thermo Scientific, South Africa). For each ml of cell suspension, 100µl of 12% NaCl solution was carefully added while swirling the tube. The suspension was left for 5 minutes at room temperature after which 9 volumes of 1.6% NaCl were added and the solution was gently mixed. The supernatant was removed after centrifugation at 500xg for 10 minutes at 4°C in an Eppendorf centrifuge 5702R (Eppendorf, Germany). Freshly washed erythrocytes (section 2.1.3) were added to obtain a haematocrit of 5% in a final volume of 15ml made up with fresh complete medium supplemented with 20% plasma. The suspension was transferred to a 50ml flat culture flask (NuncTM, Denmark) and gassed for 45 seconds with a gas mixture consisting of 5.5% CO₂, 2.75% O₂ and 91.25% N₂ (African Oxygen Ltd., South Africa). The culture flask was closed tightly and incubated at 37°C for 24hrs. Complete medium supplemented with 20% plasma was used for the initial 7 days of culturing to initiate parasite growth. Continuous stock cultures were maintained as described in section 2.1.5.

2.1.2 Heat inactivation of plasma

Blood donated by the South African Blood Bank was collected in acid citrate dextrose (ACD) tubes (Becton Dickinson Biosciences, USA) and centrifuged at

750xg for 10 minutes at 4°C in an Eppendorf centrifuge 5702R. The plasma was sterilely removed and placed in a 50ml sterile Falcon tube and heat inactivated at 56°C by incubating it for 2 hours in a waterbath. The heat inactivated plasma was centrifuged at 750xg for 10 minutes at 20°C. The clear supernatant was aliquoted into 10ml aliquots in 15ml sterile Falcon tubes in a laminar flow hood and stored at -70°C. The plasma was heat inactivated because plasma from healthy humans can cause lysis of *Plasmodium falciparum* infected erythrocytes *in vitro* via complement-mediated lysis of cells bound with immunoglobulin (Turrini *et al.*, 1992). The plasma is thus heat inactivated to destroy complement, thus reducing the growth-inhibitory activity of normal plasma.

2.1.3 Erythrocyte preparation

Fresh blood was collected in ACD tubes and centrifuged at 1000xg for 15 minutes at 4°C in a MSE Coolspin centrifuge (*Fisons Scientific, UK*). The plasma and buffy coat were sterilely removed. The erythrocytes were washed twice by adding 2 volumes of sterile phosphate buffered saline (PBS). After mixing, the suspension was centrifuged at 400xg for 10 minutes at 4°C. The washed erythrocytes were resuspended in 1 volume of incomplete medium and stored at 4°C in sterile 15ml Falcon tubes for a maximum of 7 days after which the cells were discarded.

2.1.4 Preparation of smears and calculating parasitaemia

A blood smear of the culture was made on a daily basis to assess the state of the culture. The culture flask was gently tilted at a 60° angle to expose the parasitised red blood cells (pRBCs) at the bottom of the flask. A drop of the pRBCs was placed onto a microscope slide using a glass Pasteur pipette and a thin blood smear was made. After the smear has dried the cells were fixed with methanol for 5 seconds and stained using the Rapindiff Staining Kit (*Global Diagnostics, South Africa*). After rinsing the slide with water it was allowed to air dry and viewed under a microscope (*Zeiss Axiostar, Germany*) using a 1000x magnification and mineral oil.

The thin blood smear was used to study ten fields of vision. The number of infected and uninfected erythrocytes was counted in each field. An average % parasitaemia in each field was calculated using the following formula:

$$\% \text{ Parasitaemia} = (\text{number of infected cells} / \text{total number of cells}) \times 100$$

2.1.5 Culture maintenance

Cultures should be maintained at 5 - 10% parasitaemia. The culture flask was gently tilted at an angle of 60°C and the old medium was sterilely removed every 24 hours in a laminar flow hood using a glass Pasteur pipette and a vacuum pump. A volume of 15ml fresh complete medium (containing 10% plasma) was pre-warmed to 37°C and added to the 50ml culture flask. The flask was then gassed (section 2.1.1) and the culture was incubated at 37°C. For continuous stock cultures, fresh erythrocytes were added every 2 – 4 days to maintain 5 - 10% parasitaemia and 5% haematocrit.

2.1.6 Dividing the culture

A culture was divided when the parasitaemia exceeded 10% or when the majority of pRBCs were used for parasite deoxyribonucleic acid (DNA) extraction and a culture stock flask had to be maintained. Complete medium (12ml) and 3ml parasitised red blood cell suspension were sterilely added to a 50ml culture flask. Washed erythrocytes were added to the flask to obtain a final haematocrit of 5% and a final parasitaemia of approximately 2%. The flask was gassed and incubated as described in section 2.1.1.

2.1.7 Culture synchronisation

Sorbitol treatment according to the method of Lambros and Vanderberg (1979) was used to synchronise the culture. The method is based on the increased permeability of the erythrocyte membrane to take up this sugar alcohol when infected with mature stage parasites. In an isotonic solution, schizont- and trophozoite- infected erythrocytes will continuously import sorbitol via parasite-induced channels which produces an osmotic imbalance within the cell. This in turn leads to a continuous influx of water into the cell causing cell lysis and the

selective removal of mature stage parasites. Immature ring stage forms do not cause an increase in permeability.

A thin blood smear was made of the culture prior to synchronisation to determine whether the parasitaemia was approximately 10% and if the parasites were mainly in the early ring stage. The culture was sterilely transferred to a 50ml Falcon tube and centrifuged at 1000xg for 5 minutes at 20°C in an Eppendorf centrifuge 5702R. The supernatant was removed and the pellet was resuspended in 10 volumes of 5% D-sorbitol (*Sigma-Aldrich Corporation, USA*). The suspension was left at room temperature for 20 minutes. Thereafter it was centrifuged at 250xg for 5 minutes at 20°C and the supernatant was removed. The pellet was resuspended in 15ml complete medium and transferred to a 50ml culture flask. The flask was gassed (section 2.1.1) and the culture was incubated at 37°C.

2.1.8 Preparation of parasite stock suspension for long term storage

A ring stage culture at approximately 10% parasitaemia was centrifuged for 5 minutes at 250xg at 20°C in an Eppendorf centrifuge 5702R. The packed cells were resuspended in a 1:1 ratio with 60% glycerol/PBS (v/v). 1ml of the cell suspension was aliquoted into sterile cryo-tubes (*NuncTM, Denmark*) and placed in liquid nitrogen for storage.

2.2 Cloning

2.2.1 *Plasmodium falciparum* DNA extraction

DNA was isolated from a culture with late stage parasites (trophozoites and/or schizonts) using the method described by Schlichterle *et al.* (2000). The content of a medium culture flask (50ml) containing 15ml *P. falciparum* culture at 8-10% parasitaemia was transferred to a sterile 50ml Falcon tube. The cells were pelleted by centrifugation at 1 000xg for 5 minutes at 4°C in an Eppendorf 5702R centrifuge. The supernatant was carefully discarded and the parasitised red blood cell (pRBC) pellet washed once by resuspending it in 20ml phosphate buffered saline (PBS, pH 7.4) and centrifuging at 1 000xg for 5 minutes at 4°C. The

supernatant was discarded. Ten microlitres 5% saponin (final concentration of 0.05%) (*USB Corporation, USA*) was added to the washed pRBC pellet and made up to a final volume of 1ml using PBS. The solution was mixed by inverting the tube a few times and incubated for 5 minutes at room temperature to lyse the RBCs. The parasites were pelleted via centrifugation at 1 000xg for 5 minutes at 4°C. After discarding the supernatant the parasites were washed by vortexing them in 50ml PBS and centrifugation at 1 000xg for 5 minutes at 4°C. The wash step was repeated twice until the supernatant was clear. The cell pellet was resuspended in 1ml lysis solution supplemented with PCR grade recombinant Proteinase-K (*Roche Applied Science, Germany*) to obtain a final concentration of 0.1mM. Proteinase K is a broad-spectrum serine protease and is stable over a wide pH range (4 – 12) (Hilz *et al.*, 1975), making it useful during nucleic acid extraction. Proteinase K is used in DNA extractions to digest contaminating proteins and prokaryotic or eukaryotic nucleases which may otherwise degrade DNA. The lysed parasite suspension was incubated at 37°C for 3 hours in a waterbath with occasional mixing to promote parasite lysis. The suspension was then aspirated with a syringe and 21 gauge needle to ensure that parasites were completely lysed for maximal DNA isolation. After the incubation step, DNA was extracted with phenol followed by ethanol precipitation. The phenol used had a pH of 8.2 and was saturated with 10mM Tris (pH 8.0) and 1mM EDTA. A 1ml volume of a 1:1 ratio of Tris-buffered phenol (*Sigma-Aldrich In.c, USA*) and chloroform (*Saarchem, South Africa*) solution was added. The sample was transferred to a 2ml Eppendorf tube and centrifuged at 18 000xg for 5 minutes at 4°C using an Eppendorf 5415R centrifuge (*Eppendorf, Germany*). The solution separated into 3 layers: the top aqueous phase containing the DNA, a white protein band at the interface and the bottom organic phase containing RNA. Approximately 80% of the aqueous phase was carefully transferred to a 1.5ml Eppendorf tube. DNA recovery was maximized by adding 100µl TE buffer (pH 8.0) to the remaining organic phase, mixing thoroughly by inversion, and centrifuging at 18 000xg for 5 minutes at 4°C. The aqueous phase was pooled with the previous one and kept on ice. RNase A (10µl) (*Fermentas, Europe*), supplied in 50mM Tris-HCl (pH 7.4) and 50% glycerol (*Saarchem, South Africa*)

was added per ml of aqueous phase to a final concentration of 100µg/ml. RNase A is a pancreatic enzyme that cleaves single stranded RNA. The sample was incubated at 37°C for 30 minutes. The phenol/chloroform extraction was repeated, followed by extraction with an equal volume of chloroform. After mixing by inversion, the solution was centrifuged at 18 000xg for 5 minutes at 4°C. The aqueous phase was carefully removed and 1:10 (v/v) 3M sodium acetate (pH 5.2) and 2.5 volumes (v/v) of ice-cold 100% ethanol were added. The DNA from the aqueous phase was allowed to precipitate at -70°C for 30 minutes. The precipitated DNA was collected by centrifuging the sample at 18 000xg for 30 minutes at 4°C. The supernatant was carefully removed not to disturb the DNA pellet and 1ml ice-cold 70% ethanol was added to the pellet and centrifuged at 18 000xg for 5 minutes at 4°C. The supernatant was discarded and the DNA pellet air dried at room temperature for 10 - 15 minutes to allow residual ethanol to evaporate. The DNA pellet was dissolved in 30µl nuclease-free water (*Promega, USA*) and stored in aliquots at -20°C.

2.2.2 Determination of DNA concentration, purity and integrity

The concentration of the extracted DNA sample was determined using a Nanodrop-ND 1000 spectrophotometer (*Nanodrop Technologies Inc, USA*) where a modified version of the Beer-Lambert equation is employed to correlate the calculated absorbance with the nucleic acid concentration.

The equation used is as follows:

$$c = (A \times E) / b \\ = (A \times 50) / 1$$

Where: c = the nucleic acid concentration (ng/µl)
 A = the absorbance in absorbance units (AU) at 260nm
 E = wavelength-dependent extinction co-efficient of 1µg/ml double stranded DNA (ng-cm/ml)
 b = the pathlength (cm)

The purity of the DNA was determined using the ratio of sample absorbance at 260nm and 280nm. A ratio of ~ 1.8 indicated pure DNA, whereas a ratio <1.8

was an indication that protein, ethanol or other contaminants that absorb light strongly at or near 280nm were present in the sample.

The DNA integrity was determined by agarose gel electrophoresis. A 0.8% agarose mini-gel was cast in a horizontal mini-gel kit model # MGU-200T (CBS Scientific, USA) and electrophoresed for 1 hour at 100V using an EPS 301 power supply (Amersham Pharmacia Biotech, Sweden) in 1x TAE buffer at room temperature. The gel was made using D-1 LE agarose (Hispanagar, Spain) in 50ml 1x TAE buffer and 2.5µl ethidium bromide (10µg/µl) (Sigma-Aldrich Inc., USA) was added to the gel solution before casting. Due to the intercalation of ethidium bromide between the nucleic acid base pairs and its UV fluorescence characteristics, the DNA was visualized and photographed under UV light using GeneSnap version 6.05 image acquisition software (Syngene, UK).

2.2.3 The polymerase chain reaction (PCR)

2.2.3.1 Primer design for amplification of the catalytic domain of PfB0150c

Sequence information of the gene (*PfB0150c*) encoding *P. falciparum* protein kinase 8 (*PfPK8*) was obtained from the *Plasmodium* genome database (*PlasmoDB* version 8.1, 2011). The DNA sequence of *PfB0150c* was used to design primers specific for the catalytic domain of the enzyme using Gene Runner Version 3.05 (Hastings Software Inc, 1994). Restriction sites for the restriction endonucleases *Bam*HI and *Xho*I were incorporated into the 5' end of the primers to facilitate the ligation of the amplified catalytic domain of *PfB0150c* into the pTriEx-3 expression vector (Novagen, USA) (refer to Appendix section 7.3.6 for the vector map). The primers were analysed using Integrated DNA Technologies SciTools Oligo Analyzer 3.0 (www.idtdna.com) to ensure that no primer dimers and hairpins would form during amplification. Inqaba Biotech (South Africa) synthesized the primers and they were received in lyophilised form. The primers were reconstituted according to manufacturer's recommendations using nuclease free water to a final concentration of 100µM and stored in aliquots at -20°C. A working stock of 10µM was prepared from the 100µM stock and stored at -20°C.

The following primers were used to amplify the kinase domain of *Pf*B0150c with a size of 1 507bp:

Forward primer (with an incorporated *Bam*HI recognition site)

5'- **CGC** **G↓GA TCC** **T**GGA TGA AAA GGA TGG ATA TG -3'

Reverse primer (with an incorporated *Xho*I recognition site)

5'- **CCG** **C↓TC GAG** TTT CTG GGA TTG TTC AGT C -3'

The bases in bold indicate the extra bases added to facilitate enzyme binding and activity at the site of cleavage. The recognition sites for the endonucleases are underlined and the arrow indicates the exact cleavage site. An extra base (purple) was added to the forward primer to ensure that the codons were in frame.

2.2.3.2 Amplification of the functional region of *Pf*B0150c

The optimal annealing temperature, primer and DNA template concentration for maximal amplification of the target were determined empirically using a GoTaq® Green Master Mix (*Promega, USA*). The reaction mixtures were prepared as indicated in Table 2.

Table 2: PCR reaction mixture using the GoTaq® Green Master Mix PCR system.

Component	Volume (µl)	Final concentration
GoTaq® Green Master Mix (2x)	12.5	1x
<i>Pf</i> B0150c forward primer (10µM)	0.25 – 2.5	0.1 - 1µM
<i>Pf</i> B0150c reverse primer (10µM)	0.25 – 2.5	0.1 - 1µM
<i>P. falciparum</i> genomic DNA	1 - 5	~ 100ng
Nuclease-free water to a final volume of 25µl	x	-

The target sequence was amplified in an Eppendorf Mastercycler® Gradient machine (*Eppendorf, Germany*) with a lid pre-heated to 95°C. A two-step PCR was performed using two successive annealing temperatures for the amplicon. A range of annealing temperatures was tested less than 8°C of the calculated T_m (for the 1st annealing temperature) or the T_m given by the primer manufacturer (for the

2nd annealing temperature) to determine the optimal conditions to yield a maximum amount of product.

The T_m for the *P. falciparum* section of the primer sequence was calculated using the following formula:

$$T_m (^{\circ}\text{C}) = 4(nG+nC) + 2(nA+nT)$$

Where T_m = melting temperature of sequence

n = number of bases

The formula above is not accurate for primers >20 bases (McPherson and Moller; 2006) and therefore the T_m supplied by the manufacturer was used for the complete primer sequence to determine the 2nd annealing temperature.

The following cycling conditions yielded the maximum amplified product and were used in subsequent PCR experiments:

5 cycles

Initial denaturation: 94°C, 2 minutes
Denaturation: 94°C, 1 minute
Annealing: 54°C, 1 minute
Extension: 68°C, 2 minutes

29 cycles

Second annealing: 60°C, 1 minute
Extension: 68°C, 2 minutes
Final extension: 68°C, 7 minutes

The Expand High Fidelity^{PLUS} PCR system (*Fermentas, Europe*) was used in the final PCR using the optimised primer concentrations, DNA template concentration and cycling conditions. The preparation of the PCR reaction mixture is described in Table 3 and the PCR was performed in duplicate.

Table 3: Preparation of the PCR reaction mixture using the Expand High Fidelity PLUS PCR system.

Component	Volume (µl)	Final Concentration
Expand High Fidelity ^{PLUS} reaction buffer (5x) with 7.5mM MgCl ₂	10	1.5mM MgCl ₂
Deoxyribonucleotide (dNTP) mix (2.5mM)	1	200µM
<i>Pf</i> B0150c forward primer (10µM)	2	0.4µM
<i>Pf</i> B0150c reverse primer (10µM)	2	0.4µM
Expand High Fidelity ^{PLUS} enzyme mix	0.5	2.5U
<i>P. falciparum</i> genomic DNA (200ng/µl)	0.6	125ng
Nuclease-free water	34.1	-

The PCR amplicons were analysed by agarose gel electrophoresis as previously described (section 2.2.2) to verify that the insert size was correct.

2.2.3.3 Purification of the PCR product

The PCR amplicons were purified using Qiaquick PCR Purification Kit (*Qiagen, USA*). This purification system combines spin-column technology with the selective binding properties of a silica membrane. DNA binds to the silica membrane in the presence of high concentrations of salt while contaminants pass through the column. The binding buffer provided the correct salt-concentration and pH for binding of DNA to the column membrane. The pure DNA can be eluted with nuclease-free water.

Five volumes of kit buffer PBI (binding buffer) were added to 1 volume of the PCR product. The colour of the solution should be yellow (similar to the colour of buffer PBI) as this is indicative of the optimal pH (pH 7.5) for DNA binding to the column membrane. If the colour is orange/violet then 10µl of 3M sodium acetate (pH 5.2) should be added. The solution with the correct pH was added to a min-elute column inside an Eppendorf tube and centrifuged for 1 minute at 18 000xg at room temperature using an Eppendorf 5415R centrifuge. During this DNA binding step, the DNA bound to the silica membrane and unwanted primers

and impurities, such as salts, enzymes and un-incorporated nucleotides were discarded with the flow-through. The column was washed by adding 750µl of ethanol-containing kit buffer PE (wash buffer) to the column and centrifuging it for 1 minute at 18 000xg at room temperature. The column was centrifuged for an additional 1 minute to remove residual ethanol present on the column which may interfere with subsequent enzymatic reactions. The DNA was eluted by adding 10µl nuclease-free water to the centre of the column membrane as elution is most efficient under hypotonic conditions and low salt concentrations. The column was left to stand for 1 minute and centrifuged for 1 minute at 18 000xg at room temperature.

The concentration, purity and integrity of the DNA were analysed as previously described (section 2.2.2). The purified PCR amplicons were pooled and stored in aliquots at -20°C.

2.2.4 Cloning of *PfB0150c* into the pTriEx-3 expression vector

2.2.4.1 Restriction enzyme digestion of the PCR product *PfB0150c*

Fermentas Fast Digest[®] (*Fermentas, Europe*) endonucleases were used to carry out double enzyme digests on the purified PCR amplicon. A 30µl reaction was prepared as described in Table 4 and incubated for 30 minutes in a waterbath at 37°C. The digested product was purified using the Qiaquick PCR product purification kit as described in section 2.2.3.3. Using a Nanodrop ND-1000 spectrophotometer the concentration of the digested product was determined.

Table 4: Preparation of a 30µl Fermentas Fast Digest[®] restriction enzyme mixture utilizing *Bam*HI and *Xho*I endonucleases.

Component	Volume (µl)	Final concentration
Nuclease-free water	20.1	-
10x Fast Digest [®] buffer	3	1x
<i>PfB0150c</i> DNA	2.9	~ 1.5µg
<i>Xho</i> I	2	2U
<i>Bam</i> HI	2	2U

2.2.4.2 pTriEx-3 expression vector preparation

pTriEx-3 plasmid (*Novagen, USA*) DNA was extracted from Subcloning EfficiencyTM DH5 α TM chemically competent cells (*Invitrogen, USA*) (refer to Appendix section 7.3.6.2 for the vector map) using the GenElute Plasmid Miniprep Kit (*Sigma-Aldrich Inc., USA*) according to the manufacturer's protocol.

Plasmid extraction using this kit employs SDS-based lysis of the *Eschericia coli* cells, followed by the adsorption of plasmid DNA onto silica in the presence of high salt concentrations. The plasmid DNA is finally eluted from the silica in a spin-wash step which also removes contaminants.

A 10ml DH5 α bacterial culture was prepared in a 50ml sterile Erlenmeyer flask by inoculating 10ml of Luria-Bertani broth (LB medium) (Bertani, 1951) with 50 μ l DH5 α pTriEx-3 glycerol stock. The LB medium contains nutrients and a buffer to provide the optimum growth conditions for the bacterial cells. The cultures were incubated at 37°C for 24 hours in an orbital shaker. Cultures with an optical density at 600nm of between 0.2 and 0.4 were used in downstream experiments. The cultures were divided into 2ml Eppendorf tubes and the cells pelleted via centrifugation at 18 000xg for 1 minute in an Eppendorf 5415R centrifuge at room temperature. After discarding the supernatant, the cell pellets were completely resuspended in 200 μ l kit Resuspension Solution until homogenous. The cells were lysed by adding 200 μ l kit Lysis Solution and mixed gently immediately. The cell debris was precipitated by the addition of 350 μ l kit Neutralization/Binding Solution and inverting the tubes a few times. Centrifugation at 18 000xg for 10 minutes at room temperature ensured that unwanted cell debris, proteins, lipids and chromosomal DNA formed a viscous precipitate. A GenElute Miniprep Binding Column (*Sigma-Aldrich Inc, USA*) was prepared by inserting a column into a microcentrifuge tube and adding 500 μ l kit Column Preparation Solution followed by centrifugation at 18 000xg for 1 minute. The cleared lysate was added to the prepared column and centrifuged at 18 000xg for 1 minute. The column was washed by adding 750 μ l of the diluted kit Wash Solution to the column and centrifuged at 18 000xg for 1 minute. This wash step removed all residual salt and other contaminants possibly introduced

while loading the column. The flow-through liquid was discarded and the column centrifuged at 18 000xg for 2 minutes to remove excess ethanol. After transferring the column to another collection tube, 100µl of 5mM Tris-HCl pH 8 was added and centrifuged at 18 000xg for 1 minute to elute the plasmid DNA from the column. The plasmid DNA was spectrophotometrically analysed using a Nanodrop-ND 1000 spectrophotometer followed by agarose gel electrophoresis (section 2.2.2). Aliquots of the extracted plasmid DNA were stored at -20°C.

2.2.4.3 Restriction digestion of pTriEx-3 plasmid

Extracted pTriEx-3 plasmid DNA was digested with Fermentas FastDigest® restriction enzymes. *Bam*HI and *Xho*I were used to perform a simultaneous double enzyme digest on the purified pTriEx-3 plasmid. A 60µl reaction mixture was prepared as described in Table 5 and incubated for 1 hour in a waterbath at 37°C. Thermo-sensitive fast alkaline phosphatase (*Roche Applied Science, Germany*) was added to the reaction mixture to prevent self-ligation of the digested plasmid. The integrity of the digested plasmid DNA was determined by agarose gel electrophoresis (section 2.2.2). The digested product was stored at -20°C.

Table 5: Preparation of a 60µl Fermentas Fast Digest® restriction enzyme mixture utilizing *Bam*HI and *Xho*I endonucleases to digest pTriEx-3 plasmid DNA.

Component	Volume (µl)	Final concentration
Nuclease-free water	8	-
10x Fast Digest® buffer	6	1x
pTriEx-3 DNA	40	~ 2µg
<i>Xho</i> I	2	2U
<i>Bam</i> HI	2	2U
Thermo-sensitive fast alkaline phosphatase	2	2U

2.2.4.4 Ligation of amplicons into pTriEx-3 plasmid

The Rapid DNA Ligation Kit (*Roche Applied Science, Germany*) was used to ligate the *Pf*B0150c (1 507bp) insert DNA to the pTriEx-3 (5 082bp) expression

vector resulting in a recombinant *PfB0150c*-pTriEx-3 plasmid with a size of 6 589bp.

The digested PCR product and pTriEx-3 vector DNA were electrophoresed on a 0.8% agarose gel (section 2.2.2) next to a DNA mass ladder to quantitate the DNA on a Geldoc SynGene GeneGenius gel documentation system (*Syngene, UK*) using SynGene GeneTools version 4.0 analysis software (*Syngene, UK*).

The 4:1 molar ratio of insert DNA to plasmid DNA needed for optimal ligation was calculated using the In-Fusion™ Molar Ratio Calculator (*Clontech Bioinformatics, USA*, <http://bioinfo.clontech.com/infusion/molarRatio.do>). The following reaction mixtures were prepared in separate PCR tubes:

Table 6: Ligation reaction mixtures.

Component	Amount
<i>PfB0150c</i> (130ng/μl)	89ng
pTriEx-3 (90ng/μl)	75ng
5x DNA Dilution Buffer	2μl
Nuclease free water	5.3μl
2x T4 DNA Ligation Buffer	10μl
T4 DNA Ligase	1μl

The samples were incubated for 30 minutes at 16°C in a pre-cooled thermocycler. The T4 DNA ligase was inactivated by incubation at 70°C for 10 minutes. The pTriEx-3 vector, *PfB0150c* insert, ligation product (*PfB0150c*-pTriEx-3) and negative control (pTriEx-3) were electrophoresed on a 0.8% agarose gel (section 2.2.2) to determine the success of the ligation step.

2.2.4.5 Transformation of competent DH5α bacterial cells with recombinant pTriEx-3 plasmid

Two 50μl aliquots of Subcloning Efficiency™ DH5α™ chemically competent cells were thawed on ice. Two transformation reactions were set up, one using the *PfB0150c*-pTriEx-3 construct and the other as a control with only the pTriEx-3

plasmid. Five microlitres of each ligation reaction was added to the thawed competent DH5 α cells. The plasmid-cell suspensions were incubated on ice for 30 minutes followed by a 20 second heat shock at 42°C and then the suspensions were placed on ice for 2 minutes. The chemically competent cells are more permeable to foreign DNA. A short exposure to heat is thought to create a thermal imbalance on either side of the cell membrane due to the lipid rearrangement of the membrane. This forces the DNA to enter the cells either through cell pores or the damaged cell wall (Hanahan, 1983).

Five hundred microlitres of LB media was added and the suspensions were placed in an orbital shaker for 1 hour at 37°C. Fifty microlitre aliquots of the recombinant *PfB0150c*-pTriEx-3 and the pTriEx-3 cell suspension were sterilely spread onto two separate agar culture plates supplemented with ampicillin (refer to Appendix section 7.1.3). The plates were inverted after spreading and placed in an incubator set to 37°C overnight. The plasmid contains an ampicillin resistance gene and this was used as a selectable marker. Only plasmid-bearing bacterial colonies were able to proliferate on the plates.

2.2.4.6 PCR screening of DH5 α colonies post transformation

Colony screening of transformed DH5 α cells was done to determine which colonies contained the recombinant *PfB0150c*-pTriEx-3 plasmid construct or the pTriEx-3 control plasmid. Three colonies were sterilely picked from the *PfB0150c*-pTriEx-3 culture plate and 1 colony picked from the pTriEx-3 control plate using a pipette and resuspended in 10 μ l nuclease free water. Five microlitres of the bacterial cell suspension were lysed by heating at 95°C for 5 minutes in an Eppendorf Mastercycler[®] Gradient machine. Twenty five microlitre PCR reaction mixtures for each picked colony and a no DNA control were set up in PCR tubes using primers specific for the cloned region of *PfB0150c* as follows:

Table 7: PCR reaction mixture for screening *Escherichia coli* colonies.

Component	Colony DNA	No DNA control
GoTaq® Green Master Mix (2x)	12.5µl	12.5µl
<i>Pf</i> B0150c forward primer [10µM]	1µl	1µl
<i>Pf</i> B0150c reverse primer [10µM]	1µl	1µl
DH5α bacterial cell suspension	5µl	-
Nuclease-free water	5.5µl	10.5µl

The target sequence was amplified in an Eppendorf Mastercycler® Gradient machine with a lid pre-heated to 95°C.

The following cycling conditions were used:

29 Cycles

Initial denaturation: 94°C, 2 minutes
Denaturation: 94°C, 1 minute
Annealing: 60°C, 1 minute
Extension: 68°C, 2 minutes
Final extension: 72°C, 7 minutes

The PCR products were resolved on a 0.8% agarose gel (section 2.2.2) to determine which colonies contained the recombinant *Pf*B0150c-pTriEx-3 plasmid.

The remaining 5µl of the positive colony cell suspensions were placed in separate 10ml BD Falcon™ round bottom growth tubes with 2ml LB medium and 20µl ampicillin (100µg/µl). The tubes were placed in an orbital shaker and the cells allowed to proliferate overnight at 37°C. Glycerol stock solutions of the positive colonies were made by adding 500µl of the overnight DH5α cell growths to 500µl 60% sterile glycerol. The glycerol stocks were stored at -70°C. The remaining cell cultures were used to extract recombinant *Pf*B0150c-pTriEx-3 plasmid and pTriEx-3 control plasmid using the GenElute Plasmid Miniprep Kit as previously described (section 2.2.4.2). The plasmid DNA concentrations were determined (section 2.2.2) and digestion with *Bam*HI and *Xho*I (section 2.2.4.3) followed by agarose gel electrophoresis (section 2.2.2) to confirm the presence of the

PfB0150c insert. A positive colony containing the *PfB0150c* insert was sequenced (section 2.2.5).

2.2.4.7 Transformation of Rosetta 2 (DE3) cells and analysis of the recombinant *PfB0150c*-pTriEx-3 plasmid

Rosetta 2 cells were transformed with the recombinant *PfB0150c*-pTriEx-3 and control pTriEx-3 plasmids as described previously (section 2.2.4.5). A *PfB0150c*-pTriEx-3 plasmid with no errors in the kinase domain was used for the transformation.

Three 20µl aliquots of Rosetta 2 (DE3) cells (*Novagen, USA*) stored at -70°C were thawed on ice. One of these was used as a transformation negative control with no added plasmid DNA. Two hundred nanograms of the extracted *PfB0150c*-pTriEx-3 plasmid DNA (section 2.2.4.2) was added to one of the 20µl aliquots and 200ng of the control pTriEx-3 plasmid DNA was added to the other. The cell suspensions were mixed by inversion and incubated at 4°C for 30 minutes followed by a heat shock step at 42°C for 30 seconds. The suspensions were then immediately incubated at 4°C for 2 minutes. Five hundred microlitre LB medium was added to each tube and the cells were allowed to grow in an orbital shaker at 37°C for an hour. Fifty microlitres of each cell suspension was sterilely spread on separate agar plates (refer to Appendix section 7.1.3) supplemented with ampicillin (100µg/ml) (*Roche Applied Science, Germany*) and chloramphenicol (50µg/ml) (*Sigma-Aldrich Inc., USA*). The TriEx-3 plasmid has resistance genes against ampicillin and Rosetta 2 (DE3) cells have an extra plasmid harbouring a resistance gene against chloramphenicol, therefore only transformed Rosetta 2 (DE3) cells will grow on the plate.

2.2.5 Recombinant *PfB0150c*-pTriEx-3 plasmid DNA sequencing

A positive *Escherichia coli* DH5α colony containing the *PfB0150c* insert was sequenced (section 2.2.4.6). Automated fluorescence-based cycle sequencing was performed using the ABI BigDye® v1.1 Terminator Cycle sequencing kit (*Applied Biosystems Inc., South Africa*). This sequencing method is based on Sanger sequencing but uses fluorescent dyes to label the extension products unlike the

original Sanger sequencing method which utilizes a radioactive material as a product label (Sanger *et al.*, 1974).

A twenty microlitre BigDye® terminator sequencing reaction mixture was set up using the forward and reverse primer for *PfB0150c* (section 2.2.3.2).

Table 8: Preparation of the BigDye® terminator sequencing reaction mixtures.

Component	Volume (µl)	Final concentration
Recombinant <i>PfB0150c</i> -pTriEx-3 plasmid DNA	8.4µl	500ng
2.5x Ready reaction Pre-mix	4µl	1x
5x BigDye sequencing buffer	2µl	1x
Gene specific primer (forward or reverse) (3.2µM)	1µl	3.2pmol
Nuclease-free water	4.6µl	-

The sequencing reactions were performed in a thermocycler under the following conditions:

Initial denaturation: 96°C for 1 minute

Repeat the following for 25 cycles:

96°C, 10 seconds

55°C, 5 seconds

60°C, 4 minutes

The reaction mixture was kept on ice in the dark and sent to the HIV Genotyping Laboratory (NHLS, Charlotte Maxeke Academic Hospital, Johannesburg, South Africa) for sequencing. The sequence chromatograms were analysed using Finch TV version 1.4.0 (Geospiza Inc.).

2.2.6 Retransformation of Rosetta 2 (DE3) cells with recombinant pGEX-4T-2 plasmid

Recombinant plasmid (pGEX-4T-2-*PfB0150c*) (refer to Appendix section 7.3.6.1 for the vector map) containing the functional region of *PfB0150c* was extracted from previously transformed Rosetta 2 (DE3) *Escherichia coli* cells. The pGEX-4T-2 plasmid was used as control. Plasmid DNA was extracted from the cells

using the GenElute Plasmid Miniprep Kit as previously described in section 2.2.4.2.

A 10ml Rosetta 2 (DE3) bacterial culture was prepared by inoculating 10ml of LB medium supplemented with chloramphenicol (50µg/ml) and ampicillin (100µg/ml) with 10µl of pGEX-4T-2-*Pf*B0150c glycerol stock. The plasmid DNA was extracted and analysed using a Nanodrop-ND 1000 spectrophotometer followed by agarose gel electrophoresis (section 2.2.2). Aliquots of the extracted plasmid DNA were stored at -20°C.

Rosetta 2 (DE3) cells were transformed separately with 200ng of the extracted pGEX-4T-2 -*Pf*B0150c or control pGEX-4T-2 plasmid DNA as previously described in section 2.2.4.7. Colony PCR screening (section 2.2.4.6) confirmed the presence of the recombinant pGEX-4T-2-*Pf*B0150c plasmid in the retransformed Rosetta 2 (DE3) cells. Recombinant pGEX-4T-2-*Pf*B0150c and pGEX-4T-2 control plasmid DNA were extracted from overnight growths of transformed Rosetta 2 (DE3) cells. The recombinant plasmid DNA was analysed (section 2.2.2) and stored in aliquots at -20°C.

2.3 Prokaryotic protein expression system

2.3.1 Recombinant *Pf*PK8 protein expression in *Escherichia coli* Rosetta 2 (DE3) cells

Rosetta 2 (DE3) cells are used to express eukaryotic proteins from genes that contain codons rarely used in *Escherichia coli*. This bacterial strain supplies tRNAs driven by their native promoters for codons AUA, AGG, AGA, CUA, CCC, GGA and CGG on a compatible chloramphenicol resistant plasmid (Novy *et al.*, 2001). This makes universal translation possible that would otherwise be limited by the exclusive use of *Escherichia coli* codons (Novagen, Competent Cells, User protocol TB009 Rev. F0104).

Frozen Rosetta 2 (DE3) glycerol stocks containing recombinant pGEX-4T-2-*Pf*B0150c, control plasmid pGEX-4T-2, recombinant *Pf*B0150c-pTriEx-3 and the

control plasmid pTriEx-3 were used to prepare overnight growths. Twenty microlitres of the glycerol stock was sterilely added to 1ml LB medium supplemented with ampicillin (100µg/ml) and chloramphenicol (50µg/ml) in 10ml BD Falcon™ round bottom growth tubes. The cells were allowed to proliferate overnight at 37°C in an orbital shaker. Agar plates (refer to Appendix section 7.1.3) were sterilely streaked with the overnight growths and placed in an incubator set at 37°C overnight. The plates were removed and stored at 4°C.

Overnight growths from colonies were prepared by adding 1 colony scraped from the agar plate with a pipette tip to 1ml LB medium supplemented with ampicillin (100µg/ml) and chloramphenicol (50µg/ml) in a 10ml BD Falcon™ round bottom growth tube. The cells were grown overnight in an orbital shaker at 37°C. The optical density of the cultures was measured at 600nm using a Biomate 5 spectrophotometer (*Thermo Electron Corporation, UK*). The optical density measurement is an indication of the number of cells present in the culture and was used to determine when the bacterial cells were in their log growth phase and at their prime to produce proteins. Cultures with an optical density of between 0.2 and 0.4 were used to induce protein expression using the Overnight Express™ Auto-induction System (*Novagen, USA*).

Auto-induction of recombinant protein expression is tightly regulated by the *lac* operon. Transcription is influenced by the level of cAMP (adenosine 3',5'-cyclic monophosphate) present in the bacterial cells and cAMP levels are strongly regulated by the carbon source present in the medium in which the cells are growing (Grossman *et al.*, 1998).

Glucose is the preferred carbon source during the initial growth phase of *Escherichia coli*. Protein expression is low during this phase due to binding between *lac* repressors and *lac* operators and also the repression of catabolites of alternative carbon source dependent metabolic pathways. The depletion of glucose leads to a decrease in catabolite repression and triggers the import of lactose and glycerol which causes a transition from the un-induced to the induced state of the expression host.

The Overnight ExpressTM auto-induction medium contains the following three components: a protein induction component, a buffering component and a source of magnesium needed for obtaining maximum cell densities. The induction component is a combination of carbon sources which allows for tightly regulated un-induced growth of bacterial cells to high densities followed by induction by lactose. The buffering component maintains the pH throughout the production of metabolic wastes and provides an additional supply of nitrogen to increase protein synthesis. These three components promote growth of bacterial cells to high densities and induce protein expression from *lac* promoters (Novagen, 71757 Overnight ExpressTM Instant LB Medium Package Insert, March 2012).

Twenty millilitre cultures were used for small scale expression and 250ml cultures for large scale recombinant protein production. Twenty millilitre Overnight ExpressTM Instant TB medium were inoculated with 12.5µl and 150µl overnight growths, respectively. Cultures not induced to express the recombinant protein were used as an induction control and prepared by adding 12.5µl of overnight growths to 20ml LB medium supplemented with 2% glucose (*Saarchem, South Africa*), which prevents the transition of the expression host from the un-induced to the induced state of protein expression.

The cultures were grown at 37°C for 18 hours in an orbital shaker followed by 20 hours growth at 20°C with constant shaking. The cultures were transferred to 50ml Beckman tubes and centrifuged in a Beckman Avanti® JE centrifuge at 3 500xg for 10 minutes at 4°C. The supernatant was discarded and the cell pellet was frozen at -70°C.

2.3.2 Recombinant protein extraction

The cell pellet was thawed on ice followed by another freezing step of 15 minutes at -70°C and again thawed on ice. These freeze-thawing steps facilitated the lysis of the bacterial cells. The Magne-GSTTM Protein purification system (*Promega, USA*) was used to purify the recombinant proteins. The cell pellets were resuspended in 10ml GST (glutathione-S-transferase) wash-bind buffer pH 8.23. DNase (*Fermentas Inc., Canada*) (1µl/ml) and Protease inhibitor cocktail set III (*Novagen Inc., USA*) (1µl/ml) were added to the cell suspension prior to

sonication on ice using a Bandelin Sonoplus UW 2070 sonicator (*Bandelin Electronics, Germany*). Six 30 second cycles (1 second sonication and 0.5 second pause) with a 45 second cooling on ice in between each cycle were used to completely lyse the bacterial cells in the suspension. A 100µl aliquot (Table 9) was taken to analyse the total protein content (section 2.3.5). The lysed cell suspensions were centrifuged in a Beckman Avanti® JE centrifuge (*Beckman Coulter, USA*) at 15 000rpm for 20 minutes at 4°C to separate soluble proteins from insoluble proteins. The supernatant was placed in a 15ml Falcon tube and kept on ice. The cell pellet constituted the insoluble protein fraction and was resuspended in 10ml GST wash-bind buffer pH 8.23. A 100µl aliquot (Table 9) of the insoluble proteins and the supernatant containing the soluble proteins were stored at 4°C for a maximum of 30 minutes, until they were solubilised. Each 100µl protein sample was added to 26µl 5x suspension solution, 3µl of 100% β-mercaptoethanol (*Merck, Germany*) and 3.4µl bromophenol blue solution (0.5% bromophenol blue (*BDH Laboratory Supplies, UK*) and 2.5% sucrose (*Saarchem, South Africa*). The protein samples were boiled for 2 minutes and stored at -20°C prior to electrophoresis (section 2.3.5).

2.3.3 Recombinant GST-PfPK8 purification using MagneGST™ beads

MagneGST™ beads (*Promega, USA*) were used to purify soluble recombinant Glutathione-S-Transferase tagged PfPK8 (rGST-PfPK8) from Rosetta 2 cells containing recombinant pGEX-4T-2-PfB0150c and rGST from control plasmid pGEX-4T-2. This rapid purification system utilises magnetic beads with glutathione immobilized on their surface. The beads are added to a crude soluble cell lysate and GST-fusion proteins bind to the beads. A magnetic particle separator (*Roche Applied Science, Germany*) is used to wash away unbound proteins. The GST-fusion protein is recovered from the beads by using a high concentration of glutathione, which competes with the GST-fusion proteins for binding to the beads resulting in the elution of the target protein from the beads.

One hundred microlitre aliquots (Table 9) of sample were taken throughout the purification process for protein analysis (section 2.3.5). Twenty microlitres of MagneGST™ beads were used to purify soluble GST-tagged recombinant

proteins from a 20ml bacterial culture and 50µl beads for a 250ml culture. According to the manufacturer, 20µl beads have a binding capacity of 50µg fusion protein. The particles were resuspended and transferred to a 2ml Eppendorf tube. The tube was placed in a magnetic particle separator to allow the particles to be attracted to the magnet. The supernatant was discarded without disrupting the beads captured by the magnet and 100µl MagneGSTTM wash-bind buffer pH 8.23 was added to the beads. Care was taken not to allow the beads to dry out. The beads were resuspended and the tube placed in the magnetic separator. The supernatant was discarded and the wash step was repeated three times. The beads were resuspended in 100µl MagneGSTTM wash-bind buffer pH 8.23 before adding it to the soluble protein fraction (section 2.3.2). The suspension was incubated for 12 hours at 4°C with constant gentle mixing on an Intelli-mixer RM 2M Skyline (*ELMI Ltd, Latvia*) to prevent the beads from settling which will decrease the yield of purified protein. The incubation was performed at 4°C to minimise the activity of proteases that might still be present in the soluble cell lysate which will degrade rGST-PfPK8. The manufacturer recommended an incubation time of 30 minutes at room temperature, but an incubation overnight at 4°C resulted in better protein yields. The next day the suspension was transferred to 2ml Eppendorf tubes and placed in the magnetic particle separator. The supernatant was removed and stored at 4°C to be used for rebinding if the recombinant protein yield was low. Two hundred microlitres of MagneGSTTM wash-bind buffer pH 8.23 was added to each Eppendorf tube and the beads were resuspended and combined into one 2ml Eppendorf tube. The suspension was incubated for 5 minutes at room temperature with occasional mixing on an Intelli-mixer RM 2M Skyline to wash the beads. The tube was placed in the magnetic particle separator and the supernatant was discarded. The washing step was repeated a total of three times. After the final wash, 100µl of elution buffer (500mM reduced L-Glutathione) (*Sigma-Aldrich Inc., USA*) was added to the sample and incubated for 20 minutes at room temperature. The tube was placed in the magnetic particle separator and the eluted protein was transferred to a 1.5ml Eppendorf tube and kept on ice. A second elution with 100µl of elution buffer was carried out. One hundred microlitres MagneGSTTM wash-bind buffer pH 8.23 was added to the beads. The

aliquots taken throughout the purification process (Table 9) were solubilised (section 2.3.2) and electrophoresed (section 2.3.5).

Table 9: Protein samples (100µl) collected during extraction and purification of rGST-*Pf*PK8.

Protein sample (Induced / uninduced)	Source	Source volume (ml)
Total	Lysed bacterial cells in MagneGST™ wash-bind buffer	10
Insoluble	Insoluble protein cell pellet resuspended in MagneGST™ wash-bind buffer	10
Soluble	Soluble protein lysate in MagneGST™ wash-bind buffer	10
Unbound	Supernatant post over-night incubation with beads at 4°C	10
Wash 1	Supernatant after wash 1 with MagneGST™ wash-bind buffer	1
Wash 2	Supernatant after wash 2 with MagneGST™ wash-bind buffer	1
Wash 3	Supernatant after wash 3 with MagneGST™ wash-bind buffer	1
Elution 1	Eluted rGST- <i>Pf</i> PK8 in glutathione solution (500mM)	0.1
Elution 2	Eluted rGST- <i>Pf</i> PK8 in glutathione solution (500mM)	0.1
Beads	Beads resuspended in MagneGST™ wash-bind buffer post-purification	0.1

2.3.4 r*Pf*PK8-His purification using MagneHis™ beads

MagneHis™ Kit (*Promega Corporation, USA*) was used to purify soluble recombinant octa-histidine tagged *Pf*PK8 (r*Pf*PK8-His) from Rosetta 2 cells containing recombinant *Pf*B0150c-pTriEx-3. This rapid purification system utilises paramagnetic pre-charged nickel beads (MagneHis™ beads) to isolate polyhistidine tagged fusion proteins from a soluble crude bacterial cell lysate. Histidine tagged recombinant proteins will bind to the beads, unbound proteins

are washed away and the target protein is recovered by elution with imidazole (*Sigma-Aldrich Inc., USA*).

One hundred microlitre aliquots (Table 10) of sample from various steps of the purification were taken to be analysed via SDS-PAGE (section 2.3.5). Fifty microlitres MagneHis™ Nickel beads were used to purify soluble rPfPK8-His proteins from a 20ml bacterial culture. The beads are supplied as a 50% slurry and 1ml beads have a binding capacity of 1mg protein. The beads were mixed to a uniform suspension and 50µl beads were transferred to the soluble protein fraction (section 2.3.2) in a 15ml Falcon tube. The tube was inverted approximately 10 times to thoroughly mix the suspension and incubated at 4°C for 1 hour with constant gentle mixing on an Intelli-mixer RM 2M Skyline. The manufacturer recommended an incubation time of 2 minutes at room temperature but a longer incubation was found to yield a higher amount of target protein. The incubation was performed at 4°C to minimise protease activity, which will degrade the target protein. After incubation, the suspension was transferred to 2ml Eppendorf tubes and placed in a magnetic particle separator to separate the beads from the supernatant. The supernatant was removed and stored at 4°C to be used for rebinding if the recombinant protein yield was low. One hundred microlitres of kit MagneHis™ bind-wash buffer was added to each Eppendorf tube and the beads were resuspended and combined into one 2ml Eppendorf tube. The tube was placed into the magnetic separator and the supernatant was discarded. One hundred and fifty microlitres of kit MagneHis™ bind-wash buffer was added to the tube. The tube was incubated for 1 minute with gentle agitation at room temperature. The beads and supernatant were separated and a 100µl aliquot of the supernatant was taken and kept on ice (wash 1). The wash step was repeated a total of three times. One hundred microlitres of kit MagneHis™ Elution Buffer was added to the tube, mixed by pipetting up and down and incubated for 15 minutes at room temperature with constant mixing. The manufacturer recommended an elution incubation time of 2 minutes, but a longer elution time yielded more protein. The tube was placed in the magnetic separator and the eluted protein was removed to a clean 1.5ml Eppendorf tube and kept on ice. A 2nd elution was carried out in the same manner. One hundred microlitres of

kit MagneHisTM Elution Buffer was added to the beads. The aliquots taken throughout the purification process (Table 10) were solubilised (section 2.3.2) and electrophoresed (section 2.3.5).

Table 10: Protein samples (100µl) collected during extraction and purification of *rPfPK8*-His.

Protein sample (Induced / uninduced)	Source	Source volume (ml)
Total	Lysed bacterial cells in kit MagneHis TM bind-wash buffer	10
Insoluble	Insoluble protein cell pellet resuspended in kit MagneHis TM bind-wash buffer	10
Soluble	Soluble protein lysate in kit MagneHis TM bind-wash buffer	10
Soluble Uninduced	Soluble protein lysate of uninduced culture in kit MagneHis TM bind-wash buffer	10
Unbound	Supernatant post over-night incubation with beads at 4°C	10
Wash 1	Supernatant after wash 1 with kit MagneHis TM bind-wash buffer	0.150
Wash 2	Supernatant after wash 2 with kit MagneHis TM bind-wash buffer	0.150
Wash 3	Supernatant after wash 3 with kit MagneHis TM bind-wash buffer	0.150
Elution 1	Eluted (<i>rPfPK8</i> -His) in imidazole (500mM)	0.1
Elution 2	Eluted (<i>rPfPK8</i> -His) in imidazole (500mM)	0.1
Beads	Beads resuspended in kit MagneHis TM bind-wash buffer post-purification	0.1

2.3.5 Laemmli sodium dodecyl sulphate-polyacrylamide gel electrophoresis (SDS-PAGE)

Protein samples (Table 9 and Table 10) collected during the purification process were separated on a Laemmli SDS-polyacrylamide gel (Laemmli, 1970) consisting of 12 % resolving gel and 4% stacking gel. The resolving gel has a smaller pore size whereas the upper stacking gel has a lower pH and larger pores. The 8cm x 10cm casting cassette was assembled in a Hoefer Mighty Small II SE250 gel cassette (*Hoefer Scientific Instruments, USA*). The gel solutions were prepared as set out in Table 11:

Table 11: Laemmli SDS-PAGE gel solutions.

Reagent	12 % Resolving gel		4% Stacking gel	
	Final concentration	Volume	Final concentration	Volume
30% Acrylamide	12%	4ml	4%	433µl
1% Bis-acrylamide	0.11%	1.076ml	0.11%	333µl
4x Resolving gel buffer	1x	2.5ml	-	-
4x Stacking gel buffer	-	-	1x	833µl
10% SDS	0.005%	53.3µl	0.02%	6.7µl
Milli-Q water	-	2.33ml	-	1.63ml
10% APS	0.07%	67µl	0.2%	67µl
TEMED	-	5µl	-	2.5µl

Acrylamide and bisacrylamide form a cross-linked polymer network when APS is added. This polymerization reaction is catalysed by the addition of TEMED which promotes the production of free radicals by APS. Freshly prepared 10% ammonium persulphate (APS) (*Promega, USA*) and tetramethylethylenediamine (TEMED) (*Promega, USA*) were therefore added to the resolving gel solution just before the gel was poured. The solution was swirled to gently mix and poured into the gel cassette to a height of approximately 7cm. The gel was overlaid

with 1ml isopropanol (*Merck, Germany*) to ensure a flat interface between the resolving gel and the stacking gel. The gel was allowed to polymerise at room temperature for 30 – 45 minutes. The isopropanol was carefully rinsed from the top of the gel with Milli-Q water and was drained by inverting the gel cassette. The APS and TEMED were added to the stacking gel solution, swirled to mix and poured into the gel cassette to fill it to the top. A comb with the appropriate well-width and number of wells was inserted and the stacking gel was allowed to polymerise at room temperature for 30 – 45 minutes. Different volumes of the protein samples (Table 9 and Table 10) were loaded on the gels next to a Pre-stained protein ladder (*Fermentas Inc., Canada*) to determine the size of the bands and different concentrations of bovine serum albumin (BSA) (*Roche Diagnostics, Germany*) to quantitate the yield of protein. The gels were electrophoresed using Laemmli running buffer for 120 minutes at 20mA per gel, using a Mighty SlimTM SX250 power supply (*Hoefer Scientific Instruments, USA*). The gels were cooled during electrophoresis to 4°C using a Labcon CPE 50 circulator (*Labcon, South Africa*). Gels were stained overnight in 0.05% Coomassie R-250 blue (*BDH Laboratory Supplies, UK*) stain and destained in 10% acetic acid (*SMM Instruments, South Africa*)/10% methanol (*SMM Instruments, South Africa*) solution for 4 hours at room temperature with constant agitation on an Labotec[®] Orbital shaker (*Labotec, South Africa*). The 10% acetic/10%methanol solution was changed every hour. The gels were destained further in 10% acetic acid overnight until the gel background was clear. The protein yield and percentage purity of the recombinant proteins were determined by performing densitometric analysis on the stained SDS-PAGE gels. A non-saturated image of the stained gels was captured using a Geldoc SynGene GeneGenius gel documentation system (*Syngene, UK*) and analysed using SynGene GeneTools version 4.0 analysis software (*Syngene, UK*).

2.3.6 Immunoblotting of GST-tagged recombinant proteins

Unstained Laemmli gels, four pieces of blotting paper and a piece of HybondTM-C Extra Nitrocellulose membrane (*Amersham Biosciences, UK*) cut to size were soaked for 10 minutes in Towbin transblot buffer (Towbin, 1979) at room temperature. The western transfer cassettes (*Hoefer Scientific Instruments, USA*)

were assembled with the gel on the cathode side and the nitrocellulose membrane facing the anode and placed in the transfer tank (*TE Series Transphor electrophoresis unit, Hoefer Scientific Instruments, USA*). The tank was filled with approximately 1.5L of pre-cooled (4°C) transblot buffer. The proteins were transferred overnight at 4°C onto the nitro-cellulose membrane at 35V, 70 – 90mA with gentle stirring on a magnetic stirrer.

The next day the nitrocellulose membranes were washed in TBS for 10 minutes and the gels were placed in Coomassie blue stain to determine the transfer efficiency. The membranes were coated with 1ml Ponceau S (*Sigma-Aldrich Inc, USA*) for 2 minutes to detect protein transfer. The excess dye was rinsed off using Milli-Q water and the banding of the molecular weight marker was recorded on the stained membrane. The membrane was incubated in 50ml 3% bovine serum albumin (BSA)/TBS blocking solution on a shaking platform for 1 hour at room temperature to coat areas of the membrane not containing any transferred protein, which prevents non-specific antibody binding.

The membrane was incubated on a shaking platform in 50ml 1:100 000 dilution of anti-GST horse radish peroxidase (HRP) – conjugated primary antibody (*Amersham Biosciences, UK*) at room temperature for 1 hour with gentle shaking. The antibody solution was stored at -20°C for re-use. The membrane was washed 3 times on a shaking platform, each for 10 minutes with 100ml TBS containing 0.05% Tween[®] 20 detergent (*CalBiochem, South Africa*) (TBST) to remove any unbound antibody from the membrane followed by a rinse in TBS for 10 minutes.

The GST-Antibody complexes were visualised with the SuperSignal[®] West Pico Chemiluminescent Substrate (*Pierce Biotechnology Inc, USA*) according to the manufacturer's instructions. When adding the substrate and luminol to the protein-HRP-conjugated antibody complexes, the HRP enzyme catalyses the oxidation of luminol (Sasse and Gallagher, 2003). This oxidation process releases energy in the form of light which is recorded on an X-ray film as a band.

The chemiluminescent detection was performed in a dark room. One ml of the stable peroxide solution and 1ml of the luminol enhancer solution from the kit

were added to a 2ml Eppendorf tube and mixed by pipetting up and down. The working solution was added to the membrane surface to which the proteins had been transferred. The membrane was left for 5 minutes to allow the chemiluminescent reaction to take place. Care was taken to completely cover the membrane with the solution. The excess solution was drained off the membrane and the membrane was covered with clear plastic before placing it in an x-ray film cassette with the protein side facing upward. A piece of CP-G plus medical X-ray film (*Agfa, Germany*) was placed over the blot and exposed to the membrane for 30 seconds. The exposed X-ray film was developed manually using X-ray developer diluted 1:4 with water (*Axim, South Africa*) then fixed in Perfix high speed X-ray fixer (*Champion photochemistry, South Africa*). The film was allowed to dry at room temperature. The nitrocellulose membrane was stained with amido black stain (*ApploChem, Germany*) for 10 minutes to detect the transferred proteins on the membrane. The background dye was removed from the stained membrane by destaining it in 10% acetic acid/10% methanol solution for 10 minutes.

2.3.7 Immunoblotting of His-tagged recombinant proteins

Unstained Laemmli gels, pieces of blotting paper and a piece of HybondTM-C Extra Nitrocellulose membrane (*Amersham Biosciences, UK*) cut to size were soaked for 10 minutes in Towbin transblot buffer (Towbin, 1979) at room temperature. The western transfer cassettes (*Hoefel Scientific Instruments, USA*) were assembled as described in section 2.3.6. The tank was filled with approximately 1.5L of pre-cooled (4°C) transblot buffer. The proteins were transferred overnight at 4°C onto the nitro-cellulose membrane at 35V (70 – 90mA) with gentle stirring on a magnetic stirrer.

A QIAexpress® Detection and Assay kit with Anti-His HRP Conjugates (*Qiagen, USA*) was used for the immunoblotting of Histidine-tagged recombinant proteins. The nitrocellulose membranes were washed twice in TBS (10mM Tris and 150mM NaCl at pH7.5) for 10 minutes each at room temperature after overnight protein transfer to remove excess glycine. The transfer gels were placed in Coomassie blue stain to determine the transfer efficiency. The membranes were

incubated for 1 hour at room temperature in blocking buffer (0.5% (w/v) kit blocking reagent in kit blocking reagent buffer, 0.1% (v/v) Tween 20). The membranes were washed twice for 10 minutes each with TBS-Tween/Triton X (10mM Tris-HCl at pH7.5, 150mM NaCl, 0.05% Tween 20 v(v/v) and 0.2% Triton X-100 (v/v)) and once with TBS, with vigorous shaking. The membranes were incubated with gentle shaking in 20ml of HRP-conjugated mouse anti-penta-His antibody (1:2 000 in 1x Anti-His HRP Conjugate blocking buffer) for 1 hour at room temperature. The membranes were again washed twice in TBS-Tween/Triton X and once with TBS for 10 minutes each with vigorous shaking. The membranes were washed twice on a shaking platform at room temperature, each time for 10 minutes with TBS-Tween/Triton X buffer to remove any unbound antibody from the membrane. The final wash step was in TBS for 10 minutes at room temperature before continuing with the chemiluminescent detection reaction and exposure of the membrane to X-ray film as previously described in section 2.3.6.

2.4 Eukaryotic protein expression system

2.4.1 *Sf9* insect cell culturing techniques

2.4.1.1 Thawing *Sf9* and TriEx™ *Sf9* insect cells

Sf9 and TriEx™ *Sf9* insect cells (Novagen, USA) were cultured and maintained according to manufacturer's recommendations. BacVector® Insect Cell Medium (Novagen, USA) was used for *Sf9* insect cell culturing and TriEx™ Insect Cell Medium (Novagen, USA) was used for the culturing of TriEx™ *Sf9* insect cells.

The medium was pre-warmed to 28°C in a water bath. An aliquot (1ml) of *Sf9* Insect Cells or TriEx™ *Sf9* insect cells was removed from liquid nitrogen and quickly thawed by immersing the vial about half way into a 28°C water bath. The vial was gently swirled until the cells were fully thawed. The outside of the vial was sterilized with 70% ethanol before slowly pipetting the vial contents into a sterile 15ml Falcon tube in a laminar flow hood. Pre-warmed medium (9ml) was added drop-wise to the cells. After gently mixing the cell suspension by pipetting

up and down 3 times, the cells were centrifuged at 400xg for 3 minutes at 20°C in an Eppendorf centrifuge 5702R. The medium was removed after centrifugation and 10ml fresh pre-warmed medium was added to the cells. The cells were gently resuspended before transferring them to a sterile 250ml Erlenmeyer culture flask (*Corning, Biocom Biotech, South Africa*). The suspension culture was incubated at 28°C with constant shaking (100rpm) in a Shaking Incubator 150LT Model 355 (*Separations Scientific, South Africa*). After 48hrs the growth and viability of the culture were determined by the Trypan Blue dye exclusion method. The cell number at this stage should be above 1×10^6 cells/ml and a viability of $\geq 85\%$. The growth rate of recently thawed cells is initially slow and cells have a low viability, but after one week, the viability should be above 95% and the cell growth should be steady with a doubling time of approximately 1 – 1.5 days.

2.4.1.2 Determination of cell viability by Trypan Blue dye exclusion

The cell viability of the suspension culture was determined every 48hrs using a Trypan Blue dye solution (*Sigma-Aldrich Inc, USA*). Trypan Blue dye stains only dead cells, which will appear blue under a microscope compared to shiny translucent viable cells. It is important to count the live cells soon after the Trypan Blue solution is added because live cells will lose their capacity to exclude dye with time. A volume of 100µl cells was aseptically removed from the shaking culture in a laminar flow hood and added to a sterile 1.5ml Eppendorf tube containing 100µl of the Trypan Blue solution. After mixing the suspension using a pipette, the solution was incubated at room temperature for 3 minutes. With the cover slip in place, a small aliquot of the trypan blue-cell suspension was added to both sides of a haemocytometer. Four counts of the same sample were performed using a phase contrast inverted microscope (*Olympus Optical Corporation Ltd., Japan*).

All the cells in the 1mm centre square of each chamber of the haemocytometer, representing a total volume of 0.1mm^3 , were counted. Since 1cm^3 is equivalent to approximately 1ml, the total number of cells per ml (cell density) can be calculated using the following formulas:

$$\text{Cell density (cells/ml)} = \text{average cell count} \times \text{dilution factor} \times 10^4$$

$$\text{Cell viability (\%)} = \left[\frac{(\text{average \# viable cells})}{(\text{average \# viable + unviable cells})} \right] \times 100$$

2.4.1.3 Passage of suspension cultures

The cells were passaged every 2 – 3 days when the cell density reached 2×10^6 cells/ml. The cells were discarded when passaged more than 20 times. To maintain viability and for successful recombinant virus and protein production, the cells were maintained at a concentration of 1.5×10^6 cells/ml. Over-dilution of a culture will result in cell death, therefore a culture with a cell density less than 1×10^6 cells/ml was avoided. The culture was diluted with pre-warmed 28°C BacVector® Insect Cell Medium or TriEx™ Insect Cell Medium to the desired cell density and the calculated volume of cells were transferred to another sterile 250ml Erlenmeyer culture flask. A culture volume to flask volume did not exceed a ratio of 1:5. The flasks were incubated at 28°C with constant shaking at 100rpm.

2.4.1.4 Maintenance of a stock monolayer culture

A 5ml stock monolayer culture of *Sf9* and TriEx™ *Sf9* insect cells was maintained in a 50ml culture flask. A monolayer culture is used as the stock culture due to the lower proliferation rate of attached cells compared to cells in a suspension culture and therefore it is technically less demanding to maintain.

Based on the cell count of the suspension culture, *Sf9* cells or TriEx™ *Sf9* were seeded in a 50ml culture flask to a final cell density of 0.5×10^6 cells/ml. Pre-warmed 28°C BacVector® Insect Cell Medium or TriEx™ Insect Cell Medium was added to a final culture volume of 5ml. The monolayer culture was incubated at 28°C and examined daily under an inverted microscope to determine if the cells were healthy and if the monolayer confluency was high enough (85 – 95%) to divide the culture. An over-confluent culture will lead to flotation of insect cells and the cells will start to divide in the medium because these cells are not subject to contact inhibition. Under a microscope, healthy insect cells appear rounded and bright with distinct cell boundaries, whereas unhealthy cells appear dark and

granular with irregular shaped cell boundaries. A large number of floating cells within the culture was used as an indication that the culture was unhealthy. Typically, cells grown in a monolayer were divided 1:5 (ratio of existing culture to fresh medium) every 3 – 4 days according to needs, when the confluency was between 85 – 95% and the cell density was $2.0 - 2.5 \times 10^6$ cells/flask. The medium was sterilely aspirated from the flask in a laminar flow hood and 5ml pre-warmed 28°C BacVector® Insect Cell Medium or TriEx™ Insect cell medium was added to the flask. The cells were gently rinsed off the bottom of the flask using the medium by pipetting repeatedly. An aliquot (100µl) of dislodged cells was used to determine the cell density and viability of the culture using the Trypan Blue dye exclusion method. Based on the cell count, the cells were seeded in a 250ml Erlenmeyer culture flask, according to needs or discarded. The volume of the monolayer 50ml culture flask was adjusted to 5ml using pre-warmed 28°C BacVector® Insect Cell Medium or TriEx™ Insect Cell medium and incubated at 28°C.

2.4.1.5 Preparation of *Sf9* and TriEx™ *Sf9* insect cells for long term storage in liquid nitrogen

Insect cells were frozen in liquid nitrogen to provide a fresh source of cells when the working stocks became too old or had been passaged more than 20-25 times. Exponentially growing cells from a suspension culture with viability between 85 – 95% were transferred to a sterile 15ml Falcon tube and centrifuged at 400xg for 3 minutes at 20°C in an Eppendorf centrifuge 5702R centrifuge. The medium was aseptically removed using a pipette in a laminar flow hood. The cells were resuspended in enough pre-warmed 28°C BacVector® Insect Cell Medium or TriEx™ Insect Cell medium to have a final cell density of 2×10^6 cells/ml. For each 1ml resuspended cells, 200µl BacVector® Insect Cell Medium and 100µl high-grade dimethyl sulphoxide (DMSO) (10%) (*BDH Laboratory Supplies, UK*) were added. The cell suspension was mixed by gently pipetting up and down several times to ensure complete mixing. The cell suspension was divided into 1ml aliquots in sterile 1.5ml Eppendorf tubes and transferred to liquid nitrogen for long term storage.

2.4.2 Production of recombinant baculovirus

2.4.2.1 Transfection of *Sf9* insect cells with recombinant *PfB0150c*-pTriEx-3 vector

BacMagic™ DNA kit (*Novagen, USA*) was used to generate baculovirus recombinants containing the *PfB0150c* insert (BacVirus-*PfB0150c*). The transfer plasmid (*PfB0150c*-pTriEx-3) is co-transfected with the BacMagic single stranded DNA (DNAs) and homologous recombination will take place within the insect cells. A portion of the essential open reading frame 1629 (ORF1629) of the BacMagic DNAs has been deleted and it contains a bacterial artificial chromosome (BAC). The partial deletion of ORF1629 prevents non-recombinant virus replication within transfected insect cells. After recombination, the ORF1629 is restored and the BAC sequence is replaced by the target sequence (*PfB0150c*). This results in a homogeneous population of BacVirus-*PfB0150c*.

Two 35mm petri-dishes (*NuncTM, Denmark*) were seeded with 1×10^6 cells/dish in 2ml BacVector® Insect Cell medium 1 hour before use. One petri-dish was used for the transfection and the other as a negative transfection control (no vector). The petri-dishes were gently rocked in a side-to-side and back-and-forth manner to ensure an even cell monolayer. The seeded cells were allowed to attach to the plates for 4 hours in a Shaking Incubator 150LT Model 355 set to 28°C without shaking. The co-transfection mixtures of DNA and Insect GeneJuice® Transfection Reagent (*Novagen, USA*) were prepared during the incubation period (Table 12).

Table 12: Preparation of insect cell transfection mixtures.

Component	Volume (µl) needed for transfection mixture	Volume (µl) needed for negative control transfection mixture
BacVector [®] Insect cell medium	1000	1000
Insect GeneJuice [®]	5	5
BacMagic DNA (100ng)	5	5
Recombinant <i>Pf</i> B0150c-pTriEx-3 transfer vector DNA (500ng)	5	-
BacVector [®] Insect cell medium	-	5
Final volume	1 015	1 015

The transfection solutions were mixed with gentle agitation and incubated at room temperature for 30 minutes to allow recombination complexes to form. The culture medium was removed from the 35mm petri-dishes just prior to the end of the transfection mixture incubation time. Care was taken not to disrupt the cell monolayer by tilting the dish at a 45° - 60° angle to allow the liquid to pool to one side of the dish. Immediately after the medium had been removed from the cells, 1ml transfection mixture was added drop-wise to the centre of the petri-dish. The petri-dishes were incubated overnight at 28°C in a sterile container humidified with wet cottonwool. The following day, 1ml BacVector[®] Insect cell medium was carefully added to each petri-dish followed by incubation in the same manner for 4 days at 28°C. The medium containing recombinant baculovirus was harvested and placed in a 1.5ml Eppendorf tube. The viral seed stock was stored in the dark at 4°C.

2.4.2.2 Amplification of recombinant virus

A 10ml suspension culture of *Sf9* cells was prepared at a density of 2×10^6 cells/ml in a sterile 150ml Erlenmeyer culture flask. The cells were infected with virus by adding 500µl of the recombinant viral seed stock to the culture. The culture was incubated at 28°C with constant shaking at 100 rpm until the cells were sufficiently infected with the recombinant virus. The cells were analysed on a

daily basis using a phase-contrast inverted microscope. An 80µl aliquot of the cell suspension was sterilely removed from the culture and placed in a 1.5ml Eppendorf tube. Forty microlitres of the cells were placed on a haemocytometer with a cover slip and viewed under the microscope. Cells infected with virus appeared grainy when compared to healthy cells and the infected cells became uniformly rounded and enlarged with distinct enlarged nuclei. The remaining 40µl of the cell suspension was used to determine the cell viability and cell density on a daily basis using the Trypan Blue dye exclusion method (section 2.4.2.1). The cell culture medium was harvested when the cells appeared to be well infected with virus (4 – 5 days). The cell suspension was placed in a 15ml Falcon tube and centrifuged at 1 000xg for 20 minutes at 4°C in an Eppendorf centrifuge 5702R. The supernatant was sterilely removed and this amplified recombinant virus stock was stored at 4°C in the dark. The supernatant contained recombinant baculovirus since a high viral load caused lysis of the insect cells releasing virus into the medium.

A 1ml aliquot of this viral stock was stored in a sterile 1.5ml Eppendorf tube at -70°C for long term storage as the titre of the stock stored at 4°C will drop after 3 – 4 months. The amplification process was repeated 6 times before determining the viral titre.

2.4.2.3 Titre determination of recombinant baculovirus

The FastPlax™ Titer kit (Novagen, USA) was used for rapid viral titre determination. This system is based on the detection of the baculovirus surface glycoprotein 64 (gp64) (Hohmann and Faulker (1983); Monsma and Blissard (1995)) which appears on the surface of viral infected cells as early as 8 – 24 hours post-infection (Oomens *et al.*, 1995). Glycoprotein 64 is detected using a monoclonal antibody directed against this external viral epitope. Goat Anti-Mouse IgG β-Galactosidase conjugate is used as secondary antibody to detect the gp64-antibody complex with a colour reaction. The colour reaction is due to an enzymatic reaction where the chromogenic stain 5-bromo-4-chloro-3-indoyl-β-D-galactopyranoside (X-Gal) is converted by β-Galactosidase to the insoluble blue enzymatic product 5,5'-dibromo-4,4'-dichloro-indigo in the presence of nitroblue

tetrazolium (NBT). Single infected cells and infected cell clusters (foci) are easily distinguished from uninfected cells by this blue colour.

An exponentially growing culture of *Sf9* cells was prepared prior to the start of the FastPlax titer assay. Three pairs of 35mm petri-dishes were labelled “-5”, “-6” and “-7” according to the viral dilutions that will be added to these plates. A total of 1×10^6 cells in 2ml BacVector[®] Insect cell medium were seeded in each plate. After adding the cells, the plates were moved in a side-to-side and back-and-forth manner to ensure an even monolayer. The cells were allowed to attach to the plates for 4 hours in an incubator set to 28°C. Virus dilutions were prepared in 1.5ml Eppendorf tubes during this time. The dilution series was prepared as follows: 990µl of BacVector[®] Insect cell medium was added to tubes labelled “-2” and “-4” and 900µl of medium was added to tubes labelled “-5”, “-6” and “-7”. The dilution series was started by adding 10µl of the viral seed stock (section 2.4.2.1) to the “-2” labelled tube. This constitutes the 10^{-2} virus stock dilution used to perform a serial dilution. Care was taken to pipette accurately and to avoid viral stock droplets that may cling to the outside of the pipette tip, since all other dilutions were derived from this dilution.

The 2ml medium was aspirated from the petri dishes by slowly tipping the petri dishes at a 30° angle and removing the liquid from the edge of the petri dish to avoid disturbing the cell monolayer. One hundred microlitres of each virus dilution were added drop-wise to the centre of each of the 2 duplicate petri dishes labelled accordingly and incubated at 28°C for 1 hour. The petri dishes were tipped back and forth at 10 minute intervals to ensure that the cell monolayer did not dry out. Two millilitres BacVector[®] Insect cell medium were added to each petri dish after the incubation period and the petri dishes were incubated at 28°C for 24 hours in a sterile sealed container. Moist cottonwool was added to the container to prevent the cells from drying out.

The subsequent steps were performed on a laboratory bench top since sterile technique was not necessary. The medium was removed from the petri dishes at 24 hours post-infection and disposed of as biological waste, since it contained infectious baculovirus. The cells in each petri dish were washed twice with 2ml

PBS. The cells were fixed with 2ml 3.7% formaldehyde (*Sigma-Aldrich Inc., USA*) - PBS solution and incubated for 15 minutes at room temperature. The formaldehyde solution was removed and the cells in each petri dish washed twice with 2ml PBS. One percent gelatine (*Novagen, USA*) in kit TBST was used as blocking agent to avoid non-specific binding of the antibody to other proteins. Two millilitres of the blocking solution was added to the petri dishes followed by an incubation period of 30 minutes at room temperature with gentle rocking on a slow orbital shaker. The cells were washed twice with 2ml PBS after removing the gelatine solution. The FastPlax Antibody (*Novagen, USA*) was diluted 1:10 000 in 1x TBST. One millilitre of the diluted antibody was added to each petri dish and incubated for 1 hour with gentle rocking to allow for the protein-antibody complexes to form. The FastPlax antibody solution was removed and the cells were washed 3 times for 10 minutes with 2ml per petri dish of 1x TBST. One millilitre of Goat Anti-Mouse β -gal Conjugate (1:1000) in 1x TBST was added to each petri dish and incubated for 60 minutes with gentle rocking at room temperature. After removing the conjugate antibody solution the cells were washed 3 times for 10 minutes with 2ml per petri dish of 1x TBST. The developing solution was prepared during the last wash by adding 60 μ l of X-Gal (*Novagen, USA*) and 60 μ l of NBT (*Novagen, USA*) to 15ml of PBS containing 5mM MgCl₂. The wash solution was removed and 2ml of the developing solution was added to each petri dish. The petri dishes were incubated at 37°C for 15 – 60 minutes. To avoid over-developing of the infected cells, the petri dishes were examined under a microscope at 10 minute intervals. Infected cells appeared medium blue to dark purple with the colour either completely filling the area of the cell or it may appear as dark purple foci of staining. The cells were washed twice with 1x TBST per petri dish to stop the colour development. The colour may continue to develop and darken with time, even after this wash step. Therefore care was taken to count the stained cells immediately after washing. Un-infected cells may appear lightly stained if over developed. The infected cells and foci (clusters of stained cells) were counted immediately after washing, using a phase-contrast inverted microscope. Single cells that stained strongly stained were counted as well as small clusters of stained cells.

The following formula was used to calculate the titre (plaque forming units (pfu)/ml) of the viral seed stock:

$$\text{pfu/ml} = 10 \times \text{number infected cells or foci} \times \text{dilution factor}$$

The average of the 6 petri dishes with different viral dilutions was used to determine the final viral titre.

2.4.3 Recombinant *Pf*PK8-His expression analysis in *Sf9* insect cells

2.4.3.1 Expression in TriExTM-*Sf9* insect cells

TriExTM-*Sf9* cells are optimised for vigorous cell growth and will yield high amounts of recombinant protein once infected with a recombinant baculovirus. The *Pf*B0150c-pTriEx-3 expression vector construct has a baculovirus p10 promoter which is essential for recombinant protein expression in infected *Sf9* insect cells. The p10 promoter is highly active during the later phase of baculovirus infection during which maximal expression is achieved.

For expression, 12x 20ml exponentially growing TriExTM-*Sf9* cell suspension cultures at a density of 2×10^6 cells/ml were prepared (section 2.4.1.3). Recombinant viruses were added to the cultures in triplicate at an MOI of 1, 2, 5 and 10, respectively. Uninfected TriExTM-*Sf9* cells were used as a protein expression control and were also cultured in triplicate. The cells were cultured for 24, 48, 72 and 96 hours at 28°C with constant shaking at 100rpm. The cell density and viability were determined at each time point using the Trypan Blue dye exclusion method (section 2.4.1.2). The experiment was repeated twice using different TriExTM-*Sf9* cell suspensions.

2.4.3.2 Immunoblotting of His-tagged recombinant proteins

Approximately 5×10^5 TriExTM-*Sf9* cells taken from infected (MOI of 1, 2, 5 and 10) and uninfected cultures were pelleted after 24, 48, 72 and 96 hours post-infection via centrifugation at 1 000xg for 20 minutes in an Eppendorf 5415R centrifuge. The supernatants were removed and stored separately on ice together with the cell pellets until protein analysis was performed.

The cell pellets infected with an MOI of 1, 2, 5 and 10 taken at the various time points post-infection were resuspended in 200µl PBS. Fifty microlitres of the resuspended cell samples and the supernatant samples were solubilised and prepared for Laemmli SDS-PAGE analysis as previously described (section 2.3.2 and section 2.3.5). A Spectra Molecular Weight marker (*Fermentas, Europe*) and recombinant Pfl0675c-C-His (40kDa) or Qiagen His ladder (*Qiagen, USA*) were used as controls. Twelve and 25 microliters of the solubilised cell and supernatant sample were loaded on two SDS-PAGE gels for Coomassie Blue staining and immunoblotting, respectively. A histidine ladder or rPFL0675c-C-His (40 kDa) were used as immunoblot positive controls.

Unstained Laemmli gels, pieces of blotting paper and a piece of HybondTM-C Extra Nitrocellulose membrane (*Amersham Biosciences, UK*) cut to size were soaked for 10 minutes in Towbin transblot buffer (Towbin, 1979) at room temperature. The western transfer cassettes (*Hoefler Scientific Instruments, USA*) were assembled as described in section 2.3.6. The tank was filled with approximately 1.5L of pre-cooled (4°C) transblot buffer. The proteins were transferred overnight at 4°C onto the nitro-cellulose membrane at 35V (70 – 90mA) with gentle stirring on a magnetic stirrer.

A QIAexpress® Detection and Assay kit with Anti-His HRP Conjugates (*Qiagen, USA*) was used for the immunoblotting of Histidine-tagged recombinant proteins. The nitrocellulose membranes were washed twice in TBS for 10 minutes each at room temperature after overnight protein transfer to remove excess glycine. The gels were placed in Coomassie blue stain to determine the transfer efficiency. The membranes were incubated for 1 hour at room temperature in blocking buffer (0.5% (w/v) kit blocking reagent in kit blocking reagent buffer, 0.1% (v/v) Tween 20). The membranes were washed twice for 10 minutes each with TBS-Tween/Triton X and once with TBS, with vigorous shaking. The membranes were incubated with gentle shaking in 20ml of HRP-conjugated mouse anti-penta-His antibody (1:2 000 in 1x Anti-His HRP Conjugate blocking buffer) for 1 hour at room temperature. The membranes were again washed twice in TBS-Tween/Triton X and once with TBS for 10 minutes each with vigorous shaking.

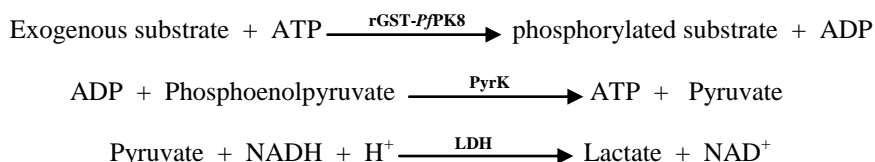
The membranes were washed twice on a shaking platform at room temperature, each time for 10 minutes with TBS-Tween/Triton X buffer to remove any unbound antibody from the membrane. The final wash step was in TBS for 10 minutes at room temperature before continuing with the chemiluminescent detection reaction and exposure of the membrane to X-ray film as previously described in section 2.3.6.

2.5 Non-radio-active coupled protein kinase assay

2.5.1 Kinetic analysis of rGST-PfPK8

The assay method is based on a coupled closed system reaction where a kinase catalyzes the transfer of a phosphate group from ATP to a specific amino acid residue of a protein substrate in the presence of auxiliary enzymes pyruvate kinase (PyrK) and lactate dehydrogenase (LDH) (Bergmeyer, 1974).

The reactions are as follows:



The rate of decrease in the absorbance at 340nm is directly and continuously measured in a temperature controlled Biomat 5 spectrophotometer (*Thermo Electron Corporation, UK*) over 20 minutes at 30 second intervals. The change in absorbance due to the oxidation of nicotinamide adenine dinucleotide (NADH) is directly proportional to the activity of rGST-PfPK8 in the presence of an exogenous substrate.

The kinase activity of rGST-PfPK8 (2.5 – 2.73µg pure enzyme) in the presence of three different substrates was determined according to the method described by Worthington and Worthington (2011). The K_m and V_{max} for casein (*Sigma-Aldrich Inc., USA*), myelin basic protein (MBP) (*Sigma-Aldrich Inc., USA*) and histone protein 1 (H1) (*EMD Biosciences Inc., USA*) were determined with

adenosine triphosphate (ATP) (*Roche diagnostics GmbH, Germany*) at a constant concentration of 2.5mM and the substrates in a range between 0.05 μ M – 5 μ M (39.8 μ g - 398 μ g for casein, 9.2 μ g - 92 μ g for MBP and 10.8 μ g - 108 μ g for H1). The K_m and V_{max} for ATP were determined by varying the concentration of ATP between 0.025mM and 2.0mM and keeping the amount of casein constant at 0.5 μ M (400 μ g). The kinetic analysis was performed using GraphPad Prism 5 for Windows version 5.01 software (*GraphPad software Inc., www.graphpad.com*).

A standard reagent solution containing 1.22mM reduced NADH, 2mM phosphoenolpyruvate (PEP) (*Roche Diagnostics GmbH, Germany*), 28mM MgSO₄ (*Sigma-Aldrich Inc., USA*), 26mM reduced glutathione (*Sigma-Aldrich Inc., USA*), 7 units/ml PyrK (*Roche diagnostics GmbH, Germany*) and 15 units/ml LDH (*Roche diagnostics GmbH, Germany*) was prepared and kept on ice. Two hundred and thirty three microliters of the reagent solution was used per ml reaction. The buffer (0.1M Tris-HCl at varying pH values), ATP and the exogenous substrates, either casein, MBP or H1 for rGST-*Pf*PK8 and glycerol for *Escherichia coli* glycerol kinase (*Ec*GK) were added at different concentrations (Table 13 and Table 14) to the reagent solution on ice just prior to starting the assay. The reagent solution was kept on ice. The final reaction mixture (1ml) contained: 0.3mM NADH, 0.5mM PEP, 3.5 units/ml LDH, 1.6 units/ml PyrK, 6.5mM MgSO₄, 6mM reduced glutathione, 70mM Tris-HCl (at varying pH values) or 70mM sodium acetate (at varying pH values), ATP (at varying concentrations) and substrate (at varying concentrations). An arbitrary amount of 2.5 μ g pure rGST-*Pf*PK8 enzyme was used in the initial enzyme assay with a standard reagent solution containing 2.5mM ATP and 200 μ g casein as exogenous substrate. Addition of 3 μ l of the eluted rGST-*Pf*PK8 fraction containing 2.5 – 2.73 μ g pure enzyme initiated the coupled enzyme reactions. This resulted in a decreased absorbance at 340nm and the same conditions were therefore used in downstream kinetic assays.

A standard volume (3 μ l) of the prepared rGST-*Pf*PK8 was used for each assay. After performing each assay, purified rGST-*Pf*PK8 was quantified using densitometric analysis of a Coomassie stained Laemmli SDS-PAGE gel to

determine the amount and purity of soluble rGST-PfPK8 used in the assay to calculate K_m and V_{max} values. A standard curve was constructed using different known amounts of BSA (section 2.3.5) and the concentration of rGST-PfPK8 was determined accordingly.

The reaction mixtures were set up on ice in 1.5ml Eppendorf tubes according to Table 13 and Table 14. Each 1ml solution was added to a 10mm Helma quartz cuvette (*Sigma-Aldrich Inc., USA*) and was pre-incubated for 1 minute at 37°C in the spectrophotometer followed by the addition of the enzyme (refer to Table 13 and Table 14 for volumes) before measuring and recording the decrease in absorbance at 340nm over 20 minutes at 37°C using a temperature controlled Biomate 5 spectrophotometer (*Thermo Electron Corporation, UK*) and the VISIONlite™ version 2.2 kinetics software (*Thermo Fisher Scientific, Inc., Germany*).

A blank measurement was taken for each enzyme substrate used in the assay. The blank contained the reagent solution, ATP and substrate (200µg casein, 100µg MBP or 100µg H1). The absorbance values of the blank reaction mixtures were subtracted from the experimental absorbance values to eliminate any background signal. Recombinant GST was used as the negative protein kinase activity control instead of rGST-PfPK8. The phosphorylation of glycerol (5mM) (*Saarchem Pty Ltd., South Africa*) in the presence of *Escherichia coli* glycerol kinase (*EcGK*) (*Sigma-Aldrich Inc., USA*) was used as the assay positive control.

The linear part of the reaction curve was used to calculate the initial rate of substrate conversion with NADH decreasing in an equimolar ratio to ATP converted to ADP by rGST-PfPK8.

The enzyme activity and velocity of rGST-PfPK8 in the presence of casein, MBP and H1 was calculated using the following formulas:

$$V = \frac{\Delta A_{340} \times \text{reaction volume}}{\epsilon \text{ of NADH}}$$

$$\text{Enzyme activity} = V / \text{mg enzyme}$$

Where:

V = velocity of the reaction ($\mu\text{mole}/\text{min}$)

ΔA_{340} = change in NADH absorbance measured during the linear part of curve (min)

Reaction volume = 1ml

ϵ = extinction coefficient of NADH ($\text{mM}^{-1} \text{cm}^{-1}$)

Table 13: Protein kinase assay control and blank reaction mixture (1ml) preparations.

Control/Blank sample	Reagent solution	ATP (final 2.5mM)	Substrate	Enzyme
<i>Escherichia coli</i> glycerol kinase (EcGK) blank	233 μl	25 μl of a 100mM ATP stock	50 μl of a 100% Glycerol stock	0
EcGK assay positive control	233 μl	25 μl of a 100mM ATP stock	50 μl of a 100% Glycerol stock	1 μl of a 1:100 dilution of 532U/ml EcGK stock
EcGK assay negative control (no substrate)	233 μl	25 μl of a 100mM ATP stock	0	1 μl of a 1:100 dilution of 532U/ml EcGK stock
rGST blank	233 μl	25 μl of a 100mM ATP stock	40 μl of a 5mg/ml Casein stock (final: 200 μg)	0
rGST negative control (no substrate)	233 μl	25 μl of a 100mM ATP stock	0	3 μl of a ~5 $\mu\text{g}/\mu\text{l}$ purified soluble rGST stock (final: ~15 μg)
rGST- <i>Pj</i> PK8 casein blank	233 μl	25 μl of a 100mM ATP stock	40 μl of a 5mg/ml Casein stock (final: 200 μg)	0
rGST- <i>Pj</i> PK8 MBP blank	233 μl	25 μl of a 100mM ATP stock	100 μl of a 1mg/ml MBP stock (final: 100 μg)	0
rGST- <i>Pj</i> PK8 H1 blank	233 μl	25 μl of a 100mM ATP stock	100 μl of a 1mg/ml H1 stock (final: 100 μg)	0

* The reaction mixture was made up to a final volume of 1ml using 0.1M Tris-HCl buffer with a pH of 7.4 at 37°C.

Table 14: Protein kinase assay sample reaction mixture (1ml) preparations.

Sample	Reagent solution	ATP (final: 2.5mM)	Substrate	rGST-<i>Pf</i>PK8 (final: 2.5 – 2.73µg pure enzyme)
rGST- <i>Pf</i> PK8 in the presence of exogenous Casein	233µl	25µl of a 100mM ATP stock	40µl of a 5mg/ml Casein stock (final: 200µg)	3µl
rGST- <i>Pf</i> PK8 in the presence of exogenous MBP	233µl	25µl of a 100mM ATP stock	100µl of a 1mg/ml MBP stock (final: 100µg)	3µl
rGST- <i>Pf</i> PK8 in the presence of exogenous H1	233µl	25µl of a 100mM ATP stock	100µl of a 1mg/ml H1 stock (final: 100µg)	3µl
rGST- <i>Pf</i> PK8 in the presence of exogenous casein with varying ATP concentrations	233µl	2.5µl - 200µl of a 10mM ATP stock	40µl of a 5mg/ml Casein stock (final: 200µg)	3µl

* The reaction mixture was made up to a final volume of 1ml using 0.1M Tris-HCl buffer with a pH of 7.4 at 37°C.

2.5.2 Effect of temperature on the enzyme activity of rGST-*Pf*PK8

The enzyme activity (U/mg) of rGST-*Pf*PK8 at temperatures of 26°C, 28°C, 32°C, 37°C and 40°C was spectrophotometrically determined as previously described (section 2.5.1).

A reaction mixture for each temperature was prepared according to Table 15 in 1.5ml Eppendorf tubes and kept on ice. The reaction mixture was pre-incubated for 2 minutes at the assay temperature prior to analysis using a temperature controlled Biomate 5 spectrophotometer. The reaction mixtures were made up to a final volume of 1ml and the change in absorbance at 340nm recorded as previously described (section 2.5.1). The enzyme activity of rGST-*Pf*PK8 was calculated and graphically represented using GraphPad Prism 5 for Windows version 5.01 software.

Table 15: Reaction mixture preparation used to determine the effect of temperature on rGST-*Pf*PK8 enzyme activity.

Sample	Reagent solution	ATP (final: 2.5mM)	Casein	rGST- <i>Pf</i> PK8 (final: 2.5 – 2.73µg pure enzyme)
rGST- <i>Pf</i> PK8 in the presence of exogenous Casein	233µl	25µl of a 100mM ATP stock	40µl of a 5mg/ml Casein stock (final: 200µg)	3µl

* The reaction mixture was made up to a final volume of 1ml using 0.1M Tris-HCl buffer with a pH of 7.4 at temperatures 26°C, 28°C, 32°C, 37°C and 40°C , respectively.

2.5.3 Effect of pH on enzyme activity of rGST-*Pf*PK8

The effect of a change in pH on enzyme activity of rGST-*Pf*PK8 was investigated using the spectrophotometric coupled enzyme assay previously described (section 2.5.1). A 0.1M sodium acetate buffer system was used to determine the enzyme activity of rGST-*Pf*PK8 between pH5 – 6. A 0.1M Tris-HCl buffer was used for pH 6.8 – 9.

The reaction mixtures were prepared as described in Table 16 and kept on ice until analysis. The reaction mixtures were made up to a final volume of 1ml using a buffer with the correct pH. The enzyme assays were performed as previously described in section 2.5.1.

Table 16: Reaction mixture preparation to study the effect of pH on rGST-*Pf*PK8 activity.

pH	Reagent solution	Buffer	ATP (final: 2.5mM)	Casein	rGST- <i>Pf</i> PK8 (final: 2.5 – 2.73µg pure enzyme)
pH 5 pH 5.5 pH 6	233µl	0.1M Sodium acetate	25µl of a 100mM ATP stock	40µl of a 5mg/ml Casein stock (final: 200µg)	3µl
pH 6.8 pH 7.0 pH 7.4 pH 8.0 pH 8.2 pH 9.0	233µl	0.1M Tris-HCl	25µl of a 100mM ATP stock	40µl of a 5mg/ml Casein stock (final: 200µg)	3µl

* The reaction mixture was made up to a final volume of 1ml using the various buffers described in the table at 37°C.

2.5.4 rGST-PfPK8 enzyme stability

Purified samples of rGST-PfPK8 and rGST with a known concentration and percentage purity were used to test the stability of rGST-PfPK8 every 24 hours over a period of 3 days in the presence of 73.7µl of a 5% casein stock at 37°C as previously described (section 2.5.1). The purified rGST-PfPK8 sample was stored at 4°C between readings.

2.6 Protein-protein interactions between RBCM proteins and rGST-PfPK8

2.6.1 Red blood cell membrane (RBCM) protein preparation

Red blood cell membrane (RBCM) proteins were extracted from human blood according to the method described by Coetzer and Palek (1986). Blood (6ml) was collected in ACD tubes and centrifuged at 1 200xg for 15 minutes at 4°C in an Eppendorf 5702R centrifuge. The plasma and buffy coat were aspirated from the blood cells with a Millipore Vacuum Pump Type PF 710-75 (*Millipore, South Africa*) before washing the red cells 3 times with cold 0.9% NaCl, and centrifuging each time for 10 minutes at 1 200xg at 4°C in an Eppendorf 5702R centrifuge. The saline and residual buffy coat were carefully aspirated from the cells and discarded. After the final wash 4ml freshly prepared cold lysis buffer was added to the packed red cells. The cell suspension was vortexed with a MT19 Chiltern AutoVortex mixer (*CBS Scientific, USA*) to lyse the red blood cells (RBCs) and the lysate was transferred to a pre-cooled 40ml Beckman centrifuge tube (*Beckman Coulter, USA*). Four millilitres lysis buffer was added to the ACD tube and the vortex step was repeated to maximize the yield of red cells. Lysis buffer was added to the cell lysate in the 40ml Beckman tube to a final volume of 30ml before centrifuging it at 14 000xg for 15 minutes at 4°C in a Beckman Avanti® JE centrifuge (*Beckman Coulter, USA*). The supernatant was removed and discarded. The RBC pellet was swirled thoroughly and the tightly packed button of residual white blood cells at the bottom of the centrifuge tube was removed by aspiration. The RBCMs were washed with lysis buffer 3 – 4 times

until the supernatant was clear. The supernatant was aspirated from the RBCMs after the final wash, leaving a 1:1 ratio of buffer to RBCMs. A 1:1 000 ratio of 0.1M Pefabloc (*Roche Diagnostics GmbH, Germany*) to RBCMs were added and the suspension was incubated on ice for 5 minutes. A 20µl and three 100µl aliquots were placed into 1.5ml Eppendorf tubes and prepared for SDS-PAGE protein analysis and quantitation (section 2.3.5). The remainder of RBCMs were stored at -20°C.

2.6.2 Red blood cell membrane protein (RBCM) quantitation

The Bradford colorimetric protein determination method (Bradford, 1976) is designed to quantitate 1 - 10µg of protein and was used to quantitate the extracted RBCMs. The Bradford dye assay is based on the equilibrium between three forms of Coomassie PlusTM Protein Assay Reagent dye (*Pierce, USA*). The dye is mostly stable under acid conditions as a double-protonated red form and upon binding to a protein it is stable as an unprotonated blue complex. The absorbance at 595nm of the blue protein-dye complex is spectrophotometrically determined and compared to that of different known amounts of a standard protein, bovine serum albumin (BSA). A standard curve can then be used to calculate the concentration of the RBCM proteins.

Twenty microlitres of 5N NaOH (*Saarchem Pty Ltd., South Africa*) was added to a 20µl aliquot of RBCMs (section 2.6.1), inverted to mix and kept on ice. A standard curve with duplicates ranging from 2 - 16µg using a 2mg/ml BSA stock solution was prepared in 5ml glass tubes.

Ten microlitres of the RBCM-NaOH solution was added in duplicate to 5ml glass tubes. One and a half millilitres of Coomassie PlusTM Protein Assay reagent was added to each tube including a blank with no protein present. The solutions were vortexed and incubated at room temperature for 10 minutes. The absorbance was measured at a wavelength of 595nm in 1.5ml Semi Micro UV cuvettes (*Plastibrand[®], Germany*) using a Biomate 5 spectrophotometer. A standard curve was generated and the RBCM protein concentration of the sample was automatically calculated by the VISIONliteTM software version 2.2.

2.6.3 Red blood cell membrane blot overlays

Binding studies were performed by blot overlays of extracted RBCM proteins (section 2.6.3) with purified rGST-*Pf*PK8 (section 2.3.3).

The membrane proteins were separated on 12% Laemmli SDS-PAGE gels (section 2.3.5) and 4% - 17% Fairbanks gels. The separated RBCM proteins were then transferred to nitrocellulose membranes (section 2.3.6).

2.6.3.1 Dot blots

rGST-*Pf*PK8 (16µg - 20µg), RBCM proteins (5µg, 7.5µg, 10µg) and rGST (approximately 20µg) (section 2.3.3) were slowly spotted in duplicate onto two HybondTM-C nitrocellulose membranes using a pipette. The membranes were allowed to air dry.

2.6.3.2 SDS-PAGE gel blots

Gradient Fairbanks gels (4% - 17%) were prepared according to the method described by Fairbanks *et al.* (1971). The gel solutions were prepared as set out in Table 17.

Table 17: Fairbanks SDS-PAGE gel solutions.

Reagent	4%	17%
	Volume (ml)	
40% Acrylamide + 1.5% Bis-acrylamide	3.4	3.4
10x TAE buffer	3.4	0.8
10% SDS	0.68	0.16
25% Glycerol	-	2
Milli-Q water	26.109	0.94
10% APS	0.4	0.2
0.5% TEMED	0.011	0
TEMED	-	0.5

Eighteen micrograms RBCM proteins and 20µg RBCM proteins were loaded next to each other in triplicate on the gel and electrophoresed in a Hoefer SE400 Sturdier Vertical Electrophoresis system (*Hoefer Scientific Instruments, USA*) for 17 hours at room temperature in Fairbanks running buffer (1x TAE, 0.1% SDS) at 45V. The lanes were carefully cut out to have three separate gel sections, each with 18µg and 20µg separated RBCM proteins. Three Laemmli SDS-PAGE gels were loaded with 5µl Page Ruler™ Prestained Protein Ladder (*Fermentas Inc., Canada*), 5µg BSA (negative control), 5µg rGST (negative control) (section 2.3.3), 0.8µg – 1.2µg rGST-PfPK8 (positive control), 5µg RBCM proteins, 7.5µg RBCM proteins and 10µg RBCM proteins and electrophoresed as previously described. The proteins of two Fairbanks unstained gel sections and two Laemmli unstained gels were transferred onto a Hybond™-C nitrocellulose membranes overnight (section 2.3.6). The other gels were stained with Coomassie blue (section 2.3.5).

2.6.3.3 Blot overlays

The blots were blocked for 1 hour in 5% BSA in TBS (w/v) at room temperature. One membrane and one dot blot were placed in 6ml 50mM Tris-HCl buffer (pH 7.5) containing 182 - 200 µg pure rGST-PfPK8. The duplicate nitrocellulose membranes were used as controls and were placed in 6ml 50mM Tris-HCl buffer (pH 7.5). The membranes were incubated for 2.5 hours with constant gentle shaking at room temperature. The membranes were then washed three times for 10 minutes each in TBST and once in TBS to remove all unbound proteins. The proteins were fixed on the membranes for 20 minutes with 0.5% formaldehyde (*Sigma-Aldrich Inc., USA*) in TBS (v/v) before incubating for 20 minutes with 2% glycine in TBS (w/v) at room temperature to inactivate reactive aldehyde groups that are still present on the membranes (Tisdale, 2002). The membranes were washed three times in TBST followed by one 10 minute wash in TBS before incubating them for 1 hour at room temperature in 1:100 000 anti-GST HRP-conjugated primary anti-body. The membranes were washed three times in TBST followed by one 10 minute wash in TBS to remove any unbound antibody. The antibody was detected by chemiluminescence using the SuperSignal® West Pico

Chemiluminescent Substrate and the nitrocellulose membranes were stained with amido black as described in section 2.3.6.

2.7 Bio-informatic analysis of *Pf*PK8

2.7.1 Sequence alignment of *Pf*PK8 with other protein kinases

The *Pf*PK8 protein sequence of the cloned region (Figure 5) was submitted in FASTA format to the Basic Local Alignment Search Tool version 2.2.27 (BLAST) (<http://blast.ncbi.nlm.nih.gov>) to identify possible homologues of the target protein sequence.

N-terminal end

EKDGYEEMNGGDKNEEMNGGDKNEEMNVGDKNGGIEHKNEGINEEEHKDELINKEHKNE
RINEEHKNERINEEHKNEGINEEEHKNEGINEEEHKNERINEEHKNEGINEEKLTYHNMKNNNIS
NENNYNDDDSYDEDNLVSLKIINLKYLSSKNSLKNILREVNFKMCEHPNVVKYFESFFWP
PCYLVIVCEYLSGGTLYDLKKNYGRISEDLLVYILDDVLNGLNYLHNECSSPLIHRDIKPTN
IVLSKDGIAKIIDFGSCEELKNSDQSKELVGTIYYISPEILMRTNYDSSDIWSLGITIYEIVLCT
LPWKRNRQSFENYIKTIINSSPKINITEGYSKHLCYFVEKCLQKKPENRGNVVDLLNHNKFLIK
KRYIKKKPSSIYEIRDILKIYNGKGKTNIFRNFFKNLFFFNDKNKKKPNKMISSKSCDAEMF
FEQLKRENFDFEIKLKDDENSRLNTFNINISKERDDISYSSLNLEKIKEHSLNMVASVVG
TEQQK

C-terminal end

Figure 5: Protein sequence of the cloned region of *Pf*PK8 (PlasmoDB version 8.1, 2011).

The black amino acids indicate the cloned region of *Pf*PK8 (497 aa) with the central kinase domain (274 aa) denoted in red.

2.7.2 Structure prediction of recombinant *Pf*PK8

The complete protein sequence of *Pf*PK8 (2 485 aa) (Appendix section 7.3.2) was used to perform an in-silico 3D structural prediction of the target enzyme, using the protein-homology/analogy recognition engine (Phyre2) (<http://www.sbg.bio.ic.ac.uk/phyre2/html/page.cgi?id=index>) and the ExPASy Bio-informatics Resource Portal SWISS-MODEL version 8.05 Workspace (<http://swissmodel.expasy.org/workspace/>) (Arnold *et al.*, 2006; Schwede *et al.*, 2003; Guex and Peitsch, 1997). This approach compares the target protein to the 3D structure of its homologues in the Protein Data Bank. This template-based homology modelling is the most reliable approach to protein structure prediction and relies on experimentally determined structure by X-ray crystallography.

The cloned kinase domain of *PfPK8* (497 aa) (Appendix section 7.3.2) without an affinity tag (Figure 5) was submitted to Phyre2 and the predicted secondary structure including various proposed characteristics of the enzyme were retrieved.

2.7.3 *PfPK8* protein parameter prediction

The theoretical pI, molecular weight, amino acid composition, half-life and stability of *PfPK8* were predicted using the ProtParam tool (<http://web.expasy.org/protparam/>) on the ExPASy Bioinformatics Research Portal. ProtParam allows the in-silico computational prediction of physical and chemical parameters of a given protein sequence (Gasteiger *et al.*, 2005).

The cloned protein kinase region of *PfPK8* with an N-terminal glutathione-S-transferase tag (Appendix section 7.3.3) and a C-terminal octa-histidine tag were submitted to ProtParam to obtain the protein parameters for the recombinant proteins of interest.

3 RESULTS

3.1 *Plasmodium falciparum* culturing

Plasmodium falciparum cultures were maintained at a parasitaemia of 5% - 10%. The parasites within the erythrocytes were stained blue-purple (Figure 6) using the Rapindiff Staining Kit.

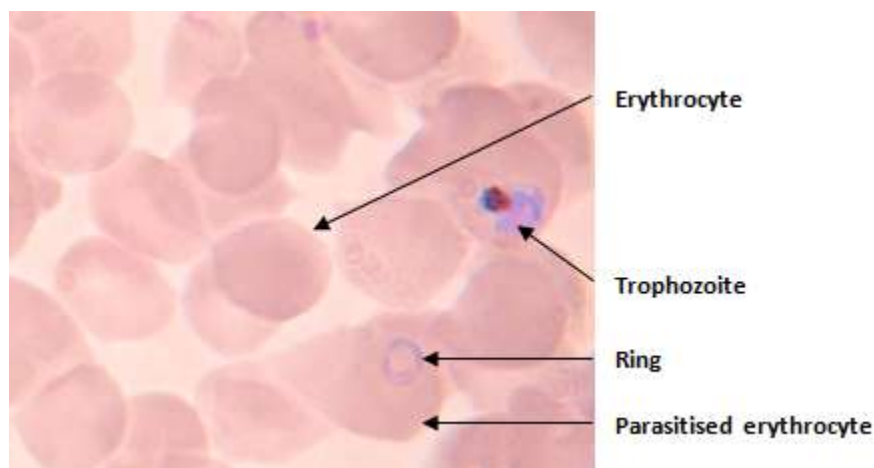


Figure 6: Photograph of the ring and trophozoite intra-erythrocytic stages of *Plasmodium falciparum*.

3.2 *Plasmodium falciparum* DNA extraction

Plasmodium falciparum (3D7) DNA was extracted from parasitised erythrocytes and the purity and concentration were spectrophotometrically determined. The ratios of absorbance at 260nm and 280nm (A_{260}/A_{280}) of samples 1, 3 and 4 were greater than 2 (Table 18) indicating RNA contamination as shown on the agarose gel (Figure 7). Pure DNA has an A_{260}/A_{280} of between 1.8 and 2. The DNA was intact and was seen as a high molecular weight band on the gel.

Table 18: Spectrophotometric data of *Plasmodium falciparum* 3D7 genomic DNA.

3D7 DNA sample	Concentration (ng/ μ l)	A_{260}/A_{280}	Total DNA	
			μ l	μ g
1	230	2.29	30	7
2	591	1.98	30	18
3	313	2.41	30	9
4	291	2.16	30	9

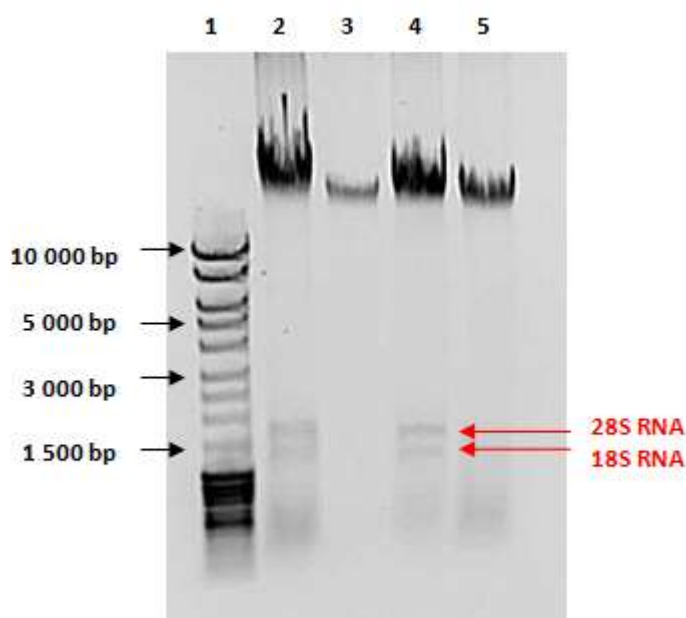


Figure 7: *Plasmodium falciparum* 3D7 genomic DNA resolved on a 0.8% agarose gel.

Lane 1 – MassRuler DNA Ladder Mix (5 μ l), Lane 2 – DNA sample 1, Lane 3 – DNA sample 2, Lane 4 – DNA sample 3, Lane 5 – DNA sample 4. Samples 1, 3 and 4 are contaminated with RNA.

The DNA samples were treated with ribonuclease A (RNase A) to remove the RNA contamination in the samples. DNA samples with an absorbance ratio between 1.6 and 1.9 were considered pure enough and used for downstream applications. DNA samples 1 and 2 and samples 3 and 4 were pooled and yielded better A_{260}/A_{280} ratios (Table 19). The samples were free from RNA and the integrity of the DNA was maintained as seen on the agarose gel (Figure 8).

Table 19: Spectrophotometric data of pooled *Plasmodium falciparum* 3D7 genomic DNA after RNase A treatment.

3D7 DNA sample	Concentration (ng/ μ l)	A_{260}/A_{280}	Total DNA	
			μ l	μ g
1+2	447	1.88	30	13.41
3+4	480	1.90	30	14.40

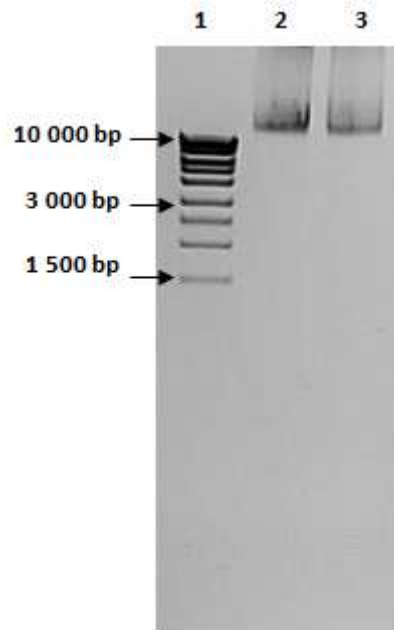


Figure 8: RNase A-treated *Plasmodium falciparum* 3D7 genomic DNA resolved on a 0.8% agarose gel.

Lane 1: MassRuler DNA Ladder High Range (5 μ l), Lane 2: Pooled DNA samples 1+2 (~ 200ng), Lane 3: Pooled DNA samples 2+3 (~ 200ng).

3.3 Amplification of the kinase domain of *PfB0150c*

The *PfB0150c* gene consists of a single exon and is situated on chromosome 2 of the *P. falciparum* genome. The gene has Crick-orientation, meaning that the coding sequence is found on the antisense (3' to 5') strand of the chromosomal DNA (Figure 9). The 7.457 kb gene spans from base pair 149 524 to base pair 156 981 according to PlasmoDB version 8.3, 2011.

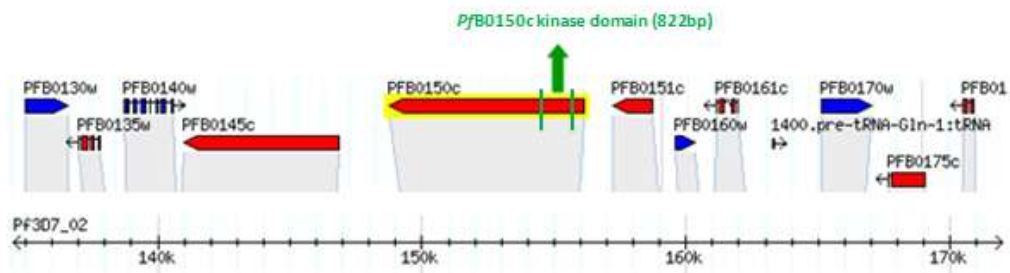


Figure 9: A section of chromosome 2 of the *Plasmodium falciparum* genome (PlasmoDB version 8.1, 2011).

PfB0150c codes for a *P. falciparum* putative protein kinase 8 (*PfPK8*). The predicted kinase domain of *PfPK8* was subcloned. A 1 507bp fragment of the *PfB0150c* gene containing the centrally located predicted kinase domain (822bp) was chosen for subcloning because the entire gene coding for *PfPK8* was too large to amplify and express. Flanking primers were designed to amplify the 1 507bp fragment (Figure 10) and an extra base (Figure 11) was added to the forward primer to ensure that the codons were in-frame.

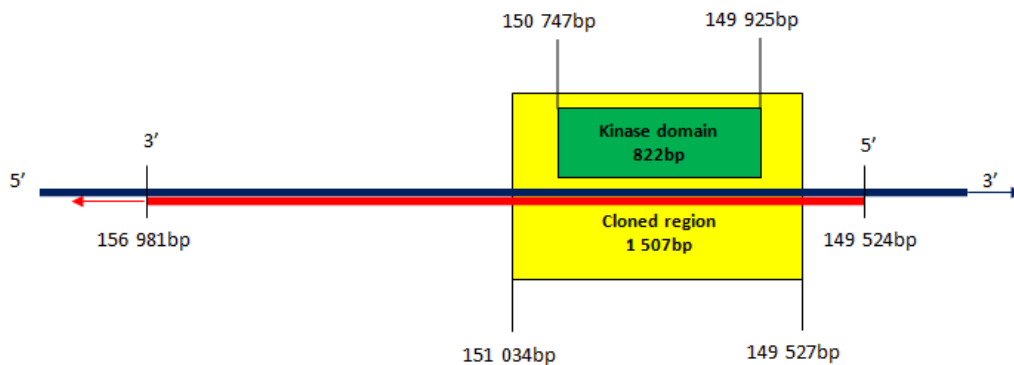


Figure 10: Diagrammatic representation of *PfB0150c* and the sections of interest. *Plasmodium falciparum* chromosome 2 is represented by the blue bar. The *PfB0150c* gene (red bar) consists of a single exon 7 458bp in length and has Crick orientation. The kinase domain is central to the amplified region.

5'

GATCC**T**GATGAAAAGGATGGATATGAAAGAAATGAATGGGGGAGATAAGAATGAAGA
AATGAATGGGGGAGATAAGAATGAAGAAATGAATGTGGGAGATAAAAAATGGAGGAA
TAAATGAGGAACATAAAAAATGAGGAATAAATGAGGAACATAGGATGAACTAATAAA
TAAGGAACATAAAAAACGAGCGAATAAATGAGGAACATAAAAAACGAACGAATAAATG
AGGAACATAAAAAATGAAGGAATAAATGAGGAACATAAAAAATGAAGGAATAAATGAGA
ACATAAAAAACGAA**CGAATAAATGAGGAACATAAAAAATGAAGGAATAAATAAACTGA**
CCTATCATAATATGAATAAAAAATAATTTTCAAATGAAAATAATTATAAGATGACGAT
TCTTATGATGAAGATAATTTGGTATCCCTGAAGATAATAAACTTAAAAATATTTAAGTA
AAAAGAATAGTTTAAAAAACATTTTGAGAGAAGTAAATTTTTTAAAAATGTGTGAAC
ATCAAATGTAGTAAAAATATTTTGAATCTTTTTTTTGGCCTCCTTGTTATTTAGTTATTGT
GTGTGAATATTTATCAGGAGGAACATTATATGATTTATATAAAAAATTATGGTAGAATA
TCAGAAGATCTTTAGTATATATCTTAGATGATGTATTAAATGGTTTAAATTATTTACAT
AATGAATGTAGTTCACCACTTATACATAGAGATATAAAACCAACAAATATCGTTCCTT
CCAAAGATGGTATAGCTAAGATATTGATTTTGGTTCTTGTGAAGAATTGAAAAATAGT
GATCAGTCTAAAGAATTAGTGGGTACTATATATTATATATCACCTGAAATATTGATGA
GACTAATTATGATTGTTTCATCTGATATATGGTATTGGGTATTACAATATATGAAATT
GTTTTATGTACCTTACCATGGAAAAGAAATCAATCATTGAAAATTATATAAAAAACCA
TAATTAATTCATCACCAAAAAATTAACATAACAGAAGGATATAGTAACACTTATGTTAT
TTTGTTGAGAAAGTGTTTACAAAAGAAACCTGAGAACAGAGGAAATGTGAAAGATTTA
TAAATCATAAATTTTTGATTAAAAAGAGGTATATTA AAAAGAAACCTAGTTCTATTA
TGAAATAAGAGATATATTA AAAATATATAATGGTAAAGGTAAAACAAATATCTTCCG
AAATTTTTTTTAAAGAACCTTTTTTCTTCAATGATAAAATAAAAAAAAAAAAAACCAATA
AAATGATCATTCCAAATCCTGTGATGCAGAAATGTTCTTTGAACAGTTAAAAAGGGAA
AATTTTGATTTTTTTGAAATTAAATTA AAAAGATGATGAAAATAGTAGATCCTTGAATA
CGTTTAATATAAATATATCTAAGAAAGAGACGACATATCATATTCTTCTTAAATTTGG
AAAAATCAAAGAACAGTCTCAATATGGTAGCATCTGTTGTCGGG**ACTGAACAATC**
CCAGAACTCGAG 3'

Figure 11: Region of *Pf*B0150c used for subcloning.

Primer positions are indicated in green. The restriction sites are included. The red segment denotes the kinase domain (822bp) of *Pf*B0150c. An extra base (purple) was added to the forward primer to ensure that the codons are in-frame.

PCR reactions were performed with GoTaq[®] Green Master Mix to determine optimal DNA concentrations, primer concentrations and annealing temperature. The optimised parameters were then used for the Expand High Fidelity enzyme system. The purified amplicons of the correct size (1 507bp) are shown in Figure 12.

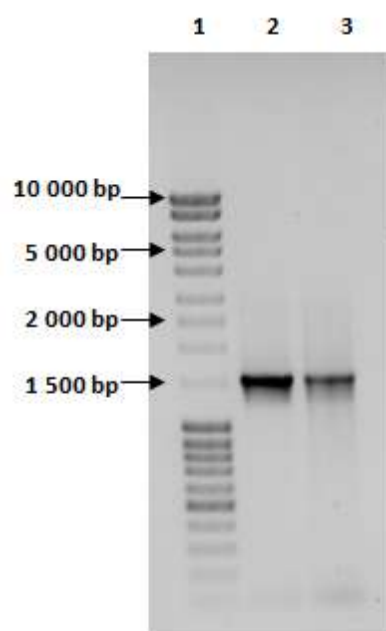


Figure 12: *PfB0150c* amplicons resolved on a 0.8% agarose gel.

Lane 1: MassRuler DNA Ladder Mix (2µl), Lane 2: 10µl PCR product (sample 1), Lane 3: 10µl PCR product (sample 2). The size of the resolved bands is approximately 1500bp, as expected.

The concentration of the amplicons was spectrophotometrically determined (Table 20) before cloning into the pTriEx-3 expression vector.

Table 20: Spectrophotometric data of the purified *PfB0150c* amplicons.

<i>PfB0150c</i> amplicon	Concentration (ng/µl)	Total	
		µl	µg
Sample 1	670	50	33.50
Sample 2	540	50	27

3.4 Cloning

3.4.1 Plasmid preparation

Transformed *Escherichia coli* Rosetta (DE3) cells were used to extract recombinant pGEX-4T-2-*PfB0150c* plasmid DNA (6 466bp) (clone was donated by Brigit Smit, previous member of the *Plasmodium* Molecular Research Unit), pGEX-4T-2 control plasmid DNA (4 970bp) and pTriEx-3 plasmid DNA (5

082bp). The concentration and purity of the extracted plasmids were spectrophotometrically determined (Table 21) and the integrity assessed by agarose gel electrophoresis (Figure 13 and 14). The plasmid DNA resolved into multiple bands representing the native plasmid conformations (super-coiled, coiled and circular).

Table 21: Spectrophotometric data of extracted plasmid DNA.

Plasmid sample	Concentration (ng/ μ l)	A_{260}/A_{280}	Total DNA	
			μ l	μ g
pGEX-4T-2- <i>Pf</i> B0150c	68	1.93	100	6.8
pGEX-4T-2	73	1.99	100	7.3
pTriEx-3	85	1.89	100	8.5

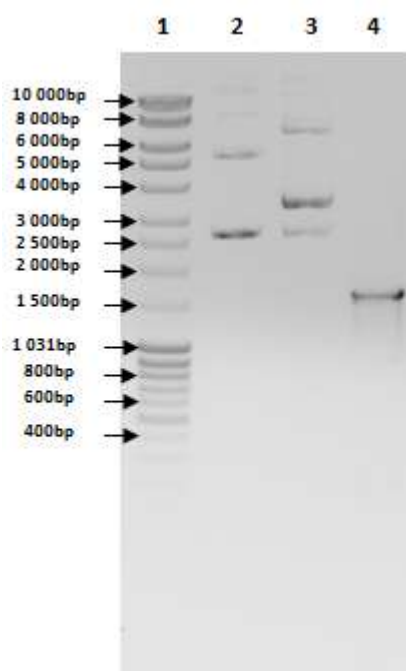


Figure 13: Recombinant pGEX-4T-2-*Pf*B0150c and pGEX-4T-2 plasmid DNA.

Lane 1: MassRuler DNA Ladder Mix (5 μ l), Lane 2: pGEX-4T-2 (4 970bp) (200ng), Lane 3: pGEX-4T-2-*Pf*B0150c (6 466bp) (200ng), Lane 4: *Pf*B0150c amplicon (1 507bp) (100ng). The DNA bands migrated slightly higher than expected.

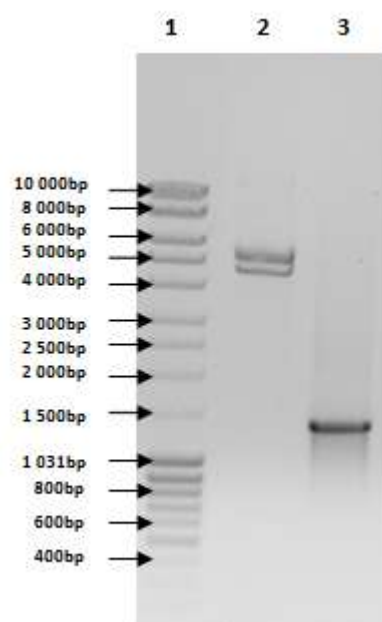


Figure 14: Agarose gel of DNA samples used for cloning the *PfB0150c* amplicon into the pTri-Ex-3 expression vector.

Lane 1: MassRuler DNA Ladder Mix (5µl), Lane 2: pTriEx-3 expression vector DNA (200ng) with a size of 5 082bp, Lane 3: *PfB0150c* amplicon (200ng) with a size of 1 507bp.

3.4.2 Restriction endonuclease digestion and ligation

pTriEx-3 plasmid DNA and the *PfB0150c* amplicon were digested with *Bam*HI and *Xho*I endonucleases to linearise the plasmid and to create compatible ends for cloning. The vector and amplicon were resolved on an agarose gel (Figure 15) and the amounts quantitated by densitometry to calculate the 4:1 molar ratio of amplicon to vector for the ligation reaction.

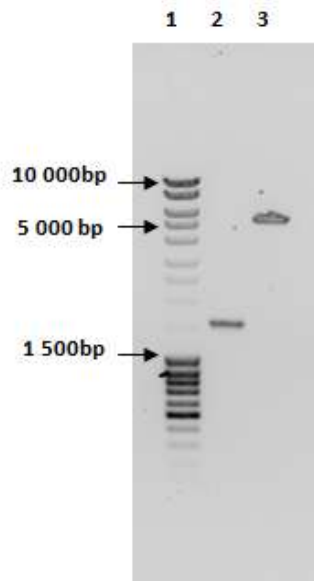


Figure 15: Digested *PfB0150c* amplicon and pTriEx-3 expression vector resolved on a 0.8% agarose gel.

PfB0150c and pTriEx-3 expression vector were digested using endonucleases *Bam*HI and *Xho*I. Lane 1: MassRuler DNA Ladder Mix (5μl), Lane 2: *PfB0150c* amplicon (100ng) (1 507bp), Lane 3: linearized pTriEx-3 plasmid (100ng) (5 082bp).

3.4.3 Transformation of *Escherichia coli* DH5α cells with *PfB0150c*-pTriEx-3

After ligation of pTriEx-3 (5 082bp) with the amplicon *PfB0150c* (1 507bp), *Escherichia coli* DH5α cells were transformed with recombinant *PfB0150c*-pTriEx-3. Colonies were screened by PCR using primers specific for *PfB0150c* to determine which transformed bacterial colonies contained the target insert. Colonies 1 and 3 contained the *PfB0150c* insert, as seen in lanes 2 and 4 of Figure 16. The amplified insert migrated to approximately 1 500bp, as expected. The dark bands at the bottom of the gel are presumably primer-dimers that formed during the PCR process due to non-specific annealing and primer elongation.

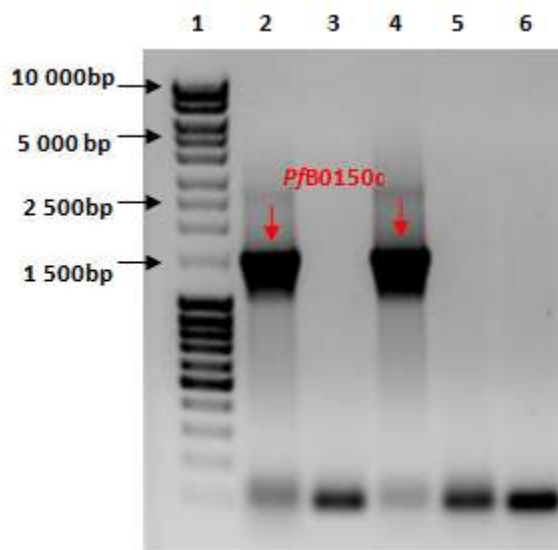


Figure 16: Positive colony selection PCR of *Escherichia coli* DH5 α cells transformed with recombinant *PfB0150c*-pTriEx-3 resolved on a 0.8% agarose gel.

Lane 1: MassRuler DNA Ladder Mix (5 μ l), Lane 2 - 4: PCR product from bacterial colonies 1 to 3 from the recombinant *PfB0150c*-pTriEx-3 culture plate, Lane 5: Bacterial colony from the pTriEx-3 control culture plate, Lane 6: No DNA PCR control. An insert with the correct size of 1 507 (red arrows) was amplified using primers specific for the amplified region of *PfB0150c*. Colonies 1 and 3 were positive for recombinant *PfB0150c*-pTriEx-3.

Restriction digests with endonucleases *Bam*HI and *Xho*I were carried out on plasmids extracted from transformed *Escherichia coli* DH5 α colonies 1 and 3 (Table 22) to confirm that the *PfB0150c* insert was the correct size, prior to sequence analysis (Figure 17).

Table 22: Plasmids from *Escherichia coli* DH5 α colonies transformed with *PfB0150c*-pTriEx-3.

Plasmid sample	Concentration (ng/ μ l)	A_{260}/A_{280}	Total plasmid DNA	
			μ l	μ g
<i>PfB0150c</i> -pTriEx-3 from colony 1	59	1.92	100	5.9
<i>PfB0150c</i> -pTriEx-3 from colony 3	60	1.93	100	6.0
pTriEx-3 from control colony	57	1.91	100	5.7

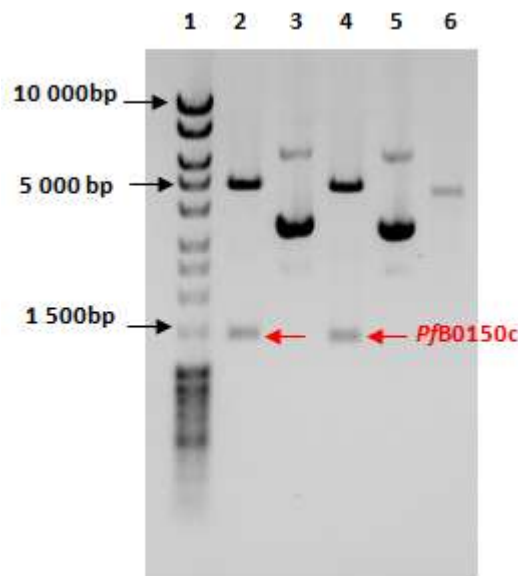


Figure 17: Restriction endonuclease digestion of plasmid DNA extracted from DH5 α cells transformed with recombinant *P/B0150c*-pTriEx-3.

The plasmids were digested with *Bam*HI and *Xho*I and electrophoresed on a 0.8% agarose gel to verify that the cells contained the *P/B0150c* insert (1 507bp). Lane 1: MassRuler DNA Ladder Mix (5 μ l), *P/B0150c*-pTriEx-3 construct 1 digested (Lane 2) and undigested (Lane 3), *P/B0150c*-pTriEx-3 construct 3 digested (Lane 4) and undigested (Lane 5), Lane 6: digested control plasmid TriEx-3 (5 083bp) resolved as only one band due to the *P/B0150c* insert not being present.

The digested *P/B0150c*-pTriEx-3 (6 590bp) constructs resolved as two distinct bands. One with the approximate size of the amplicon (1 507bp) and the other with the approximate size of the pTriEx-3 vector (5 083bp). The undigested *P/B0150c*-pTriEx-3 constructs resolved as multiple bands which is indicative of the native plasmid conformations. The digested control plasmid TriEx-3 migrated lower than the recombinant plasmids due to the absence of the amplicon (Figure 17).

3.4.4 Sequence analysis of recombinant *P/B0150c*-pTriEx-3

P/B0150c-pTriEx-3 construct 3 was sequenced with forward and reverse vector specific pTriEx-3 primers (Inqaba).

The forward primer yielded a good read from base pair 1 of the *P/B0150c* insert to base pair 898. The reverse primer covered base pairs 1 507 to 898. Refer to Appendix section 7.3.7 for the complete sequence chromatograms. The chromatogram for the 5' section of the *P/*PK8 DNA sequence (Figure 18) sequenced using the forward primer resolved with high amplitude peaks which

were distinct and a low baseline noise. This is an indication that the sequence is of a high quality. The peaks at the 3' end had lower amplitude, overlapped and deteriorated quite rapidly. To ensure reliable sequence data and complete coverage of *PfPK8*, the DNA was also sequenced from the 3' end using a reverse primer specific for the vector (Figure 19).

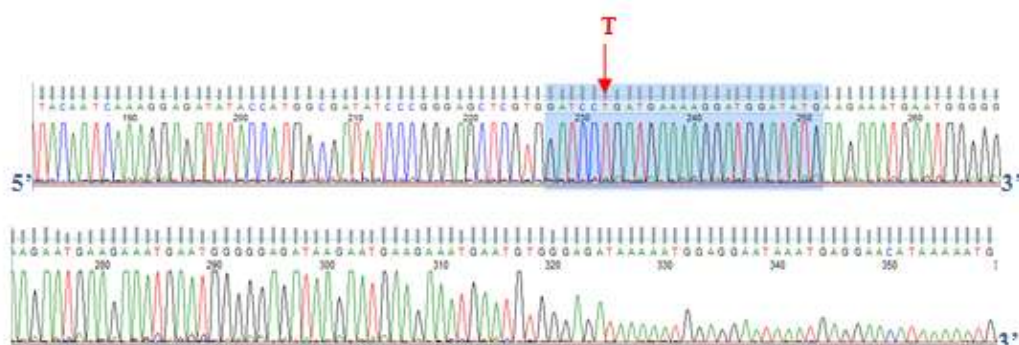


Figure 18: A section of the sequence chromatogram of recombinant *PfB0150c-Tri-Ex-3* construct 2 sequenced with a forward vector-specific primer.
The *PfB0150c* forward primer is highlighted in blue with the added base to ensure the correct reading frame indicated in red.

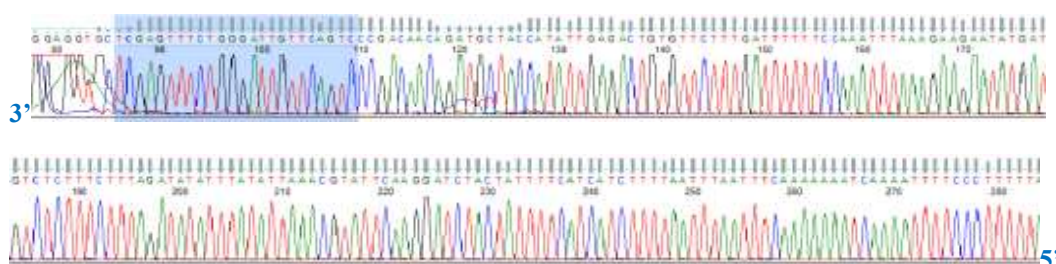


Figure 19: A section of the sequence chromatogram of recombinant *PfB0150c-Tri-Ex-3* construct 2 sequenced with a reverse vector-specific primer.
The *PfB0150c* reverse primer is highlighted in blue.

The two sequences were aligned (Figure 20) to confirm that the sequence of the amplified region of *PfB0150c* subcloned into the pTriEx-3 expression vector was identical to the original sequence obtained from the PlasmDB version 8.1 (2011) database.

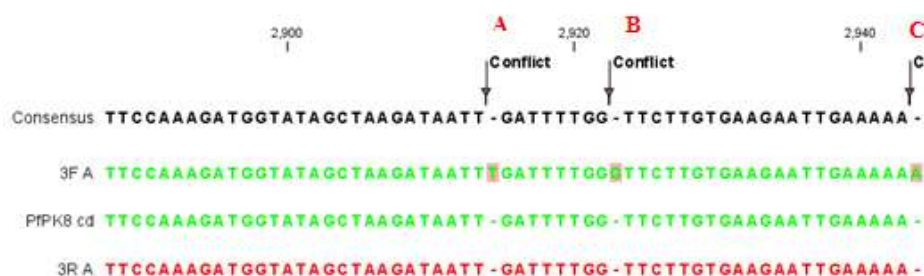


Figure 20: A section of the sequence alignment of the rPfB0150c-pTriEx-3 construct 2 sequence.

The DNA sequences of the subcloned *PfB0150c* sequenced using a forward (3F A, green) and reverse (3R A, red) vector specific primer were aligned with the original *PfB0150c* functional region sequence (green) obtained from the PlasmDB version 8.1 (2011) database. The consensus sequence is indicated in black.

A non-alignment is indicated by a conflict-flag in the consensus sequence (black). Three conflicts are illustrated in Figure 20, where the forward primer sequence contained an extra base, presumably due to sequencing artefacts. Since the reverse sequence corresponded to the PlasmDB sequence, the insert sequence was presumed to be correct. Refer to Appendix section 7.3.8 for the complete sequence alignment.

3.4.5 Transformation of *Escherichia coli* Rosetta 2 (DE3) cells with *PfB0150c*-pTriEx-3

Escherichia coli Rosetta 2 (DE3) cells supply tRNAs driven by their native promoters for codons rarely used in *Escherichia coli* and these cells were therefore transformed with recombinant *PfB0150c*-pTriEx-3 plasmid. Universal translation of the protein product of *PfB0150c*, designated as rPfPK8-His, in *Escherichia coli* Rosetta 2 (DE3) was now possible which would have been limited when expressing this plasmodial protein in *Escherichia coli* DH5α cells.

Transformation was verified by colony plasmid digestion with *Bam*HI and *Xho*I (Figure 21). *PfB0150c*-pTriEx-3 digested with both restriction enzymes yielded two bands (Lane 4 of Figure 21) as expected. A band with a size of approximately 6 000bp (pTriEx-3 vector, 5 082bp) and a band of approximately 1 500bp indicating the presence of the *PfB0150c* insert.

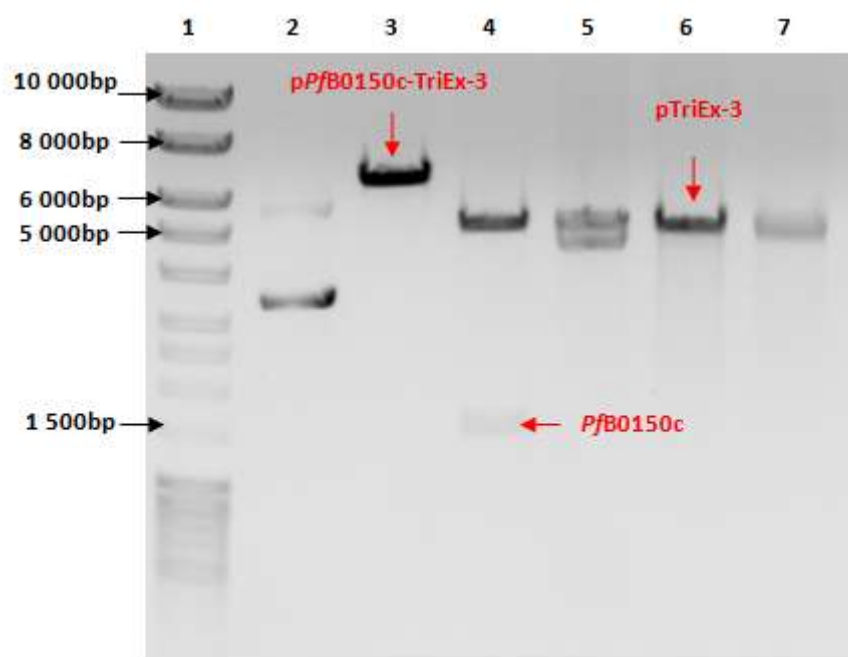


Figure 21: Digested recombinant plasmids (*PfB0150c*-pTriEx-3) extracted from transformed *Escherichia coli* Rosetta 2 (DE3) cells.

Lane 1: MassRuler DNA Ladder Mix (5µl), Lane 2: undigested recombinant *PfB0150c*-pTriEx-3, Lane 3: *PfB0150c*-pTriEx-3 digested with *Xho*I (5 083bp), Lane 4: *PfB0150c*-pTriEx-3 (6 590bp) digested with *Xho*I and *Bam*HI, Lane 5: undigested pTriEx-3, Lane 6: pTriEx-3 digested with *Xho*I (5 082bp), Lane 7: pTriEx-3 digested with *Xho*I and *Bam*HI.

3.5 Expression of recombinant r*Pf*PK8-His protein

The pTriEx-3 vector allows for rapid expression of recombinant eukaryotic proteins in prokaryotic, eukaryotic and mammalian expression systems. Protein expression in *Escherichia coli* bacterial cells, *Spodoptera frugiperda* insect cells and vertebrate cells are possible with a single recombinant pTriEx-3 plasmid.

Recombinant *Pf*PK8-His is 505 amino acids in length and contains a C-terminal octa-Histidine tag (Figure 22). It has a predicted size of approximately 60kDa.

N-terminal end

EKDGYEEMNGGDKNEEMNGGDKNEEMNVGDKNGGIEHKNEGINEEEHKDELINKEHKNE
RINEEHKNERINEEHKNEGINEEEHKNEGINEEEHKNE **RINEEHKNEGIN**KLTYHNMNKNNIS
NENNYNDDDSYDEDNLVSLKIINLKYLSKKNSLKNILREVNFKMCEHPNVVKYFESFFWP
PCYLVIVCEYLSGGTLYDLYKNYGRISEDLLVYILDDVLNGLNYLHNECSSPLIHRDIKPTN
IVLSKDGIAKIIDFGSCEELKNSDQSKELVGTIYYISPEILMRTNYDSSDIWSLGITIYEIVLCT
LPWKRNQSFENYIKTIINSSPKINITEGYSKHLCYFVEKCLQKKPENRGNVVDLLNHNKFLIK
KRYIKKKPSSIYEIRDILKIYNGKGKTNIFRNFFKNLFFFNDKNKKKPNKMISSKSCDAEMF
FEQLKRENFDFFEIKLKDDENSRLNTFNINISKERDDISYSSLNLEKIKEHSLNMVASVVG
TEQK**HHHHHHHH**

C-terminal end**Figure 22: Protein sequence of the translated rPfPK8-His protein.**

The black amino acids indicate the cloned region of *Pf*PK8 (497 aa) with the central kinase domain (274 aa) (red). The blue amino acids are the octa-Histidine tag, encoded by the vector, which is located on the C-terminal end of the recombinant proteins.

3.5.1 Prokaryotic protein expression of rPfPK8-His

Twenty milliliters *Escherichia coli* Rosetta 2 (DE3) cells containing the recombinant plasmid *Pf*B0150c-pTriEx-3 (6 590bp) were induced to express rPfPK8-His. Recombinant protein was purified and protein fractions were collected throughout the purification process, separated on a Laemmli SDS-PAGE gel (Figure 23) and analysed by immunoblotting (Figure 24).

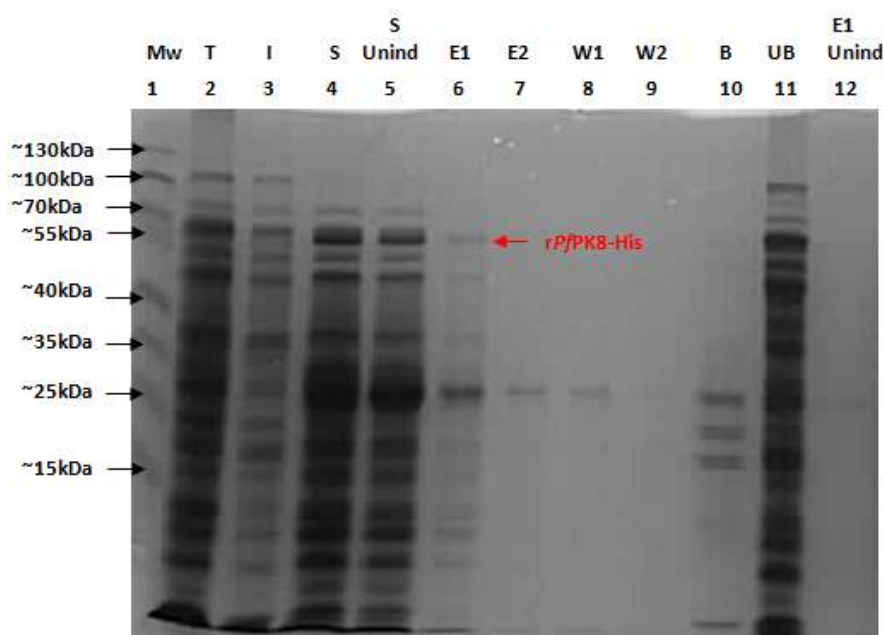


Figure 23: Coomassie stained 12% Laemmli gel of purified rPfPK8-His from a 20ml *Escherichia coli* Rosetta 2 (DE3) culture.

Lanes 2 – 11 are protein samples from an induced 20ml *Escherichia coli* Rosetta 2 (DE3) pPfB0150c-TriEx-3 culture. The protein fractions were electrophoresed in the following order: Lane 1: PageRuler Pre-stained protein ladder (5µl), Lane 2: Total protein fraction (5µl out of 10ml), Lane 3: Insoluble proteins (5µl out of 10ml), Lane 4: Soluble proteins (5µl out of 10ml), Lane 5: Soluble proteins of uninduced (5µl out of 10ml), Lane 6: Elution 1 (10µl out of 100µl), Lane 7: Elution 2 (10µl out of 100µl), Lane 8: Wash 1 (10µl out of 150µl), Lane 9: Wash 2 (10µl out of 150µl), Lane 10: MagneHis Nickel beads (10µl out of 100µl), Lane 11: Unbound protein fraction (10µl out of 10ml), Lane 12: Elution 1 of an uninduced rPfB0150c-His culture (10µl out of 100µl). A prominent unidentified histidine-containing protein contaminant was visualised in elution 1 and 2 with a size of ~25kDa.

Recombinant rPfPK8-His was visible in the insoluble fraction. This is an indication that some inclusion bodies formed. A major band with a size between 25 – 35kDa was observed in the elution fractions and in wash 1. The soluble fraction was purified on Nickel-containing MagneHisTM beads and proteins with no affinity for the MagneHisTM beads were washed from the beads in three wash steps. Recombinant PfPK8-His was not detected in the washes. The unbound fraction had a high protein concentration as expected. Proteins not eluted from the beads are present in the bead fraction. No residual rPfPK8-His was detected, indicating that the elution conditions were appropriate to elute all of the target protein from the MagneHisTM beads. A major contaminant with a size between 25 – 35kDa was observed in the elutions.

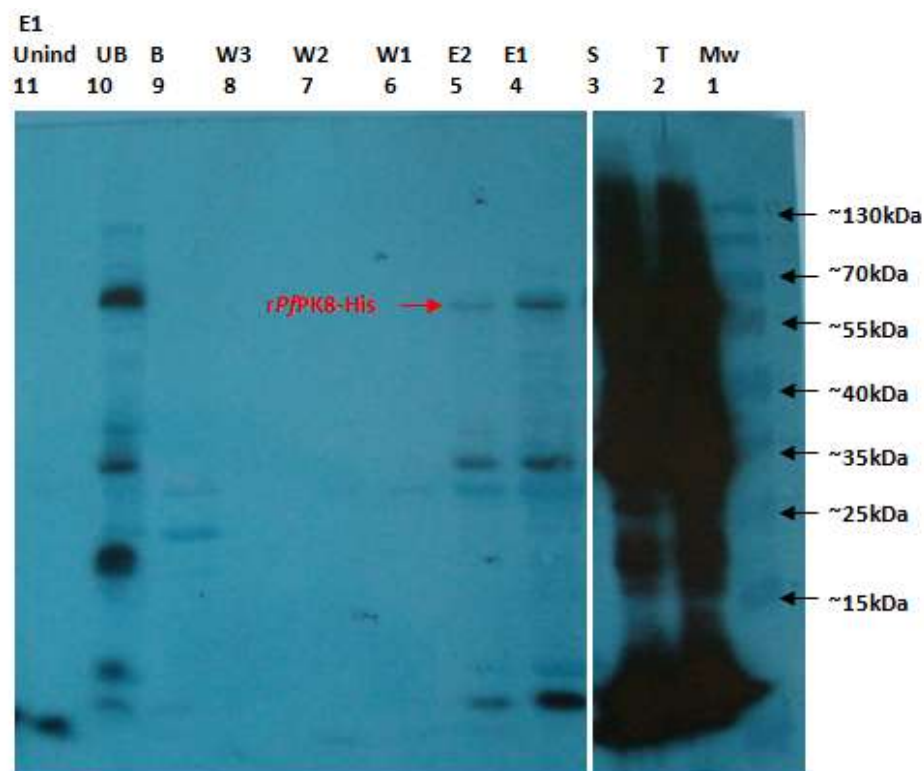


Figure 24: Immunoblot of rPfPK8-His proteins.

Stained nitrocellulose membrane overlaid with autoradiograph. Lanes 2 – 10 are electrophoresed proteins from purification samples of an induced 20ml *Escherichia coli* Rosetta 2 (DE3) pPfB0150c-TriEx-3 culture that were transferred to nitrocellulose membranes and probed with Anti-His HRP conjugated antibody. The protein fractions were electrophoresed in the following order: Lane 1: PageRuler Pre-stained protein ladder (5µl), Lane 2: Total protein fraction (5µl out of 10ml), Lane 3: Soluble proteins (5µl out of 10ml), Lane 4: Elution 1 (10µl out of 100µl), Lane 5: Elution 2 (10µl out of 100µl), Lane 6: Wash 1 (10µl out of 150µl), Lane 7: Wash 2 (10µl out of 150µl), Lane 8: Wash 3 (10µl out of 150µl), Lane 9: MagneHis Nickel beads (10µl out of 100µl), Lane 10: Unbound protein fraction (10µl out of 10ml), Lane 11: Elution 1 of an uninduced rPfB0150c-His culture (10µl out of 100µl). An unidentified histidine-containing protein was visualised in elution 1 and 2 with a size between 25 – 35kDa.

The dark bands detected by the anti-His antibody in the total fraction of the rPfPK8-His immunoblot (Figure 24) were partly due to overloading of the gel, giving rise to non specific bands, but also reflected histidine-rich *Escherichia coli* proteins present in the cell lysate. An unknown protein with a molecular weight of approximately 25kDa was visualised in the first and second elution protein fractions (lanes 4 and 5 of Figure 24).

3.5.2 Eukaryotic protein expression of rP/PK8-His

3.5.2.1 Production of recombinant baculovirus

Preparation of *Sf9* insect cell cultures for transfection

The trypan blue dye exclusion method was used to assess *Sf9* insect cells. Viable cells appeared shiny and translucent compared to non-viable cells which stained blue when viewed under a microscope (Figure 25). Cells in the log phase of growth with viability above 85% were needed for recombinant baculovirus production.

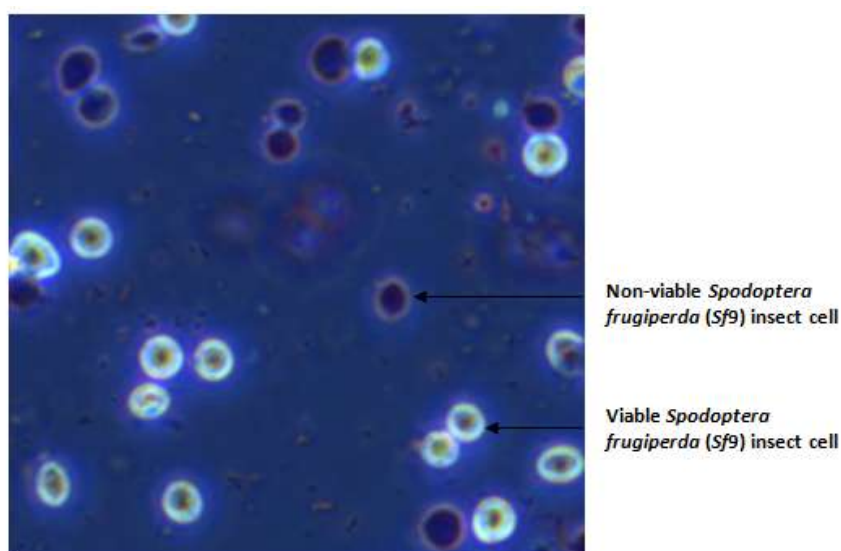
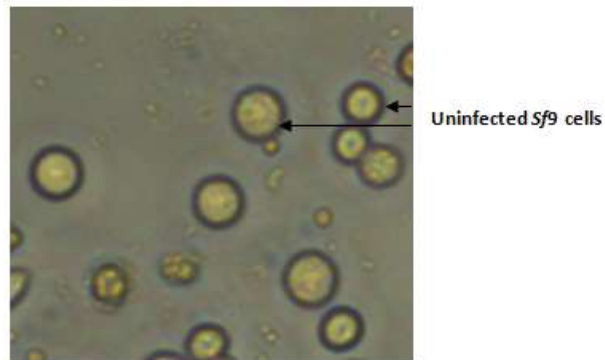


Figure 25: Photograph of a healthy *Spodoptera frugiperda* (Sf9) cell culture stained with Trypan Blue dye solution as seen under a phase contrast inverted microscope with a 40x magnification.

3.5.2.2 Amplification of recombinant baculovirus (BacVirus-PfB0150c)

Recombinant baculovirus particles (BacVirus-PfB0150c) were generated using the PfB0150c-pTriEx-3 transfer plasmid and BacMagic single stranded DNA. A suspension culture of *Sf9* cells with a cell density of 2×10^6 cells/ml was infected with BacVirus-PfB0150c to amplify the recombinant baculovirus. Normal uninfected *Sf9* insect cells (Figure 26 A) were regular shaped with distinct cell boundaries whereas infected *Sf9* insect cells were enlarged and appeared granular with an irregular shape when viewed under a phase contrast microscope (Figure 26 B).

A. *Sf9* cells prior to infection.



B. 48 hours post-infection with recombinant BacVirus-*PfB0150c*.

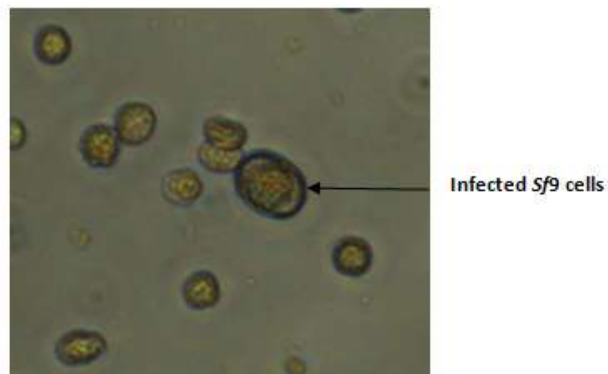
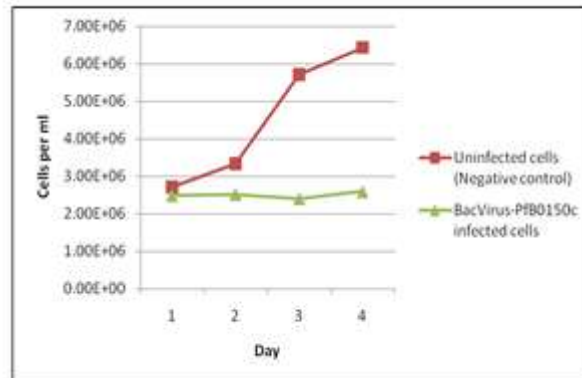


Figure 26: *Spodoptera frugiperda* (*Sf9*) insect cells pre- and post infection with BacVirus-*PfB0150c*.

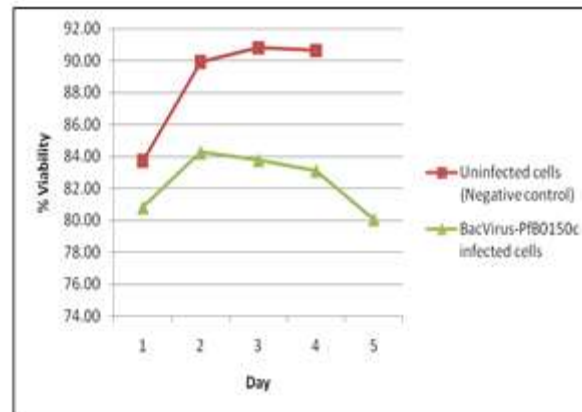
Photograph of *Sf9* insect cells pre-infection (A) and 48 hours post-infection (B) with BacVirus-*PfB0150c* as seen under a phase contrast microscope with a 40x magnification.

BacVirus-*PfB0150c* infected *Sf9* insect cells were monitored over a period of 5 days to assess the progress of recombinant virus amplification. The proliferation rate (Figure 27 A), percentage cell viability (Figure 27 B) and number of viable cells per ml of culture (Figure 27 C) were compared to a control uninfected *Sf9* culture.

A. Proliferation rate of *Sf9* insect cells.



B. Viability of *Sf9* insect cells.



C. Number of viable *Sf9* insect cells per ml culture.

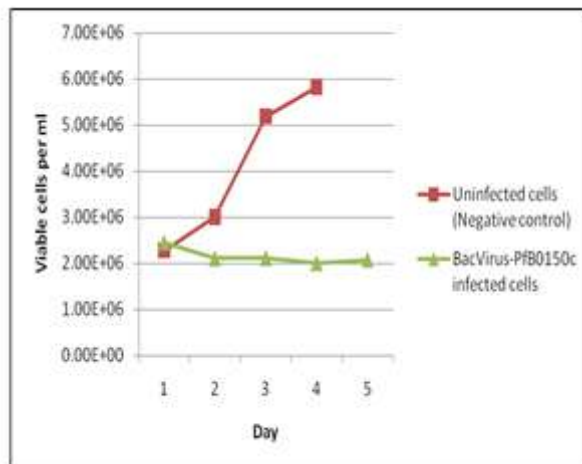


Figure 27: Growth curves of *Spodoptera frugiperda* (*Sf9*) insect cell suspension cultures infected with recombinant BacVirus-PfB0150c.

A *Sf9* cell culture was infected with recombinant BacVirus-PfB0150c viral stock and monitored over 5 days. A control culture was set up without adding any BacVirus-PfB0150c. The proliferation rate (A), percentage cell viability (B) and number of viable cells per ml (C) were determined daily.

The host cell is prepared by the baculovirus for viral DNA replication shortly after infection. Viral DNA synthesis takes place between 0.5 – 6 hours post infection followed by early viral gene expression. The infected cell starts to form buds on its surface 12 hours post infection, this process shuts down the host's gene expression system which will cause a decrease in the growth rate of the baculoviral culture. No increase in the growth rate (Figure 27 A) of the *Sf9* insect cell culture infected with BacVirus-*PfB0150c* was seen post infection and a decrease in the number of viable cells after 24 hours was observed (Figure 27 C). The reason for this is due to bud formation on the host cell surface, which peaks at 18 – 36 hours post infection. These buds rupture and produce extracellular viruses which contain the plasma membrane envelope and glycoprotein 64 (gp64) needed for virus entry by means of endocytosis. The released viruses will invade new host cells. Between 36 and 96 hours post infection, genes under control of the p10 promoter are expressed and cell lysis begins which releases the expressed proteins into the culture medium. The percentage viable cells (Figure 27 B) started to decrease dramatically 48 hours after infection due to cell lysis and the spread of the BacVirus-*PfB0150c*, compared to viability of the uninfected control culture which continued to increase. The proliferation rate (Figure 27 A) of the control culture continued to increase during the course of the study, as expected.

3.5.2.3 Viral titre determination of the BacVirus-*PfB0150c* stock solution

Sf9 insect cells in log phase of growth were infected with different concentrations of BacVirus-*PfB0150c* stock. Using the FastPlax™ Titer kit, baculovirus-infected *Sf9* insect cells expressing gp64 on the cell surface were counted 24 hours post infection. Dark blue plaques or infected cell clusters (foci) were easily distinguished from uninfected cells when viewed under a phase-contrast inverted microscope (Figure 28).

The average number of plaques or foci of infected cells found with different viral dilutions was used to calculate the final viral titre of 3.1×10^9 plaque forming units (pfu) per ml of viral seed stock after 6 rounds of amplification in suspension cultures (Table 23).

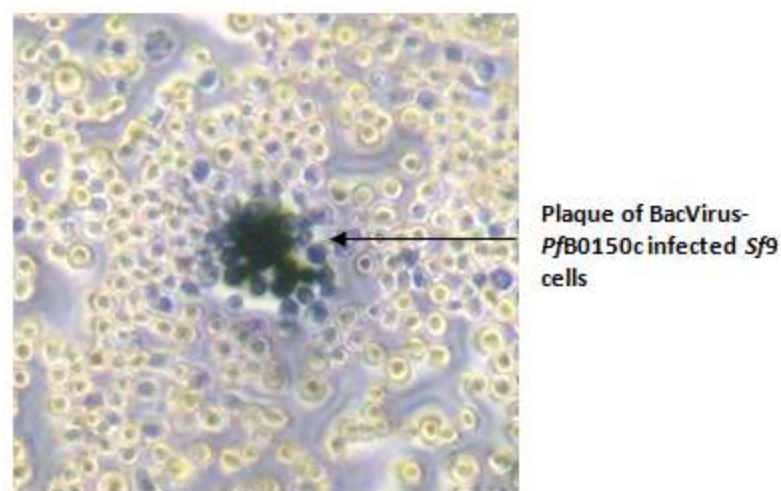


Figure 28: Recombinant baculovirus-infected *Spodoptera frugiperda* (Sf9) cells 24 hours post infection visualized with the FastPlax™ Titer kit.

Recombinant baculovirus (BacVirus-PfB0150c) infected cells were detected by the appearance of gp64 glycoprotein on the cell surface of Sf9 insect cells 24 hours post-infection. Dark blue plaques or foci were visible under a phase-contrast inverted microscope with a 10x objective.

Table 23: Sf9 plaques formed by BacVirus-PfB0150c.

Dilution	Number of infected cells/plaques	Titre (pfu/ml)
10^{-6}	20	2.0×10^8
	22	2.2×10^8
10^{-7}	19	1.9×10^9
	12	1.2×10^9
10^{-8}	6	6.0×10^9
	9	9.0×10^9
Final titre (average)		3.1×10^9

3.5.3 Protein expression and purification of rPfPK8-His

Spodoptera frugiperda (Sf9) insect cells were infected with recombinant BacVirus-PfB0150c to produce rPfPK8-His. SDS-PAGE analysis and immunoblotting of rPfPK8-His proteins in Sf9 insect cells were performed.

Shaking flasks containing 20ml of Sf9 insect cells were infected at MOI 1, MOI 2, MOI 5 and MOI 10 respectively, with recombinant BacVirus-PfB0150c to

determine whether the *rPfPK8*-His target protein will express in the eukaryotic baculoviral expression system. A control culture was also set up containing uninfected *Sf9* insect cells. The cells were monitored over 96 hours, determining the cell viability and cell density every 24 hours. Cell pellets and supernatants of approximately 5×10^5 cells were harvested at 24, 48, 72 and 96 hours respectively post infection and solubilised for SDS-PAGE analysis. The cell pellet protein samples (Figure 29 A) and the supernatant protein samples (Figure 29 B) were electrophoresed on a 12% Laemmli gel and stained with Coomassie blue to visualise the protein bands.

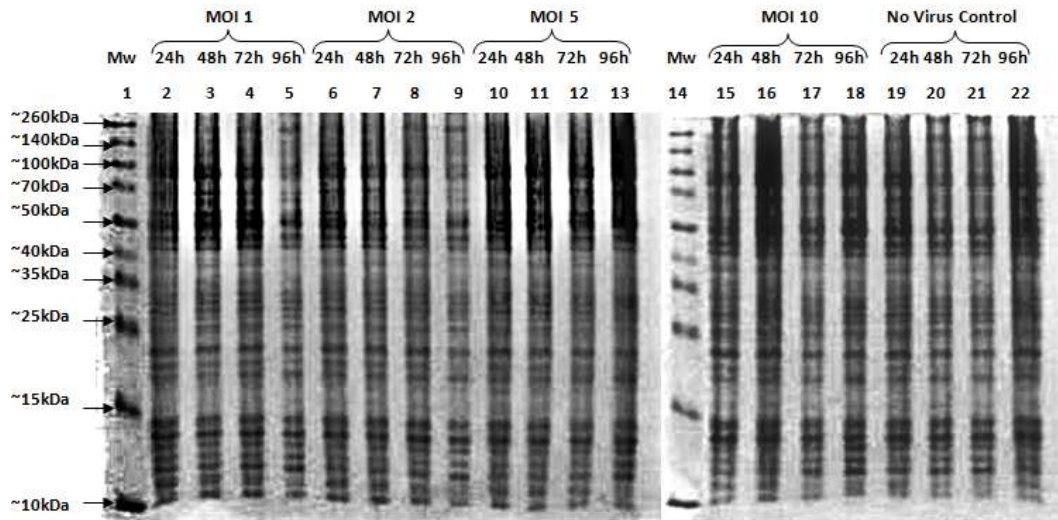
There was no distinct difference in the observed protein banding pattern between the MOI 1, MOI 2, MOI 5 and MOI 10 cell pellet and supernatant protein samples compared to that of the uninfected control. The 60kDa target protein *rPfPK8*-His was not visualised after staining the gels (Figure 29 A and B).

Unstained gels of the *Sf9* cell pellet and supernatant protein samples were transferred to a nitrocellulose membrane and probed for expression by horseradish peroxidase-conjugated mouse anti-penta-Histidine antibody (1:2 000). The proteins were visualised by exposing the probed membrane to X-ray film for 5 minutes until the histidine positive control (*rPFL0675c*-C-His or Qiagen Histidine ladder) was observed.

Recombinant *PFL0675c*-C-His, a 40kDa histidine tagged protein, which was used as the experimental positive control gave a positive signal in the cell pellet autoradiograph (Figure 30 A) which indicated that the immunoblot result was reliable. An intense ~ 60kDa protein band in the recombinant baculovirus infected insect cells would have indicated the successful expression of *rPfPK8*-His.

The experiment was repeated using different starting TriExTM-*Sf9* cell suspensions. The results of only one experiment are shown but the inability to express *rPfPK8*-His in recombinant BacVirus-*PfB0150c* infected *Sf9* insect cells remained unchanged.

A. SDS-PAGE of cell pellet samples.



B. SDS-PAGE of supernatant samples

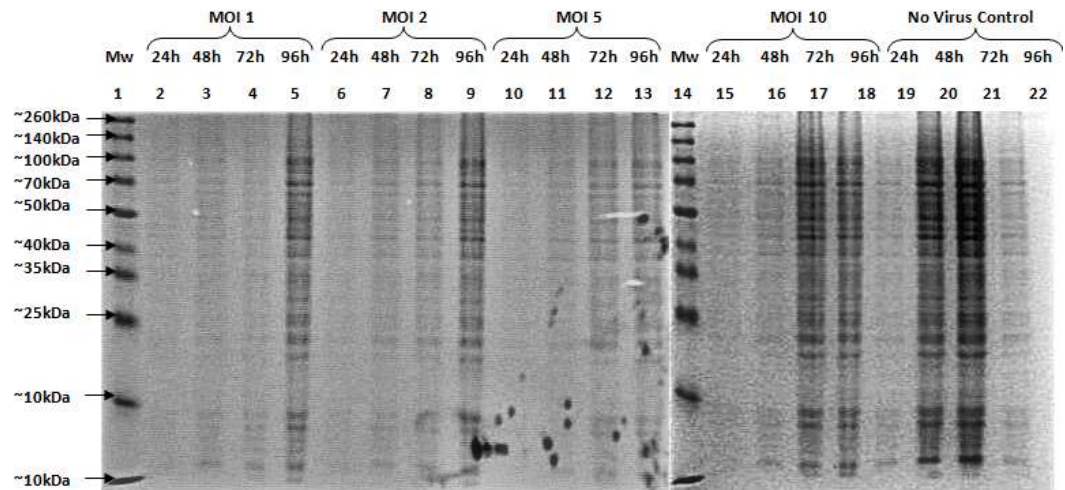
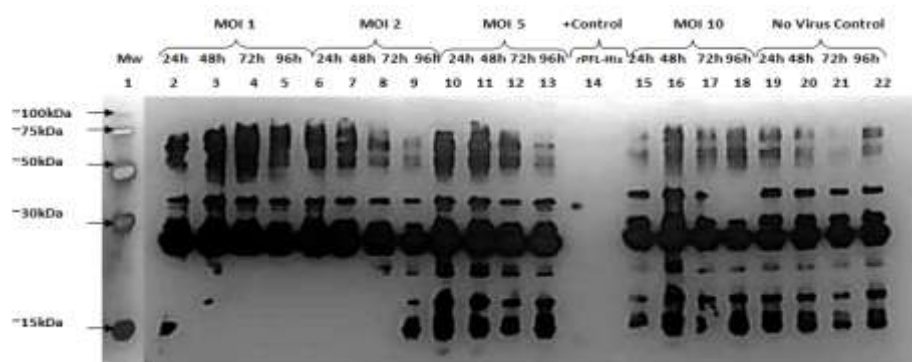


Figure 29: Coomassie Blue stained 12% Laemmli gel analysis of *rP/*PK8-His expression in recombinant *BacVirus-P/B0150c* infected *Sf9* insect cells.

Figure A shows the stained gel of the cell pellet samples and Figure B shows the stained gel of the supernatant samples. Samples (approximately 5×10^5 cells) were taken at 24, 48, 72 and 96 hours post infection at different MOIs and were electrophoresed. Lanes 1 and 14 show a Spectra Broad Range Multi Colour protein ladder (5 μ l). Lanes 2-5 show MOI 1 samples, Lanes 6-9 show MOI 2 samples, Lanes 10-13 MOI 5 samples, Lanes 15-18 show MOI 10 samples and Lanes 19-22 samples of the uninfected control. No expression of the 60kDa target protein (*rP/*PK8-His) was observed after staining the gel with Coomassie Brilliant Blue Dye.

A. Autoradiograph of cell pellet samples



B. Autoradiograph of supernatant samples

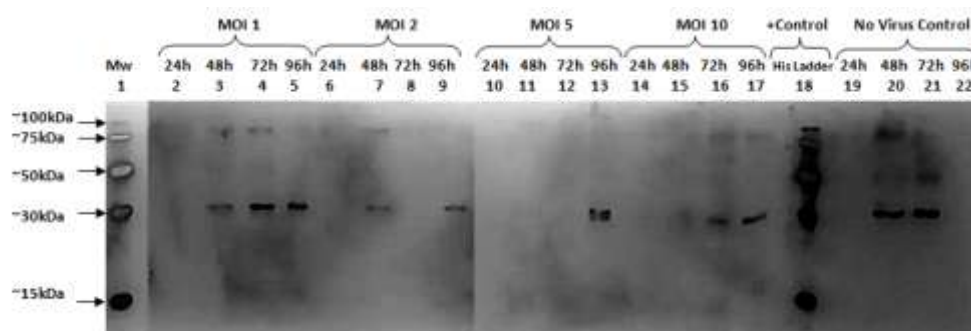


Figure 30: Immunoblot of rP/PPK8-His proteins expressed in *Sf9* insect cells infected with recombinant BacVirus-P/B0150c.

Figure A shows the autoradiograph of the cell pellet samples and Figure B shows the autoradiograph of the supernatant samples after 5 minute exposure to anti-his antibody-probed nitrocellulose membranes. Lanes 1 in Figure A and B show a Histidine ladder (5 μ l) ranging from approximately 100kDa to 15kDa. Cell pellet (Figure A) and supernatant samples (Figure B) (approximately 5×10^5 cells) were taken at 24, 48, 72 and 96 hours post infection at different MOIs and were electrophoresed and exposed to X-ray film. Figure A: Lanes 2-5 show MOI 1 cell pellet samples, Lanes 6-9 show MOI 2 cell pellet samples, Lanes 10-13 show MOI 5 cell pellet samples, Lane 14 is the immunoblot histidine positive control PFL0675c-C-His (10 μ l) (~ 40kDa), Lanes 15-18 show MOI 10 cell pellet samples and Lanes 19-22 show cell pellet samples of the uninfected control. Figure B: Lanes 2-5 show MOI 1 supernatant samples, Lanes 6-9 show MOI 2 supernatant samples, Lane 10 is the positive control Histidine ladder, Lanes 11-14 show MOI 5 supernatant samples, Lanes 15-18 show MOI 10 supernatant samples and Lanes 19-22 show supernatant samples of the uninfected control. No target protein rP/PPK8-His was visualised in the cell pellet or supernatant fractions.

3.6 Expression of recombinant rGST-P/PPK8 protein

Recombinant rP/PPK8-His was not successfully expressed in baculovirus infected *Spodoptera frugiperda* insect cells and the low purity and yield of expressed soluble rP/PPK8-His in *Escherichia coli* Rosetta 2 (DE3) was not good enough to

characterise the kinetic parameters of the enzyme. It was therefore decided to explore the expression of *Pf*PK8 as a GST-tagged recombinant protein in *Escherichia coli*. The recombinant pGEX-4T-2-*Pf*B0150c construct was donated by Brigit Smit (previous member of the Red Blood Cell Malaria Unit).

Escherichia coli Rosetta 2 (DE3) cells, transformed with plasmid pGEX-4T-2-*Pf*B0150c were induced to express recombinant GST-tagged *Pf*PK8, which was analysed by means of SDS-PAGE and immunoblotting.

Recombinant GST-*Pf*PK8 is 723 amino acids in length consisting of an N-terminal GST-tag, which has 220 amino acids and a predicted size of 25kDa. Recombinant GST-*Pf*PK8 has a predicted size of 85kDa.

N-terminal end

MSPILGYWKIKGLVQPTRLLLEYLEEKYEEHLYERDEGDKWRNKKFELGLEFPNLPYYID
 GDVKLTQSMAIIRYIDKHNMLGGCPKERAIEISMLEGAVLDIRYGVSRAYSKDFETLKVDF
 LSKLPLKMFEDRLCHKTYLNGDHVTHPDFMLYDALDVVLYMDPMCLDAFPKLVCFFKKRI
 EAIPQIDKYLKSSKYIAWPLQGWQATFGGGDHPPKSDEKDGYEEMNGGDKNEEMNGGD
 KNEEMNVGDKNGGIEHKNEGINEEHKDELINKEHKNERINEEHKNERINEEHKNEGINEE
 HKNEGINEEHKNE**RINEEHKNEGIN**KLTYHNMNKNNISNENNYNDDDSYDEDNLVSLKII
NLKYLSKKNSLKNILREVNFKMCEHPNVVKYFESFFWPPCYLVIVCEYLSGGTLYDLYKN
 YGRISEDLLVYILDDVLNGLNYLHNECSSPLIHRDIKPTNIVLSKDGIAKIIDFGSCEELKNS
 DQSKELVGTIYYISPEILMRTNYDSSDIWSLGITIYEIVLCTLPWKRNQSFENYIKTIINSSPKI
NITEGYSKHLCYFVEKCLQKKPENRGNVKDLLNHKFLIKKRYIKKKPSSIYEIRDILKIYNG
 KGKTNIFFRNFFKNLFFFNDDKNKKKPNKMISSEKSCDAEMFFEQLKRENFDFEIKLKDDENS
 RSLNTFNINISKERDDISYSSLNLEKIKEHSLNMVASVVGTEQQK **C-terminal end**

Figure 31: Protein sequence of rGST-*Pf*PK8.

Blue amino acids indicate the GST-tag, red indicates the kinase domain of *Pf*PK8 and the black amino acids the cloned region of *Pf*PK8.

Protein fractions were collected throughout the purification process of rGST-*Pf*PK8 from 250ml Rosetta 2 (DE3) *Escherichia coli* cultures. Soluble recombinant protein with the expected approximate molecular weight of 85kDa was present in eluted fractions 1 and 2 as seen in lanes 8 and 9 of Figure 32. The fraction labelled B in Figure 32 represents residual MagneGSTTM magnetic beads and contained proteins that had not been eluted from the beads after two elution steps. The GST-tag was used as a control and was expressed in *Escherichia coli* cells containing non-recombinant pGEX-4T-2 plasmids. The GST-tag resolved as a low molecular weight band (lane 13 of Figure 32) just above the 25kDa mark, as expected.

Recombinant GST-*Pf*PK8 was present in the insoluble fraction (as seen in Figure 32 and 33). This is an indication that insoluble inclusion bodies had formed. Proteins with no affinity for the MagneGSTTM beads were washed from the beads in three wash steps. More proteins were present in the wash 1 fraction compared to wash 2 and 3, as expected. Unbound rGST-*Pf*PK8 was washed from the magnetic beads during the washes 1 and 2, possibly due to the binding time being too short. The unbound fraction had a high protein concentration and contained all of the unbound proteins in the cell lysate including some rGST-*Pf*PK8 (as seen in Figure 32 and 33). Proteins not eluted from the beads are present in the bead fraction. It is evident from Figure 32 that insufficient elution of rGST-*Pf*PK8 occurred during the purification steps.

Uninduced protein samples were electrophoresed to check for leaky expression of the target protein. Leaky expression of rGST-*Pf*PK8 was however not detected as seen in Figure 32.

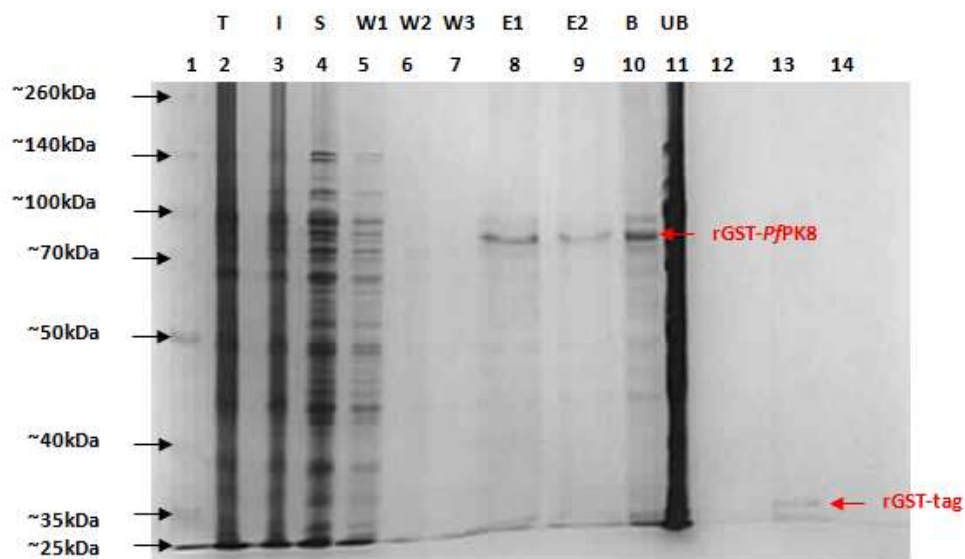


Figure 32: Coomassie stained 12% Laemmli gel of purified rGST-*Pf*PK8 from a 250ml *Escherichia coli* Rosetta 2 (DE3) culture.

Lane 1: Spectra Broad Range Multi Colour protein ladder, Lane 2: Total protein fraction (T) (2µl out of 10ml), Lane 3: Insoluble proteins (I) (2µl out of 10ml), Lane 4: Soluble proteins (S) (2µl out of 10ml), Lane 5: Wash 1 (W1) (10µl out of 150µl), Lane 6: Wash 2 (W2) (10µl out of 150µl), Lane 7: Wash 3 (W3) (10µl out of 150µl), Lane 8: Elution 1 (E1) (10µl out of 100µl), Lane 9: Elution 2 (E2) (10µl out of 100µl), Lane 10: MagneGSTTM beads (B) (10µl out of 100µl), Lane 11: Unbound fraction (UB) (10µl out of 10ml), Lane 12: Elution 1 of a 20ml uninduced rGST-*Pf*PK8 culture (10µl out of 100µl), Lane 13: Elution 1 of a 20ml induced rGST control culture (5µl out of 100µl), Lane 14: Elution 1 of a 20ml uninduced rGST control culture (5µl out of 100µl).

All fractions from the purification steps were separated on a Laemmli gel, transferred to a nitrocellulose membrane, probed by anti-glutathione-S-transferase horseradish peroxidase-conjugated (anti-GST HRP- conjugated) antibody and exposed to X-ray film to obtain an auto-radiograph (Figure 33).

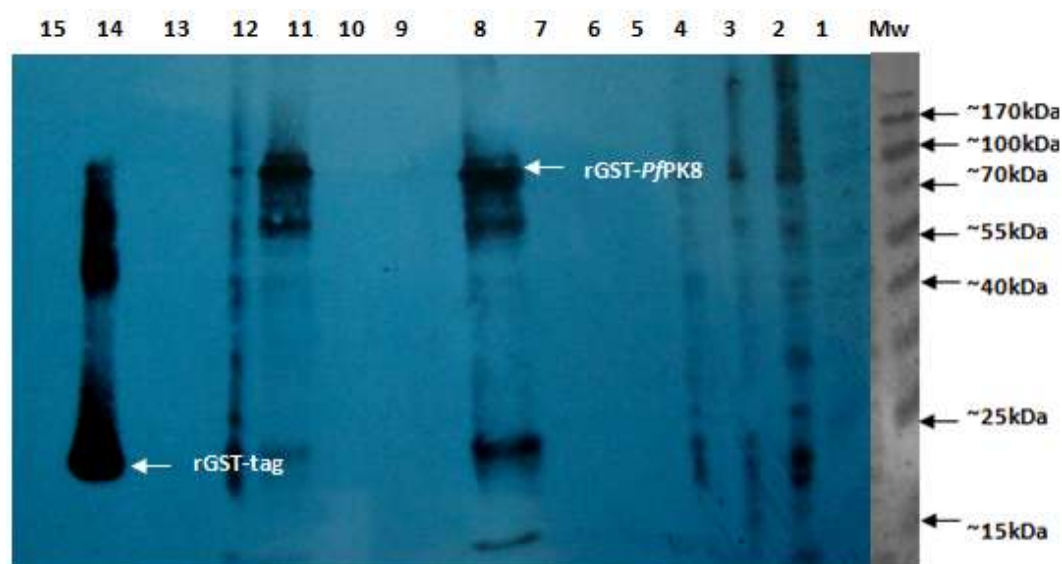


Figure 33: Immunoblot of rGST-*Pf*PK8 proteins probed with anti-GST-HRP conjugated antibody.

Lanes 2 – 12 are electrophoresed proteins from purification samples of an induced 250ml *Escherichia coli* Rosetta 2 (DE3) pGEX-4T-2-*Pf*B0150c culture probed with Anti-GST conjugated antibody. Lane 1: PageRuler Pre-stained protein Ladder (5µl), Lane 2: Total protein fraction (1µl out of 10ml), Lane 3: Insoluble proteins (1µl out of 10ml), Lane 4: Soluble proteins (1µl out of 10ml), Lane 5: Wash 1 (10µl out of 150µl), Lane 6: Wash 2 (10µl out of 150µl), Lane 7: Wash 3 (10µl out of 150µl), Lane 8: Elution 1 (10µl out of 100µl), Lane 9: Elution 2 (10µl out of 100µl), Lane 10: Elution 3 (10µl out of 100µl), Lane 11: Residual MagneGST™ beads (10µl out of 100µl), Lane 12: Unbound protein fraction (1µl out of 10ml), Lane 13: Elution 1 of a 20ml uninduced pGEX-4T-2-*Pf*B0150c culture (10µl out of 100µl), Lane 14: Elution 1 of a 20ml induced pGEX-4T-2 culture (10µl out of 200µl), Lane 15: Elution 1 of a 20ml uninduced pGEX-4T-2 culture (10µl out of 200µl).

The black smear observed in Lane 14 of Figure 33 was due to the expression of large amounts of GST (~ 25kDa) and possible dimeric forms. The X-ray film was exposed for 30 seconds to see a clear positive signal of rGST-*Pf*PK8 in Lanes 8 with the correct size of approximately 85kDa. In the rGST-*Pf*PK8 Elution 1 fraction (Lane 8 of Figure 33) and in the residual MagneGST™ beads fraction (Lane 11 of Figure 33), two additional positive bands were observed on the auto-radiograph. The first band had a size of between 55 - 70kDa and may represent a

truncated form of the protein, which would still be detected by the antibody since the GST tag is on the N-terminal of the recombinant protein. The second ~25kDa band was presumably endogenous *Escherichia coli* GST that had co-purified.

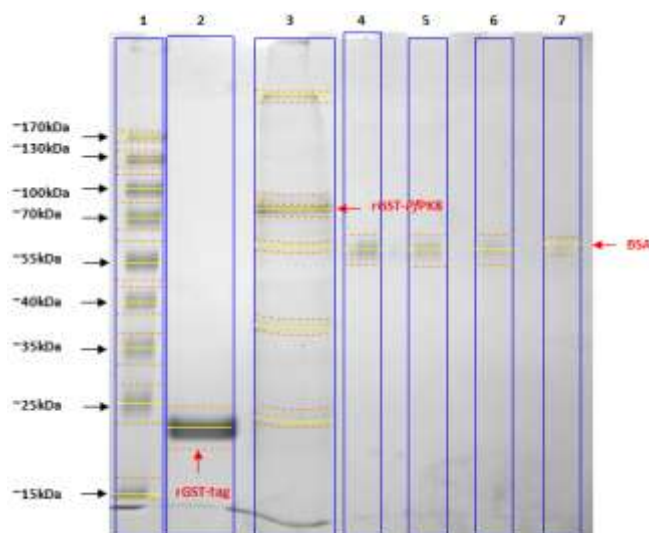


Figure 34: Densitometric analysis of a Coomassie stained 12% Laemmli gel.

The percentage purity and amount of extracted rGST-PfPK8 from a 250ml *Escherichia coli* Rosetta 2 (DE3) culture were determined using densitometry of a Laemmli gel. Lane 1: PageRuler Pre-stained protein ladder (5µl), Lane 2: Elution 1 of pGEX-4T-2 induced 20ml culture (10µl out of 100µl), Lane 3: Elution 1 of pGEX-4T-2-PfB0150c induced culture (10µl out of 100µl), Lane 4: 5µg BSA, Lane 5: 3.75µg BSA, Lane 6: 2.5µg BSA, Lane 6: 1.25µg BSA. The purity of rGST-PfPK8 was calculated to be approximately 63%.

Densitometric analysis was performed on a Coomassie stained 12% Laemmli gel (Figure 34) to determine the percentage purity of the eluted rGST-PfPK8 and the total protein yield from a 250ml Rosetta 2 (DE3) *Escherichia coli* culture transformed with the recombinant pGEX-4T-2-PfB0150c plasmid. Peaks 2 and 3 in Figure 35 represent rGST-PfPK8 in Elution 1. By taking the contaminating proteins into account, the purity of rGST-PfPK8 was calculated to be approximately 63%. The amount of protein eluted was calculated by constructing a standard curve of the densitometric data summarized in Table 24.

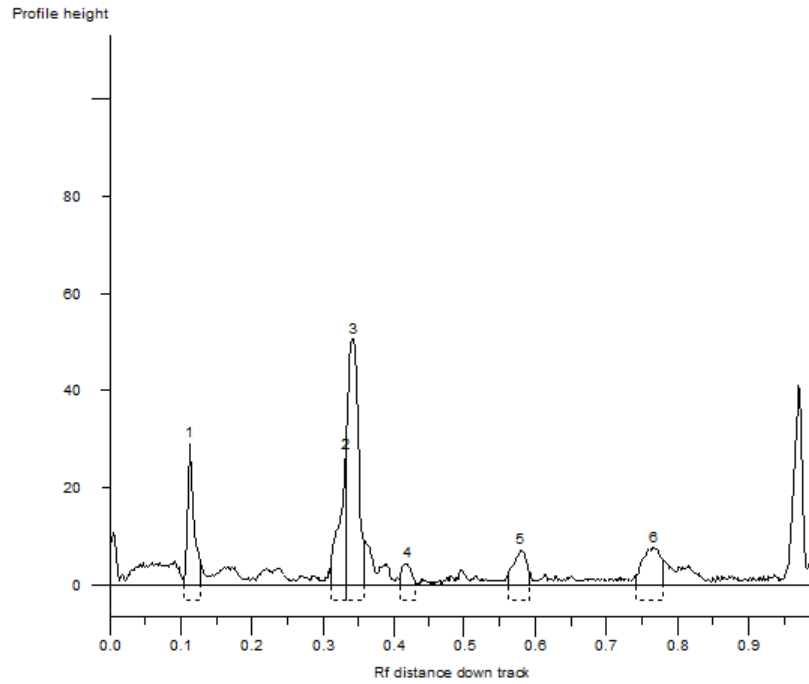


Figure 35: Densitometric scan of the first elution fraction of rGST-PfPK8.

This graph is representative of Elution 1 of rGST-PfPK8 from a *Escherichia coli* Rosetta 2 (DE3) culture (Lane 3 in Figure 34). Peaks 2 and 3 show the amount of rGST-PfPK8 present in the elution. The other peaks are indicative of contaminating proteins.

Table 24: Densitometric analysis data of rGST-PfPK8 Elution 1.

Lane*	Peak no.	Sample	Raw volume of peak	Protein amount loaded (µg)	Total volume eluted (µl)	Total Protein amount eluted (µg)
3	1	rGST-PfPK8 Elution 1 (10µl)	15 038	2.78	100	27.8
	2		54 191	9.96		99.6
	3		3 584	0.74		7.4
	4		7 529	1.48		14.8
	5		11 040	2.04		20.4
4		BSA	27 002	5	NA	
5		BSA	16 775	3.75		
6		BSA	13 309	2.5		
7		BSA	4 868	1.25		

* Refer to Figure 34 for the lane details.

The total amount of protein eluted in the first elution was 170µg per 250ml culture. With a purity of 63%, the yield of pure rGST-*Pf*PK8 from a 250ml culture was approximately 107µg.

3.7 Non-radioactive coupled protein kinase assays

Purified soluble rGST-*Pf*PK8 was used to perform protein kinase assays to determine the kinetic parameters of *Pf*PK8. A non-radioactive coupled protein kinase assay was used. This coupled protein kinase assay is based on a well-documented enzyme assay used for *Escherichia coli* glycerol kinase (*Ec*GK) kinetic studies first described by Hyashi and Lin (1967). *Ec*GK catalyzes the transfer of a phosphate group from ATP to its substrate (glycerol) in the presence of auxiliary enzymes pyruvate kinase (PyrK) and lactate dehydrogenase (LDH). Oxidation of NADH occurs during the kinase assay and this oxidation is directly proportional to the phosphorylated product formed and the activity of *Ec*GK in the presence of glycerol. The rate of product formation is monitored by measuring the absorbance at 340nm as a function of time in a closed system (Worthington and Worthington, 2011).

The activity of rGST-*Pf*PK8 in the presence of three exogenous substrates was continuously measured as the decrease in NADH absorbance over 20 minutes and used to calculate the enzyme activity and kinetic parameters. *Ec*GK in the presence of glycerol was used as assay positive control and without substrate as assay negative control. Recombinant GST was used as a negative control to ascertain the effect of the GST tag and a sample without rGST-*Pf*PK8 was used as a blank. The absorbance readings of the blank samples were subtracted from the enzyme samples since they take into account the contribution of the reaction mixture and substrate towards the absorbance value taken at 340nm.

To test the kinase activity of rGST-*Pf*PK8, the amount of enzyme purified per biological sample had to be increased and thus 500ml cultures of transformed *Escherichia coli* Rosetta 2 (DE3) cells were induced to express the recombinant protein. The purified rGST-*Pf*PK8 was eluted in 200µl GST-elution buffer. This

provided enough rGST-*Pf*PK8 protein for several assay points. The yield ranged from 289µg - 370µg of crude eluted rGST-*Pf*PK8 per 500ml culture. The purity of the enzyme preparations used in the assays ranged from 58% - 63%. An initial experiment was performed using different amounts of rGST-*Pf*PK8 and 3µl (approximately 2.5µg) of the recombinant enzyme was found to be the best.

The enzyme activity of rGST-*Pf*PK8 varied between biological samples. Possible reasons for this could be a different amount of contaminating proteins in the enzyme preparation, a difference in protein folding during expression in Rosetta 2 (DE3) *Escherichia coli* cells and variable effects of protein manipulation during the extraction and purification process. Each kinetic assay to determine V_{max} and K_m for the three substrates was therefore performed using a single preparation of rGST-*Pf*PK8.

3.7.1 Stability of rGST-*Pf*PK8

The stability of rGST-*Pf*PK8 (2.25 – 2.73µg pure enzyme) (Figure 36) was analysed over a period of 3 days using casein (200µg) as exogenous substrate and 2.5mM ATP. The assay was performed at 37°C in a 0.1M Tris-HCl buffer system with a pH of 7.4. The day of rGST-*Pf*PK8 purification was regarded as day 1. The enzyme sample was stored in GST-buffer at 4°C over the course of the study to minimize any protease activity within the sample. The experiment was repeated twice using a different biological sample of the enzyme.

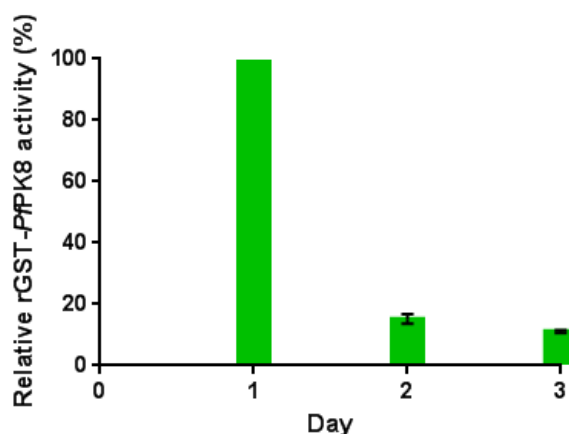


Figure 36: Stability of rGST-PfPK8.

The stability of rGST-PfPK8 at 4°C was spectrophotometrically analysed over a period of 3 days using casein (200µg) as exogenous substrate. The assay was performed at 37°C in a 0.1M Tris-HCl buffer system with a pH of 7.4. The day of rGST-PfPK8 purification is regarded as day 1. The experiment was repeated using a different biological sample of the enzyme. The error bars represent standard error of the mean of two experiments. The graphs were generated with GraphPad Prism 5 for Windows version 5.01.

The relative kinase activity of rGST-PfPK8 decreased significantly from 100% on day 1 to 15% on day 2 and 11% on day 3. Recombinant rGST-PfPK8 is therefore unstable *in vitro*. This instability may be due to the low protein concentration of rGST-PfPK8. Glycerol, sucrose or BSA could have been added to stabilise the enzyme as a result of the macromolecular crowding effect (Wang *et al.*, 2012). However, it was preferred to prepare a fresh enzyme sample before each assay, which was used on the same day. The concentration and purity of the sample was determined by electrophoresis and densitometric quantitation to calculate the activity of the enzyme.

3.7.2 Substrate specificity of rGST-PfPK8

The natural substrate of PfPK8 in *P. falciparum* is unknown. Known protein kinase substrates were therefore used in the *in vitro* kinase assay. Recombinant rGST-PfPK8 (2.25 – 2.73µg pure enzyme) in the presence of casein (200µg), MBP (100µg) and H1 (100µg) were tested. Figure 37 is a representation of one of the kinase assay experiments.

The A_{340} absorbance values (Figure 37) of the samples without any enzyme (blank) were high because the reaction mixture contained 0.5mM reduced NADH

which absorbs light at this wavelength. *EcGK* in the presence of glycerol showed a steady decrease in absorbance at 340nm and there was no change in absorbance when glycerol was omitted indicating that the assay was functional. The rGST sample (line F in Figure 37) was used to control for the possible effect of the GST tag on enzyme activity. The absorbance at 340nm remained unchanged for rGST, as expected. The rGST-*PfPK8* un-induced sample (lines H, I and J) was used to test for leaky expression of the target enzyme. The absorbance remained unchanged over 20 minutes for these samples and therefore indicated that the plasmid did not normally express rGST-*PfPK8*. Recombinant rGST-*PfPK8* phosphorylated all three substrates.

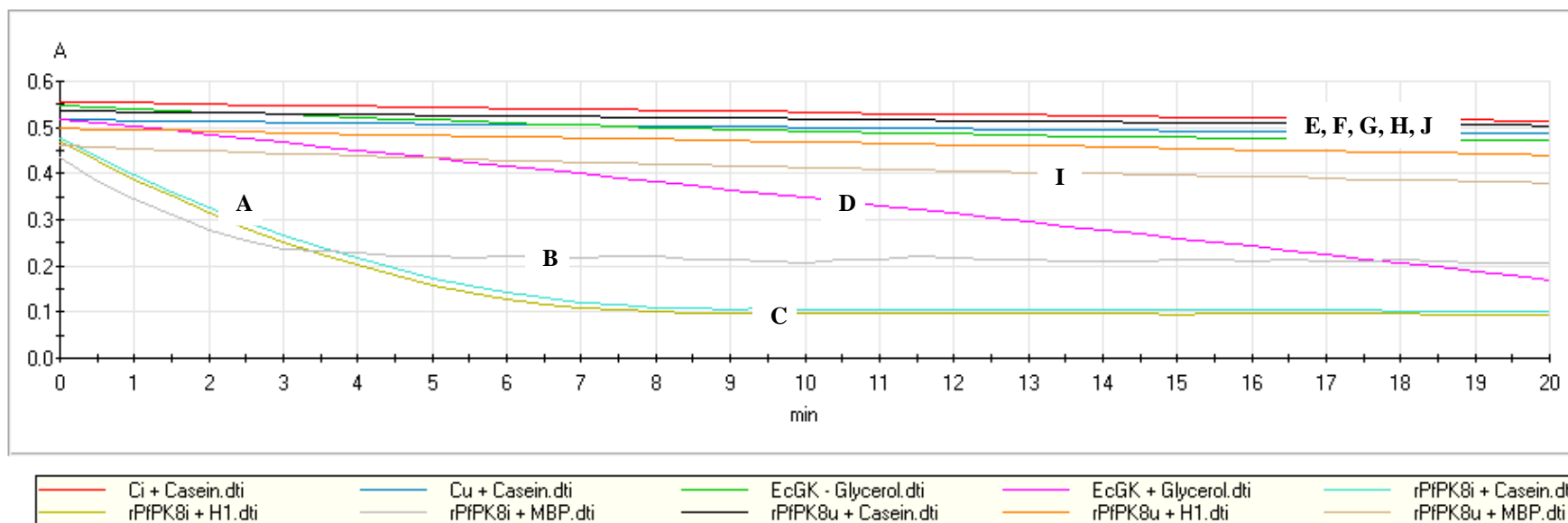


Figure 37: Spectrophotometric data of the non-radioactive coupled enzyme assay showing the decrease of NADH due to the kinase activity of recombinant rGST-PjPK8 in the presence of exogenous substrates.

The absorbance of each reaction mixture was directly and continuously measured at 340nm in a temperature controlled spectrophotometer at 37°C over 20 minutes. The rate of decrease in the absorbance is directly proportional to the activity of rGST-PjPK8 (2.25 µg) in the presence of 200µg casein (sloping light blue line - A), 100µg myelin basic protein (MBP) (sloping grey line - B) and 100µg histone protein 1 (H1) (sloping yellow line - C). *Escherichia coli* glycerol kinase (EcGK) (53.2U/ml) in the presence of 5µM glycerol was used as assay positive control (decreasing pink line - D) and 53.2U/ml M EcGK without glycerol as substrate was used as assay negative control (green line - E). The enzyme activity of 2.25µg recombinant Glutathione-S-transferase (rGST) (Ci) (red line - F) was used as the enzyme negative control and no-rGST (Cu) (blue line - G) was used as the enzyme negative control blank. The activity of uninduced rGST-PjPK8 (rPjPK8u) in the presence of 200µg casein (straight black line - H), 100µg MBP (brown line - I) and 100µg H1 (orange line - J) was used to detect leaky expression of the recombinant enzyme.

3.7.3 Kinetic analysis of rGST-*Pf*PK8

Plasmodium falciparum protein kinase 8 has not yet been characterised and therefore basic kinetic studies of rGST-*Pf*PK8 in the presence of exogenous substrates casein, MBP and H1 as well as for ATP were performed.

The linear part of the reaction curve (Figure 37) was used to calculate the initial rate of substrate conversion (velocity) with NADH decreasing in an equimolar ratio to ATP converted to ADP by rGST-*Pf*PK8. The velocity (V) of the reaction is defined as the amount (μmol) of NADH oxidized per minute. The enzyme activity (μmol/min/mg enzyme) is defined as the velocity of the reaction per mg of rGST-*Pf*PK8.

The following formula was used to calculate velocity and enzyme activity of rGST-*Pf*PK8:

$$V = \frac{\Delta A_{340} \times \text{reaction volume}}{\epsilon \text{ of NADH}}$$

$$\text{Enzyme activity} = V / \text{mg enzyme}$$

Where:

V = velocity of the reaction (μmole NADH/min)

ΔA₃₄₀ = change in NADH absorbance measured during the linear part of curve (min)

Reaction volume = 1ml

ε = extinction coefficient of NADH (mM⁻¹ cm⁻¹) = 6.22

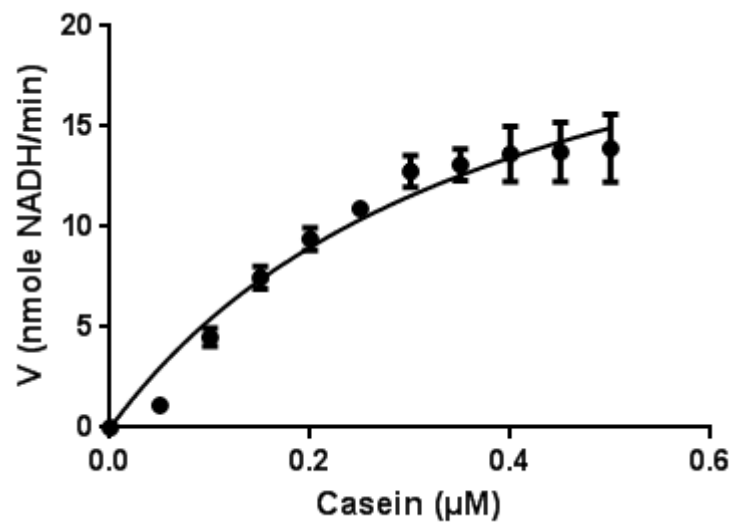
The Michaelis-Menten constant (K_m) and maximum velocity (V_{max}) (Table 25) of rGST-*Pf*PK8 were determined from the non-radioactive coupled protein kinase assays in the presence of exogenous substrates casein, myelin basic protein (MBP) and histone protein 1 (H1). The rate of the rGST-*Pf*PK8 reaction (μmole/min) of each assay was calculated and plotted against the substrate amount (μM) used in each reaction.

The graphs (Figure 38) were used to calculate the V_{\max} and K_m according to the Michaelis-Menten equation:

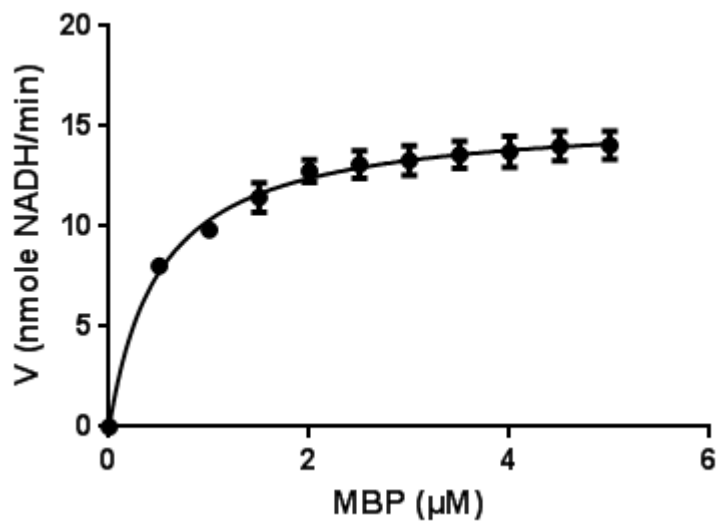
$$V_0 = (V_{\max} \times [S_0]) / ([S_0] + K_m)$$

where V_0 = initial velocity and S_0 = initial substrate concentration

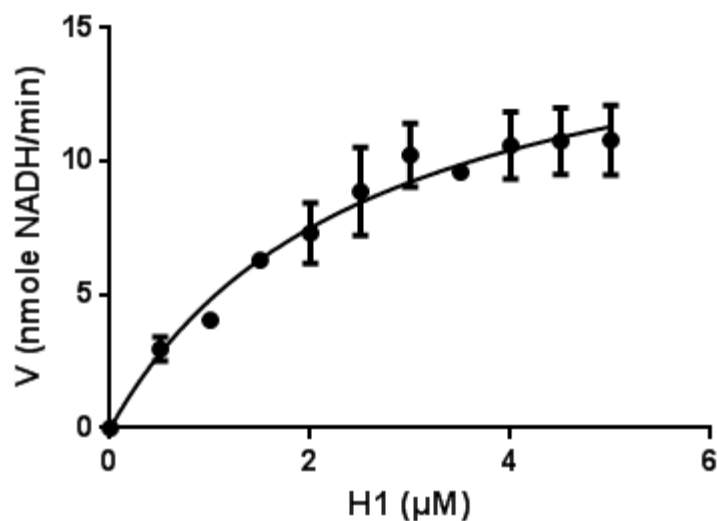
A. Casein substrate



B. MBP substrate



C. H1 substrate



D. ATP

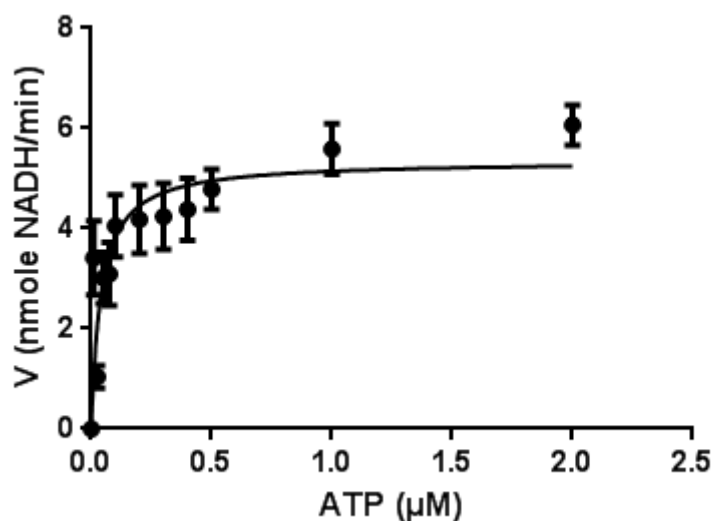


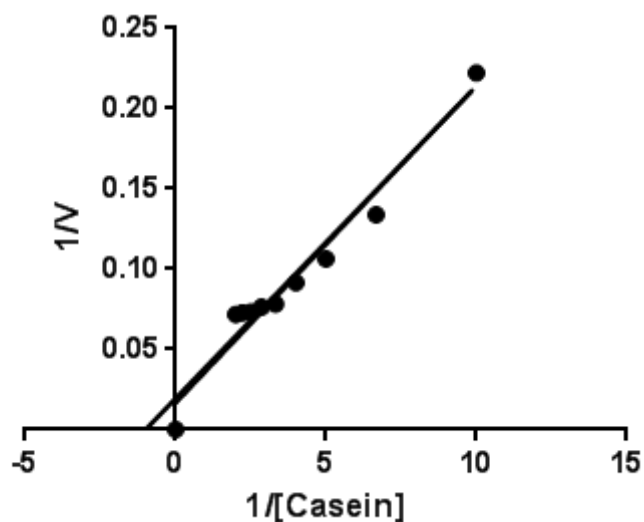
Figure 38: Michaelis-Menten plots for rGST-P/PK8 in the presence of three exogenous substrates and ATP.

Plots of the rate of the rGST-P/PK8 reaction (nmole/min) against substrate concentration (μM). Casein (A), myelin basic protein (MBP) (B), histone protein 1 (H1) (C) and ATP (D). The experiments were performed in duplicate using a different biological protein sample. The error bars represent standard error of the mean. The graphs were generated with GraphPad Prism 5 for Windows version 5.01.

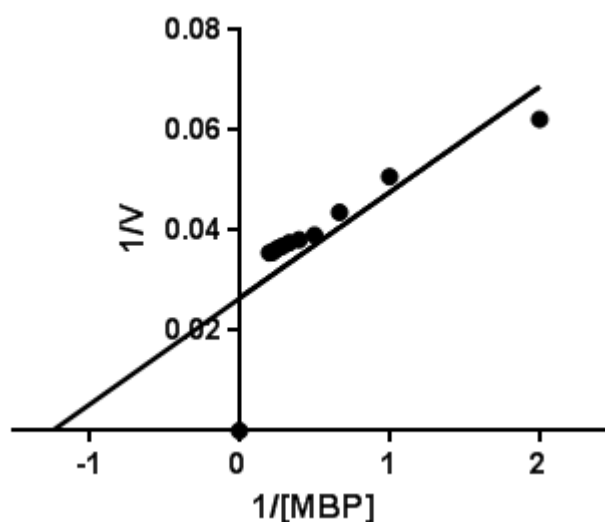
A Lineweaver-Burk plot (Figure 39) for each substrate was constructed by plotting the $1/V$ readings against the $1/[S]$ values. The Michaelis-Menten equation does not take substrate inhibition into account and therefore Lineweaver-

Burk plots were used to determine the approximate K_m and V_{max} values for rGST-PfPK8 (Table 25). The graphs were generated with GraphPad Prism 5 for Windows version 5.01 software.

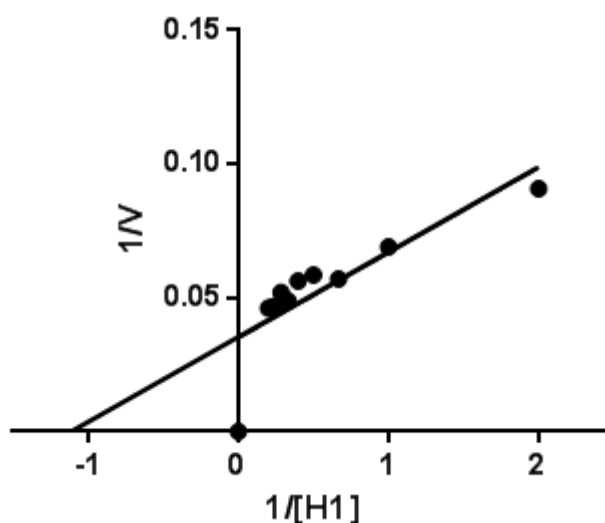
- A. Double reciprocal plot of rGST-PfPK8 in the presence of casein (0.05 μ M – 0.5 μ M) with constant ATP (2.5mM).**



- B. Double reciprocal plot of rGST-PfPK8 in the presence of MBP (0.5 μ M - 5 μ M) with constant ATP (2.5mM).**



- C. Double reciprocal plot of rGST-*Pf*PK8 in the presence of H1 (0.5 μ M - 5 μ M) with constant ATP (2.5mM).



- D. Double reciprocal plot of rGST-*Pf*PK8 in the presence of ATP (0.025mM – 2mM) with constant casein (0.5 μ M).

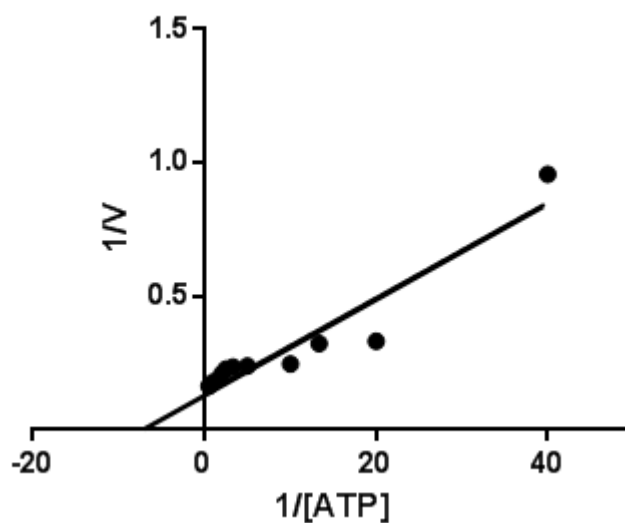


Figure 39: Lineweaver-Burk plots for rGST-*Pf*PK8 in the presence of three exogenous substrates and ATP.

Double reciprocal plot of 1/Velocity against 1/Substrate concentration for rGST-*Pf*PK8 in the presence of casein (A), myelin basic protein (MBP) (B), histone protein 1 (H1) (C) and ATP (D). The graphs were generated with GraphPad Prism 5 for Windows version 5.01 software.

Table 25: Approximate Km and Vmax values for rGST-*Pf*PK8 for three exogenous substrates and ATP.

Exogenous substrate	Km (μ M)	Vmax (nmole NADH/min) \pm SEM*	Specific activity (V/mg) \pm SEM*
Casein	0.9	14.8 \pm 0.07	6 188 \pm 747.8
MBP	1.3	14.1 \pm 0.01	12 497 \pm 616.4
H1	1.1	11.1 \pm 0.02	9 611 \pm 1 162.1
ATP	7.7	5.28 \pm 0.1	5 395 \pm 353.7

SEM: Standard error of the mean

* Sample size = 2

The Vmax is reached when all of the rGST-*Pf*PK8 sites are saturated with substrate. Recombinant GST-*Pf*PK8 had the highest specific enzyme activity in the presence of MBP (12 497 \pm 616nmole NADH/min per mg enzyme).

3.7.4 Effect of temperature on rGST-*Pf*PK8 activity

Enzyme activity can be affected by temperature. The temperature of a female *Anopheles sp.* mosquito ranges between 22°C and 28°C while not feeding and can increase up to 34°C when a blood meal is taken (Lahondere and Lazzari, 2012). The normal body temperature of a human is 37°C and during a fever spike caused by malaria infection may rise to 40°C. The enzyme activity (Figure 40) of rGST-*Pf*PK8 was therefore determined by varying the assay temperature between 26°C and 40°C.

Casein (200 μ g) was used as exogenous substrate in the presence of rGST-*Pf*PK8 (2.25 – 2.73 μ g) and 2.5mM ATP at pH 7.4. The experiment was repeated using a different biological sample of rGST-*Pf*PK8. Recombinant GST-*Pf*PK8 showed maximal kinase activity at a temperature of 40°C.

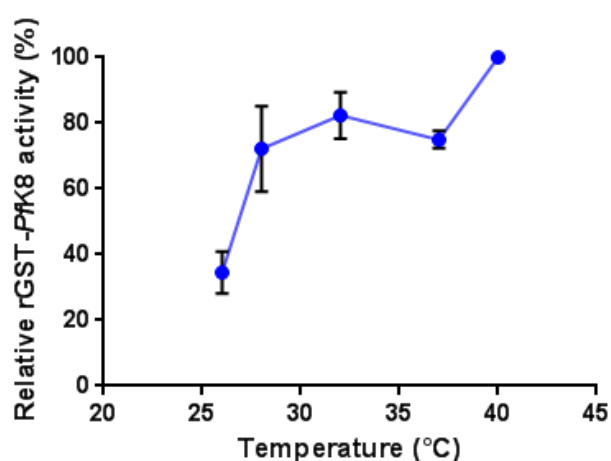


Figure 40: Effect of temperature on rGST-PfPK8 enzyme activity.

The graph shows the relative activity (%) of rGST-PfPK8 (2.25 – 2.73µg pure enzyme) over a temperature range in the presence of 200µg casein at a pH of 7.4. The experiment was repeated using a different rGST-PfPK8 sample. The relative activity enzyme results were as follows: 26°C (35%), 28°C (72%), 34°C (82%), 37°C (75%), 40°C (100%). The error bars represent standard error of the mean of two experiments using two different biological samples. The graphs were generated with GraphPad Prism 5 for Windows version 5.01.

Because enzymes are proteins, their activity depends upon the integrity of the native protein conformation, and denaturation of the protein, or the dissociation of the enzyme into subunits, therefore destroys the catalytic activity. The enzyme had the lowest relative activity at a temperature of 26°C (35%) and remained active at a temperature of 40 °C (100%). Temperatures above 60°C will cause a permanent change in the shape of an enzyme's active site and a fever spike in the human host will not affect the activity of rGST-PfPK8. Recombinant GST-PfPK8 remains active at a temperature corresponding to the body temperature of an *Anopheles sp.* mosquito (28°C: 72% and 34°C: 82%) and its human host (37°C: 75%).

3.7.5 Effect of pH on rGST-PfPK8 activity

All enzymes are sensitive to pH changes. *Plasmodium falciparum* is exposed to a range of pH conditions during its asexual and sexual life cycle. The pH of the parasite's cytoplasm is near neutral (pH 7.15 – 7.3) and that of the digestive vacuole is acidic (pH 4.5 – 5.5) (Kuhn *et al.*, 2007)). The parasite is briefly exposed to human blood plasma (pH 7.35 – 7.45) (Waugh and Grant, 2007) before spending most of its asexual life cycle within an erythrocyte with a

pH of 7.4. Gametocytes are ingested by a female mosquito during a blood meal and travel to the acidic (pH 5 – 6.5) midgut of the mosquito (Gusmao *et al.*, 2007).

The target protein *Pf*PK8 is mostly expressed in the ring, trophozoite and schizont stages of *P. falciparum*'s life cycle. The activity of rGST-*Pf*PK8 (2.25 – 2.73µg pure enzyme) was therefore tested over a pH range of 5 – 9 (Figure 41) in the presence of 2.5mM ATP and 200µg casein as exogenous substrate.

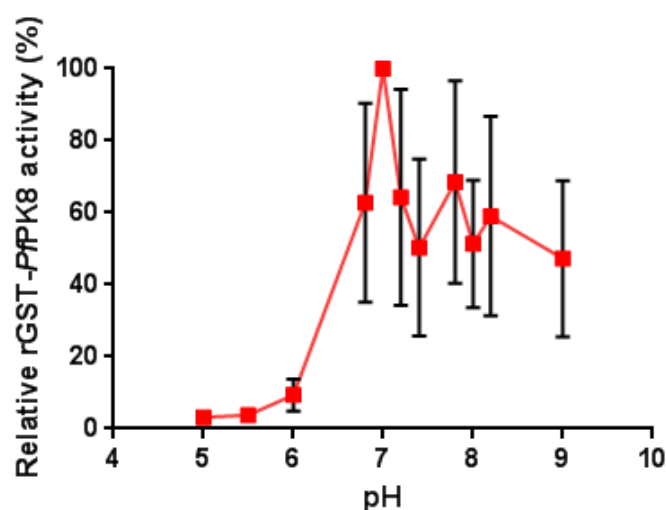


Figure 41: Effect of pH on rGST-*Pf*PK8 enzyme activity.

The graph shows the relative enzyme activity (%) of rGST-*Pf*PK8 (2.25 – 2.73µg pure enzyme) over a pH range in the presence of 200µg casein at a temperature of 37°C. The reactions were set up with different buffers. For pH 5, pH 5.5 and pH 6 a 0.1M sodium acetate buffer was used. For pH 6.8 – 9, 0.1M Tris-HCl buffer was used. The experiment was repeated using a different rGST-*Pf*PK8 sample. The results were as follows: pH 5 (No relative activity), pH 5.5 (4%), pH 6 (9%), pH 6.8 (63%), pH 7.2 (64%), pH 7 (100%) pH 7.4 (50%), pH 7.8 (69%), pH 8 (51%), pH 8.2 (59%), pH 9 (47%). The values at pH 7 were the same and thus there are no error bars. There was no margin of error at pH 7. The graphs were generated with GraphPad Prism 5 for Windows version 5.01.

The enzyme assay relies on the auxiliary enzymes pyruvate kinase and lactate dehydrogenase. The margin of error was generally high, as indicated by the error bars in Figure 41. A change in the pH will not only have an effect on the target enzyme in the closed system but will affect the other enzymes as well and cause a shift in product formation and equilibrium of the coupled reactions. Recombinant GST-*Pf*PK8 was the most active at pH 7 which is close to what is regarded as physiological pH and had extremely low activity at a pH below 6 (<9%) and was

inactive at pH 5. The target enzyme had a similar relative activity at pH 6.8 (63%) and pH 7.2 (64%). The relative enzyme activity fluctuated slightly between pH 7.2 and pH 9.

3.8 Recombinant GST-*Pf*PK8 and red blood cell membrane protein-protein interactions

Red blood cell membrane (RBCM) proteins were extracted from human blood to investigate whether rGST-*Pf*PK8 interacts with any of these proteins.

3.8.1 Red blood cell membrane protein quantitation

The concentration of RBCM proteins was determined by using the Coomassie PlusTM Protein Assay Reagent and a BSA standard curve (Table 26).

Table 26: Absorbance values of the Coomassie protein determination assay of BSA standards and red blood cell membrane protein sample.

Sample	Absorbance at 595nm		Average absorbance at 595nm
2µg BSA	0.092	0.077	0.0845
4µg BSA	0.13	0.123	0.1265
8µg BSA	0.255	0.258	0.2565
12µg BSA	0.336	0.355	0.3455
16µg BSA	0.442	0.442	0.442
RBCM	0.0752	0.0802	0.0777

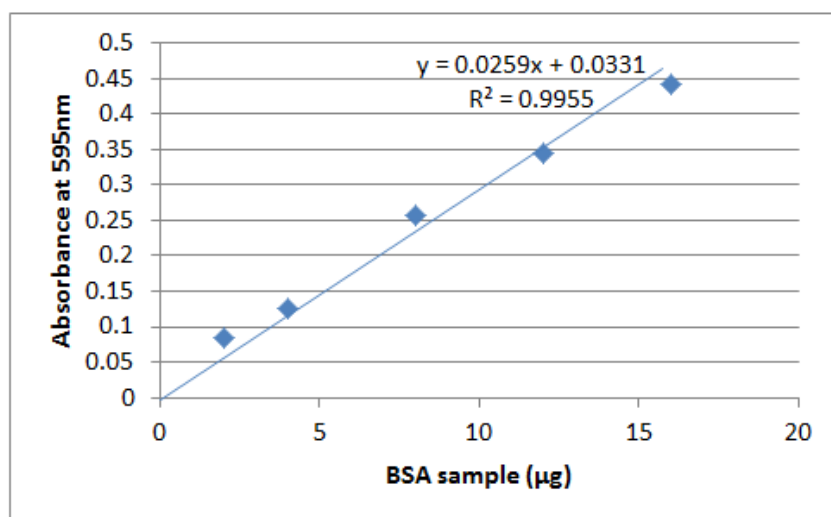


Figure 42: BSA standard curve.

The Coomassie Plus™ Protein Reagent assay was used to determine the concentration of the red blood cell membrane (RBCM) protein sample. A standard curve with an R^2 value of 0.9955 was obtained using bovine serum albumin (BSA) as standard.

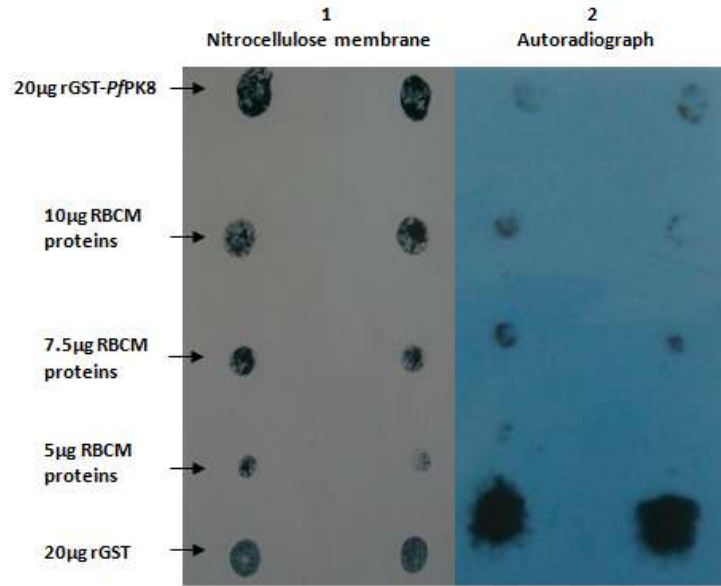
The concentration of the RBCM protein sample was calculated to be $1.7\mu\text{g}/\mu\text{l}$ using the BSA standard curve (Figure 42).

3.8.2 Binding studies

Binding studies were performed by dot blot overlays of RBCM proteins with purified rGST-*Pf*PK8 to determine if there is a parasite-host protein-protein interaction between RBCM proteins and rGST-*Pf*PK8.

Different amounts of RBCM proteins, $20\mu\text{g}$ rGST-*Pf*PK8 and $20\mu\text{g}$ rGST as positive controls were spotted on two separate nitrocellulose membranes. One membrane was overlaid with $182\mu\text{g}$ purified rGST-*Pf*PK8 in a 50mM Tris-HCl buffer pH 7.5 (Figure 43 A) and the control blot (Figure 43 B) with only buffer. The membranes were probed with anti-GST horseradish peroxidase conjugate antibody and exposed to X-ray film overnight to obtain an autoradiograph.

A. Recombinant GST-*Pf*PK8 dot blot overlay.



B. Control buffer overlay.

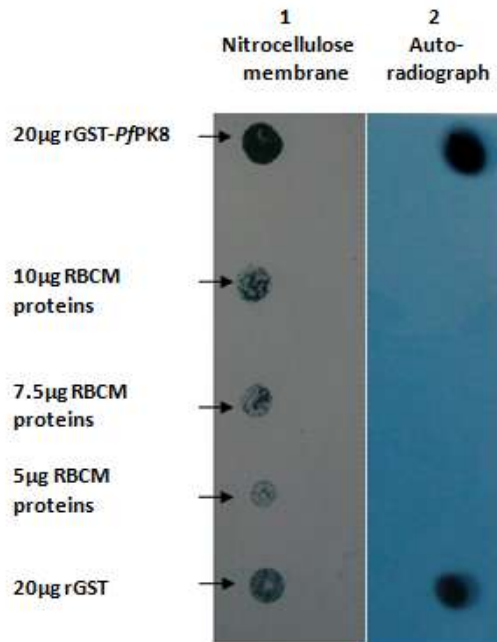


Figure 43: Dot blots of immobilised red blood cell membrane proteins overlaid with rGST-*Pf*PK8.

Photographs of dot blots with 20µg rGST-*Pf*PK8 as positive control and RBCM proteins immobilised on a nitrocellulose membrane. The experimental membrane (A) was overlaid with 182µg purified rGST-*Pf*PK8 in 50mM Tris-HCl buffer at pH 7.4 and the control membrane with only 50mM Tris-HCl buffer. Panel 1: Amido black stained nitrocellulose membranes with the immobilised proteins, Panel 2: Recombinant GST-*Pf*PK8 and rGST were detected with Anti-GST horseradish peroxidase Conjugate antibody (1:100 000). The autoradiograph was obtained by overnight exposure to the probed membranes.

A positive signal was detected on the dot blot autoradiograph overlaid with rGST-*Pf*PK8 as seen in Figure 43 A compared to no signal on the control autoradiograph (Figure 43 B). This indicates that a parasite-host protein-protein interaction does exist between RBCM proteins and rGST-*Pf*PK8.

Laemmli gels were used to determine exactly with which RBCM protein rGST-*Pf*PK8 interacted. RBCM proteins, rGST-*Pf*PK8, rGST and BSA were separated on SDS-PAGE gels and transferred to nitrocellulose membranes (Figure 44).

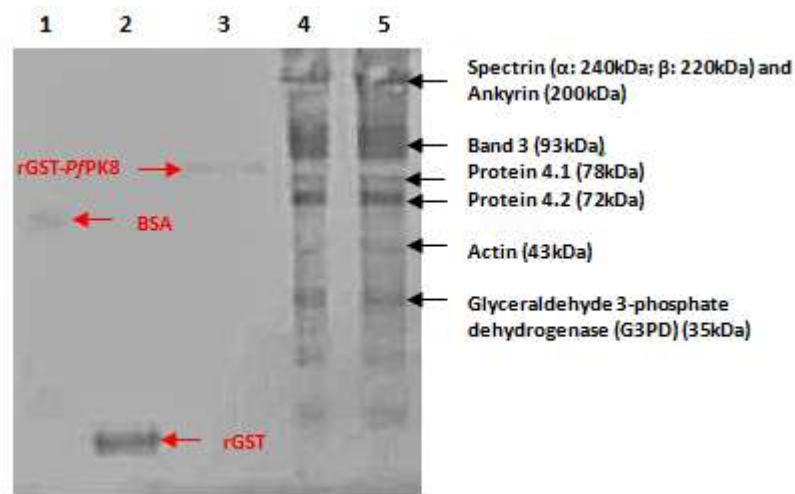
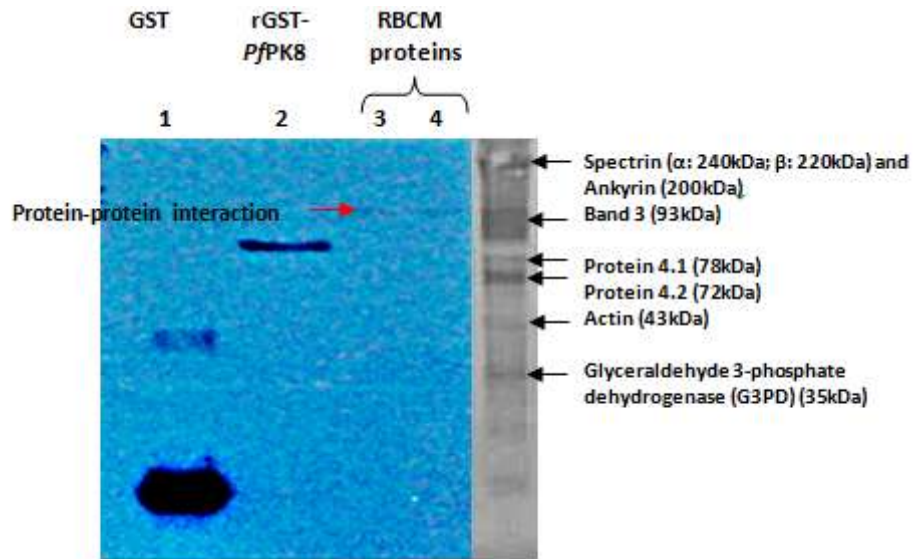


Figure 44: Amido black stained nitrocellulose membrane used in the binding study of rGST-*Pf*PK8 with RBCM proteins.

Proteins were electrophoresed on a Laemmli gel and transferred to a nitrocellulose membrane. Lane 1: BSA (1μg), Lane 2: rGST (5μg), Lane 3: rGST-*Pf*PK8 (1μg), Lane 4: RBCM proteins (7.5μg) and Lane 5: RBCM proteins (10μg).

One nitrocellulose membrane was overlaid with 182μg pure rGST-*Pf*PK8 in 50mM Tris-HCl buffer and the other membrane overlaid with buffer only. The membranes were probed with anti-GST HRP-conjugated primary anti-body and exposed to X-ray film overnight to detect protein-protein interaction between rGST-*Pf*PK8 and the immobilised RBCM proteins (Figure 45 A and B).

A. Autoradiograph of rGST-*Pf*PK8 overlay.



B. Autoradiograph of control buffer overlay.

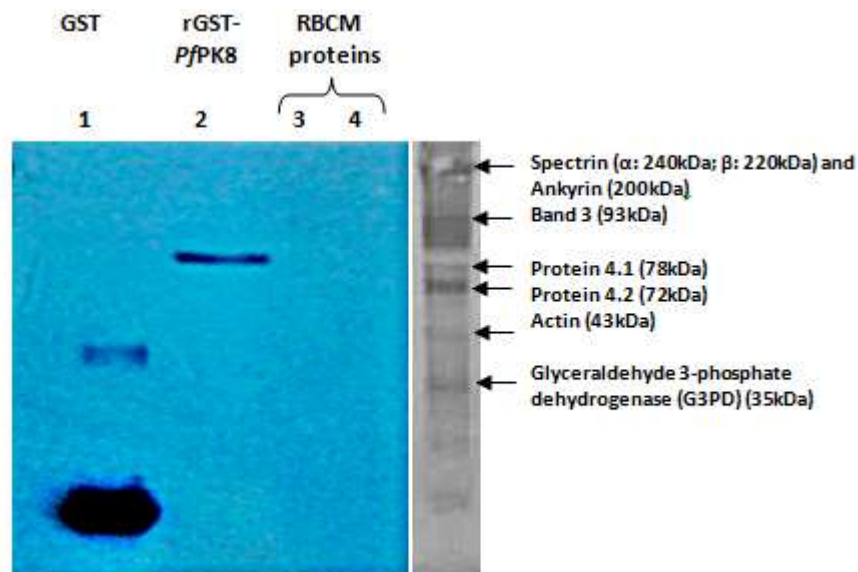


Figure 45: Immunoblots of RBCM – rGST-*Pf*PK8 overlays using anti-GST HRP-conjugated antibody.

Autoradiographs of nitrocellulose membranes overlaid with (A) 182μg rGST-*Pf*PK8 and (B) buffer. A host-parasite protein-protein interaction between rGST-*Pf*PK8 and RBCM protein Band 3 was detected as seen in Figure A.

A positive signal was detected on the autoradiograph overlaid with 182μg rGST-*Pf*PK8 in 6ml 50mM Tris-HCl. Using the amido black stained nitrocellulose membrane and the autoradiograph (Figure 45 A), measurements of the distance

travelled by the proteins showed that the RBCM protein with which rGST-*Pf*PK8 interacted is Band 3. The experiment was repeated with another immunoblot of a Laemmli gel using a different biological purified sample of rGST-*Pf*PK8, which confirmed the result (data not shown).

3.9 Bioinformatic analysis of *Pf*PK8

3.9.1 Identification of *Pf*PK8 homologues and functional regions using BLAST

The 497 residue protein sequence (Figure 31) of *Pf*PK8 containing the centrally located protein kinase domain (274 aa) was submitted to BLAST and sequences with a significant percentage identity (identity >35% and E-value <0.05) (Altschul *et al.*, 1997) with the target sequence were identified. Refer to Appendix section 6.4.1 for details on the sequences that produced a significant protein sequence alignment to *Pf*PK8. The results of the BLAST query provided insight into the possible function of *Pf*PK8. The majority of the identified homologues were those from the STE kinase family classified as serine/threonine kinases (STKs).

The first recognized significant alignment (Appendix section 6.4.1) with a query cover of 100% and an E-value of 0 is the *Pf*PK8 target sequence in PlasmoDB recognized by BLAST. A STK from *Plasmodium cynomolgi* strain B had the highest sequence identity of 68% to the target sequence and the most significant E-value of 2×10^{-154} , followed by a STK from *Plasmodium vivax* Sal-1 (66% identity, E-value = 2×10^{-132}) and a protein kinase from *Plasmodium knowlesi* strain H1 (62% identity, E-value = 7×10^{-143}) (Figure 46). The other identified homologues had an identity of less than 40% to the target sequence of *Pf*PK8 and included human mammalian sterile 20-like kinase 3 (MST3) (also known as STE-20-like kinase 3 or STK PK24) and MST1 (also known as STK PK25).

serine/threonine-specific protein kinase [Plasmodium cynomolgi strain B]

Sequence ID: [ref|XP_004225467.1](#) Length: 1471 Number of Matches: 1

[▶ See 1 more title\(s\)](#)

Range 1: 1072 to 1408 GenPept Graphics						▼ Next Match ▲ Previous Match	
Score	Expect	Method	Identities		Positives	Gaps	
488 bits(1255)	2e-154	Compositional matrix adjust.	229/339(68%)		280/339(82%)	4/339(1%)	
Query 125		NDDDSYDEDNLVSLKIINLKYLSKKNLSLKNILREVNF-KMCEHPNVVVKYFESFFWPPCYL					183
Sbjct 1072		+D+ +YDE+NLV+LKIINL+YLSKKNLSL+ I++EV+F + C+HPN+VKY ESFFWPPCYL					1131
Query 184		SDEGNYDEENLVTILKIINLRYLSKKNLSLRIMKEVHFLQCDHPNIVKYHESFFWPPCYL					243
Sbjct 1132		VIVCEYLSGGTLYDLYKNGRISEDLVYILDDVLNGLNYLHNECSSPLIHRDIKPTNIV					1191
Query 244		VIVCE+LSGGTL+DLYK GRI+ED+LV+ILDDVL L YLHNEC L+HRDIKPTNIV					302
Sbjct 1192		VIVCEFLSGGTFLDLYKKCGRITEDVLVHILDDVLKALKYLHNECPLCLVHRDIKPTNIV					1250
Query 303		LSKDGIAKIIDFGSCEELKNSDQSKELVGTIYYISPEILMRTNYD-SSDIWSLGITIIYEI					362
Sbjct 1251		SK G+AKIIDFGSCE+++ + E+VGT+YYISPEIL R YD S+DIWSLGITIIYE+					1310
Query 363		FSKSGMAKIIDFGSCEKVEDV-KLHEVVGTLYYISPEILKREKYDCSADIWSLGITIIYES					422
Sbjct 1311		VLCTLPWKRNSQSFENYIKTIINSSPKINITEGYSKHLCYFVEKCLQKKPENRGNVKDLLN					1370
Query 423		V+C LPWK + E I+ I++SSPKIN+ G+SK C+FVE CLQ P R V+ LL					
Sbjct 1371		VMCALPWKGKKDIEESIQIVDSSPKINLCSGFSKQFCFFVESCLQNNPGKRAKVEHLLG					
Query 125		HKFLIKKRYIKKKPSSIIYEIRDILKIYNGKGKTNIFRNFFKNLFFNDKNKKKPNKMISS					
Sbjct 1311		HKFL KKR +++KPSSI+EIRDILK+ NGKGK NIFRNFFKNLFF ND NK++ NK +SS					
Query 423		HKFLTCKRLLRRKPSSIFEIRDILKVNNKGKKNIFRNFFKNLFFLNDMKNRRRNKALSS					
Query 423		KSCDAEMFFEQLKRENFDFFEIKLKDDENSRSLNFTNIN			461		
Sbjct 1371		KSC+ EMF++QLKRENFDFFEIKL+ DENSRSL ++			1408		
Sbjct 1371		KSCEPEMFYQQLKRENFDFFEIKLR-DENSRSLGHLHVG			1408		

serine/threonine-specific protein kinase [Plasmodium vivax Sal-1]

Sequence ID: [ref|XP_001612957.1](#) Length: 2125 Number of Matches: 1

[▶ See 1 more title\(s\)](#)

Range 1: 1715 to 2050 GenPept Graphics						▼ Next Match ▲ Previous Match	
Score	Expect	Method	Identities		Positives	Gaps	
489 bits(1260)	2e-152	Compositional matrix adjust.	224/338(66%)		277/338(81%)	4/338(1%)	
Query 125		NDDDSYDEDNLVSLKIINLKYLSKKNLSLKNILREVNF-KMCEHPNVVVKYFESFFWPPCYL					183
Sbjct 1715		D +SYDE+ LV+LKI+NL+YLSKKNLSL+ I++EV+F ++C+HPN+VKY ESFFWPPCYL					1774
Query 184		GDQESYDEEKLVTLKIVNLRYLSKKNLSLRIMKEVHFLQCDHPNIVKYHESFFWPPCYL					243
Sbjct 1775		VIVCEYLSGGTLYDLYKNGRISEDLVYILDDVLNGLNYLHNECSSPLIHRDIKPTNIV					1834
Query 244		VIVCE+LSGGTL+DLYK GRI+ED+LV+ILDDVL L YLHNEC+S L+HRDIKPTNIV					302
Sbjct 1835		VIVCEFLSGGTFLDLYKKCGRITEDVLVHILDDVLKALQYLHNECTSCLVHRDIKPTNIV					1893
Query 303		LSKDGIAKIIDFGSCEELKNSDQSKELVGTIYYISPEILMRTNYD-SSDIWSLGITIIYEI					362
Sbjct 1894		SK G+AKI+DFGSCE +++ + E+VGT+YYISPEIL R YD S+DIWSLGITIIYE+					1953
Query 363		FSKSGVAKIVDFGSCERVEDL-KMHEVVGTLYYISPEILKREKYDCSADIWSLGITIIYEV					422
Sbjct 1954		VLCTLPWKRNSQSFENYIKTIINSSPKINITEGYSKHLCYFVEKCLQKKPENRGNVKDLLN					2013
Query 423		V+C LPWK + E IK I+ SSPKIN+ G++K C+FVE CLQ P R N LL					
Sbjct 2014		VMCALPWKGKKHIEESIKQIVGSSPKINLCSGFTKQFCFFVESCLQNDPGKRANAHHLLG					
Query 423		HKFLIKKRYIKKKPSSIIYEIRDILKIYNGKGKTNIFRNFFKNLFFNDKNKKKPNKMISS					
Sbjct 2014		HKFL KKR +++KPSSI+EIRDILK+ NGKGK NIFRNFFKNLFF NDKNK++ NK + S					
Query 423		HKFLTCKRLLRRKPSSIFEIRDILKVNNKGKKNIFRNFFKNLFFLNDKKNRRRNKALGS					
Query 423		KSCDAEMFFEQLKRENFDFFEIKLKDDENSRSLNFTNIN			460		
Sbjct 2014		KSC+ EMF+ +LKRENFDFFEI+L+D +SRSL ++			2050		
Sbjct 2014		KSCEPEMFYRKLKRENFDFFEIRLDG-SRSLGHLHV			2050		

protein kinase [Plasmodium knowlesi strain H]

Sequence ID: [refjXP_002258003.1](#) Length: 2129 Number of Matches: 1

[▶ See 1 more title\(s\)](#)

Range 1: 1708 to 2065		GenPept	Graphics			▼ Next Match	▲ Previous Match
Score	Expect	Method	Identities	Positives	Gaps		
462 bits(1189)	7e-143	Compositional matrix adjust.	233/360(65%)	293/360(81%)	4/360(1%)		
Query 103		EGINKLTYHNMNKNISNENNYNDDDSYDEDNLVSLKIINLKYLSKKNLKNILREVNF-				161	
Sbjct 1708		+GI+K ++ ++ + + +D++ YDE+NLV+LKIINL+YLSK+NSL+ I++EV+F					1767
		QGIDKGSHQGNDEGSHQGNKDSDDEEYDEENLVTLKIINLRYLSKENSRLRRIMKEVHFL					
Query 162		KMCEHPNVVKYFESFFWPPCYLVIVCEYLSGGTLYDLYKNYGRISEDLLVYILDDVLNGL				221	
Sbjct 1768		+ C HPN+VKY ESFFWPPCYLVIVCE+LSGGTL+DLYK GRI+ED+LV+ILDDVL L					1827
		QNCNHPNIVKYHESFFWPPCYLVIVCEFLSGGTFLDLYKKCGRITEDVLVHILDDVLKAL					
Query 222		NYLHNECSSPLIHRDIKPTNIVLSKDGIAKIIDFGSCEELKNSDQSKELVGTIYYISPEI				281	
Sbjct 1828		YLHNECS L+HRDIKPTNIV SK G+AKI+DFGSCE++++ + E+VGT+YYISPEI					1886
		KYLHNECSLCLVHRDIKPTNIVFSKSGVAKIVDFGSCEKVEDL-KLHEVVGTLYYISPEI					
Query 282		LMRTNYD-SSDIWSLIGITIYEIVLCTLPWKRNSQSFENYIKTIINSSPKINITEGYSKHL				340	
Sbjct 1887		L R YD S+DIWSLIGITIYE V+C LPW+ + E IK I++SSPKIN+ G+SK C					1946
		LKREKYDCSADIWSLIGITIYESVMCALPWRGKKDIEESIKQIVDSSPKINLCSGFSKQFC					
Query 341		YFVEKCLQKKPENRGNVKDLLNHKFLIKKRYIKKKPSSIYEIRDILKIYNGKGKTNIFRN				400	
Sbjct 1947		+FVE CLQ P R V +LL HKFL KKR I++KPSSI+EIRDILK+ NGKGK NIFRN					2006
		FFVESCLQNNPGKRAKVANLLGHKFLTKRLIRRKPSIIFEIRDILKVNGKGKNNIFRN					
Query 401		FFKNLFFFNDKNNKKPNKMISSKSCDAEMFFEQLKRENFDFFEIKLKDDENSRSLNTFNI				460	
Sbjct 2007		FFKNLFFFNDKNNK++ NK +SSKSC+ EMF+++LKRENFDFFEIKL+ DENSRSL ++					2065
		FFKNLFFFNDKNNKRRTNKALSSKSCEPEMFYQKLKRENFDFFEIKLR-DENSRSLGHLHV					

Figure 46: An alignment of the kinase domain of *rPf*PK8 with its closest serine/threonine-like kinase homologues.

The cloned region sequence of *rPf*PK8 (497 aa) was submitted to BLAST to obtain a sequence alignment between the target sequence and its closest homologues. A STK from *Plasmodium cynomolgi* strain B had the highest sequence identity of 68%, followed by a STK from *Plasmodium vivax* Sal-1 (66% identity) and a protein kinase from *Plasmodium knowlesi* strain H1 (62% identity). The term “% identity” refers to the number of residues that are identical in the alignment and “% positives” refers to the number of residues that belong to the same class.

Putative conserved domains within *Pf*PK8 sharing homology with the catalytic domain of protein kinases from the STE kinase family (PKc_STEs) and that of the serine/threonine kinases (STKcs) were identified with the BLAST search. These domains include the ATP binding site containing the activation-loop (A-loop) and the substrate binding site of the enzyme’s catalytic domain (Figure 48 and 49). Fifty six percent (9 out of 16) of the residues that compose the conserved feature of the ATP binding site of PKc_STEs (amino acids 157 – 180 of the kinase domain) (Figure) and 57% (8 out of 14) of the residues of the substrate binding site (residues 10 – 221 of the kinase domain) were identified as identical or highly conserved in the target sequence of *Pf*PK8. The substrate binding site is based on the binding of the human PAK4 serine/threonine kinase to a consensus peptide. The areas of sequence identity between *Pf*PK8, PKc_STEs and STKcs are shown in Figure 47.

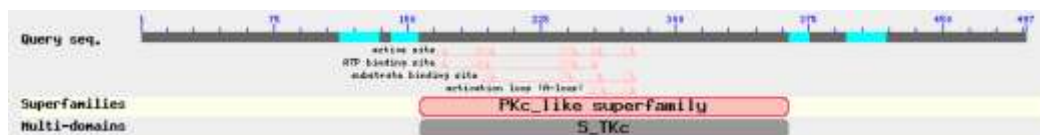


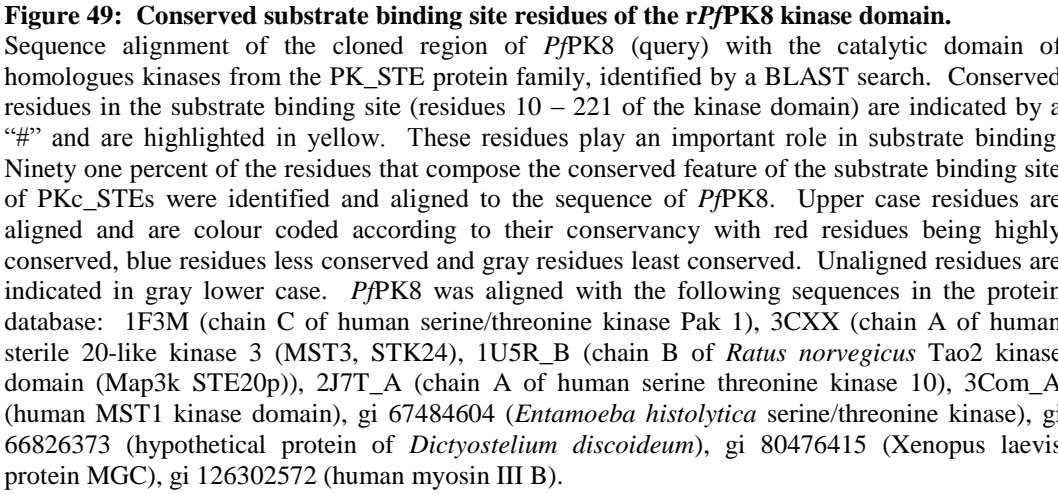
Figure 47: Areas of identity between the cloned region of *Pj*PK8, PKc_STEs and S_TKcs.

The pink triangles depict the areas where sequence identity between the target 497 residue protein sequence of *Pj*PK8 (query sequence) and the catalytic domain of protein kinases from the STE kinase family (PKc_STEs) and that of the serine/threonine kinases (S_TKcs) has been identified by BLAST. The kinase domain of *rPj*PK8 ranges from residue 95 – 368. Putative sequence domains identified within the active site include the ATP binding site containing the activation loop and the substrate binding site. Sixty percent of the residues that compose the conserved features of the ATP binding site of PKc_STEs and 91% of the residues of the substrate binding site were mapped to the target sequence of *Pj*PK8.



Figure 48: Conserved ATP-binding pocket residues of the rPfPK8 kinase domain

Sequence alignment of the cloned region of *Pf*PK8 (query) with the catalytic domain of homologues kinases from the PK_STE protein family, identified by a BLAST search. Conserved residues in the ATP binding site (residues 157 – 180) are indicated by a “#” and are highlighted in yellow. These residues are important in ATP binding. Sixty percent of the residues that compose the conserved feature (activation-loop) of the ATP binding site of PKc_STEs were identified and aligned to the sequence of *Pf*PK8. Upper case residues are aligned and are colour coded according to their conservancy with red residues being highly conserved, blue residues less conserved and gray residues least conserved. Unaligned residues are indicated in gray lower case. *Pf*PK8 was aligned with the following sequences in the protein database: 1F3M (chain C of human serine/threonine kinase Pak 1), 3CKX (chain A of human sterile 20-like kinase 3 (MST3, STK24)), 1U5R_B (chain B of *Ratus norvegicus* Tao2 kinase domain (Map3k STE20p)), 2J7T_A (chain A of human serine threonine kinase 10), 3Com_A (human MST1 kinase domain), gi 67484604 (*Entamoeba histolytica* serine/threonine kinase), gi 66826373 (hypothetical protein of *Dictyostelium discoideum*), gi 80476415 (*Xenopus laevis* protein MGC), gi 126302572 (human myosin III B).



3.9.2 Secondary structure prediction of *Pf*PK8

The cloned sequence including the kinase domain of *Pf*PK8 was submitted to the protein-homology/analogy recognition engine (Phyre2) to predict the secondary structure of the target enzyme. A detailed summary output of the secondary structure (α -helices, β -strands or coils) and disorder prediction of the kinase domain of *Pf*PK8 given by Phyre2 is shown in Figure 50. Phyre2 uses a program called DisoPred (Ward *et al.*, 2004a) to identify areas of the query that are most likely to be structurally disordered. These areas can be used to identify structurally flexible regions that may inhibit protein crystallization.

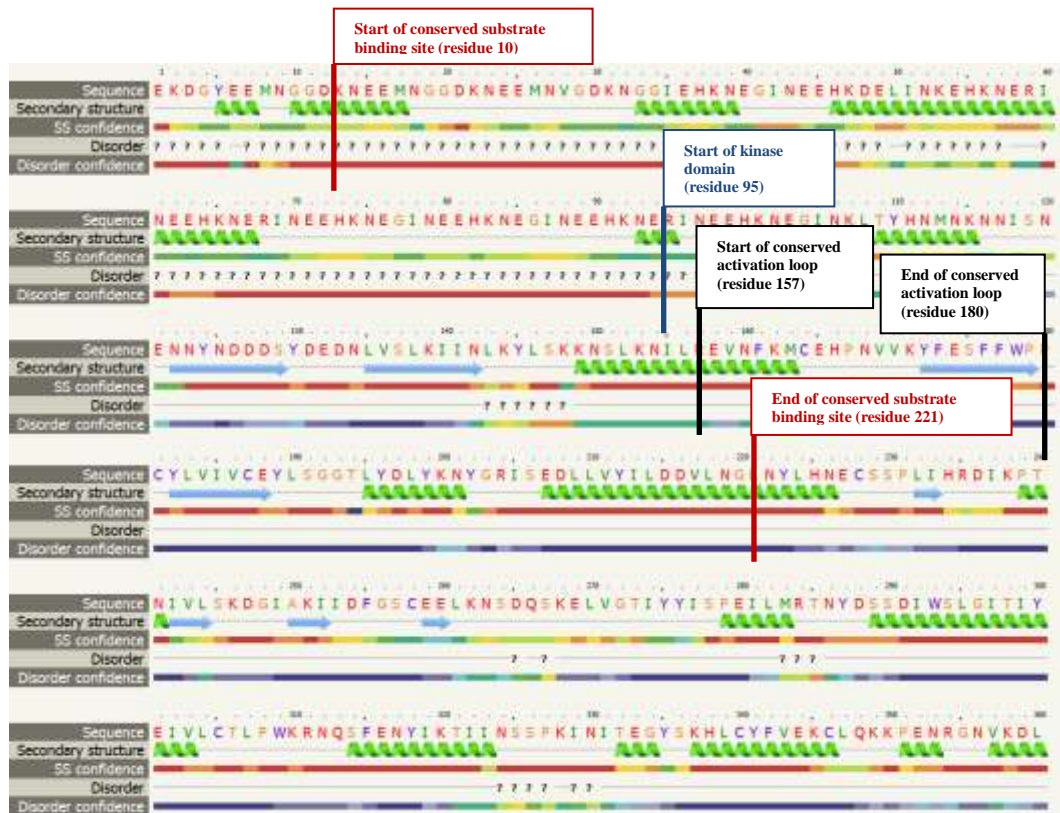




Figure 50: Secondary structure and disorder prediction of the cloned region of *PfPK8*.

A summary of the secondary structure and disorder prediction of the cloned region (497aa) of *PfPK8* according to the protein-homology/analogy recognition engine (Phyre2). The protein sequence of the kinase domain of *PfPK8* submitted to Phyre2 is indicated with corresponding amino acid positions. The position of the kinase domain and conserved residues of the substrate binding site and activation loop is indicated. A green swirl indicates the position of a predicted alpha helix, a blue arrow the position of a predicted beta strand and a grey line the position of a predicted coil. The secondary structure (SS) confidence row indicates the confidence of the prediction at each position from low confidence (dark blue - 0) to high confidence (red - 9). The areas of predicted disorder within the 3D secondary structure are indicated by a "?".

3.9.3 Three dimensional structure prediction of *PfPK8*

Only 54% (268 aa of the kinase domain) of the cloned region of *PfPK8* (497 aa) was modelled by the protein-homology/analogy recognition engine (Phyre2) with a confidence score of 90% (Figure 51).

Due to the low percentage of residues modelled, another query was submitted to Phyre2 with only the amino acid sequence of the kinase domain of *PfPK8*. This domain consists of 274 amino acids of which 98% of the residues were modelled with a confidence score >90% (Figure 52). Phyre2 used the top 120 homologues identified in the Protein Data bank with known crystal structures to construct the 3D structure model of the kinase domain of *PfPK8*. The high level of confidence (100%) of the top 20 homologues (Figure 53) is attributed to the conservancy of the protein kinase domain across eukaryotic protein kinases.

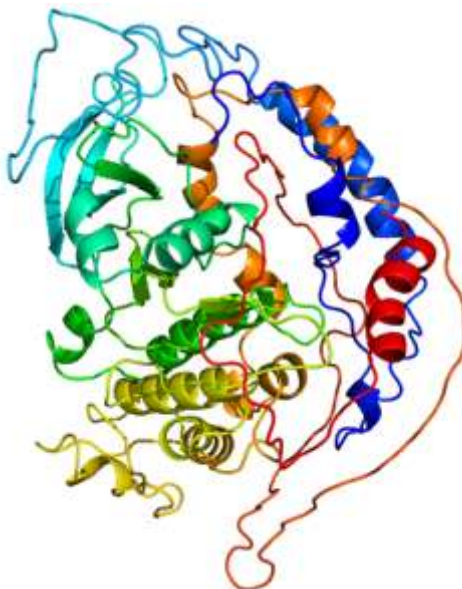


Figure 51: Predicted 3D structure of the cloned region of *Pf*PK8.

The amino-acid sequence of the cloned region of *Pf*PK8 was submitted to the protein-homology/analogy recognition engine (Phyre2) to obtain the three-dimensional structure. Fifty four percent of the amino acids submitted to the query were modelled with >90% confidence level. The N-terminal end of the protein is indicated in red and the C-terminal domain is indicated in blue.

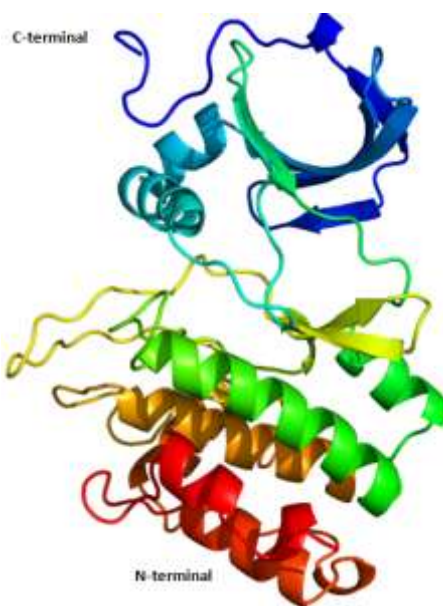













Figure 52: Predicted 3D structure of the kinase domain of *Pf*PK8.

The amino-acid sequence of the kinase domain of *Pf*PK8 was submitted to the protein-homology/analogy recognition engine (Phyre2) to obtain the three-dimensional secondary structure. Ninety eight percent of the amino acids submitted to the query were modelled with >90% confidence level. The N-terminal end of the protein is indicated in red and the C-terminal domain is indicated in blue.

#	Template	Alignment Coverage	3D Model	Confidence	% I.d.	Template Information
1	c2c30A_	Alignment		100.0	29	PDB header: transferase Chain: A; PDB Molecule: serine/threonine-protein kinase pak 6; PDBTitle: crystal structure of the human p21-activated kinase 6
2	c2acx8_	Alignment		100.0	22	PDB header: transferase Chain: 8; PDB Molecule: g protein-coupled receptor kinase 6; PDBTitle: crystal structure of g protein coupled receptor kinase 6 bound to2 amppnp
3	c3pfqA_	Alignment		100.0	23	PDB header: transferase Chain: A; PDB Molecule: protein kinase c beta type; PDBTitle: crystal structure and allosteric activation of protein kinase c beta2 ii
4	c3q5iA_	Alignment		100.0	26	PDB header: transferase Chain: A; PDB Molecule: protein kinase; PDBTitle: crystal structure of pbanka_031420
5	c3nyo8_	Alignment		100.0	22	PDB header: transferase Chain: 8; PDB Molecule: g protein-coupled receptor kinase 6; PDBTitle: crystal structure of g protein-coupled receptor kinase 6 in complex2 with amp
6	c4fijA_	Alignment		100.0	30	PDB header: transferase Chain: A; PDB Molecule: serine/threonine-protein kinase pak 4; PDBTitle: catalytic domain of human pak4
7	c4fie8_	Alignment		100.0	30	PDB header: transferase Chain: 8; PDB Molecule: serine/threonine-protein kinase pak 4; PDBTitle: full-length human pak4
8	c2qg5D_	Alignment		100.0	24	PDB header: transferase Chain: D; PDB Molecule: calcium/calmodulin-dependent protein kinase; PDBTitle: cryptosporidium parvum calcium dependent protein kinase cgd7_1840
9	c1koaA_	Alignment		100.0	23	PDB header: kinase Chain: A; PDB Molecule: twitichin; PDBTitle: twitchin kinase fragment (c.elegans), autoregulated protein2 kinase and immunoglobulin domains
10	c3hztA_	Alignment		100.0	29	PDB header: transferase Chain: A; PDB Molecule: calcium-dependent protein kinase 3; PDBTitle: crystal structure of toxoplasma gondii cdpk3, tgme49_105860
11	d1yhwa1	Alignment		100.0	28	Fold: Protein kinase-like (PK-like) Superfamily: Protein kinase-like (PK-like) Family: Protein kinases, catalytic subunit










12	d2j4zal	Alignment		100.0	23	Fold: Protein kinase-like (PK-like) Superfamily: Protein kinase-like (PK-like) Family: Protein kinases, catalytic subunit
13	d1phka_	Alignment		100.0	22	Fold: Protein kinase-like (PK-like) Superfamily: Protein kinase-like (PK-like) Family: Protein kinases, catalytic subunit
14	c2bdwB_	Alignment		100.0	18	PDB header: transferase Chain: 8; PDB Molecule: hypothetical protein k11e8.1d; PDBTitle: crystal structure of the auto-inhibited kinase domain of2 calcium/calmodulin activated kinase II
15	c3l1jA_	Alignment		100.0	28	PDB header: transferase Chain: A; PDB Molecule: calcium/calmodulin dependent protein kinase with PDBTitle: crystal structure of full length cpd3 (cgd5_820) in2 complex with ca2+ and amppnp
16	c1ym7C_	Alignment		100.0	19	PDB header: transferase Chain: C; PDB Molecule: beta-adrenergic receptor kinase 1; PDBTitle: g protein-coupled receptor kinase 2 (grk2)
17	c3c4wB_	Alignment		100.0	22	PDB header: transferase Chain: 8; PDB Molecule: rhodopsin kinase; PDBTitle: crystal structure of g protein coupled receptor kinase 1 bound to atp2 and magnesium chloride at 2.7a
18	c2cgvA_	Alignment		100.0	25	PDB header: transferase Chain: A; PDB Molecule: serine/threonine-protein kinase chk1; PDBTitle: identification of chemically diverse chk1 inhibitors by2 receptor-based virtual screening
19	c3qa8H_	Alignment		100.0	25	PDB header: immune system, signaling protein Chain: H; PDB Molecule: mgc80376 protein; PDBTitle: crystal structure of inhibitor of kappa b kinase beta
20	c2jamB_	Alignment		100.0	22	PDB header: transferase Chain: 8; PDB Molecule: calcium/calmodulin-dependent protein kinase type PDBTitle: crystal structure of human calmodulin-dependent protein2 kinase i g

Figure 53: Template information of homologues used to predict the 3D structure of the kinase domain of *Pf*PK8.

The 3D structure of the kinase domain of *Pf*PK8 was predicted using the protein-homology/analogy recognition engine (Phyre2). The above listed *Pf*PK8 homologues were identified by Phyre2 as the top 20 matches with the highest confidence. The 3D crystal structures of these homologues were used to predict the 3D structure of the kinase domain of *Pf*PK8. The 100% confidence score is attributed to the high conservancy between the kinase domains of eukaryotic protein kinases.

Plasmodium falciparum PK8 is a large protein consisting of 2 485 residues according to PlasmoDB 2011. The protein size was too large for Phyre2 to predict the structure of the complete protein. Phyre2 is only able to predict a protein's structure with high confidence if the protein has between 30 and 1 200 residues (Kelley and Sternberg, 2009). The ExPASy Bio-informatics Resource Portal SWISS-MODEL Workspace was used to predict the whole protein structure (Figure 54). The SWISS-MODEL Repository is a European database of 3D structure models and consists of more than 3.2 million protein structures of

which approximately 2.3 million are unique sequences to the UniProt database (Kiefer *et al.*, 2009).

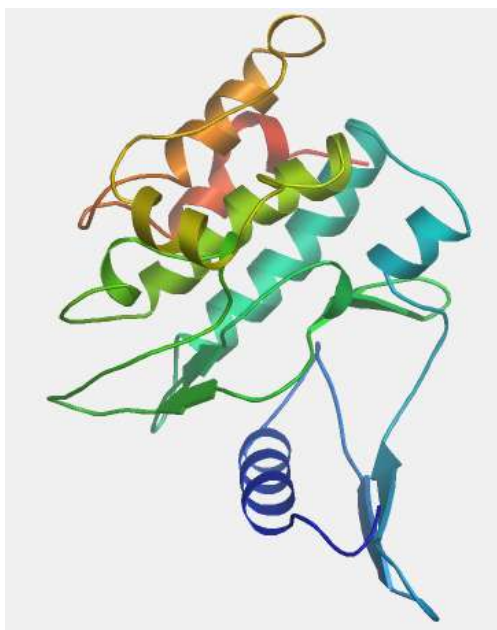


Figure 54: Predicted 3D structure of *Pf*PK8.

The complete amino-acid sequence *Pf*PK8 was submitted to the SWISS-MODEL Workspace to obtain a predicted three-dimensional structure. Approximately 10% of the protein was modelled (depicted in figure) with a sequence similarity of 33.19% to the template (mammalian sterile 20-like kinase, MST1).

Residues 2 130 to 2 356 (10%) of the submitted *Pf*PK8 sequence (2 485 aa) were modelled (Figure 50) based on a template of MST1 which is a human serine/threonine kinase. SWISS-MODEL Workspace identified the crystal structure of MST1 as the template with the most sequence similarity to *Pf*PK8. If there is a sequence identity of less than 40% between the target sequence and the template sequence, errors in the algorithms used for sequence alignment and 3D modelling may occur. The sequence identity between the target sequence and the template sequence was only 33.19%. The 3D structure prediction of *Pf*PK8 by the SWISS-MODEL Workspace is not reliable due to possible alignment errors during modelling.

3.9.4 Predicted protein parameters of recombinant *Pf*PK8

The protein parameters of the recombinant target proteins were predicted by Prot Param. The *Pf*PK8 (715 aa) protein was predicted to consist of 0.6% alanine, 3.0% arginine, 12.7% asparagine, 5.8% aspartic acid, 1.8% cysteine, 1.2% glutamine, 11.3% glutamic acid, 5.0% glycine, 3% histidine, 9.5% isoleucine, 7.8% leucine, 11.9% lysine, 1.8% methionine, 4.0% phenylalanine, 2.2% proline, 7.0% serine, 2.4% threonine, 0.6% tryptophan, 4.8% tyrosine and 3.4% valine. The predicted molecular weight of the protein was 83.84kDa with a theoretical pI of 5.92. The estimated *in vivo* half-life of the protein was predicted to be approximately 10 hours in *Escherichia coli*. The instability index of the protein was computed to be 41.87 which classified the protein as unstable (Gasteiger *et al.*, 2005).

Recombinant *Pf*PK8-His (505 aa) had a predicted molecular weight of 59.51kDa with a theoretical pI of 6.12. There was no change in the half-life between that of rGST-*Pf*PK8 and r*Pf*PK8-His in *Escherichia coli* cells. The instability index of rGST-*Pf*PK8 was predicted to be slightly higher than that of rGST-*Pf*PK8 with a value of 43.87.

The predicted molecular weight of the recombinant proteins corresponds to the molecular weight visualized from stained SDS-PAGE gels (Figures 23 and 32).

4 DISCUSSION

A 1507bp section of the *Pf*B0150c gene, containing 822bp of a putative kinase domain was cloned into pTriEx-3 and pGEX-4T-2 expression vectors. Soluble recombinant proteins containing either an octa-histidine or a GST tag were expressed in *Escherichia coli*. Purified rGST-*Pf*PK8 had kinase activity and phosphorylated casein, MBP and H1 *in vitro*. Binding studies revealed an interaction between rGST-*Pf*PK8 and band 3, one of the major proteins of the host red cell membrane.

4.1 Expression of r*Pf*PK8 in heterologous hosts

Reliable cost-effective and fast high-throughput production of newly identified proteins like r*Pf*PK8 is needed to perform X-ray crystallographic studies, enzyme characterization, enzyme kinetic studies and novel drug target discovery initiatives. *Pf*PK8 is approximately 294kDa according to PlasmoDB version 8.1 (2011) and since the expression of soluble proteins with a molecular weight greater than 56kDa is problematic (Mehlin *et al.*, 2006), only a section of the *Pf*B0150c containing the kinase domain was cloned. The pTriEx-3 expression vector was used because it provides the possibility to express high-levels of recombinant *Pf*PK8 in multiple systems (bacteria, insect cells and mammalian cells) with the use of only one recombinant plasmid. Plasmodial proteins are known to express with difficulty. If problems arose with the expression of soluble r*Pf*PK8 in *Escherichia coli* cells, expression with the same recombinant plasmid was possible in *Spodoptera frugiperda* (*Sf*9) insect cells infected with a recombinant baculovirus. The pTriEx-3 vector utilizes cytomegalovirus (CMV) enhancer-promoter combinations and a T7 *lac* promoter to direct recombinant protein expression in *Escherichia coli* cells and a p10 promoter for expression in *Sf*9 cells. In-frame cloning is made possible by various restriction enzyme sites and open reading frames (ORF) that are found at both ends of the multiple cloning sites (MCS). The pTriEx-3 vector has an octa-histidine tag at the C-terminal end of the MCS which allows for the expression of fusion proteins that can easily be purified by affinity chromatography. Baculovirus genomic DNA is incorporated

on each side of the promoter and ORF regions which facilitates *Pf*B0150c-TriEx-3-baculovirus recombinant generation by homologous recombination at the viral *polh* locus.

Alternative protein expression systems may also be employed to improve the expression of the kinase domain of r*Pf*PK8. These include expression in *Saccharomyces cerevisiae*, *Toxoplasma gondii*, mammalian cells, *Xenopus laevis*, plants and a cell free protein expression system (reviewed in Birkholtz *et al.*, 2008). Molecular chaperones have also been used to improve the solubility of plasmodial proteins. Co-expression of chaperones from the heat shock protein family ensures that recombinant proteins in the non-natural host cell are properly folded. *Plasmodium falciparum* has at least six identified genes encoding heat shock protein 70 – type proteins (Shonhai *et al.*, 2007). These proteins can be co-expressed in *Escherichia coli* cells together with r*Pf*PK8 in order to provide a specialized folding pathway and an increased yield of soluble recombinant protein (Birkholtz *et al.*, 2008).

4.1.1 Expression of r*Pf*PK8-His in *Escherichia coli*

The *Escherichia coli* expression system is the most widely used due to the rapid production of large amounts of target-producing biomass at a relatively low cost and with relatively little non-sophisticated laboratory equipment. The kinase domain of *Pf*PK8 was therefore first expressed on a small scale as an octa-histidine tagged protein in *Escherichia coli* Rosetta 2 (DE3) cells. Rare codons of plasmodial proteins (arginine, leucine, isoleucine and proline) inhibit the translation process in *Escherichia coli* cells as a result of tRNA exhaustion (Flick *et al.*, 2004). The inhibition is caused by ribosome stalling due to the limited availability of these tRNAs which results in truncated forms of the expressed recombinant proteins. The cloned section of *Pf*B0150c contains 3.0% arginine, 7.8% leucine, 9.5% isoleucine and 2.2% proline. The DE3 strain of *Escherichia coli* Rosetta 2 was therefore chosen as host cell for expression of *Pf*PK8 recombinant proteins because this strain was engineered to supply tRNAs driven by their native promoters for the codons rarely used in *Escherichia coli* (Novy *et al.*, 2001). The auto-induction method was used to initiate protein translation and

the growth medium was supplemented with glucose which is the preferred carbon source of *Escherichia coli* during the initial growth phase.

Recombinant *Pf*PK8-His was expressed in the soluble and insoluble fractions (Figure 23). The expression of incorrectly folded insoluble plasmodial proteins in bacterial cells is a common occurrence. Recombinant proteins are sometimes expressed in confined structures which cause them to precipitate (Carrio and Villaverde, 2002) and form inclusion bodies. The formation of inclusion bodies is a coping mechanism of the bacterial cell caused by metabolic stress (Vedadi *et al.*, 2007). In this instance *rPf*PK8-His may have had a toxic effect and the difference in amino acid composition of *rPf*PK8 and the bacterial proteins could have burdened the metabolic functioning of the host cell. Inclusion bodies are composed of denatured protein molecules condensed to form particles. Although methods have been developed to extract these incorrectly folded proteins from the host cell's inclusion bodies (Carrio and Villaverde, 2001), successful renaturation is not always possible. Refolding of enzymes like *rPf*PK8 is problematic since the enzymes lose their activity. It is difficult to prove that renatured proteins have folded correctly into their native state. Circular dichroism is a method that can be used to estimate the secondary structure of refolded proteins (Greenfield, 2006). It is based on the irregular absorption of right- and left-handed circular polarized light. When an asymmetric molecule like a protein interacts with light, it absorbs right- and left-handed polarized light unequally and exhibits different refraction indices for the two light waves. These absorption spectra and refraction indices are unique to a specific protein and can be compared to a correctly folded protein in its native state to deduce the secondary structure of a renatured protein. In the case of *rPf*PK8-His, circular dichroism is not useful since the polarized light refraction indices of native *Pf*PK8 have not yet been determined.

The time-point at which expression is induced in a bacterial culture is critical for producing high yield soluble recombinant proteins (Peti and Page, 2007). It is best to induce protein expression at the post-log growth phase, as demonstrated for *Pf*EMP1 domains (Flick *et al.*, 2004). The low growth rate results in slower protein synthesis allowing the host cell's processing machinery to assemble the

newly produced proteins in the correctly folded form, which would render them soluble. *rPfPK8-His* was induced at the log growth phase of the *Escherichia coli* Rosetta 2 (DE3) culture and this possibly contributed to the insolubility of the protein.

The majority of plasmodial proteins are successfully expressed as soluble recombinant proteins at a more basic isoelectric point (pI). The pI of plasmodial proteins is inversely correlated with solubility and expression (Mehlin *et al.* (2006). The predicted theoretical pI of *rPfPK8-His* (pI 6.12) falls within the ideal parameters (pI 3.45 – 6.8) defined by Mehlin *et al.* (2006).

According to Peti and Page (2007) the soluble expression of heterologous recombinant proteins in *Escherichia coli* cells can be enhanced by optimizing the incubation temperature. In an expression study of *PfEMP1* domains conducted by Flick *et al.*, 2004, an incubation temperature of 16°C was used and this lead to improved expression. In this study a pre- and post-induction temperature of 20°C was used to express *rPfPK8-His*. Decreasing the incubation temperature from 20°C to 16°C would possibly have yielded more soluble *rPfPK8-His*, but this would however have influenced the growth rate of the culture and ultimately the total yield of expressed *rPfPK8-His*.

The soluble fraction of *rPfPK8-His* was purified and the stained Laemmli gels were used to estimate the molecular weight (the predicted molecular weight was 59.1kDa). Rather than relying solely on the predicted *rPfPK8-His* protein size to confirm protein expression and protein identity on the stained Laemmli gels, another reliable method would be to peptide sequence the isolated *rPfPK8-His* protein band of interest using peptide mass fingerprinting. This approach would provide a better measure of certainty about the identity and integrity of the expressed protein and should be considered in future studies.

Multiple protein bands were visualised on the stained Laemmli gels in the *rPfPK8-His* eluted fractions (Figure 23 and 24). According to Robichon *et al.*, (2011) histidine-tagged recombinant proteins expressed at low levels in *Escherichia coli* cells are known to co-elute with native bacterial proteins when

purified by metal affinity chromatography. The contaminating bacterial proteins have a high affinity for divalent nickel ions due to the occurrence of non-consecutive histidine residues and metal binding motifs exposed on the proteins surface. The paramagnetic MagneHisTM beads used in the affinity purification process are coated with nickel and the low purity of the eluted rPfPK8-His protein fractions can be attributed to the co-elution of some of the 17 metal binding proteins of *Escherichia coli* described by Robichon *et al.*, (2011).

4.1.2 Expression of rPfPK8-His in *Spodoptera frugiperda* insect cells

Due to the low yield and poor purity of rPfPK8-His expressed in *Escherichia coli*, the *Spodoptera frugiperda* (Sf9) baculoviral eukaryotic protein expression system was tested. The recombinant proteins are expressed via a secretory pathway in a baculovirus infected insect cell, an intracellular environment that promotes correct protein folding and allows post-translational modification of the foreign target protein. The large baculovirus genome makes the insertion of large foreign DNA possible and leads to the successful expression of active high molecular weight heterologous proteins at higher concentrations compared to *Escherichia coli* expression. Plasmodial proteins expressed in this system are usually correctly folded and expressed with a higher yield compared to bacterial expression, for example: domains of MSP-1 (Pizarro *et al.*, 2003), PfEBA-175 (Liang *et al.*, 2000) and PfAMA-1 (Narum *et al.*, 1993). In a study of plasmodial proteins conducted by Mehlin *et al.* (2006) seven *P. falciparum* proteins were expressed as soluble at high yields in a baculoviral Sf21 system which was previously expressed as insoluble in bacterial cells.

Drawbacks of this expression system is the amount of time that needs to be invested, the high costs involved to express the target protein and the inability to predict the outcome of successful expression of plasmodial proteins.

Heterologous expression of rPfPK8-His in the baculoviral Sf9 insect cell system was unsuccessful. Expression of the target protein was monitored for 96 hours in suspension Sf9 insect cell cultures infected with recombinant BacVirus-PfB0150c at a MOI of 1 – 10. No difference in the protein banding pattern of Sf9 cell lysates and supernatants compared to the uninfected control was observed (Figure

29 and 30). A possible reason for this could be the degradation of the expressed recombinant protein (Kost *et al.*, 2005). A high recombinant viral load within insect cells leads to a disruption of the cellular biochemistry and cell lysis 3 - 5 days post-infection. A disruption of the infected *Sf9* cells occurred and may have led to an increase in protease activity in the cells and degradation of r*Pf*PK8-His. In a study conducted by Ho *et al.* (2004) this difficulty was circumvented by constructing a mutant virus with reduced capability for initiating recombinant protein degradation. It was selected by a novel fluorescence resonance energy transfer-based assay and random mutagenesis, and decreased the amount of lysis of baculovirus infected *Sf21* cells to 7% compared to 60% caused by the parent virus. This resulted in a detectable amount of expressed recombinant luciferase protein.

4.1.3 Expression rGST-*Pf*PK8 in *Escherichia coli*

The solubility of recombinant proteins can be improved by using different affinity tags, such as Glutathione-S-transferase (GST) or the maltose-binding protein. The latter enhanced the solubility of *P. falciparum* falcipain-2 in *Escherichia coli* cells (Goh *et al.*, 2003). A *Pf*B0150c construct in the pGEX-4T2 vector was available in the laboratory (created by Brigit Smit), which produced recombinant *Pf*PK8 with an N terminal GST tag. The predicted pI of rGST-*Pf*PK8 is 5.92, which is within the range of soluble recombinant proteins. GST is a large protein of 25kDa, but despite the increase in size, soluble rGST-*Pf*PK8 was expressed in *Escherichia coli* Rosetta 2 (DE3) cells. The protein was purified with glutathione-coated magnetic beads and yielded 170µg crude protein per 250ml bacterial culture. SDS PAGE analysis indicated that the rGST-*Pf*PK8 had a molecular weight of ~85kDa, which corresponds to the expected size of the protein. The protein yield was low, since at least 5mg/ml of protein is needed to perform X-ray crystallographic structural analysis and to elucidate the biochemical function of the protein of interest (Chayen and Saridakis, 2008). The yield of soluble rGST-*Pf*PK8 may have been higher if the conditions for magnetic bead affinity purification were optimised. The elution of rGST-*Pf*PK8 from the magnetic beads was not sufficient as evident from the amount of recombinant protein detected in the beads protein fraction after two consecutive elution steps (Figure 32 and

Figure 33). The elution of larger target proteins from a soluble fraction of bacterial lysate can be improved by changing the stringency of the elution buffer (Harper and Speicher, 2011). The majority of the ionic bonds between the tagged proteins and the magnetic beads will be disrupted by increasing the sodium chloride concentration of the elution buffer, thereby yielding a higher concentration of rGST-*Pf*PK8 in the eluted protein fraction. A significant amount of rGST-*Pf*PK8 was also detected in the unbound fraction after purification (Figure 32 and Figure 33). An increase in the incubation time of the soluble r*Pf*PK8 with the magnetic beads could possibly increase the yield of the target protein.

The purity of rGST-*Pf*PK8 was deduced from densitometric analysis (Figure 34 and 35) of a stained Laemmli gel where protein samples taken at various steps during the affinity purification process were separated (Figure 32). The amount of pure rGST-*Pf*PK8 was 0.43µg/ml *Escherichia coli* culture and the purity was on average 63%. Possible truncated forms of rGST-*Pf*PK8 were expressed as evident from unexpected protein bands of approximately 60kDa present in the eluted fractions after recombinant protein purification (Figure 32 and 33). In the case of rGST-*Pf*PK8 one of the protein bands had a molecular weight of approximately 25kDa, which probably represents endogenous *Escherichia coli* GST. Peptide mass fingerprinting of rGST-*Pf*PK8 should be considered in future studies as a reliable method to confirm the identity of these unexpected protein bands, which could be truncated and posttranslationally modified protein forms of rGST-*Pf*PK8. The yield and purity of the rGST-*Pf*PK8 preparations were however sufficient to carry out enzyme kinetic assays.

4.2 *Pf*B0150c mRNA and protein expression

Plasmodium falciparum PK8 is encoded by *Pf*B0150c of the *P. falciparum* 3D7 genome. The mRNA expression levels of *Pf*B0150c during seven asexual life stages of the parasite are depicted in Figure 55 (Le Roch *et al.*, 2003) obtained from PlasmoDB version 8.1 (2011). It can be deduced from this photolithographic oligo-array data that the expression of the *Pf*B01500c gene

occurs throughout the lifecycle of the parasite, including the sexual gametocytes and the sporozoites that invade the liver.

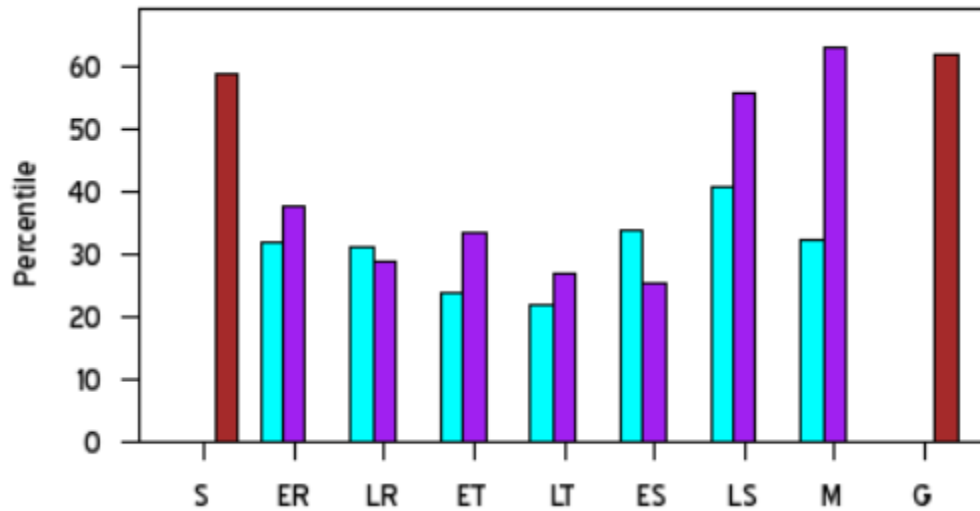


Figure 55: mRNA expression levels of *PfB0150c* during the asexual stages of development in the human host erythrocyte.

The percentile value is the ranking percentage of *PfB0150c*'s expression relative to all the other genes of *P. falciparum* 3D7 for a given experiment according to PlasmoDB version 8.1 (2011). The analysed developmental stages and expression percentiles are schizont (S) (unknown percentile), early ring (ER) (37.5%), late ring (LR) (29.0%), early trophozoite (ET) (33.4%), late trophozoite (LT) (27.0%), early schizont (ES) (25.5%), late schizont (LS) (55.6%), merozoite (M) (62.8%) and gametocyte (G) (unknown percentile). The stages were synchronized by sorbitol (blue) and temperature (purple). Data for gametocyte sample corresponds to synchronisation only by sorbitol and for sporozoite sample represents an average of temperature synchronised and sorbitol synchronised experiments.

A later study on the transcriptome confirmed the expression throughout the asexual stages Figure 56 (Bozdech *et al.*, 2003). Mass spectrometry data indicated that the *PfPK8* protein was present in merozoites (Florens *et al.*, 2002). The parasite proteome has not been studied as extensively as the transcriptome, which probably accounts for the discrepancy between the mRNA and protein expression levels, although not all mRNA transcripts are immediately translated into protein.

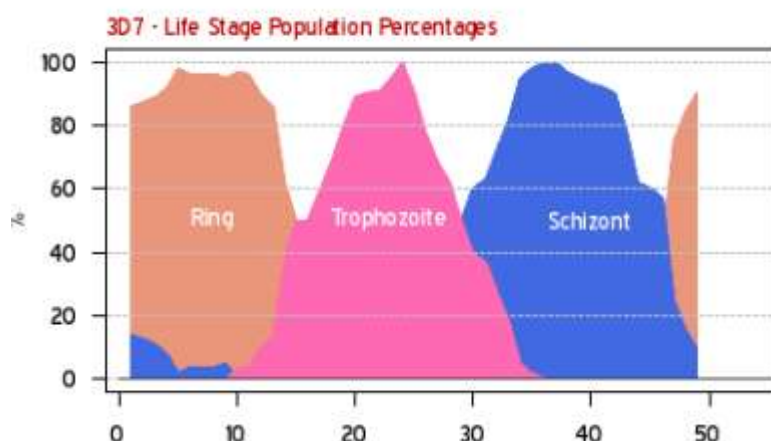


Figure 56: Expression of *PfB0150c* in *Plasmodium falciparum* 3D7 parasites.

The data represent the percentage *PfPK8* expressed during the intraerythrocytic life cycle stages of *P. falciparum*. The x-axis indicates the time in hours after adding synchronized culture of 3D7 parasites to fresh blood and the y-axis the expression intensity percentile of *PfB0150c*. The data represented in the graph were obtained from PlasmoDB version 8.1 (2011.).

4.3 Recombinant *PfPK8* is an active protein kinase

Protein kinases play an essential role in the regulation of cellular proliferation and differentiation in eukaryotes. Phosphorylation of parasite proteins and that of the parasite's host cell is essential for the survival of the intraerythrocytic parasite. This crucial role that plasmodial kinases play, makes them attractive potential targets for novel drugs against malaria. Knowledge about the function of the enzyme and its enzymatic mechanism needs to be explored before it can be identified as a potential novel drug target.

Plasmodium falciparum PfB0150c is described in the PlasmoDB database as a putative protein kinase. A non-radioactive spectrophotometric coupled enzyme assay was used to test if rGST-*PfPK8* is an active protein kinase and to establish the kinetic parameters (K_m and V_{max}) of the enzyme. The activity of rGST-*PfPK8* at various temperatures and pH values was determined and the enzyme's stability was investigated.

Eukaryotic protein kinases (Hanks *et al.*, 2003) and prokaryotic protein kinases (Kennelly, 2002) catalyse the transfer of a phosphate group of ATP or GTP to a specific amino acid residue of a protein substrate. The functional activity of protein kinases have commonly been studied by incorporating a radioactive

γ -phosphoryl group from a radiolabel (^{32}P -ATP or ^{32}P -GTP) into an exogenous substrate and subsequently determining the amount of phosphorylated substrate by scintillation counting (Sefton and Shenolikar, 1996). The radiolabel used in this type of kinase assay is costly and the disposal of radioactive waste products is expensive. Another negative aspect of this enzyme assay is the strictly regulated safety measures when working with a radioactive material. The use of this enzyme assay is becoming increasingly uncommon even though it has advantages with regards to high throughput drug screening (Glickman and Ferrand, 2008).

In this study, a spectrophotometric, non-radioactive, coupled enzyme method, based on a well-documented enzyme assay used for *Escherichia coli* glycerol kinase (*EcGK*) (Worthington and Worthington, 2011) was adapted to measure the rGST-*Pf*PK8 kinase activity. This assay method provides a direct and continuous recording of the enzyme activity in a controlled closed system over a given time, as measured by the decrease in NADH absorption, and is an easy, rapid, sensitive and less costly means to determine the kinetic properties of the enzyme.

Recombinant GST-*Pf*PK8 had kinase activity in the presence of three exogenous substrates, casein, MBP and H1. The activity of the enzyme was monitored over several days, which revealed that the enzyme was unstable. The kinase assays were therefore performed as soon as possible after enzyme purification.

A different enzyme preparation was used in each assay because not enough rGST-*Pf*PK8 was expressed and purified from one *Escherichia coli* Rosetta 2 (DE3) culture to perform all of the kinetic assays using the same enzyme sample. Each rGST-*Pf*PK8 preparation is likely to vary slightly since a biological system is used to produce the target enzyme and a difference in the purity and folding of the target enzyme is possible. The K_m and V_{max} values of rGST-*Pf*PK8 are therefore only approximate. The same rGST-*Pf*PK8 sample was however used to test the effects of pH and temperature on the enzyme and for performing Michaelis-Menten assays.

The maximum catalytic rate of an enzyme is achieved when all of the active sites are occupied by a substrate. The K_m is described as the inverse of the affinity of

an enzyme for a specific substrate. Recombinant GST-*Pf*PK8 had the lowest K_m value, which reflects the highest affinity for substrate casein, followed by H1 and MBP. Recombinant GST-*Pf*PK8 efficiently phosphorylated 200 μ g casein with a specific activity of $6.2 \pm 0.7 \mu\text{mole NADH/min/mg enzyme}$, 100 μ g MBP with a specific activity of 12 ± 0.6 and 100 μ g H1 with a specific activity of $9.6 \pm 1 \mu\text{mole NADH/min/mg enzyme}$. These values are low compared to the specific activity ($\sim 1\,020 \mu\text{mole/min}$) of recombinant *P. falciparum* casein kinase 1 (r*Pf*CK1) in the presence of its true substrate, casein (Barik *et al.*, 1997). The low specific activity of rGST-*Pf*PK8 is presumably because the exogenous substrates tested, are not the native substrates targeted by *Pf*PK8.

An active site titration assay of the r*Pf*PK8 can be performed in future studies to eliminate the differences in recombinant and possible misfolded enzymes from different preparations, which will limit errors when determining enzyme parameters like V_{max} , K_m and specific activity (Brocklehurst *et al.*, 2001). This type of assay determines the molarity of an enzyme's active binding sites present under specific conditions by using an irreversible inhibitor. A limitation of this assay is that the enzyme must have a specific type of residue within its active site that is sensitive to certain covalent modifications.

Plasmodium falciparum is exposed to various temperatures during its life cycle. The parasite spends its sexual life cycle within the *Anopheles sp.* mosquito with a body temperature range of 22°C - 28°C while not feeding and increasing up to 34°C while taking a blood meal. The asexual life cycle is completed within the human host where the parasite is exposed to a temperature range of 37°C - 41°C. Interestingly, rGST-*Pf*PK8 was most active at 40°C, a temperature synonymous with a severe fever spike in an individual infected with *P. falciparum*. Periodic episodes of fever, triggered by the rupture of infected erythrocytes releasing new merozoites, haemozoin and other toxins into the bloodstream of its host will therefore not inhibit the enzyme. The activity of rGST-*Pf*PK8 remained relatively stable between 28-37°C, ranging from 70-80% of maximal activity. It was least active (relative enzyme activity of $\sim 35\%$) at 26°C, the body temperature of a resting *Anopheles sp.* mosquito. This low level of activity is therefore presumably

sufficient to phosphorylate target substrates in the mosquito host. However, the assay relies on a coupled reaction between pyruvate kinase and lactate dehydrogenase, so these enzymes may have been affected by the decrease in temperature.

The fluctuations in activity at different temperatures are a common phenomenon in all enzymes. As the temperature of an enzyme reaction increases, the relative activity of the enzyme increases proportionally. Enzyme molecules have low kinetic energy at low temperatures and collide less frequently with their substrate molecules which results in a low enzyme activity. As the temperature increases, the kinetic energy of the enzyme molecules increase, enzyme-substrate collisions are more frequent and lead to an increase in enzyme activity. According to Worthington and Worthington (2011) a 10°C rise in temperature will cause an enzyme's activity to increase five to ten fold for most enzymes. The enzyme activity will however reach a maximum and a further increase in temperature will lead to a disruption of the forces that maintain the shape of the enzyme. This denaturing effect leads to a decrease in enzyme activity and the enzyme will eventually be inactive.

Plasmodium falciparum is exposed to a range of pH conditions during its asexual and sexual life cycle and all enzymes are sensitive to pH changes. It was for this reason that the effect of a pH change on rPfPK8 was investigated. Recombinant GST-PfPK8 was virtually inactive at a pH of 6.5 and below (Figure 41), but this could again have been influenced by low activities of the coupled enzymes in the reaction. The pH of the digestive vacuole of the malaria parasite is acidic (pH 4.5 – 5.5) (Kuhn *et al.*, 2007), so presumably PfPK8 has no digestive vacuole related function. The pH in the midgut of the mosquito is 5 – 6.5 (Gusmao *et al.*, 2007) and the sexual stages of the life cycle of the parasite will be exposed to this environment. The relative enzyme activity of rGST-PfPK8 was highest at pH 7 which corresponds to the near neutral pH of the parasite's cytoplasm (pH 7.15 – 7.3) (Kuhn *et al.*, 2007) and fluctuated slightly between pH 7.2 and 9. *Plasmodium falciparum* PK8 could therefore be functionally active within the parasite cytoplasm of the ring, trophozoite and/or schizont stages (Figure 56) and

would also be active at the host cell membrane where the intra-cellular environment of the human erythrocyte has a pH of 7.4 (Waugh and Grant, 2007).

4.4 Structural aspects of rPfPK8

The three-dimensional structure of rPfPK8 was investigated using two modelling programs. The research applications of predicting the secondary and three dimensional structure of a protein includes the elucidation of functional characteristics, possible enzyme mechanisms, identification of mutagenesis sites and ultimately for the use in drug design.

4.4.1 Homologues of rPfPK8

Eukaryotic protein kinases of malaria parasites are classified into seven clusters according to their primary structure (Doerig *et al.*, 2008). BLAST was used to identify the homologues of rPfPK8 and the results revealed that it clustered with serine/threonine-specific protein kinases (STKs). The highest sequence similarity was found to be between a STK from *Plasmodium cynomolgi* strain B, a STK from *Plasmodium vivax* Salvadore-1 and putative protein kinase from *Plasmodium knowlesi* strain H1 (Figure 46). The percentage identical residues ranged between 63 and 68. The invariable residues were mostly those of the protein kinase domain of PfPK8, which demonstrates the high sequence conservancy of the kinase domain of eukaryotes (Hanks, 2003).

4.4.2 Secondary structure of rPfPK8

Eukaryotic PKs usually display a conserved kinase domain comprising approximately 250 – 300 aa (Doerig *et al.*, 2008). Recombinant PfPK8 conforms to this rule with a kinase domain consisting of 274 aa. Eukaryotic PKs do not only exhibit a conserved kinase domain but also conserved secondary subdomains and structural elements (Hanks, 2003). The secondary structure of the kinase domain rPfPK8 was investigated to determine the position of these subdomains and structural elements.

Conserved ePK domains of the active site of r*Pf*PK8 include the substrate binding site and the ATP-binding pocket. The ATP-binding pocket is located within the substrate binding site (Figure 47). An activation-loop was identified and stretched from residues 157-180. This corresponded to the conserved residues of the ATP-binding pocket. This activation-loop is presumably essential for the functioning of r*Pf*PK8.

Flexibility of the activation-loop of ePK kinases is important due to the extensive conformational changes that occur upon ATP binding. Conserved glycine residues within the activation-loop of ePKs have been implicated in these conformational changes (Bartova *et al.*, 2004). According to Anamika *et al.* 2005, 65 of 99 kinase domain-containing gene products studied, have at least one glycine in the activation-loop. The r*Pf*PK8 activation-loop has two conserved glycine residues (Figure 48). Glycine-159 and glycine-176 of the r*Pf*PK8 activation-loop can possibly be involved in the conformational flexibility of the enzyme upon ATP binding.

The identified disordered regions in the secondary structure of r*Pf*PK8 (Figure 50) may have influenced the soluble expression of the protein (Mehlin *et al.*, 2006). It is interesting to note that the majority of these disordered regions are situated at both ends of the kinase domain of r*Pf*PK8 and that no disordered regions within the essential activation-loop have been identified. This was expected due to the sequence conservation of the ATP-binding pocket of ePKs.

4.4.3 Three dimensional structure of r*Pf*PK8

The protein folding mechanism in nature appears to be conserved and various homologous protein sequences take on a similar 3D structure. The amino acid sequence of the cloned functional region of *Pf*PK8 (497 aa) was entered into the protein-homology/analogy recognition engine (Phyre2) and a secondary structure prediction of 54% of the submitted residues was obtained with a confidence score greater than 90% (Figure 51). The protein kinase domain sequence of *Pf*PK8 was then submitted to Phyre2 to determine if the predicted 54% of the cloned functional region was the actual centrally located kinase domain. Most of the residues (98%) of the kinase region of r*Pf*PK8 were modelled by the Phyre2

modelling engine according to the crystal structures of its homologues with a confidence score >90% (Figure 52). It was therefore assumed that the initial modelled residues (54%) of the cloned region of rPfPK8 were in fact that of the kinase domain. The accuracy of the predicted structure depends on the similarities between the query sequence and the homologous template sequence. A confidence score >90% was achieved, and according to Kelley and Sternberg (2009) the predicted model of the rPfPK8 kinase domain can therefore be regarded as correct with an accurate central core (Kelley and Sternberg, 2009). As evident from the Phyre2 3D model, the kinase domain of rPfPK8 displays the common bi-lobal fold (Anamika *et al.*, 2005) of ePK kinase domains with an α -helix rich N-terminal lobe (Figure 52). This seems to differ from the common fold of ePK kinase domains where the N-terminal lobe is rich in β -sheets and the larger C-terminal domain rich in α -helices (Anamika *et al.*, 2005). The prediction confidence of the kinase domain structure at the N-terminal end was higher compared to the C-terminal end. This was expected since the cofactor ATP-binding pocket is situated at the N-terminal end of the protein kinase domain in eukaryotes (Hanks, 2003). It is however difficult to comment on how the C-terminal lobe of rPfPK8 compares with that of other ePKs due to the lower confidence modelling score of this domain.

Approximately 10% of the complete rPfPK8 protein model was predicted by the ExPASy Bio-informatics Resource Portal SWISS-MODEL Workspace with a sequence similarity of 33.19% to MST1. The obtained model (Figure 54) was unreliable due to a sequence similarity less than 40%. According to Schwede *et al.*, 2003) a sequence similarity of <40% will result in an unreliable three dimensional model due to the high probability of errors that might occur when the sequence is computed using the alignment algorithms (Schwede *et al.*, 2003).

4.5 Host-parasite protein-protein interactions and a possible function for *Pf*PK8

With regards to *P. falciparum*, protein kinases play a crucial role in signal transduction between the parasite proteins and the proteins of the human host cell during intraerythrocytic development. A possible role of *Pf*PK8 was investigated by performing binding studies with red blood cell membrane proteins extracted from a whole blood sample. The existence of a potential host-parasite protein-protein interaction was investigated by firstly performing a dot blot overlay of RBCM proteins with purified rGST-*Pf*PK8. An interaction was observed and was further investigated by using RBCM proteins separated on a Laemmli gel to determine exactly with which proteins rGST-*Pf*PK8 interacted. It was evident from these results that a band 3 - rGST-*Pf*PK8 interaction existed.

Plasmodium falciparum PK8 needs to be trafficked to the host cell membrane to come into contact with red blood cell membrane proteins band 3 and protein 4.1. *Plasmodium falciparum* PK8 does not possess the well-known five amino acid PEXEL motif which has been identified at the N-terminal end of known *P. falciparum* proteins trafficked to the host cell membrane. This RxLxQ/E amino acid motif is present in *Pf*EMP1 where it has been implicated in the export of green fluorescent protein in *P. falciparum* infected erythrocytes (Hiller *et al.*, 2004; Marti *et al.*, 2004). Hiss *et al.* (2008) found that 28% of the putative *P. falciparum* proteins contain the PEXEL motif but it has been shown that this motif alone is not sufficient to traffic proteins across and beyond the plasmodium vacuolar membrane (Nunes *et al.*, 2007). Malaria parasites have evolved different exporting mechanisms for various protein types (Deponte *et al.*, 2012) and *P. falciparum* PK8 could possibly be trafficked to the red blood cell membrane via another exporting pathway.

In normal human red blood cells (RBC), the major membrane proteins, including spectrin, ankyrin, band 3, protein 4.1 and protein 4.2 serve as substrates for numerous protein kinases (Cohen and Gascard, 1992). A characteristic distorted phosphorylation pattern of the host's RBC membrane is seen in the intraerythrocytic stage of the malaria parasite. The phosphorylation of protein 4.1

and band 3 has been shown to down-regulate their interaction *in vitro*, thereby destabilising the erythrocyte membrane (Chishti *et al.*, 1994). The role of the major membrane proteins, such as band 3, is to stabilize the erythrocyte membrane skeleton and phosphorylation of these proteins by a kinase like *Pf*PK8, could lead to destabilization resulting in an increased flexibility of the host cell membrane. It has been postulated that a destabilisation of the erythrocyte membrane skeleton promotes the parasite's growth and survival within the erythrocyte by facilitating the insertion of parasite proteins into the membrane to establish transport pathways (Chishti *et al.*, 1994; Cooke *et al.*, 2004). *Plasmodium falciparum* PK8 may also play a role during invasion of red blood cells, since a destabilisation of the membrane would facilitate entry of the parasite.

5 CONCLUSION

The conclusion was changed to include the examiner's suggestions. The conclusion on p187 now reads as follows: "To conclude, the *P. falciparum* protein kinase 8 is an active enzyme with the ability to phosphorylate multiple substrates. This enzyme is mostly expressed in the asexual stages of the parasite life cycle where it interacts with the major red blood cell membrane protein, band 3. Peptide mass fingerprinting of rPfPK8 should be considered in future studies to validate the identity of the expressed protein. It would be important to validate substrate phosphorylation by rPfPK8 by using two dimensional phosphoprotein gels. Sequencing of phosphorylated substrates should be considered to identify which amino acids are phosphorylated by rPfPK8. For future studies, the expression of PfPK8 with a higher yield of soluble protein could possibly be achieved by using a *Saccharomyces cerevisiae*, *Dictyostelium discodium*, *Tetrahymena thermophile* or a cell free expression system. The ultimate goal of expressing PfPK8 in large amounts is to perform X-ray crystallographic studies to elucidate the structure of the complete enzyme, including the active site. Transgenic parasites expressing PfPK8 linked to a fluorescent tag, such as green fluorescent protein (GFP), will enable the *in vivo* localisation of the enzyme and should confirm the interaction with the host red cell membrane. Gene knock-out studies will establish if PfPK8 is essential for parasite survival and if this should be the case then it will be a good candidate for novel drug development.

6 REFERENCE LIST

- Abdi, A; Eschenlauer, S; Reininger, L; Doerig, C. (2010). SAM domain-dependent activity of PfTKL3, an essential tyrosine kinase-like kinase of the human malaria parasite *Plasmodium falciparum*. *Cellular and Molecular Life Sciences*. 67: (19), p3355-3369.
- Agarwal, S; Kern, S; Halbert, J; Przyborski, JM; Baumeister, S; Dandekar, T; Doerig, C; Pradel, G. (2011). Two nucleus-localised CDK-like kinases with crucial roles for malaria parasite erythrocytic replication are involved in phosphorylation of splicing factor. *Journal of Cellular Biochemistry*. 112, p1295-1310.
- Aikawa, M; Miller, LH; Johnson, J, Rabbege, J. (1978). Erythrocyte entry by malarial parasites. A moving junction between erythrocyte and parasite. *The Journal of Cell Biology*. 77, p72–82.
- Altschul, SF; Madden, TL; Schaffer, AA; Zhang, J; Zhang, Z; Miller, W; Lipman, DJ. (1997). Gapped BLAST and PSI BLAST: A new generation of protein database search programs. *Nucleic Acid Research*. 25, p3389-3402.
- An, X, Debnath, G, Guo, X, Liu, S; Lux, SE; Baines, A; Gratzer, W; Mohandas, N. (2005). Identification and functional characterization of protein 4.1R and actin-binding sites in erythrocyte beta-spectrin: regulation of the interactions by phosphatidylinositol-4,5-bisphosphate. *Biochemistry*. 44, p10681-10688.
- An, X; Mohandas, N. (2010). Red cell membrane and malaria. *Transfusion Clinique et Biologique*. 17, p197-199.
- An, X; Salomao, M; Guo, X; Gratzer, W; Mohandas, N. (2007). Tropomyosin modulates erythrocyte membrane stability. *Blood*. 109: (3), p1284-1288.
- An, X; Zhang, X, Debnath, G; Baines AJ, Mohandas, N. (2006). Phosphatidylinositol-4,5-Biphosphate (PIP2) Differentially Regulates the Interaction of Human Erythrocyte Protein 4.1 (4.1R) with Membrane Proteins. *Biochemistry*. 45, p5725-5732.
- Anamika, NS; Krupa, A. (2005). A genomic perspective of protein kinases in *Plasmodium falciparum*. *Proteins*. 58, p180-189.
- Andrade, JG; Andrade, AL; Araujo, ES; Oliveira, RM; Silva, AS; Martelli, CM; Zicker, F. (1992). A randomized clinical trial with high dose of chloroquine for treatment of *Plasmodium falciparum* malaria. *Revista do Instituto de Medicina Tropical de Sao Paulo*. 34: (5), p467-473.
- Anong, WA; Franco, T; Chu, H; Weis, TL; Devlin, EE; Bodine, DM; An, X; Mohandas, N; Low, PS. (2009). Adducin forms a bridge between the erythrocyte membrane and its cytoskeleton and regulates membrane cohesion. *Blood*. 114: (9), p1904-1912.

- Arawind, L; Iyer, LM; Wellems, TE; Miller, LH. (2003). *Plasmodium* biology: genomic gleanings. *Cell*. 115: (7), p771-785.
- Arnold, K; Bordoli, L; Kopp, J; Schwede, T. (2006). The SWISS-MODEL Workspace: A web-based environment for protein structure homology modelling. *Bioinformatics*. 22, p195-201.
- Baca, AM; Hol, WG. (2000). Overcoming codon bias as a method for high-level over expression of *Plasmodium* and other AT-rich parasite genes in *Escherichia coli*. *International Journal of Parasitology*. 30, p113-118.
- Baines, AJ; Bennett, PM; Carter, EW; Terracciano, C. (2009). Protein 4.1 and the control of ion channels. *Blood Cells, Molecules, and Diseases*. 42, p211-215.
- Balu, B; Adams, JH. (2007). Advancements in transfection technologies for *Plasmodium*. *International Journal of Parasitology*. 37, p1-10.
- Bannister, LH; Hopkins, JM; Fowler, RE. (2000). A brief illustrated guide to the ultrastructure of *Plasmodium falciparum* asexual blood stages. *Parasitology Today*. 16, p427-433.
- Barik, S; Taylor, RE; Chakrabarti, D. (1997). Identification, cloning and mutational analysis of the Casein kinase 1 cDNA of the Malaria Parasite *Plasmodium falciparum* – Stage specific expression of the gene. *The Journal of Biological Chemistry*. 272, p26132-26138.
- Bartova, I; Otyepka, M; Zdenek, K; Koca, J. (2004). Activation and inhibition of cyclin-dependent kinase-2 by phosphorylation; a molecular dynamics study reveals the functional importance of the glycine-rich loop. *Protein Science*. 13: (6), p1449-1457.
- Basic Local Alignment Search Tool vesion 2.2.27 (BLAST). Available: <http://blast.ncbi.nlm.nih.gov>.
- Battacharjee, AK; Geyer, JA; Woodard, CL; Kathcart, AK; Nichols, DA; Prigge, ST; Li, Z; Mott, BT; Waters, NC. (2004). A three-dimensional in silico pharmacophore model for inhibition of *Plasmodium falciparum* cyclin-dependent kinases and discovery of different classes of novel *Pfmrk* specific inhibitors. *Journal of Medicinal Chemistry*. 47, p5418-5426.
- Baum, J; Papenfuss, AT; Baum, B; Speed, TP; Cowman, AF. (2006). Regulation of apicomplexan actin-based motility. *Nature Reviews*. 4, p621-628.
- Bennet, V; Stenbuck, PJ. (1979). The membrane attachment protein for spectrin is associated with band 3 in human erythrocyte membranes. *Nature*. 280, p468-473.
- Bennett V. (1988). The spectrin-actin junction of erythrocyte membrane skeletons. *Biochimica et Biophysica Acta*. 988, p107-121.
- Benz, EJ (r. (2010). Learning about genomics and disease from the anucleate human red blood cell. *Journal of Clinical Investigation*. 120: (12), p4204-4206.

- Beraldo, FH; Almeida, FM; da Silva, AM; Garcia, CRS. (2005). Cyclin AMP and calcium interplay as second messengers in melatonin-dependent regulation of *Plasmodium falciparum* cell cycle. *Journal of Cell Biology*. 17, p551-557.
- Bergmeyer, HU. (1974). Methods of Enzymatic Analysis Volume 1 2nd ed. Verlag Chemie Weinheim & Academic Press, New York-London.
- Bertani, G. (1951). Studies on lysogenesis. I. The mode of phage liberation by lysogenic *Escherichia coli*. *Journal of Bacteriology*. 62, p293-300.
- Bilker, O; Dechamps, S; Tewari, R; Wenig, G; Franke-Fayard, B; Brinkmann, V. (2004). Calcium and a calcium-dependent protein kinase regulate gamete formation and mosquito transmission in malaria parasites. *Cell*. 117, p503-514.
- Birkholtz, L; Blatch, G; Coetzer, TL; Hoppe, HC; Human, E; Morris, EJ; Ngcete, Z; Oldfield, L; Roth, R; Shonhai, A; Stephens, L; Louw, AI. (2008). Heterologous expression of plasmodial proteins for structural studies and functional annotation. *Malaria Journal*. 7, p179.
- Blisnick, T; Vincensini, L; Fall, G; Braun-Breton, C. (2006). Protein phosphatase 1, a *Plasmodium falciparum* essential enzyme, is exported to the host cell and implicated in the release of infectious merozoites. *Cellular Microbiology*. 8, p591-601.
- Bozdech, Z; Llinas, M; Pulliam, BL; Wong, ED; Zhu, J; DeRisi, JL. (2003). The Transcriptome of the Intraerythrocytic developmental cycle of *Plasmodium falciparum*. *PLOS Biology*. 1: (1), e5.
- Bradford, MM. (1976). A rapid and sensitive method for the quantitation of microgram quantities of protein utilizing the principle of protein-dye binding. *Analytical Biochemistry*. 72: (1-2), p248-254.
- Brocklehurst, K; Resmini, M; Topham, CM. (2001). Kinetic and titration methods for determination of active site contents of enzyme and catalytic antibody preparations. *Methods*. 24: (2), p153-167.
- Carrio, MM; Villaverde A. (2001). Protein aggregation as bacterial inclusion bodies is reversible. *FEBS Letters*. 489, p29-33.
- Carrio, MM; Villaverde, A. (2002). Construction and deconstruction of bacterial inclusion bodies. *Journal of Biotechnology*. 96, p3-12.
- Chasis, JA; Mohandas, N. (1992). Red blood cell glycophorins. *Blood*. 80, p1869-1879.
- Chayen, NE; Saridakis, E. (2008). Protein crystallization: from purified protein to diffraction-quality crystal. *Nature Methods*. 5: (2), p147-153.
- Cheng, Q; Cloonan, N; Fisher, K; Thompson, J; Waine, G; Lanzer, M; Saul, A. (1998). *Stevor* and *rif* are *Plasmodium falciparum* multicopy gene families which potentially encode variant antigens. *Molecular Biochemical Parasitology*. 97, p161-176.

Chien, S; Sung, LA. (1987). Physiochemical basis and clinical implications of red cell aggregation. *Clinical Hemorheology*. 7, p71-91.

Chishti, AH; Levin, A; Branton, D. (1988). Abolition of actin-bundling by phosphorylation of human erythrocyte protein 4.9. *Nature*. 334, p718-721.

Chisthi, AH; Maalouf, GJ; Marfatia, S; Palek, J; Wang, W; Fisher, D; Liu, SC. (1994). Phosphorylation of protein 4.1 in *Plasmodium falciparum*-infected human red blood cells. *Blood*. 83, p3339-3345.

Coetzer, TL; Palek, J. (1986). Partial spectrin deficiency in hereditary pyropoikilocytosis. *Blood*. 67, p919-924.

Cohen CM, Gascard P. (1992). Regulation and post-translational modification of erythrocyte membrane and membrane-skeletal proteins. *Seminars in Haematology*. 29: (4), p244-292.

Cohen, P. (2002). Protein kinases – the major drug targets of the twenty first century? *Nature Reviews Drug Discovery*. 1, p309-315.

Cooke, BM; Buckingham, DW; Glenister, FK. (2006). A Maurer's cleft-associated protein is essential for expression of the major malaria virulence antigen on the surface of infected red blood cells. *Journal of Cell Biology*. 172, p899-908.

Cooke, BM; Mohandas, N; Coppel, RL. (2004). Malaria and the Red Blood Cell Membrane. *Seminars in Haematology*. 41, p173-188.

Coppi, A; Tewari, R; Bishop, JR; Bennet, BL; Lawrence, R; Esko, JD; Billker, O; Sinnis, P. (2007). Heparin sulphate proteoglycans provide a signal to *Plasmodium* sporozoites to stop migrating and productively invade host cells. *Cell Host & Microbe*. 2, p316-327.

Cowman, AF; Berry, D; Baum, J. (2012). The cellular and molecular basis for malaria parasite invasion of the human red blood cell. *The Journal of Cell Biology*. 198: (6), p961-971.

Cowman, AF; Crabb, BS. (2006). Invasion of red blood cell malaria parasites. *Cell*. 124, p755-766.

Crabb, BS; de Koning-Ward, TF; Gilson, PR. (2010). Protein export in *Plasmodium* parasites: from the endoplasmic reticulum to the vacuolar export machine. *International Journal of Parasitology*. 40: (5), p509-513.

Decherf, G; Egee, S; Staines, m; Ellroy, JC; Thomas, SL. (2004). Anionic channels in malaria-infected human red cells. *Blood cells, Molecules and Diseases*. 3293, p366-371.

Deponte, M; Hoppe,HC; Lee,MC; Maier, AG; Richard, D; Rug, M; Spielmann, T; Pryzborski, JM. (2012). Wherever I may roam: protein and membrane trafficking in *P. falciparum*-infected red blood cells. *Molecular Biochemical Parasitology*. 186: (2), p95-116.

Doerig, C; Bilker, O; Haystead, T; Sharma, P; Tobin, AB; Waters, NC. (2008). Protein kinases of malaria parasites: an update. *Trends in Parasitology*. 24, p570-577

Doerig, C; Billker, O; Pratt, D; Endicott, J. (2005). Protein kinases as targets for antimalarial intervention: Kinomics, structure-based design, transmission-blockade and targeting host cell enzymes. *Biochimica et Biophysica Acta*. 1754, p132-150.

Doerig, C; Endicott, J; Chakrabarti, D. (2002). Cyclin-dependent kinase homologues of *Plasmodium falciparum*. *International Journal of Parasitology*. 32, p1575-1585.

Dondorp, AM; Nosten, F; Yi, P; Das, D; Phyto, AP; Trnning, J; Lwin, KM; Arie, F; Hanpithakpong, W; Lee, SJ; Ringwald, P; Silamut, K; Imwong, M; Chotivanich, K; Lim, P; Herdman, T; An, SS; Yeung, S; Singhasivanon, P; Day, NPJ; Lindegardh, N; Socheat, D; White, NJ. (2009). Artemisinin resistance in *Plasmodium falciparum* malaria. *New England Journal of Medicine*. 361: (5); p455-467.

Dorin, D; Le Roch, K, Sallicandro, P; Alano, P; Parzy, D; Pullet, P; Meijer, L, Doerig, C. (2001). *Pfnek-1*, a NIMA-related kinase from the human malaria parasite *Plasmodium falciparum*. Biochemical properties and possible involvement in MAPK regulation. *European Journal of Biochemistry*. 268, p2600-2608.

Dorin-Semblat, D; Quashie, N; Halbert, J, Sicard, A, Doerig, C, Peat, E; Ranford-Cartwright, L, Doerig, C. (2007). Functional characterization of both MAP kinases of the human malaria parasite *Plasmodium falciparum* by reverse genetics. *Molecular Microbiology*. 65, p1170-1180.

Dorin-Semblat, D; Sicard, A; Doerig, C; Ranford-Cartwright, L; Doerig, C. (2005). *PfPK7*, an atypical MEK-related protein kinase reflects the absence of typical three-component MAP kinase pathways in the human malaria parasite *Plasmodium falciparum*. *Molecular Microbiology*. 55, 185-196.

Droucheau, E; Primot, A; Thomas, V; Mattei, D; Knockaert M, Richardson, C; Sallicandro, P, Alano, P; Jafarshad, A; Baratte, B; Kunick, C; Parzy, D; Pearl, L; Doerig, C; Meijer, L. (2004). *Plasmodium falciparum* glycogen synthase kinase-3: molecular model, expression, intracellular localisation and selective inhibitors. *Biochimica et Biophysica Acta – Proteins and Proteomics*. 1697, p181-1960.

Eby, JJ; Holly, SP; van Drogen, F; Grishin, AV; Peter, M; Drubin, DG, Blumer, KJ. (1998). Actin cytoskeleton organization regulated by the PAK family of protein kinases. *Current Biology*. 8, p967–970.

ExPASy Bio-informatics Resource Portal SWISS-MODEL version 8.05 workspace. Available: <http://swissmodel.expasy.org/workspace/>.

- Fairbanks, G; Steck, TL; Wallach, DHF. (1971). Electrophoretic analysis of the major polypeptides of the human erythrocyte membrane. *Biochemistry*. 10, p2606-2617.
- Fernandez-Robledo, JA; Vasta, GR. (2010). Production of Recombinant proteins from protozoan parasites. *Trends in Parasitology*. 26: (5), p244-254.
- Flick, K; Ahuja, S; Chene, A; Bejarano, MT; Chen, Q. (2004). Optimized expression of *Plasmodium falciparum* erythrocyte membrane protein I domains in *Escherichia coli*. *Malaria Journal*. 3: (50), doi 10.1186/1475-2875-3-50.
- Florens, L; Washburn, MP; Raine, JD; Anthony, RM; Grainger, M; Haynes, JD; Moch, JK; Muster, N; Sacci, JB; Tabb, DL; Witney, AA; Wolters, D; Wu, Y; Gardner, MJ; Holder, AA; Sinden, RE; Yates, JR; Carucci, DJ. (2002). A proteomic view of the *Plasmodium falciparum* life cycle. *Nature*. 419, p520-526.
- Fowler, VM; Bennet V. (1984). Erythrocyte Membrane Tropomyosin. *The Journal of Biological Chemistry*. 259: (9): p5978-5989.
- Franco, T; Low, PS. (2010). Erythrocyte adducin: A structural regulator of the red blood cell membrane. *Transfusion Clinical Biology*. 17: (3), p87-94.
- Fujioka, H; Aikawa, M. (1999). The malaria parasite and its life-cycle. In: Wahlgren, M; Perlmann, P. *Malaria: Molecular and Clinical Aspects*. Singapore: Harwood Academic Publishers.
- Gardner, MJ; Hall, N; Fung, E; White, O; Berriman, M; Hyman, RW; Carlton, JM; Pain, A; Nelson, KE; Bowman, S; Paulsen, IT; James, K; Eisen, JA; Rutherford, K; Salzberg, SL; Craig, A; Kyes, S; Chan, MS; Nene, V; Shallom, SJ; Suh, B; Peterson, J; Angiuoli, S; Pertea, M; Allen, J; Selengut, J; Haft, D; Mather, MW; Vaidya, AB; Martin, DM; Fairlamb, AH; Fraunholz, MJ; Roos, DS; Ralph, SA; McFadden, Gi; Cummings, LM; Subramanian, GM; Mungall, C; Venter, JC; Carucci, DJ; Hoffman, SL; Newbold, C; Davis, RW; Fraser, CM; Barrell, B. (2002). Genome sequence of the human malaria parasite *Plasmodium falciparum*. *Nature*. 419: (6906), p498-511.
- Gasteiger, E; Hoogland, C; Gattiker, A; Duvaud, S; Wilkins, MR; Appel, RD; Bairoch, A. (2005). *The Proteomics Protocols Handbook: Protein Identification and Analysis Tools on the ExPASyServer*. Totowa: Humana Press Inc. p571-607.
- Glickman, JF; Ferrand, S. (2008). Scintillation Proximity Assay In High Throughput Screening. *Assay and Drug Development Technologies*. 6: (3), p433-455.
- Goh, LL; Loke, P; Singh, M; Sim, TS. (2003). Soluble expression of a functionally active *Plasmodium falciparum* falcipain-2 fused to maltose-binding protein in *Escherichia coli*. *Protein Expression and Purification*. 32: (2), p194-201.
- Gowda, DC; Davidson, EA. (1999). Protein glycosylation in the malaria parasite. *Parasitology Today*. 14: (4), p147-152.

- Gray, N; Detivaud, L; Doerig, C; Meijer, L. (1999). ATP-site directed inhibitors of cyclin dependent kinases. *Current Medicinal Chemistry*. 6, p859-870.
- Greenfield, NJ. (2006). Using circular dichroism spectra to estimate protein secondary structure. *Nature Protocols*. 1: (6), p2876-2890.
- Grossman, TH; Kawasaki, ES; Punreddy, SR; Osburne, MS. (1998). Spontaneous cAMP-dependent derepression of gene expression in stationary phase plays a role in recombinant expression instability. *Gene*. 209, p95-103.
- Guex, N; Peitsch, M C. (1997). SWISS-MODEL and the Swiss-PdbViewer: An environment for comparative protein modeling. *Electrophoresis*. 18, p 2714-2723.
- Gusmao, DS; Santos, AV; Marini, DC; de Souza Russo, E; Peixoto, AMD; Bacci, M; Berbert-Molina, MA; Lemos, FJA. (2007). First isolation of microorganisms from the mid diverticulum of a mosquito (Diptera: Culicidae): new perspectives for an insect-bacteria association. *Memorias do Instituto Oswaldo Cruz*. 102: (8), p919-924.
- Haas, L. (1999). Charles Louis Alphonse Laveran (1845-1922). *Journal of Neurology, Neurosurgery and Psychiatry*. 67: (4), p520.
- Halbert, J; Ayong, L; Equinet, L; Le Roch, K; Hardy, M; Goldring, D; Reininger, L; Waters, NC; Chakrabarti, D; Doerig, C. (2010). A *Plasmodium falciparum* transcriptional cyclin-dependent kinase-related kinase with a crucial role in parasite proliferation associates with histone deacetylase activity. *Eukaryotic Cell*. 9: (6), p952-959.
- Haldar, K; Mohandas N. (2007). Erythrocyte remodelling by malaria parasites. *Current Opinions in Hematology*. 14, p203-209.
- Hanahan, D. (1983). Studies on transformation of *Escherichia coli* with plasmids. *Journal of Molecular Biology*. 166: (4), p557-580.
- Hanks, SK. (2003). Genomic analysis of the eukaryotic protein kinase superfamily: a perspective. *Genome Biology*. 14: (111), p1-7.
- Harper, S; Speicher, DW. (2011). Purification of proeins fused to Glutathione S-Transferase. *Methods in Molecular Biology*. 681, p259-280.
- Hiller, NL; Bhattacharjee, S; van Ooij, C; Liolios, K; Harrison, T; Lopez-Estrano, C; Haldar, K. (2004). *Science*. 306: (5703), p1934-1937.
- Hilz, H; Wieggers, U; Adamietz, P. (1975). Stimulation of proteinase K action by denaturing agents: application to the isolation of nucleic acids and the degradation of 'masked' proteins. *European Journal of Biochemistry*. 56: (1), p103-108.
- Hiss, JA; Pryzborski, JM; Schwarte, F; Lingelbach, Schneider G. (2008). The *Plasmodium* Export Element Revisited. *PLOS One*. 3: (2), e1560.

- Ho, Y; Lo, HR; Lee, TC; Wu, CPY; Chao, YC. (2004). Enhancement of correct protein folding *in vivo* by a non-lytic baculovirus. *Biochemistry Journal*. 382, p695-702.
- Hohmann, AW; Faulkner, P. (1983). Monoclonal antibodies to baculovirus structural proteins: determination of specificities by Western blot analysis. *Virology*. 125: (2), p432-434.
- Holten, S; Merchx, A; Burgess, D; Doerig, C; Noble, M; Endicott, J. (2003). Structure of *Plasmodium falciparum* PfPK5 test the CDK regulation paradigm and suggest mechanisms of small molecule inhibition. *Structure*. 1, p1329-1337.
- Hora, R; Bridges, DJ; Craig, A; Sharma, A. (2009). Erythrocytic casein kinase II regulates cytoadherence of *Plasmodium falciparum* infected red blood cells. *Journal of Biological Chemistry*. 284: (10), p6260-6269.
- Hyashi, S; Lin, E. (1967). Purification and Properties of Glycerol Kinase from *Escherichia coli*. *Journal of Biological Chemistry*. 242, p1030-1035.
- Ipsaro, JJ; Harper, SL; Messick, TE; Mamorstein, R; Mondragon, A; Speicher, DW. (2010). Crystal structure and functional interpretation of the erythrocyte spectrin tetramerization domain complex. *Blood*. 115, p4843-4852.
- Kato, N; Kumar, KA; Marr, F; Mason, D; McNamara, C; Plouffe, D; Ramachandran, V; Spooner, M; Tuntland, T; Zhou, Y; Peters, EC; Sakata, T; Chatterjee, A; Schultz, PG; Ward, GE; Gray, N; Harper, J; Winzeler, EA; Breton, G; Le Roch, KG; Nagle, A; Andersen, C; Bursulaya, B; Henson, K; Johnson, J. (2008). Gene expression signatures and small-molecule compounds link a protein kinase to *Plasmodium falciparum* motility. *Nature Chemical Biology*. 4, p347-356.
- Kelley, LA; Sternberg, MJE. (2009). Protein structure prediction on the Web: a case study using the Phyre server. *Nature Protocols*. 4: (3): p363-371.
- Kennelly, PJ. (2002). Protein kinases and protein phosphatases in prokaryotes: a genomic perspective. *FEMS Microbiology Letters*. 206: (1), p1-8.
- Khan, AA; Hanada, T; Mohseni, M; Jeong, J-J; Zeng, L; Gaetani, M; Li, D; Reed, BC; Speicher, DW; Chishti, AH. (2008). Dematin and adducin provide a novel link between the spectrin cytoskeleton and human erythrocyte membrane by directly interacting with glucose transporter-1. *Journal of Biological Chemistry*. 283, p14600-14609.
- Khanna, R; Chang, SH; Andrabi, S; Azam, M; Rivera, A; Brugnara, C; Low, PS; Liu, S; Chishti, AH. (2002). Headpiece domain of dematin is required for the stability of the erythrocyte membrane. *Proceedings of the National Academy of Science*. 99: (10), p6637-6642.
- Kiefer, F; Arnold, K; Künzli, M; Bordoli, L; Schwede, T. (2009). The SWISS-MODEL Repository and associated resources. *Nucleic Acids Research*. 37, p387-p392.

- Kissinger, JC; Miligram, AJ; Fraunholz, MJ; Roos, DS; Brunk, BP; Crabtree, J; Diskin, SJ; Schug, J; Overton, GC; Stoeckert, CJ; Coppel, RL; Huestis, RL. (2001). PlasmoDB: An integrative database of the *Plasmodium falciparum* genome. Tools for accessing and analysing finished and unfinished sequence data. *Nucleic Acids Research*. 29: (1), p66-69.
- Korsgren, C; Cohen, CM. (1988). Associations of human erythrocyte band 4.2 binding to ankyrin and to the cytoplasmic domain of band 3. *Journal of Biological Chemistry*. 263, p10212-10218.
- Koshino, I; Mohandas, N; Takakuwa. (2012). Identification of a novel role for dematin in regulating red cell membrane function by modulating spectrin –actin interactions. *The American Society for Biochemistry and Molecular Biology*. 287: (42), p35244 - 35250.
- Kost, TA; Condreay, JP; Jarvis, DL. (2005). Baculovirus as versatile vectors for protein expression in insect and mammalian cells. *Nature Biotechnology*. 23: (5), p567-575.
- Kuhn, Y; Rohrbach, P; Lanzer, M. (2007). Quantitative pH measurements in *Plasmodium falciparum*-infected erythrocytes using pHluorin. *Cellular Microbiology*. 9, p1004-1013.
- Kun, JF; Hibbs, AR; Saul, A; McColl, DJ; Coppel, RL; Anders, RF. (1997). A putative *Plasmodium falciparum* exported serine/threonine protein kinase. *Molecular Biochemical Parasitology*. 85, p41-51.
- Kun, JF; Hibbs, AR; Saul, A; McColl, DJ; Coppel, RL; Anders, RF. (1997). A putative *Plasmodium falciparum* exported serine/threonine protein kinase. *Molecular and Biochemical Parasitology*. 85: (1), p41-51.
- Laemmli. (1970). Cleavage of Structural Proteins during the Assembly of the Head of Bacteriophage T4. *Nature*. 227, p680-685.
- Lahondere, C; Lazzari, CR. (2012). Mosquitoes cool down during blood feeding to avoid overheating. *Current Biology*. 22: (1), p40-45
- Lambert, S; Yu, H; Prchal, JT; Lawler, J; Ruff, P; Speicher, D; Cheung, MC; Kan, YW, Palek, J. (1990). cDNA sequence for the human erythrocyte ankyrin. *Proceedings of the National Academy of Science of the USA*. 87, p1730-1734.
- Lambros C; Vanderberg JP. (1979). Synchronization of *Plasmodium falciparum* erythrocytic stages in culture. *Journal of Parasitology*. 65: (3), p418-420.
- Lauterbach, SB; Lanzillotti, R; Coetzer, TL. (2003). Construction and use of *Plasmodium falciparum* phage display libraries to identify host parasite interactions. *Malaria Journal*. www.malariajournal.com/content/pdf/1475-2875-2-47.pdf.
- Le Roch, KG; Zhou, Y; Blair, PL; Grainger, M; Moch, JK; Haynes, JD; De La Vega, P; Holder, AA; Batalov, S; Carucci, DJ; Winzeler, EA. (2003). Discovery

of gene function by expression profiling of the malaria parasite life cycle. *Science*. 301: (5639), p1503-1508.

Leroy, D; Doerig, C. (2008). Drugging the *Plasmodium* kinome: the benefits of academia-industry synergy. *Trends in Pharmacological Science*. 29: (5), p241-249.

Liang, H; Narum, DL; Fuhrmann, SR; Luu, T; Sim, BK. (2000). A recombinant baculovirus-expressed *Plasmodium falciparum* receptor-binding domain of erythrocyte binding protein EBA-175 biologically mimics native protein. *Infection and Immunology*. 68, p3564-3568.

Liao, F. (2009). Discovery of Artemisinin (Qinghaosu). *Molecules*. 14, p5362-5366.

Ling Gho, L; Loke, P; Singh, M; Suan Sim, T. (2003). Soluble expression of a functionally active *Plasmodium falciparum* falcipain-2 fused to maltose-binding protein in *Escherichia coli*. *Protein Expression and Purification*. 32, p194-201.

Ling, E; Danilov, YN; Cohen, CM. (1988). Modulation of red cell band 4.1 function by cAMP-dependent kinase and protein kinase C phosphorylation. *Journal of Biological Chemistry*. 263, p2209-2216.

Liu, L; Johnson, HL; Cousens, S; Perin, J; Scott, S; Lawn, JE; Rudan, I; Campbell, H; Cibulskis, R; Li, M; Mathers, C; Black, RE. (2012). Global, regional, and national causes of child mortality: an updated systematic analysis for 2012 with time trends since 2000. *The Lancet*. 379: (9832), p2151-2161.

Maier, AG; Cooke, BM; Cowman, AF; Tilley, L. (2009). Malaria parasite proteins that remodel the host erythrocyte. *Nature Reviews Microbiology*. 7, p341-354.

Maier, AG; Rug, M; O'Neil, MT; Brown, M; Chakravorty, S; Szeszak, T; Chesson, J; Wu, Y; Hughes, K; Coppel, RL; Newbold, C; Beeson, JG; Craig, A; Crabb, BS; Cowman, AF. (2008). Exported proteins required for virulence and rigidity of *Plasmodium falciparum* infected human erythrocytes. *Cell*. 134: (1), p48-61.

Makrides, SC. (1996). Strategies for achieving high-level expression of genes in *Escherichia coli*. *Microbiology Revolution*. 60, p512-538.

Mandal, D; Moitra, PK; Basu, J. (2002). Mapping of a spectrin-binding domain of human erythrocyte membrane protein 4.2. *Biochemistry Journal*. 364, p841-847.

Manning, G; Whyte, DB; Martinez, R; Hunter, T; Sudarsanam, S. (2002). The protein kinase complement of the human genome. *Science*. 295, p1912-1934.

Manno, S; Takakuwa Y; Mohandas N. (2002). Identification of a functional role for lipid asymmetry in biological membranes: Phosphatidylserine-skeletal protein interactions modulate membrane stability. *Proceedings of the National Academy of Science USA*. 99, p1943-1948.

- Manno, S; Takakuwa, Y; Mohandas, N. (2004). Modulation of erythrocyte membrane mechanical function by protein 4.1 phosphorylation. *The Journal of Biological Chemistry*. 280: (9), p7581-7587.
- Marti, M; Good, RT; Rug , M, Knuepfer, E; Cowman AF. (2004). Targeting malaria virulence and remodelling proteins to the host erythrocyte . *Science*. 306, p1930-1933.
- Martin, RE; Kirk K. (2007). Transport of the essential nutrient isoleucine in human erythrocyte infected with malaria parasite *Plasmodium falciparum*. *Blood*. 109: (5), p2217-2224.
- McPherson, M; Moller, S (2006). *PCR The basics*. 2nd ed. New York: Taylor & Francis Group. 29.
- McRobert, L; Taylor, CJ; Deng, W; Fivelman, QL; Cummings, RM; Polley, SD; Billker, O; Bake, DA. (2008). Gametocytogenesis in malaria parasites is mediated by the cGMP-dependent protein kinase. *Plos Biology*. 6, e139.
- Mehlin, C; Boni, E; Buckner, FS; Engel, L; Feist, T; Gelb, MH; Haji, L; Kim, D; Liu, C; Mueller, N; Myler, PJ; Reddy, JT; Sampson, JN; Subramanian, E; van Voorhis, WC; Worthey, E; Zucker, F; Hol, WGJ. (2006). Heterologous Expression of proteins from *Plasmodium falciparum*: Results form 1000 genes. *Molecular and Biochemical Parasitology*. 148, p144-160.
- Merckx, A; Echali  r, A; Langford, K; Sicard, A; Langsley, G; Joore, J; Doerig, C; Noble, M; Endicott, J. (2008). Structure of PfPK7 an atypical protein kinase from *Plasmodium falciparum* identify novel activation motif and leads for inhibitory design. *Structure*. 16: (2), p228-238.
- Merckx, A; Nivez M-P; Bouyer, G; Alano, P; Langsley, G; Deitsch, K; Thomas, S; Doerig, C; Ege, S. (2008). *Plasmodium falciparum* regulatory subunit of cAMP-dependent PKA and anion channel conductance. *Plos Pathogens*. 4, e19.
- Metzenberg, AB; Gitscheir, J. (1992). The gene encoding the palmitoylated erythrocyte membrane protein, p55, originates at the CpG island 3' to the VIII gene. *Human Molecular Genetics*. 1: (2), p97-101.
- Miles, AP; Zhang, Y; Saul, A; Stowers, AW. (2002). Large-scale purification and characterization of malaria vaccine candidate antigen Pvs25H for use in clinical trials. *Protein Expression and Purification*. 25, p87-96.
- Mohandas, N; Gallagher PG. (2008). Red cell membrane: past, present, and future. *Blood*. 112, p3939-3948.
- Monsma, SA; Blissard, GW. (1995). Identification of a domain fusion domain and an oligomerization domain in the baculovirus GP64 envelope fusion protein. *Journal of Virology*. 69: (4), p2583-2595.
- Moskes, C; Burghaus, PA; Wernli, B; Sauder, U; Durrenberger, M; Kappes, B. (2004). Export of *Plasmodium falciparum* calcium-dependent protein kinase 1 to

the parasitophorous vacuole is dependent on three N-terminal membrane anchor motifs. *Molecular Microbiology*. 54, p676-691.

Murphy, SC; Samuel, BU; Harrison T. (2004). Erythrocyte detergent-resistant membrane proteins: their characterization and selective uptake during malarial infection. *Blood*. 103, p1920-1928.

Narum, DL; Welling, GW; Thomas, AW. (1993). Ion-exchange-immunoaffinity purification of a recombinant baculovirus *Plasmodium falciparum* apical membrane antigen, Pf83/AMA-1. *Journal of Chromatography*. 657, p357-363.

Novagen. (2012). 71757 Overnight Express™ Instant LB Medium Package Insert. Available: http://www.merck-chemicals.com/is-bin/INTERSHOP.enfinity/WFS/Merck-International-Site/en_US/-/USD/ViewPDF-Print.pdf?RenderPageType=ProductDetail&CatalogCategoryID=iYSb.s1O34EAAAEjBRp9.zLX&ProductUUID=. Last accessed 11/03/2012.

Novagen. Competent Cells, User protocol TB009 Rev. F0104. Available: <http://sites.bio.indiana.edu/~ybelab/procedures/NovagenCompetentCells.pdf>. Last accessed 23/02/2012.

Novy, R; Drott, D; Yaeger, K; Mierendorf, R. (2001). Overcoming the codon bias of *E coli*. *InNovations*. 12, p1-3.

Nunes, MC; Goldring, JP; Doerig, C; Scherf, A. (2007). A novel protein kinase family in *Plasmodium falciparum* is differentially transcribed and secreted to various cellular compartments of the host cell. *Molecular Microbiology*. 63, p391-401.

Ojo, KK; Larson, ET; Keyloun, KR; Castaneda, LJ; Derocher, AE; Inampudi, KK; Kim, EJ; Arakaki, TL; Murphy, RC; Zhang, L; Napuli, AJ; Maly, DJ; Verlinde, CL; Buckner, FS; Parsons, M; Hol, WG; Merritt, EA; Van Voorhis, WC. (2010). *Toxoplasma gondii* calcium-dependent protein kinase 1 is a target for selective kinase inhibitors. *Nature Structural and Molecular Biology*. 17: (5), p602-607.

Ojo, KK; Pfander, C; Mueller, NR; Burstroem, C; Larson, ET; Bryan, CM; Fox, AMW; Reid, MC; Johnson, SM; Murphy, RC; Kenedy, M; Mann, H; Leibly, DJ; Hewitt, SN; Verlinde, CL; Kappe, S; Merritt, EA; Maly, DJ; Billker, O; Van Voorhis, WC. (2012). Transmission of malaria to mosquitoes blocked by bumped kinase inhibitors. *The Journal of Clinical Investigation*. 122: (6), p2301-2305.

Ono, T; Cabrita-Santos, L; Leitao, R; Bettiol, E; Purcell, LA; Diaz-Pulido, O; Andrews, LB; Tadakuma, T; Bhanot, P; Mota, MM; Rodriguez, A. (2008). Adenyl cyclase α and cAMP signalling modulate *Plasmodium* sporozoite apical regulated exocytosis and hepatocyte infection. *Plos Pathogens*. 4, e1000008.

Oomens, AG; Monsma, SA; Blissard, GW. (1995). The baculovirus GP64 envelope fusion protein: synthesis, oligomerization, and processing. *Virology*. 209: (2), 592-603.

Palek, J (1995). *Williams Hematology. 5th ed.* New York: McGraw-Hill Inc. p406.

Pang, AL; Hashimoto, CN; Tam, LQ; Meng, ZQ; Hui, GS; Ho, WK. (2002). In vivo expression and immunological studies of the 42-kDa carboxy-terminal processing fragment of *Plasmodium falciparum* merozoite surface protein I in the baculovirus-silkworm system. *Infection and Immunology*. 70, p2772-2779.

Pasini, EM; Kirkeyaard, M; Mortensen, P; Lutz, HU; Thomas, AW; Mam, M. (2006). In-depth analysis of the membrane and cytosolic proteome of red blood cells. *Blood*. 108, p791-801.

Pei, X; Guo, X; Coppel, R; Bhattacharjee, S; Haldar, K; Gratzer, W; Mohandas, N; An, X. (2007). The ring-infected erythrocyte surface antigen (RESA) of *Plasmodium falciparum* stabilizes spectrin tetramers and suppresses further invasion. *Blood*. 110: (3), p1036–1042.

Persidis, A. (2000). Malaria. *Nature Biotechnology*. 18, p111-112.

Peterson, DS; Gao, Y; Asokan, K; Gaertig, J. (2002). The circumsporozoite protein of *Plasmodium falciparum* is expressed and localized to the cell surface in the free-living ciliate *Tetrahymena thermophila*. *Molecular and Biochemical Parasitology*. 122: (2), p119-126.

Peti, W; Page, R. (2007). Strategies to maximise heterologous protein expression in *Escherichia coli* with minimal cost. *Protein Expression and Purification*. 51, p1-10.

Philip, N; Haystead, TA. (2007). Characterization of a UBC13 kinase in *Plasmodium falciparum*. *Proceedings of the National Academy of Science USA*. 104, p7845-7850.

Pinder, JC; Smith, KS; Gratzer, WB. (1989). Preparation and properties of human red-cell ankyrin. *Biochemistry Journal*. 264, p423-428.

Pizarro, JC; Chitarra, V; Verger, D; Holm, I; Petres, S; Darteville, S; Nato, F; Longacre, S; Bentley, GA. (2003). Crystal structure of a Fab complex formed with PfMSP1-19, the C-terminal fragment of merozoite surface protein 1 from *Plasmodium falciparum*: a malaria vaccine candidate. *Journal of Molecular Biology*. 328, p1091-1103.

PlasmoDB version 9.3. Available: <http://plasmodb.org>. (2013).

Pombo, CM; Bonventre, JV; Molnar, A; Kyriakis, J; Force, T. (1996). Activation of a human Ste20-like kinase by oxidant stress defines a novel stress response pathway. *European Molecular Biology Organisation Journal*. 15, p4537-4546.

Protein-homology/analogy recognition engine (Phyre2). Available: www.sbg.bio.ic.ac.uk/~phyre. (2009)

Reid, ME; Takakuwa, Y; Conboy, J; Tchernia, G; Mohandas, N. (1990). Glycophorin-C content of human erythrocyte membrane is regulated by protein 4.1. *Blood*. 75, p2229-2234.

Ridley, RG. (1998). Malaria: Dissecting chloroquine resistance. *Current Biology*. 8: (10), p346-349.

Rinaldi, A. (2004). Fighting malaria at the crossroads. *EMBO Reports*. 5 (9), 847-851.

Robichon, C; Luo, J; Causey, TB; Benner, JS; Samuelson, JC. (2011). Engineering Escherichia coli BL21 (DE30) derivative strains to minimize *E. coli* protein contamination after purification by immobilized metal affinity chromatography. *Applied and Environmental Microbiology*. 77: (13), p4634-4646.

The RTS SCTP. (2011). First results of phase 3 trials of RTS,S/AS01 malaria vaccine in African children. *The New England Journal of Medicine*. 10: (365), p1863-1875.

The RTS,S Clinical Trials Partnership. (2012). A Phase 3 Trial of RTS,S/AS01 Malaria Vaccine in African Infants. *The New England Journal of Medicine*. 367:p2284-95.

Turrini, F; Ginsburg, H; Bussolino, F; Pescarmona, GP; Serra, MV; Arese, P. (1992). Phagocytosis of *Plasmodium falciparum* infected human red blood cells by human monocytes: involvement of immune and nonimmune determinants and dependence on parasite developmental stages. *Blood*. 80, p801-808.

Sanger, F; Donelson, JE; Coulson, AR; Kösse, IH; Fischer, D. (1974). Determination of a nucleotide sequence in bacteriophage f1 DNA by primed synthesis with DNA polymerase. *Journal of Molecular Biology*. 90: (2), p315-333.

Sasse, J; Gallagher ST. (2003). Detection of Proteins on Blot Transfer Membranes. *Current Protocols in Molecular Biology*. 1, p1071-1076.

Schinkmann, K; Blenis, J. (1997). Cloning and Characterization of a Human STE20-like Protein kinase with Unusual Cofactor Requirements. *The Journal of Biological Chemistry*. 272, p28695-28703.

Schlichterle, M; Wahlgren, M; Perlmann, H; Scherf, A (2000). *Methods in Malaria research*. 3rd ed. [http://www.malaria.mr4.org/mr4pages/protocolbook/methods in malaria research.pdf](http://www.malaria.mr4.org/mr4pages/protocolbook/methods%20in%20malaria%20research.pdf).

Schmidt, GD; Roberts, LS . (2005). *Foundations of Parasitology*. 7th ed. New York: McGraw-Hill Inc. p150-153.

Schwede, T; Kopp, J; Guex, N; Peitsch, MC. (2003). SWISS-MODEL: an automated protein homology-modeling server. *Nucleic Acids Research*. 31, p3381-3385.

Sefton, BM; Shenolikar, S. (1996). Overview of protein phosphorylation: Labeling studies, In: Ausubel FM, Brent R, Kingston RE, Moore DD, Seidman JG, Smith JA, Struhl K, editors. *Current Protocols in Molecular Biology*. John Wiley & Sons, Inc; Vol. 4; 18.1.1-18.1.4.

Shonhai, A; Boshoff, A; Blatch, GL. (2007). The structural and functional diversity of Hsp70 proteins from *Plasmodium falciparum*. *Protein Science*. 16, p1803-1818.

Siden-Kiamos, I; Ecker, A; Nyback, S; Louis, C; Sinden, RE; Billker, O. (2006). *Plasmodium berghei* calcium-dependent protein kinase 3 is required for ookinete gliding motility and mosquito midgut invasion. *Molecular Microbiology*. 60, p1355-1363.

Sing, S; Kennedy, MC; Long, CA; Saul, AJ; Miller, LH; Stowers, AW. (2003). Biochemical and immunological characterization of bacterially expressed and refolded *Plasmodium falciparum* 42-kilodalton C-terminal merozoite surface protein I. *Infection and Immunity*. 71, p6766-6774.

Singh, B; Kim Sung, L; Matusop, A; Radhakrishnan, A; Shamsul, SS; Cox-Sing, J; Thomas, A; Conway, DJ. (2004). A large focus of naturally acquired *Plasmodium knowlesi* infections in human beings. *Lancet*. 363: (9414), p1017-1024.

Solyakov, L; Halbert, J; Alam, MM; Semblat, J-P; Dorin-Semblat, D; Reininger, L; Bottrill, AR; Mistry, S; Abdi, A; Fennel, C; Holland, Z; Dematra, C; Bouza, Y; Sicard, A; Nivez, M-P; Eschenlauer, S; Lama, T; Thomas, DC; Sharma, P; Agarwal, S; Kerri, S; Prodel, G; Graviotti, M; Tobin, AB; Doerig, C. 2011. Global kinomic phospho-proteomic analysis of the human malaria parasite *Plasmodium falciparum*. *Nature Communications*. 2 (565), p1-12.

Souza, JM. (1992). Epidemiological distribution of *Plasmodium falciparum* drug resistance and its relevance to the treatment and control of malaria. *Memorias do Instituto Oswaldo Cruz*. 87, p343-348.

Specht, KM; Shokat, KM. (2002). The emerging power of chemical genetics. *Current Opinions in Cell Biology*. 14, p156-159.

Spycher, C; Rug, M; Klonis, N; Ferguson, DJP; Cowman, AF; Beck, H-P; Tilley, L. (2006). Genesis of and Trafficking to the Maurer's clefts of *Plasmodium falciparum*-Infected Erythrocytes. *Molecular and Cellular Biology*. 26: (1), p4074-4085.

Steck, TL. (1978). The band 3 protein of the human red cell membrane: a review. *Journal of Supramolecular Structure*. 8: (3), p311-24.

Syin, C; Parzy, D; Traincard, F; Boccaccio, I; Joshi, MB; Lin, DT, Yang, X; Assemet, K; Doerig, C; Langsley, G. (2001). The H89 cAMP-dependent protein kinase inhibitor blocks *Plasmodium falciparum* development in infected erythrocytes. *European Journal of Biochemistry*. 268, p4842-4849.

Takakuwa, Y. (2000). Protein 4.1, a multifunctional protein of the erythrocyte membrane skeleton: structure and functions in erythrocytes and nonerythroid cells. *International Journal of Hematology*. 72: (3), p298-309.

Thomas, DC; Ahmed, A; Gilberger, TW; Sharma, P. (2012). Regulation of *Plasmodium falciparum* Glideosome Associated Protein 45 (PfGAP45) phosphorylation. *Plos one*. 4, e35855.

Tisdale, EJ. (2002). Glyceraldehyde-3-phosphate dehydrogenase is phosphorylated by protein kinase Ciota /lambda and plays a role in microtubule dynamics in the early secretory pathway. *Journal of Biological Chemistry*. 277, p3334-3341.

Towbin, H; Staehelin, T; Gordon, J. (1979). Electrophoretic transfer of proteins from polyacrylamide gels to nitrocellulose sheets: procedure and some applications. *Proceedings of the National Academy of Science of the USA*. 76, p4250-4354.

Trager, W; Jensen JB. (1976). Human malaria parasites in continuous culture. *Science*. 193: (4254), p673-675.

Tyler, JM; Hargreaves, WR; Branton, D. (1979). Purification of two spectrin-binding proteins: Biochemical and electron microscopic evidence for site-specific reassociation between spectrin and bands 2.1 and 4.1. *Proceedings of the National Academy of Science of the USA*. 76 (10), p5192-5196.

Vaid, A; Thomas, DC; Sharma, P. (2008). Role of Ca²⁺/calmodulin-PfPKB signalling pathway in erythrocyte invasion of *Plasmodium falciparum*. *Journal of Biological Chemistry*. 283, p5589-5597.

Van Bemmelen, MX; Beghdadi-Rais, C; Desponds, C; Vargas, E; Herrera, S; Reymond, CD; Fasel, N. (2000). Expression and one-step purification of *Plasmodium* proteins in *Dictostelium*. *Molecular and Biochemical Parasitology*. 111: 92), p377-390.

Vedadi, M; Lew, J; Artz, J; Amani, M; Zhao, Y; Dong, A; Wasney, GA; Gao, M; Hills, T; Brokx, S; Qiu, W; Sharma, S; Diassiti, A; Alam, Z; Melone, M; Mulichak, A; Wernimont, A; Bray, J; Loppnau, P; Plotnikova, O; Newberry, K; Sundararajan, E; Houston, S; Walker, J; Tempel, W; Bochkarev, A; Kozieradzki, I; Edwards, A; Arrowsmith, C; Roos, D; Kain, K; Hui, R. (2007). Genome-scale protein expression and structural biology of *Plasmodium falciparum* and related Apicomplexan organisms. *Molecular Biochemical Parasitology*. 151: (1), p100-110.

Waller, KL; Nunomura, W; An, X; Cooke, BM; Mohandas, N; Coppel, RL. (2003). Mature parasite-infected erythrocyte surface antigen (MESA) of

Plasmodium falciparum binds to the 30-kDa domain of protein 4.1 in malaria-infected red blood cells. *Blood*. 102, p1911-1914.

Wang, Y; Sarkar, M; Smith, AE; Krois, AS; Pielak, GJ. (2012). Macromolecular Crowding and Protein Stability. *Journal of American Chemical Society*. 134: (40), p16614-16618.

Ward, JJ; McGuffin, LJ; Bryson, K; Buxton, BF; Jones, DT. (2004). The DISOPRED server for the prediction of protein disorder. *Bioinformatics*. 20, p2138-2139.

Ward, P; Packer, J; Equinet, L; Doerig C. (2004). Protein kinases of the human malaria parasite *Plasmodium falciparum*: The kinome of a divergent eukaryote. *BMC Genomics*. 5, p79.

Waugh, A; Grant, A. (2007). *Anatomy and Physiology Health in Health and White, NJ. (1999). Delaying antimalarial drug resistance with combination therapy. Parasitologia*. 41, p301-308.

White, NJ. (2008). Qinghaosu (artemisinin): the price of success. *Science*. 320, p330-334.

White, MT; Bejon, P; Olotu, A; Griffin, JT; Riley, EM; Kester, KE; Ockenhouse, CF; Ghani, AC. (2013). The Relationship between RTS,S Vaccine-Induced Antibodies, CD4(+) T Cell Responses and Protection against *Plasmodium falciparum* Infection, *PLOS One*. 8, pe61395-e61395.

WHO Malaria Report 2012. Available: http://www.who.int/malaria/publications/world_malaria_report_2012/wmr2012_n_o_profiles.pdf. (2012)

Wickert, H; Krohne, G. (2007). The complex morphology of Maurer's clefts: from discovery to three-dimensional reconstruction. *Trends in Parasitology*. 23, p502-509.

Wiersma, HI; Galuska, SE; Tomley, FM; Sibley, LD; Liberator, PA; Donald, RGK. (2004). A role for coccidian cGMP-dependent protein kinase in motility and invasion. *International Journal of Parasitology*. 34, p369-380.

World Health Organization. (2001). *The use of antimalarial drugs – report of an informal consultation*. Available: whqlibdoc.who.int/hq/2001/WHO_CDS_RBM_2001.33.pdf. Last accessed 22/02/2012.

Worthington, K; Worthington, V. (2011). *Worthington Enzyme Manual*. Available: <http://www.worthington-biochem.com/pap/default.html>. Last accessed March 2012.

Zhang, XS; Choi, JH. (2001). Molecular evolution of calmodulin-like domain protein kinases (CDPK's) in plants and protists. *Journal of Biological Evolution*. 53, p214-224.

Zuccala, ES; Baum, J. (2011). Cytoskeletal and membrane remodelling during malaria parasite invasion of the human erythrocyte. *British Journal of Haematology*. 154, p680-689.

7 APPENDIX

7.1 Reagents

7.1.1 *Plasmodium falciparum* culturing

Sterile 12% Sodium chloride (NaCl) solution

12g NaCl (2.05M)

Make up to 100ml using Milli-Q water

Autoclave and store at 4°C until needed.

Sterile 1.6% NaCl solution

1.6g NaCl (0.274M)

Make up to 100ml using Milli-Q water

Store at 4°C until needed.

Sterile 0.9% NaCl / 0.2% Glucose (w/v)

900mg NaCl (0.154M)

200mg Glucose

Make up to 100ml using Milli-Q water

Store at 4°C until needed.

Sterile phosphate buffered saline (PBS) (pH 7.2 OR pH 7.4)

8g NaCl (137mM)

2g KCl (2.7mM)

1.78g Na₂HPO₄·2H₂O (10mM)

0.2g KH₂PO₄ (1.5mM)

Add 900ml Milli-Q water and check pH.

Make up to a final volume of 1L using Milli-Q water.

Autoclave the solution and store at room temperature.

Sterile incomplete culture medium

10.4g GIBCOTM RPMI 1640 powder

5.94g HEPES (25mM)

4g Glucose (22mM)

44mg Hypoxanthine (0.336mM)

50mg Gentamycin sulphate (0.087mM)

Dissolve in 1L Milli-Q water and stir for 2 hours.

Filter sterilize the solution through a SterivexTM-GS 0.2 µm Filter unit (*Millipore Corporation, USA*) and store at 4°C until needed.

Sterile complete culture medium with Plasma

80ml sterile incomplete medium

2.8ml sterile 7.5% NaHCO₃ (893mM)

Gas the medium with 100% CO₂ until the pH indicator changes to an orange-yellow colour.

Add 10ml inactivated human AB⁺ plasma for a 10% final plasma concentration or 20ml for a 20% final plasma concentration.

Make up to a final volume of 100ml using sterile incomplete medium.

Store at 4°C for no longer than 1 week.

5 % D-sorbitol solution

500mg D-sorbitol

Make up in 10ml sterile Milli-Q water.

Store at 4°C until needed.

Cryo-preservation solution:

Phosphate buffered saline (PBS) (pH 7.2 – 7.4)

7.2g NaCl (123mM)

14.8g Na₂HPO₄.2H₂O (83mM)

4.4g KH₂PO₄ (32mM)

Make up to 1L using sterile Milli-Q water.

Add 60ml glycerol to 40ml of the above prepared PBS.
Aliquot the freezing solution into sterile 15ml Falcon tubes.
Store at -20°C until needed.

7.1.2 Cloning

5% Saponin

250mg Saponin

Make up to 5ml in sterile PBS (pH 7.4)

Lysis buffer

Make up the following stock solutions:

1M Tris-HCl (pH 8.0):

12.11g Tris (1M)

Add 90ml Milli-Q water and adjust the pH using HCl.

Make up to a final volume of 100ml using Milli-Q water.

0.5M EDTA (pH 8.0)

18g EDTA

Add 90ml Milli-Q water and adjust the pH using NaOH.

Make up to a final volume of 100ml using Milli-Q water.

Use 1M Tris-HCl (pH 8.0) and 0.5M EDTA (pH 8.0) stock solutions to make up lysis buffer:

4ml of 1M Tris-HCl (40mM final concentration)

16ml of 0.5M EDTA (80mM final concentration)

2g SDS (2%)

Make up to a final volume of 100ml using Milli-Q water.

Add PCR grade recombinant Proteinase-K (*Sigma-Aldrich Corporation, USA*) just before use to a concentration of 0.1mg/ml.

TE Buffer (pH 8.0)

0.24g Tris (10mM)

74mg EDTA (1mM)

Add 90ml Milli-Q water and adjust pH to 8.0 using HCl.

Make up to a final volume of 100ml using Milli-Q water.

3M Sodium Acetate (pH 5.2)

24.61g Sodium acetate trihydrate

Add 90ml Milli-Q water and adjust the pH to 5.2 using acetic acid.

Make up to a final volume of 100ml using Milli-Q water.

Ethidium bromide (10µg/µl)

10mg Ethidium bromide (*Sigma-Aldrich Inc. USA*)

Make up to 1ml using Milli-Q water.

Store the solution in the dark at 4°C.

50x TAE buffer (pH ~8.5)

24.2g Tris

10ml 0.5M EDTA (pH 8)

5.71ml Acetic acid

Make up to a final volume of 100ml using Milli-Q water.

1x TAE buffer

20ml of 50x TAE buffer

Make up to a final volume of 1L using Milli-Q water.

0.8% Agarose gel

0.4g Agarose D-1 LE (*Hispanager, Spain*)

Make up to a final volume of 50ml using 1x TAE buffer.

Microwave the solution until the agarose has fully dissolved.

Allow to cool for a few minutes before adding 2.5µl ethidium bromide (final concentration 0.5 µg/ml).

Swirl the mixture, pour it into the mini-gel casting tray to form wells and allow the gel to set at room temperature.

7.1.3 *Escherichia coli* cell growth reagents

Luria Bertani Broth (LB medium)

10g Bacto™ Tryptone (*Becton Dickinson Biosciences, USA*)

5g Yeast Extract (*Oxoid, UK*)

10g NaCl

10ml 1M Tris-HCl (pH 7.5)

Make up to 1L using Milli-Q water and autoclave the solution.

Allow the solution to cool before use.

Store the LB medium at room temperature.

Overnight Express™ Instant TB Medium

60g Overnight Express™

10ml Glycerol

Make up to 1L using Milli-Q water and autoclave the solution.

Allow the solution to cool before use and store at room temperature.

LB medium supplemented with 2% Glucose

Add 20g Glucose to 1L LB medium.

Autoclave the solution and allow to cool before use.

Store at room temperature.

Ampicillin (100mg/ml)

1g ampicillin (*Roche Applied Science, Germany*)

10ml Milli-Q water

Filter sterilize the solution through a Millex GP 0.22µm syringe-driven filter unit (*Millipore, Ireland*) and store in 200µl aliquots at -20°C..

Use within 6 months.

Chloramphenicol (50mg/ml)

0.5g chloramphenicol (*Sigma-Aldrich Inc., USA*)

10ml Milli-Q water

Filter sterilize the solution through a Millex GP 0.22µm syringe-driven filter unit and store in 200µl aliquots at -20°C.

Use within 6 months.

60% Glycerol

Add 60ml Glycerol to 40ml Milli-Q water.

Agar plates for bacterial cell cultures

15g Agar

1L LB medium

Autoclave the solution and allow it to cool before adding 1ml of 100mg/ml ampicillin to a final concentration of 100µg/ml and 1ml 50µg/ml chloramphenicol to a final concentration of 50µg/ml.

7.1.4 Recombinant protein extraction reagents

10x MagneGSTTM wash-bind buffer (pH 8.23)

0.75g Na₂HPO₄·H₂O (4.2mM)

0.35g KH₂PO₄ (2mM)

8.18g NaCl (140mM)

0.75g KCl (10mM)

Add 90ml Milli-Q water and adjust the pH to 8.23 using KH₂PO₄.

Make up to a final volume of 100ml using Milli-Q water.

GST elution buffer (500mM Glutathione)

0.77g Glutathione

0.5ml 50mM Tris-HCl (pH 8.1)

Make up to a final volume of 5ml.

Filter sterilize the solution through a Millex GP 0.22µm syringe-driven filter unit.

Store in aliquots at -20°C.

MagneHisTM bind-wash buffer (pH 7.5)

2.38g HEPES (100mM)

0.068g Imidazole (10mM)

Add 90ml Milli-Q water and adjust the pH using HCl.

Make up to a final volume of 100ml using Milli-Q water.

Filter sterilize the solution through a Millex GP 0.22µm syringe-driven filter unit and store at room temperature.

MagneHis™ kit elution buffer (pH 7.5)

2.38g HEPES (100mM)

3.404g Imidazole (500mM)

Add 90ml Milli-Q water and adjust the pH using HCl.

Make up to a final volume of 100ml using Milli-Q water.

Filter sterilize the solution through a Millex GP 0.22µm syringe-driven filter unit and store at -20°C in aliquots.

7.1.5 Laemmli SDS-PAGE reagents

30% Acrylamide solution (w/v)

30g Acrylamide

Make up to a final volume of 100ml with Milli-Q water.

Store in a dark bottle at 4°C.

1% Bis-acrylamide (w/v)

1g Bis-acrylamide

Make up to 100ml using Milli-Q water.

Store in a dark bottle at 4°C.

4x Resolving gel buffer (pH 8.8)

18.17g Tris (1.5M)

Add 90ml Milli-Q water and pH using HCl.

Make up to a final volume of 100ml with Milli-Q water and store at 4°C.

4x Stacking gel buffer (pH 6.8)

12.12g Tris (0.5M)

Add 190ml Milli-Q water and pH using HCl.

Make up to a final volume of 200ml with Milli-Q water.

10% SDS (w/v)

1g SDS

Make up in 10ml MilliQ-water.

The solution can be stored at room temperature.

10% APS (w/v)

0.1g APS

Make up in 1ml MilliQ-water.

The solution needs to be made up fresh each time.

Laemmli running buffer

6.06g Tris (25mM)

28.2g Glycine (192mM)

2g SDS (0.1% w/v)

Make up to 2L using Milli-Q water and store at room temperature.

10% Acetic acid/10% Methanol

Add 200ml Acetic acid and 200ml Methanol to 1.6L of Milli-Q water.

10% Methanol

Add 200ml Methanol to 1.8L Milli-Q water.

5x Suspension solution (pH 8)

0.303g Tris (50mM)

0.093g EDTA (5mM)

2.5g SDS (5%)

12.5g sucrose (25%)

Add 40ml Milli-Q water and adjust the pH with HCl.

Make up to a final volume of 50ml with Milli-Q water.

Store the solution at room temperature.

Bromophenol blue solution

0.25g sucrose (2.5% w/v)

0.05g Bromophenol blue (0.05% w/v)

Make up to a final volume of 10ml Milli-Q water and store at 4°C.

0.05% Coomassie Blue Stain

1g Coomassie blue R-250

500ml Isopropanol

200ml Acetic acid

Make up to 2L with Milli-Q water.

7.1.6 Fairbanks SDS-PAGE reagents

40% Acrylamide + 1.5% Bis-acrylamide solution (w/v)

40g Acrylamide

1.5g Bis-acrylamide

Make up to a final volume of 100ml with Milli-Q water.

10x TAE buffer

200ml of 50x TAE buffer

Make up to a final volume of 1L using Milli-Q water.

25% Glycerol

Add 2.5ml glycerol to 7.5ml Milli-Q water.

Vortex to mix thoroughly and store at room temperature.

0.5% TEMED

Add 50µl TEMED to 10ml Milli-Q water.

Store at 4°C in a dark bottle.

Fairbanks running buffer

1x TAE

0.1% SDS

7.1.7 Immunoblot analysis reagents for GST-tagged recombinant proteins

Towbin Transblot buffer

6.06g Tris (25mM)

28.8g Glycine (192mM)

Dissolve the reagents in 1.5L Milli-Q water.

Add 400ml methanol (20% v/v) and make up to a final volume of 2L using Milli-Q water.

Store at 4°C.

TBS buffer (pH 7.5)

6.06g Tris (25mM)

9g NaCl (150mM)

Add 900ml Milli-Q water and adjust the pH to 7.5 using HCl.

Make up to a final volume of 1L using Milli-Q water.

Store the solution at 4°C.

TBST

Add 0.5ml Tween-20 to 1L TBS buffer (pH 7.5).

Store the solution at 4°C.

Anti-GST HRP conjugated blocking buffer

Dissolve 0.75g BSA (3% w/v) in 25ml TBS buffer (pH 7.5)

Anti-GST HRP-conjugated antibody (1:100 000)

Dissolve 0.5g BSA in 50ml TBS buffer (pH 7.5) and add 0.5µl anti-GST HRP-conjugated antibody.

Store solution at 4°C.

Amido Black staining solution

1g Amido black (1% w/v)

10ml Methanol (10% v/v)

2ml Acetic acid (2% v/v)

Make up to a final volume of 100ml using Milli-Q water.

Store at room temperature.

Amido Black de-staining solution

250ml Methanol

35ml Acetic acid

215ml Milli-Q water.

Store at room temperature.

7.1.8 Immunoblot analysis reagents for Histidine-tagged recombinant proteins

Anti-His HRP conjugate Blocking buffer (150ml)

Dissolve 0.75g of kit Blocking reagent (0.5% (w/v)) in 149.85ml 1x Blocking reagent buffer and add 0.15ml Tween 20 (0.1% (v/v)).

Store solution at 4°C.

TBS-Tween/Triton X buffer (pH 7.5)

Add 2.42g Tris (10mM)

8.77g NaCl (150mM)

0.5ml Tween-20 (0.05% (v/v)) and

2ml Triton X-100 (0.2% (v/v)) to 950ml Milli-Q water and adjust pH to 7.5 with HCl.

Make up to a final volume of 1L.

Store solution at 4°C.

Anti-His HRP conjugated antibody (1:2 000)

10µl anti-His HRP-conjugated antibody stock solution in 20ml anti-His HRP-conjugated blocking buffer.

Store solution at 4°C.

7.1.9 Reagents for recombinant baculovirus (BacVirus-PfB0150c) production

3.7% Formaldehyde solution

Add 5ml 37% formaldehyde to 45ml sterile PBS (pH 7.4)

1x FastPlax™ titer kit TBST

Add 10ml of 10x FastPlax™ titer kit TBST to 90ml MilliQ-water.

1% Gelatin blocking solution

Place the FastPlax™ titer kit 10% Gelatin bottle in a beaker filled with hot water for a few minutes. When melted add 1.5ml of the gelatin solution to 15ml 1x FastPlax™ titer kit TBST.

FastPlax™ titer kit Antibody (1:10 000)

Add 1.2µl of FastPlax™ Antibody to 12ml 1x FastPlax™ TBST.

FastPlax™ titer kit Goat Anti-Mouse β-gal Conjugate (1:1000)

Add 120µl FastPlax™ Goat Anti-Mouse β-gal Conjugate to 12ml 1x FastPlax™ TBST.

FastPlax™ titer kit Developing solution

Prepare the following two solutions:

0.5M MgCl₂ solution

Dissolve 0.476g MgCl₂ in 10ml MilliQ-water.

PBS (pH7.4) containing 5mM MgCl₂

Add 150µl of 0.5M MgCl₂ solution to 14.85ml sterile PBS (pH 7.4)

Add 60µl FastPlax™ titer kit X-Gal and 60µl FastPlax™ titer kit NBT to 15ml sterile PBS (pH 7.4) containing 5mM MgCl₂.

7.1.10 Non-radioactive kinase assay reagents

0.1M Tris-HCl buffers at various pH values

1.21g Tris

Add 90ml Milli-Q water.

Warm the solution in a waterbath for approximately 10 minutes to a temperature of 37°C and adjust the pH using HCl (pH 6.8, pH 7.0, pH 7.4, pH 7.8, pH 8.0, pH 8.2, pH 9.0).

Make up to a final volume of 100ml using Milli-Q water.

Store the buffers at room temperature.

0.1M Sodium acetate buffer at various pH values

136g Sodium acetate trihydrate

Add 90ml Milli-Q water.

Warm the solution in a waterbath for approximately 10 minutes to a temperature of 37°C and adjust the pH using glacial acetic acid (CH₃CO₂H) (pH 5, pH 5.5, pH 6.0).

Make up to a final volume of 100ml using Milli-Q water.

Store the buffers at room temperature.

Casein stock solution (5mg/ml)

MW 613 400 - 796 000

Add 1ml of a Casein solution (50mg/ml) to 9ml Milli-Q water.

Store at 4°C.

The highest molecular weight of casein was used to calculate the molarity of casein used in the assay.

MBP stock solution (1mg/ml)

MW 18 400

Add 1ml Milli-Q water to 1mg MBP lyophilized powder.

Store in 50µl aliquots at -70°C.

Histone H1 stock solution (1mg/ml)

MW 21 500

Add 1ml Milli-Q water to 1mg H1 lyophilized powder.

Store in 50µl aliquots at -70°C.

Escherichia coli glycerol kinase (*EcGK*) working stock (1:100) (final: 5.32U/ml)

Add 1µl *EcGK* stock (532U/ml) to 100µl 0.1M Tris-HCl (pH7.4) buffer and keep on ice until use. The working stock must be made up fresh each time before use.

Reagent solution for 50 reactions (11.65ml)

Make up the reagent solution prior to performing the assay.

10.0mg NADH (1.22mM)

10.8mg PEP (2mM)

52.8mg MgSO₄ (28mM)

931mg Reduced Glutathione (26mM)

63.49µl LDH (15 units/ml (v/v))

40.78µl PyrK (7units/ml (v/v))

Make up to a final volume of 11.65ml using Milli-Q water and keep on ice.

7.1.11 Protein-protein interactions

Blocking solution

Add 5g BSA to 100ml TBS (pH 7.5).

Stir the mixture to a homogenous solution and store at 4°C until use.

50mM Tris-HCl buffer (pH 7.5)

Add 0.605g Tris to 90ml Milli-Q water.

Check the pH and adjust it to 7.5 using HCl.

Make up to a final volume of 100ml and store at room temperature.

7.2 Equipment and reagent suppliers list

A

ABI BigDye® v1.1 Terminator Cycle sequencing kit (*Applied Biosystems Inc., South Africa*)
ACD tubes (*Becton Dickinson Biosciences, USA*)
acetic acid (*SMM Instruments, South Africa*)
Acrylamide (*Merck, Germany*)
Adenosine tri-phosphate (ATP) (*Roche Diagnostics GmbH, Germany*)
Agarose D-1 LE (*Hispanager, Spain*)
Amido Black (*AppliChem, Germany*)
Amido black stain (*ApploChem, Germany*)
Ammonium persulphate (APS) (*Promega, USA*)
Ampicillin (*Roche Applied Science, Germany*)
Anti-GST horse radish peroxidase (HRP) – conjugated primary antibody (*Amersham Biosciences, UK*)
Anti-His horse radish peroxidase (HRP) – conjugated primary antibody (*Amersham Biosciences, UK*)
Axim X-ray manual developer and fixer (*CPAC, Africa*)

B

BacMagic™ DNA kit (*Novagen, USA*)
Bacto™ Tryptone (*Becton, Dickinson & Co., USA*)
BacVector® Insect Cell Medium (*Novagen, USA*)
Bandelin Sonoplus UW 2070 sonicator (*Bandelin Electronics, Germany*)
BD Falcon™ round bottom growth tubes (10ml) (*Becton Dickinson Biosciences, USA*)
Beckman Avanti® JE centrifuge (*Beckman Coulter, USA*)
Beckman model J2-21 centrifuge (*Beckman Coulter, USA*)
Beckman® J2-21 centrifuge (*Beckman Coulter, USA*)
Biolab bacteriological agar (*Merck, Germany*)
BioMate 5 Spectrophotometer (*Thermo electron Corp., Merck, South Africa*)
Bis-acrylamide (*Promega, South Africa*)
Bovine serum albumin (BSA) (*Roche Diagnostics, Germany*)
Bromophenol blue solution (*BDH Laboratory Supplies, UK*)
BSA-Standard (*Pierce, USA*)

C

Casein, bovine (*Sigma-Aldrich Inc., USA*)
Chloramphenicol (*Sigma-Aldrich Inc., USA*)
Chloroform (*Saarchem, South Africa*)
CO₂ (100%) (*African Oxygen Ltd., South Africa*)
Coomassie Blue R-250) (*BDH Laboratory Supplies, UK*)
Coomassie Plus – The Better Bradford™ Assay kit (*Pierce, USA*)

CP-G plus medical X-ray film (*Agfa, Germany*)
Cryo-tubes (*NuncTM, Denmark*)

D

Dimethyl sulphoxide – high grade (DMSO) (*BDH Laboratory Supplies, UK*)
DNase (*Fermentas Inc., Canada*)
D-sorbitol (*Sigma-Aldrich Corporation, USA*)

E

EDTA (*Merck, Germany*)
Eppendorf centrifuge 5415R (*Eppendorf, Germany*)
Eppendorf centrifuge 5702R (*Eppendorf, Germany*)
Eppendorf Mastercycler® Gradient machine (*Eppendorf, Germany*)
EPS 301 power supply (*Amersham pharmacia biotech, Sweden*)
Erlenmeyer culture flask (250ml) (*Corning, Biocom Biotech, South Africa*)
Ethanol (*Merck, South Africa*)
Ethidium bromide solution (0.5nM) (*Sigma-Aldrich Inc., USA*)
Expand High Fidelity^{PLUS} PCR system (*Fermentas, Europe*)

F

Falcon tube (*Thermo Scientific, South Africa*)
FastPlaxTM Antibody (*Novagen, USA*)
FastPlaxTM kit gelatin (*Novagen, USA*)
FastPlaxTM kit NBT (*Novagen, USA*)
FastPlaxTM kit TBST (*Novagen, USA*)
FastPlaxTM kit X-Gal (*Novagen, USA*)
FastPlaxTM Titer kit (*Novagen, USA*)
Fermentas Fast Digest® (*Fermentas, Europe*)
Finch TV version 1.4.0 (*Geospiza Inc.*)
Flat culture flask (50ml) (*NuncTM, Denmark*)
Formaldehyde (*Sigma-Aldrich Inc., USA*)

G

Gas mixture consisting of 5.5% CO₂, 2.75% O₂ and 91.25% N₂ (*African Oxygen Ltd., South Africa*)
Geldoc - SynGene GeneGenius gel documentation system (*Syngene, UK*)
Geldoc software - GeneSnap version 7.04 analysis software (*Syngene, UK*); SynGene
GeneTools version 4.0 analysis software (*Syngene, UK*)
Gene Runner Version 3.05 (*Hastings Software Inc, 1994*)
GenElute kit Column Preparation Solution (*Sigma-Aldrich Inc, USA*)
GenElute kit Lysis Solution (*Sigma-Aldrich Inc, USA*)
GenElute kit Neutralization/Binding Solution (*Sigma-Aldrich Inc, USA*)

GenElute kit resuspension Solution (*Sigma-Aldrich Inc, USA*)
GenElute kit Wash Solution (*Sigma-Aldrich Inc, USA*)
GenElute Miniprep kit Binding Column (*Sigma-Aldrich Inc, USA*)
GenElute Plasmid Miniprep Kit (*Sigma-Aldrich Inc, USA*)
GeneSnap version 6.05 image acquisition software (*Syngene, UK*)
Gentamycin sulphate (*Sigma-Aldrich Inc., USA*)
GIBCO™ RPMI medium (*Invitrogen, USA*)
Glucose (*Saarchem, South Africa*)
Glycerol (*Saarchem, South Africa*)
Glycerol kinase from *Escherichia coli* (*Sigma-Aldrich Inc, USA*)
Glycine (*Merck, Germany*)
GoTaq® Green Master Mix (*Promega, USA*)

H

HCl (*SMM Instruments, South Africa*)
Hellma quartz cuvette (10mm) (*Sigma-Aldrich, USA*)
HEPES (4-(2-hydroxyethyl)-piperazine-1-ethanesulphonic acid) (*Sigma-Aldrich Inc., USA*)
Histone 1 protein (H1) (*EMD Biosciences Inc., USA*)
Hoefer Mighty Small II SE250 gel cassette (*Hoefer Scientific Instruments, USA*)
Hoefer SE400 Sturdier Vertical Electrophoresis system (*Hoefer Scientific Instruments, USA*)
Horizontal mini-gel kit model # MGU-200T (*CBS Scientific, USA*)
Hybond™-C Extra Nitrocellulose membrane (*Amersham Biosciences, UK*)
Hypoxanthine (*Sigma-Aldrich Inc., USA*)

I

Imidazole (*Sigma-Aldrich Inc., USA*)
Incubator 20°C (*Hoefer Scientific Instruments, USA*)
In-Fusion™ Molar Ratio Calculator (*Clontech Bio-informatics, USA*)
Insect GeneJuice® Transfection Reagent (*Novagen, USA*)
Integrated DNA Technologies SciTools Oligo Analyzer 3.0 (www.idtdna.com)
Intelli-mixer RM 2M Skyline (*ELMI Ltd, Latvia*)
Isopropanol (*Merck, Germany*)

J

JA-14 Beckman centrifuge tube (250ml) (*Beckman Coulter, USA*)
JA-17 Beckman centrifuge tube (40ml) (*Beckman Coulter, USA*)

K

K₂HPO₄ (*Saarchem, South Africa*)
KCl (*Saarchem, South Africa*)

L

Labcon CPE 50 circulator (*Labcon, South Africa*)
Labotec® Orbital shaker (*Labotec, South Africa*)
L-lactate dehydrogenase (LDH) from rabbit muscle (*Roche Diagnostics GmbH, Germany*)

M

Magne-GST™ Protein purification system (*Promega, USA*)
MagneHis™ Kit (*Promega Corporation, USA*)
MagneHis™ kit Binding/Wash Buffer (*Promega Corporation, USA*)
MagneHis™ kit Elution Buffer (*Promega Corporation, USA*)
MagneHis™ kit Nickel-particles (*Promega Corporation, USA*)
Magnesium chloride (*Sigma-Aldrich Inc., USA*)
Magnetic particle separator (*Roche Applied Science, Germany*)
β-mercaptoethanol (*Merck, Germany*)
Methanol (*SMM Instruments, South Africa*)
Microscope (*Zeiss AxioStar, Germany*)
Mighty Slim™ SX250 power supply (*Hoefler Scientific Instruments, USA*)
Milipore Vacuum Pump Type PF 710-75 (*Millipore, South Africa*)
Milipore Vacuum Pump XF54 230 50 (*Millipore, South Africa*)
Millex GP 0.22µm syringe-driven filter unit (*Millipore, Ireland*)
Milli-Q water prepared with the Milli-Q™ Water System (*Millipore Corporation, USA*)
Mineral Oil (*Sigma-Aldrich Inc., USA*)
MSE Coolspin centrifuge (*Fisons Scientific, UK*)
MT19 Chiltern AutoVortex mixer (*CBS Scientific, USA*)
Myelin Basic Protein from bovine brain (*Sigma-Aldrich Inc., USA*)

N

Na₂HPO₄·2H₂O (*Saarchem, South Africa*)
NaC₂H₃O₂ (*Saarchem, South Africa*)
NaCl (*Saarchem, South Africa*)
NaHCO₃ (*Saarchem, South Africa*)
Nanodrop-ND 1000 spectrophotometer (*Nanodrop Technologies Inc, USA*)
NaOH (*Saarchem, South Africa*)
Nicotinamide adenine dinucleotide (NADH) disodium salt (*Roche Diagnostics GmbH, Germany*)
Nuclease free water (*Promega, USA*)

O

Overnight Express™ Auto-induction System (*Novagen Inc., USA*)

P

Page-Ruler™ Prestained protein ladder (*Fermentas Inc., Canada*)
PCR grade recombinant Proteinase K (*Roche Applied Science, Germany*)
Pefabloc (*Roche Diagnostics GmbH, Germany*)
Perfix high speed X-ray fixer (*Champion photochemistry, South Africa*)
Petri-dishes (35mm) (*Nunc™, Denmark*)
Petri-dishes (85mm) (*Costar, USA*)
Phase-contrast inverted microscope (*Olympus Optical Corporation Ltd., Japan*)
Phosphoenolpyruvate (*Roche Diagnostics GmbH, Germany*)
Ponceau S (*Sigma-Aldrich Inc., USA*)
Primers synthesized (*Inqaba Biotech, South Africa*)
Protease inhibitor cocktail set III (*Novagen Inc., USA*)
pTriEx-3 expression vector (*Novagen, USA*)
Pyruvate kinase (PyrK) from rabbit muscle (*Roche Diagnostics GmbH, Germany*)
Proteinase-K (*Sigma-Aldrich Corporation, USA*)

Q

QIAexpress® Detection and Assay kit with Anti-His HRP Conjugates (*Qiagen, USA*)
Qiaquick Ethanol-containing kit buffer PE (wash buffer) (*Qiagen, USA*)
Qiagen His ladder (*Qiagen, USA*)
Qiaquick kit buffer PBI (binding buffer) (*Qiagen, USA*)
Qiaquick PCR Purification Kit (*Qiagen, USA*)

R

Rapid DNA Ligation Kit (*Roche Applied Science, Germany*)
Rapindiff Staining Kit (*Global Diagnostics, South Africa*)
Reduced L-Glutathione (*Sigma-Aldrich Inc., USA*)
RNase A (*Fermentas, Europe*)
Rosetta 2 (DE3) cells (*Novagen, USA*)

S

Saponin (*USB Corporation, USA*)
Semi Micro UV cuvettes (1.5ml) (*Plastibrand®, Germany*)
Sf9 insect cells (*Novagen, USA*)
Shaking Incubator 150LT Model 355 (*Separations Scientific, South Africa*)
Sodium dodecyl sulphate (SDS) (*Merck, Germany*)
Spectra Molecular Weight Marker (*Fermentas, Europe*)
Sterivex™-GS 0.2µm Filter unit (*Millipore Corporation, USA*)
Subcloning Efficiency™ DH5™ chemically competent cells (*Invitrogen Ltd., USA*)
Sucrose (*Saarchem, South Africa*)
SuperSignal® kit luminol enhancer solution (*Pierce Biotechnology Inc, USA*)
SuperSignal® kit stable peroxide solution (*Pierce Biotechnology Inc, USA*)

SuperSignal® West Pico Chemiluminescent Substrate (*Pierce Biotechnology Inc, USA*)

T

TEMED (tetramethylethylenediamine) (*Promega, USA*)

Thermo-sensitive fast alkaline phosphatase (*Roche Applied Science, Germany*)

TriEx™-3 plasmid DNA (*Novagen, USA*)

TriEx™ Insect Cell Medium (*Novagen, USA*)

TriEx™ Sf9 insect cells (*Novagen, USA*)

Tris (*Roche Diagnostics, Germany*)

Tris-buffered phenol (*Sigma-Aldrich Inc, USA*)

Trypan Blue dye (*Sigma-Aldrich Inc, USA*)

Tween® 20 detergent (*CalBiochem, South Africa*)

W

Western transfer cassettes (*Hoefer Scientific Instruments, USA*)

Western transfer tank (*TE Series Transfer electrophoresis unit, Hoefer Scientific Instruments, USA*)

X

X-ray developer (*Axim, South Africa*)

Y

Yeast Extract (*Oxoid Ltd., UK*)

7.3 Sequence data

7.3.1 *Pf*B0150c DNA sequence (PlasmoDB version 8.1, 2011)

5'

ATGTTTTTCAGTCGAATTAGAAAATCGATCAGGTTATAAAAAAAGGAAAAAAAAAGAAA
TGGAATAATAAAAGTACTGGTCAGGATAAATTTACGAACAAAGATATTATATCAGAG
GAAAAAGAAGAAGGACTTGATATAGAATGTGGTCATAATATTCTGGGGGATGTACAA
TATGATGGTACATATAATATAAATGAACAAGTTAAGAAAAATTCATTGTTCTATTTTA
AATGTAAAGAGGAAATTAATTTAAAAGATGGAAATATAATATTGGATGATAAAAATA
GAAAAGTGGATGATATAAATATAACAGGGGATGATAAAAATATAAAAGTGGATGATA
AAAATATAAAAGTGGATGATAAAAATATAACAGGGGAGGATAAAAATATAACAGGG
GAGGATAAAAATATAACAGGGGATGATAAAAATATAATTTTTGATGTTGATGAAATA
TTAATCCATCAACATAATACATCAAATAGTAATATATATATAAATTGTAATGATAATA
ATAATGATATTAGGAACAGTTCAAATGTACAGCATTATTATAATGATAAAAATAAAG
AAAATATAAATAAACAAAATAAAAAGTATGTTTTAATAAATGATTATATAAATAATA
AATATATTTTATCAAAAAATAAGACATGTAAAATAAATAAAGGAAAAAAATTAATTA
AAAAAAGTAAATAATATTTCTAGGAGGAGGAATCATATATTATATAAATGTC
GTAATAAGTTATATAATGGAAATGTTTTTCTGACGATATTATTAAGTGAAGTGAA
TGTATGTAATTCGTAACTGTACTTCATAAGAATTATAATATTAATATGGATAATTATT
TAGATGATAATATACATACAAATAATAGCAATATTTATGATATTAATTATACAAATGA
AAATGTTATTAATTCAACATGTCGTTATTATCCCATAGGTAATAATAACACATTAAGT
AAAGATGAAGTTACAAAATCAAGTTCAAAAATTAATTCCTTTCTTATTTTGATGATA
TTATTAATGTAAATAAAAATGATATACCTATTTTACATGATAAAGAAAATATAAATAT
AATAAGTAACAAGGAAAGCTGTCATAAGGATGAAAAGGAGGAAGAGAAATATATCA
TGTATAATTCAAATTTAGTAGAAGAAAAAAACAAAAAAATGATTTGGAATTCTC
TTAATGTATTACCAATAGATATACTACTTAAAAATGGACATGATGAAATTAATAAAGA
GATATGCAAAAAAAAAAAAAAGTTTTTTTAGTCAGAATGATATAAAGTCTAAAAT
GTTATACAATAATAAAAGTTATTCAAAAAGTGAAAAAGTATTATATACAAATAATAA
AAACAGTAATACGTTTCATTCCTATATTTTCTTAAATAAGGTAGGAGACAAGTTTAA
AACTCTGAGAATATATATGATATGTATAATAATAAAAAAATGTCTATATACATGATA
AGAAGATATATACTAATATGTATTCTAATAAATTAACAGAAACATTATTATAGCAC
TTCTAATATAAATTTATTATATAATAATATAGGAAAGGTATTAGATAATGGTCTACAT
TTATCGAATAATATGTATTGTCGTTTAAATTCAAATCCACCATATAAGAGTATCTCGTT
AATTAATAACAATGTTTTTTTTTATAAAAAAGAGGAAAAGTAATAGTAATAATAAAT
AATAATAATAATATTAGTAGTAGTAGTAGTAGTAGTAAAAAAATCACGTGATC
ATTAATAAAAAAATATCATCTTATAATATTCATTATAAAGAAAGAAAGGATTCGTTTA
AAGAGAATTTTTTATTTTTCAAAGAGAAAATTTTACCATCAAAAAAGATACTTGTGT
TTTTAATGAAAGACAAAAAGATCTTTTTGAAAAAAGTAATGAACATATTAATGCGTT

TCTTCTTTTAATAATACATCAGATGATATTTCTTCACATTCAAGCGTAAATAAGAAAG
AACCTTTTTTTTGCTTTAAAAAATAATTCCATAAGGCACATACCAAAAGAAAATAATAT
AATATATACATCTGGGAAATCTTTTAATCATGTGCAGGATAAGGAAAAGACTGTTCTA
CTTAAAAAAAAGAAAGAAATAAATGATAAGAATACATTTAGCTCTTGTTTAATAAAC
CATAATATAACAACATATACATTACAAAATGGAGTAAATAAAAAATTTAAATATGTTA
GGAATAAGAGATTCTATTTATAAAATAGATGAAAAGAACAATATGTTGAAAGAATGT
TATAATGGAAATAATGATAGTAATAATAAGAAAAAAAAGAAGAAAAAAAATTATCT
TTTTCATGTGATATTATAAATGATAATTACACCTTATGAATCAGATAAGGAGAAAA
ACAATTCTAATAATATTAAGAGTATGGATATATTTAATTATGTAAAAAGAAAAAGCA
ACCTTTATAATAATTTATCTTCGAACAGGGATTCTACTGTAGATATGCATAATAATA
TAATAGTGAAGAATATATAAATATACAGAGAACAAATAAAATATATGAATTGAGTAA
TAAAAGAATTAGAAATTATAAATTGTATAGTATGGATGAAATATTTAAGGTGTCTCTT
AAGGAAAAAAAATATATAGATAAATTTCTAATAATATGGAAAGAGTAACATATAAA
AATGAAATGATAAATGAAAAGATAAGTAAGATGGACGATATATTATATCCTTGTGAC
AAAAATAAATCTTTAAACATGTCTTGTCTGTTATAATAGAAAATAATATATCAAGAG
AAGAAAATGAAAAAATTCAAGTGTTATATTAATAAAAAAAGAATGAGAATATGT
TTAATTGTGTTGGAAGGTTACATTGTCACATGGGCAAATGAATAATCAAGATAATAT
ATATGACCAAGGGAATATAAAAAAAAATGAAGAAGAAATAACCAAACATGATGAAT
ATATATCAAGGGAAGAAAAAATAAATATAATAGTAAATGTATTAGAAATTTTGATG
ACTATAAATATGAACAAGTGTTGAGTTACCATACGTTGGATGAAGACAAAAA
ATGATATGAACAATTTAATAGATATGAATAATGAGGCGATTATTGAAACGGTGAATG
GTGTTATTAATAATATTATATTGGATAGAAAAGATAATAACAGTAGGAAGGATATGG
AGAAAGAGATGGAGAAGGAGATGGAGAAGAAGATGGAGAAGGAGATGGAGAAGGT
GATGGAGAAGGAGATGGAGAAGGTGATGGAGAAGGAGGTGGAGAAAGAATTGAAAA
ATGAGATGAACAATAGGATGAACAATAGGATGAACAATGAGATGAAAAATGAAATA
AACATTTATAAAAACAATGAGATATATGTAGATAATGATAAAGAAGTAGAAATTGTA
AATGAGGAGAAGAACTTATTTACCCATTTAATTACGAATCTGATGTACATAAAAATA
TGAATATGTCAATTAATATAAATAATTGTAAAGATGATTATAATAATATATTAAGA
ATATGTAGATAATTCATGTCTTGCTCAAAAGGAAGAGAATATATTTTCGACCTTTATTC
AATTTAAATAAGAAAGATAAAGTATGGAAACGTTTTAATATAAAGAATAATATTAAG
ACAATAATACATAATGAAGAGATGAAAAGAATATATCAAATATTAATAAAAAATGTT
TTTCCTATTTATAATTTAATCGATATGAAAATTTTTTAATAAATCATTTAACATATAA
TTTTCCAAAAAATGATTTATTTAAATTATCATACAAAGTAAGTATGAATAATATAAGG
AATTTGTATATTGCTAATAAACATATAAATAAATAATTATGATTATATGAATAAATTAT
ATAATCAAATATATATACATTAATAATATCAGGTAGCTAATATAGATAATGATCATCA
TATATGTAAGAAAGGGGGAGGGTTGGATTATATAAATATGAATATATCAAAGAATG
TAAAAATAGGAAAGACAAAACATATTTAAATAAAATATTTTCATTATAAGAAGAAAA
GGATGCACGCTTTTTTATAAATGACGAAATTGGTTCTAATGATTATATGTATGATATA
AAAAAAAATATAGTAACGATGAAAATAATTATAAATTAAATGAAAAGATGAACATA

TCTATGTCAAATGATGAAGATATGATTCCCTACGTTAAATAGTGAACATGGAAATAATT
TTCCAAGTTGTCAACCGAATTTATTAGAAAAAAAAGTACTTATATAGATTTGAACTT
ATATGATAGTAATTCTATGGACGATTTTACAGAAGAAAAATATAATTTTGTTAATAAT
GAAAATGATTTATTCAATACTAAAAGATGGAAGTTTAATTTTCCAAGGGTAAAAATC
TGTTTAATAATAAATTTTTTAATGTATCTAATGAGGATGGTGTGTTTTCTTTTTTAAA
AATATGAATCTTTTTAGGGAACTTAATAAATCAAATAATAGCTTAAAAGTACTAGAGAGTG
TTAAAAATAGTAATAATAATTGTAGTAATAATAAGGGTGATGATAATATTGGAAATAT
GGAGAATATGAATACAACAAATGTTACAATTGCGAGTGATGAACATATATCTACAAA
GGGAGATATACACGACGAATCATTTTCTAGAGACGATAATGATTGTATCCTTTTTAAAA
ATTGAAGGTAGAAGTAAAAAATATAGTGATATAACCTTATATAATGAGGACAAAAGT
AATTTGGAGAATGACAATGAGACTATTAATGAATATGAAAATGTATGTAGTAACATA
GATGTTAATGAATGGGAAGATAAGGTAAATGGTACATGTAATAGTGTTGGTGATAAA
GAGACTGAAAAGAATAATGAAAAGAATAATGAAAAGAATAATGAAAAGAATAATGA
AAAGAATAATGAAAAGAATAATGAAAAGAATAATGAAAAGAATAATGAAAAGAATA
ATGAAGAAAATAATGAAGGAAATAATGAAGAAAATAATGAAGAAAATAATGAAGAA
AATAATGAAGAAAATAATGATATAGAAAAGAATGATATAAAGGATAATAATTCGGGA
CAAGTGAAAGAAAATATAATTGTTATGAATAATACAAACAATATGGATGTTGATAAT
GATGATAATAACAATAATTACAATAATGTTAGTACTGATGAAGGTATAGATATAATTA
AAAACATCAAAAGTGAGATGAATGATTATATTTATAATGATAATATTATGATTAAAGAT
AAATAATAAAAAGTATAGATCTTATGAATATAAAAAATCAAAAGAATGAACCTTTTTTA
AATTATACAAATGAAAAGGATATACATATGAAGAGCAATTCATCATATAATGTAAAT
GATAAAATGAATTTATTTAATAATAATGAGAAAACAGAAAAAATAATACTAGTTTA
AACGATTTATTATATAAAAAGAAAAGAAGATTAGATGATGAAAAAATATCTGAATAT
AAGGATACAAATTTAACAACAATACCTTTGAACATATAGCTAAAAGGATTAATTTA
ATTTTGAATGATACAATTGAATTTTTTCAAAAACATACATATCTTCATAATGGTTATGG
TAATGTTTCAGGTGTGCAAAAAGAACAAGAGGAAATTAGAAAAAAGAAGTTGAAAA
AATGGTCCTGTATTTATAAAATTAATAAAATTGTACGTAAAGGGGCCACGGGGTGGT
GTTTTCTGCGTGGAGAAGTGAGAATGTTGATTTTTTTAATCATTCGTTTTTTGAAAAC
TAAATTTGGAGAATAAAAAGAAGGGATATATCGATGAAACAAATGTTAATGAAAATT
ATGAGTCTGATAATGAATATGATAGTGATGAAGATGATACTGAAAGTGATAATGATG
ATGAGCAAAATAAAGAGAATGAAAGAGGTGATGAAAAGGATGGATATGAAGAAATG
AATGGGGGAGATAAGAATGAAGAAATGAATGGGGGAGATAAGAATGAAGAAATGAA
TGTGGGAGATAAAAATGGAGGAATAAATGAGGAACATAAAAATGAAGGAATAAATG
AGGAACATAAGGATGAACTAATAAATAAGGAACATAAAAACGAGCGAATAAATGAG
GAACATAAAAACGAACGAATAAATGAGGAACATAAAAATGAAGGAATAAATGAGGA
ACATAAAAATGAAGGAATAAATGAGGAACATAAAAACGAACGAATAAATGAGGAAC
ATAAAAATGAAGGAATAAATAAACTGACCTATCATAATATGAATAAAAATAATTTT
CAAATGAAAATAATTATAATGATGACGATTCTTATGATGAAGATAATTTGGTATCCCT
GAAGATAATAAACTTAAAATATTTAAGTAAAAAGAATAGTTTAAAAACATTTTGAG

AGAAGTAAATTTTTTAAAAATGTGTGAACATCCAAATGTAGTAAAATATTTTGAATCT
TTTTTTTGGCCTCCTTGTTATTTAGTTATTGTGTGTGAATATTTATCAGGAGGAACATT
ATATGATTTATATAAAAAATTATGGTAGAATATCAGAAGATCTTTTAGTATATATCTTA
GATGATGTATTAAATGGTTTAAATTATTTACATAATGAATGTAGTTCACCACTTATAC
ATAGAGATATAAAACCAACAAATATCGTTCCTTCCAAAGATGGTATAGCTAAGATAAT
TGATTTTGGTTCTTGTTGAAGAATTGAAAAATAGTGATCAGTCTAAAGAATTAGTGGGT
ACTATATATTATATATCACCTGAAATATTGATGAGAACTAATTATGATTGTTTCATCTGA
TATATGGTCATTGGGTATTACAATATATGAAATTGTTTTATGTACCTTACCATGGAAA
AGAAATCAATCATTTGAAAATTATATAAAAAACCATAATTAATTCATCACCAAAAATTA
ACATAACAGAAGGATATAGTAAACACTTATGTTATTTTGTGAGAAGTGTTTACAAAA
GAAACCTGAGAACAGAGGAAATGTGAAAGATTTATTAATCATAAAATTTTGATAAA
AAGAGGTATATTA AAAAGAAACCTAGTTCATATATATGAAATAAGAGATATATTA AAA
ATATATAATGGTAAAGGTAAACAAATATCTTCCGAAATTTTTTTAAGAACCTTTTTTT
CTTCAATGATAAGAATAAAAAAAAAAAAAACCAAATAAAATGATCAGTTCCAAATCCTG
TGATGCAGAAATGTTCTTTGAACAGTTAAAAAGGGAAAATTTTGATTTTTTTTGAAATT
AAATTA AAAAGATGATGAAAATAGTAGATCCTTGAATACGTTTAATATAAATATATCTA
AAGAAAGAGACGACATATCATATTCTTCTTTAAATTTGGAAAAAATCAAAGAACACA
GTCTCAATATGGTAGCATCTGTTGTCTGGGACTGAACAATCCCAGAAATGA 3'

***PfB0150c* DNA sequence length: 7 458 bp**
The red segment denotes the kinase domain (822bp).
The gene consists of a single exon.

DSYDEDNLVSLKIINLKYLSSKNSLKNILREVNFLKMCEHPNVVKYFESFFWPPCYLVIVC
EYLSGGTLYDLYKNYGRISEDLLVYILDDVLNGLNYLHNECSSPLIHRDIKPTNIVLSKDIGI
AKIIDFGSCEELKNSDQSKELVGTIYYISPEILMRTNYDCSSDIWSLGITIYEIVLCTLPWKR
NQS FENYIKTIINSSPKINITEGYSKHLCYFVEKCLQKKPENRGNVKDLLNHKFLIKKRYIK
KKPSSIYEIRDILKIYNGKGKTNIFRNFFKNLFFNDKNKKKKPNKMISSKSCDAEMFFEQL
KRENFDFFEIKLKDDENSRLNTFNINISKERDDISYSSLNLEKIKEHSLNMVASVVGTEQS
QK C-terminal end

*Pf*B0150c protein sequence length: 2 485 aa
*Pf*PK8 kinase domain (red): 274 aa

7.3.3 Recombinant GST-*Pf*PK8 protein sequence (PlasmoDB version 8.1, 2011)

N-terminal end

MSPILGYWKIKGLVQPTRLLLEYLEEKYEEHLYERDEGDKWRNKKFELGLEFPNLPYYID
GDVKLTQSMAIRYIADKHNMLGGCPKERAISMLEGAVLDIRYGVSR IAYS KDFETLKV
DFLSKLPLKMFEDRLCHKTYLNGDHVTHPDFMLYDALDVVLYMDPMCLDAFPKLVCFK
KRIEAI PQIDKYLKSSKYIAWPLQGWQATFGGGDHPPKSDEKDG YEEMNGGD KNEEMNG
GDKNEEMNVGDKNGGIEHKNEGINEEEHKDELINKEHKNERINEEHKNERINEEHKNEGIN
EEHKNEGINEEEHKNE RINEEHKNEGIN KLT YHNMNKNNISNENNYNDDDSYDEDNLVSL
KIINLK YLSKKNSLKNILREVNFKMCEHPNVVKYFESFFWPPCYLVIVCEYLSGGTLYDLY
KNYGRISEDLLVYILDDVLNGLNYLHNECSSPLIHRDIKPTNIVLSKDGI AKIIDFGSCEELK
NSDQSKELVGTIYYISPEILMRTNYDSSDIWSLGITIYEIVLCTLPWKRNQSFENYIKTIINSS
PKINTEGYSKHLCYFVEKCLQKKPENRGNVKDLLNHKFLIK KRYIKKKPSSIYEIRDILKIY
NGKGKTNIFRNFFKNLFFFNDKNKKKPNKMISSKSCDAEMFFEQLKRENFDFFEIKLKDDE
NSRSLNTFNINISKERDDISYSSLNLEKIKEHSLNMVASVVGTEQQK C-terminal end

GST-tag protein sequence length (blue): 218 aa

rGST-*Pf*PK8 protein sequence length: 715 aa

*Pf*PK8 kinase domain (red): 274 aa

7.3.4 pGEX-4T-2-PfB0150c DNA sequence

5'

ACGTTATCGACTGCACGGTGCACCAATGCTTCTGGCGTCAGGCAGCCATCGGAAGCTG
TGGTATGGCTGTGCAGGTCGTAAATCACTGCATAATTCGTGTCGCTCAAGGCGCACTC
CCGTTCTGGATAATGTTTTTTGCGCCGACATCATAACGGTTCTGGCAAATATTCTGAA
ATGAGCTGTTGACAATTAATCATCGGCTCGTATAATGTGTGGAATTGTGAGCGGATAA
CAATTTACACAGGAAACAGTATTCATGTCCCCTATACTAGGTTATTGGAAAATTAAG
GGCCTTGTGCAACCCACTCGACTTCTTTTGAATATCTTGAAGAAAAATATGAAGAGC
ATTTGTATGAGCGCGATGAAGGTGATAAATGGCGAAACAAAAAGTTTGAATTGGGTT
TGGAGTTTCCCAATCTTCCTTATTATATTGATGGTGATGTTAAATTAACACAGTCTATG
GCCATCATACGTTATATAGCTGACAAGCACAACATGTTGGGTGGTTGTCCAAAAGAGC
GTGCAGAGATTTCAATGCTTGAAGGAGCGGTTTTGGATATTAGATACGGTGTTCGAG
AATTGCATATAGTAAAGACTTTGAACTCTCAAAGTTGATTTTCTTAGCAAGCTACCT
GAAATGCTGAAAATGTTTGAAGATCGTTTTATGTCATAAAACATATTTAAATGGTGATC
ATGTAACCCATCCTGACTTCATGTTGTATGACGCTCTTGATGTTGTTTTATACATGGAC
CCAATGTGCCTGGATGCGTTCCCAAAATTAGTTTGTTTTAAAAAACGTATTGAAGCTA
TCCCACAAATTGATAAGTACTTGAAATCCAGCAAGTATATAGCATGGCCTTTGCAGGG
CTGGCAAGCCACGTTTGGTGGTGGCGGATCCTGATGAAAAGGATGGATATGAAGAAA
TGAATGGGGGAGATAAGAATGAAGAAATGAATGGGGGAGATAAGAATGAAGAAATG
AATGTGGGAGATAAAAAATGGAGGAATAAATGAGGAACATAAAAAATGAGGAATAAAT
GAGGAACATAGGATGAACTAATAAATAAGGAACATAAAAAACGAGCGAATAAATGAG
GAACATAAAAAACGAACGAATAAATGAGGAACATAAAAAATGAAGGAATAAATGAGGA
ACATAAAATGAAGGAATAAATGAGAACATAAAAAACGAACGAATAAATGAGGAACAT
AAAAATGAAGGAATAAATAAACTGACCTATCATAATATGAATAAAAAATAATTTCA
AATGAAAATAATTATAAGATGACGATTCTTATGATGAAGATAAATTTGGTATCCCTGAA
GATAATAAACTTAAAAATTTTAAGTAAAAAGAATAGTTTAAAAAACATTTTGAGAGA
AGTAAATTTTTTAAAAATGTGTGAACATCAAATGTAGTAAATATTTTGAATCTTTTTT
TTGGCCTCCTTGTTATTTAGTTATTGTGTGTGAATATTTATCAGGAGGAACATTATATG
ATTTATATAAAAAATTATGGTAGAATATCAGAAGATCTTTAGTATATATCTTAGATGAT
GTATTAAATGGTTTAAATTATTTACATAATGAATGTAGTTCACCACTTATACATAGAG
ATATAAAACCAACAAATATCGTTCCTTCCAAAGATGGTATAGCTAAGATATTGATTTT
GGTTCCTGTGAAGAATTGAAAAATAGTGATCAGTCTAAAGAATTAGTGGGTACTATAT
ATTATATATCACCTGAAATATTGATGAGAACTAATTATGATTGTTCATCTGATATATG
GTATTGGGTATTACAATATATGAAATTGTTTTATGTACCTTACCATGGAAAAGAAATC
AATCATTTGAAAATTATATAAAAAACCATAATTAATTCATCACCAAAAATTAACATAAC
AGAAGGATATAGTAACACTTATGTTATTTTGTGAGAAGTGTTTACAAAAGAAACCTG
AGAACAGAGGAAATGTGAAAGATTTATTAAATCATAAATTTTTGATTAAAAGAGGT

ATATTAAAAAGAAACCTAGTTCTATTATGAAATAAGAGATATATTAAAAATATATAAT
GGTAAAGGTAAAACAAATATCTTCCGAAATTTTTTTAAGAACCTTTTTTCTTCAATGA
TAAAATAAAAAAAAAAAAAACCAAATAAAATGATCATTCCAAATCCTGTGATGCAGAAA
TGTTCTTTGAACAGTTAAAAAGGGAAAATTTTGATTTTTTTGAAATTAAATTAAGA
TGATGAAAATAGTAGATCCTTGAATACGTTTAATATAAATATATCTAAGAAAGAGAC
GACATATCATATTCTTCTTAAATTTGGAAAAAATCAAAGAACAGTCTCAATATGGTAG
CATCTGTTGTCTGGGGACTGAACAATCCCAGAACTCGAGACTGAACAATCCCAGAAA
TGACTCGAGCGGCCGCATCGTGACTGACTGACGATCTGCCTCGCGCGTTTCGGTGATG
ACGGTGAAAACCTCTGACACATGCAGCTCCCGGAGACGGTCACAGCTTGTCTGTAAG
CGGATGCCGGGAGCAGACAAGCCCGTCAGGGCGCGTCAGCGGGTGTGGCGGGTGTCT
GGGGCGCAGCCATGACCCAGTCACGTAGCGATAGCGGAGTGTATAATTCTTGAAGAC
GAAAGGGCCTCGTGATACGCCTATTTTTATAGGTTAATGTCATGATAATAATGGTTTC
TTAGACGTCAGGTGGCACTTTTCGGGGAAATGTGCGCGGAACCCCTATTTGTTTATTTT
TCTAAATACATTCAAATATGTATCCGCTCATGAGACAATAACCCTGATAAATGCTTCA
ATAATATTGAAAAAGGAAGAGTATGAGTATTCAACATTTCCGTGTCGCCCTTATTTCC
TTTTTTGCGGCATTTTGCCTTCCTGTTTTTGCTCACCCAGAAACGCTGGTGAAAGTAAA
AGATGCTGAAGATCAGTTGGGTGCACGAGTGGGTTACATCGAACTGGATCTCAACAG
CGGTAAGATCCTTGAGAGTTTTTCGCCCCGAAGAACGTTTTCCAATGATGAGCACTTTT
AAAGTTCTGCTATGTGGCGCGGTATTATCCCGTGTTGACGCCGGGCAAGAGCAACTCG
GTCGCCGCATACACTATTCTCAGAATGACTTGGTGAGTACTACCAGTCACAGAAAA
GCATCTTACGGATGGCATGACAGTAAGAGAATTATGCAGTGCTGCCATAACCATGAG
TGATAACACTGCGGCCAACTTACTTCTGACAACGATCGGAGGACCGAAGGAGCTAAC
CGCTTTTTTGCACAACATGGGGGATCATGTAACTCGCCTTGATCGTTGGGAACCGGAG
CTGAATGAAGCCATACCAAACGACGAGCGTGACACCACGATGCCTGCAGCAATGGCA
ACAACGTTGCGCAAACTATTAACCTGGCGAACTACTTACTCTAGCTTCCCGGCAACAAT
TAATAGACTGGATGGAGGCGGATAAAGTTGCAGGACCACTTCTGCGCTCGGCCCTTCC
GGCTGGCTGGTTTATTGCTGATAAATCTGGAGCCGGTGAGCGTGGGTCTCGCGGTATC
ATTGCAGCACTGGGGCCAGATGGTAAGCCCTCCCGTATCGTAGTTATCTACACGACGG
GGAGTCAGGCAACTATGGATGAACGAAATAGACAGATCGCTGAGATAGGTGCCTCAC
TGATTAAGCATTGGTAACTGTCAGACCAAGTTTACTCATATATACTTTAGATTGATTTA
AAACTTCATTTTTTAATTTAAAAGGATCTAGGTGAAGATCCTTTTTTGATAATCTCATGAC
CAAAATCCCTTAACGTGAGTTTTTCGTTCCACTGAGCGTCAGACCCCGTAGAAAAGATC
AAAGGATCTTCTTGAGATCCTTTTTTTCTGCGCGTAATCTGCTGCTTGCAAACAAAAA
AACCACCGCTACCAGCGGTGGTTTGTGTTGCCGGATCAAGAGCTACCAACTCTTTTTCC
GAAGGTAACCTGGCTTCAGCAGAGCGCAGATACCAAATACTGTCCTTCTAGTGTAGCCG
TAGTTAGGCCACCACTTCAAGAACTCTGTAGCACCGCCTACATACCTCGCTCTGCTAA
TCCTGTTACCAGTGGCTGCTGCCAGTGGCGATAAGTCGTGTCTTACCGGGTTGGACTC
AAGACGATAGTTACCGGATAAGGCGCAGCGGTGGGGCTGAACGGGGGGTTTCGTGCAC
ACAGCCCAGCTTGGAGCGAACGACCTACACCGAACTGAGATACCTACAGCGTGAGCT

ATGAGAAAGCGCCACGCTTCCCGAAGGGAGAAAGGCGGACAGGTATCCGGTAAGCG
GCAGGGTCGGAACAGGAGAGCGCACGAGGGAGCTTCCAGGGGGAAACGCCTGGTAT
CTTTATAGTCCTGTCTGGGTTTCGCCACCTCTGACTTGAGCGTCGATTTTTGTGATGCTC
GTCAGGGGGGCGGAGCCTATGGAAAAACGCCAGCAACGCGGCCTTTTTACGGTTCCT
GGCCTTTTGCTGGCCTTTTGCTCACATGTTCTTTCCTGCGTTATCCCCTGATTCTGTGGA
TAACCGTATTACCGCCTTTGAGTGAGCTGATACCGCTCGCCGCAGCCGAACGACCGAG
CGCAGCGAGTCAGTGAGCGAGGAAGCGGAAGAGCGCCTGATGCGGTATTTTCTCCTT
ACGCATCTGTGCGGTATTTACACCCGCATAAATTCGGACACCATCGAATGGTGCAAAA
CCTTTCGCGGTATGGCATGATAGCGCCCGGAAGAGAGTCAATTCAGGGTGGTGAATG
TGAAACCAGTAACGTTATACGATGTCGCAGAGTATGCCGGTGTCTCTTATCAGACCGT
TTCCCGCGTGGTGAACCAGGCCAGCCACGTTTCTGCGAAAACGCGGGAAAAAGTGGA
AGCGGCGATGGCGGAGCTGAATTACATTCCCAACCGCGTGGCACAACAACCTGGCGGG
CAAACAGTCGTTGCTGATTGGCGTTGCCACCTCCAGTCTGGCCCTGCACGCGCCGTCG
CAAATTGTCGCGGCGATTAAATCTCGCGCCGATCAACTGGGTGCCAGCGTGGTGGTGT
CGATGGTAGAACGAAGCGGCGTCGAAGCCTGTAAAGCGGCGGTGCACAATCTTCTCG
CGCAACGCGTCAGTGGGCTGATCATTAACTATCCGCTGGATGACCAGGATGCCATTGC
TGTGGAAGCTGCCTGCACTAATGTTCCGGCGTTATTTCTTGATGTCTCTGACCAGACAC
CCATCAACAGTATTATTTTCTCCCATGAAGACGGTACGCGACTGGGCGTGGAGCATCT
GGTCGCATTGGGTCAACAGCAAATCGCGCTGTTAGCGGGCCCATTAAGTTCTGTCTCG
GCGCGTCTGCGTCTGGCTGGCTGGCATAAATATCTCACTCGCAATCAAATTCAGCCGA
TAGCGGAACGGGAAGGCGACTGGAGTGCCATGTCCGGTTTTCAACAAACCATGCAAA
TGCTGAATGAGGGCATCGTTCCCACTGCGATGCTGGTTGCCAACGATCAGATGGCGCT
GGGCGCAATGCGCGCCATTACCGAGTCCGGGCTGCGCGTTGGTGCGGATATCTCGGTA
GTGGGATACGACGATACCGAAGACAGCTCATGTTATATCCCGCCGTTAACCACCATCA
AACAGGATTTTCGCCTGCTGGGGCAAACCAGCGTGGACCGCTTGCTGCAACTCTCTCA
GGGCCAGGCGGTGAAGGGCAATCAGCTGTTGCCCCTCTCACTGGTGAAAAGAAAAAC
CACCTGGCGCCCAATACGCAAACCGCCTCTCCCCGCGCGTTGGCCGATTCATTAATG
CAGCTGGCACGACAGGTTTCCCGACTGGAAAGCGGGCAGTGAGCGCAACGCAATTAA
TGTGAGTTAGCTCACTCATTAGGCACCCCAGGCTTTACACTTTATGCTTCCGGCTCGTA
TGTTGTGTGGAATTGTGAGCGGATAACAATTTACACAGGAAACAGCTATGACCATG
ATTACGGATTCAGTGGCCGTCGTTTTACAACGTCGTGACTGGGAAAACCTGGCGTTA
CCCAACTTAATCGCCTTGACAGCACATCCCCCTTTCGCCAGCTGGCGTAATAGCGAAGA
GGCCCGCACCGATCGCCCTTCCCAACAGTTGCGCAGCCTGAATGGCGAATGGCGCTTT
GCCTGGTTTTCCGGCACCCAGAAGCGGTGCCGGAAGCTGGCTGGAGTGCGATCTTCCTG
AGGCCGATACTGTCGTCGTCCCCTCAAACCTGGCAGATGCACGGTTACGATGCGCCCAT
CTACACCAACGTAACCTATCCCATTACGGTCAATCCGCCGTTTGTTCACCGGAGAAT
CCGACGGGTTGTTACTCGCTCACATTTAATGTTGATGAAAGCTGGCTACAGGAAGGCC
AGACGCGAATTATTTTTGATGGCGTTGGAATT

3'

pGEX-4T-2-*Pf*B0150c DNA sequence length: 6 466bp

The cloned functional region of *Pf*PK8 is the underlined segment with the centrally located kinase domain (822bp) denoted by the red bases.

The pGEX-4T-2 vector sequence is indicated by the green bases.

The GST-tag (560bp) is indicated by the blue bases.

7.3.5 *Pf*B0150c-pTriEx-3 DNA sequence

5'

TCCTGCATCTTTTAATCAAATCCCAAGATGTGTATAAACGCGCCGGTATGTACAGGAA
GAGGTTTATACTAAACTGTTACATTGCAAACGTGGTTTCGTGTGCCAAGTGTGAAAAC
CGATGTTTAATCAAGGCTCTGACGCATTTCTACAACCACGACTCCAAGTGTGTGGGTG
AAGTCATGCATCTTTTAATCAAATCCCAAGATGTGTATAAACCAACCAAACTGCCAAAA
AATGAAAACGTGCGACAAGCTCTGTCCGTTTGCTGGCAACTGCAAGGGTCTCAATCCT
ATTTGTAATTATTGAATAATAAAACAATTATAAATGTCAAATTTGTTTTTTATTAACGA
TACAAACCAAACGCAACAAGAACATTTGTAGTATTATCTATAATTGAAAACGCGTAGT
TATAATCGCTGAGGTAATATTTAAAATCATTTTCAAATGATTCACAGTTAATTTGCGA
CAATATAATTTTATTTTCACATAAACTAGACGCCTTGTCGTCTTCTTCTTCGTATTCCTT
CTCTTTTTCATTTTTCTCTTCATAAAAATTAACATAGTTATTATCGTATCCATATATGTA
TCTATCGTATAGAGTAAATTTTTTGTTGTCATAAATATATATGTCTTTTTTAATGGGGT
GTATAGTACCGCTGCGCATAGTTTTTCTGTAATTTACAACAGTGCTATTTTCTGGTAGT
TCTTCGGAGTGTGTTGCTTTAATTATTAAATTTATATAATCAATGAATTTGGGATCGTC
GGTTTTGTACAATATGTTGCCGGCATAGTACGCAGCTTCTTCTAGTTCAATTACACCAT
TTTTTAGCAGCACCGGATTAACATAACTTTCCAAAATGTTGTACGAACCGTTAAACAA
AAACAGTTCACCTCCCTTTTCTATACTATTGTCTGCGAGCAGTTGTTTGTGTTAAAAA
TAACAGCCATTGTAATGAGACGCACAACTAATATCACAACTGGAAATGTCTATCA
ATATATAGTTGCTGATGGCCGGCCTATTAATAGTAATCAATTACGGGGTCAATTAGTTC
ATAGCCCATATATGGAGTTCCGCGTTACATAACTTACGGTAAATGGCCCGCCTGGCTG
ACCGCCCAACGACCCCGCCCATTGACGTCAATAATGACGTATGTTCCCATAGTAACG
CCAATAGGGACTTTCCATTGACGTCAATGGGTGGAGTATTTACGGTAAACTGCCCACT
TGGCAGTACATCAAGTGTATCATATGCCAAGTCCGCCCCCTATTGACGTCAATGACGG
TAAATGGCCCGCCTGGCATTATGCCCAGTACATGACCTTACGGGACTTTCCTACTTGG
CAGTACATCTACGTATTAGTCATCGCTATTACCATGCTGATGCGGTTTTGGCAGTACA
CCAATGGGCGTGGATAGCGGTTTGACTCACGGGGATTTCOAAGTCTCCACCCCATGA
CGTCAATGGGAGTTTGTTTTGGCACCAAAATCAACGGGACTTTCOAATGTGTAAT
AACCCCGCCCCGTTGACGCAAATGGGCGGTAGGCGTGTACGGTGGGAGGTCTATATA
AGCAGACGTCGTTTAGTGAACCGTCAGATCACTAGATGCTTTATTGCGGTAGTTTATC
ACAGTTAAATTGCTAACGCCAGTCTCGAACTTAACGTGCAGAAGTTGGTCGTGAGGCA
CTGGGCAGGTAAGTATCGGGCCCTTTGTGCGGGGGGAGCGGCTCGGGGCTGTCCGCG
GGGGGACGGCTGCCTTCGGGGGGGACGGGGCAGGGCGGGGTTTCGGCTTCTGGCGTGT
GACCGGCGGCTCTAGAGCCTCTGCTAACCATGTTTCATGCCTTCTTCTTTTCTACAGC
TCCTGGGCAACGTGCTGGTTATTGTGCTGTCTCATCATTTTGGCAAAGAATTGGATCG
GACCGAAATTAATACGACTCACTATAGGGGAATTGTGAGCGGATAACAATTCCCCGG
AGTTAATCCGGGACCTTTAATTCAACCCAACACAATATATTATAGTTAAATAAGAATT

ATTATCAAATCATTGTATATTAATTAATAAATACTATACTGTAAATTACATTTTATTTAC
 AATCAAAGGAGATCCTGATGAAAAGGATGGATATGAAGAAATGAATGGGGGAGATA
 AGAATGAAGAAATGAATGGGGGAGATAAGAATGAAGAAATGAATGTGGGAGATAAA
 AATGGAGGAATAAATGAGGAACATAAAAAATGAGGAATAAATGAGGAACATAGGATG
 AACTAATAAATAAGGAACATAAAAAACGAGCGAATAAATGAGGAACATAAAAAACGAA
 CGAATAAATGAGGAACATAAAAAATGAAGGAATAAATGAGGAACATAAAAAATGAAGGA
 ATAAATGAGAACATAAAAAACGAACGAATAAATGAGGAACATAAAAAATGAAGGAATA
AATAAACTGACCTATCATAATATGAATAAAAAATAATTTTCAAATGAAAATAATTATA
AGATGACGATTCTTATGATGAAGATAATTTGGTATCCCTGAAGATAATAAACTTAAAA
TATTTAAGTAAAAAGAATAGTTTAAAAAACATTTTGAGAGAAGTAAATTTTTTAAAAA
TGTGTGAACATCAAATGTAGTAAAATATTTTGAATCTTTTTTTTTGGCCTCCTTGTTATT
TAGTTATTGTGTGTGAATATTTATCAGGAGGAACATTATATGATTTATATAAAAAATTA
TGGTAGAATATCAGAAGATCTTTAGTATATATCTTAGATGATGTATTAAATGGTTTAA
ATTATTTACATAATGAATGTAGTTCACCACTTATACATAGAGATATAAAACCAACAAA
TATCGTTCTTTCCAAAGATGGTATAGCTAAGATATTGATTTTGGTCTTGTTGAAGAATT
GAAAAATAGTGATCAGTCTAAAGAATTAGTGGGTACTATATATTATATATCACCTGAA
ATATTGATGAGAATAATTATGATTGTTTCATCTGATATATGGTATTGGGTATTACAAT
ATATGAAATTGTTTTATGTACCTTACCATGGAAAAGAAATCAATCATTGAAAAATTAT
ATAAAAACCATAATTAATTCATCACCAAAAATTAACATAACAGAAGGATATAGTAAC
ACTTATGTTATTTTTGTTGAGAAGTGTTTACAAAAGAAACCTGAGAACAGAGGAAATGT
GAAAGATTTATTAATCATAAATTTTTGATTAAAAGAGGTATATTAAAAAGAAACCT
 AGTTCTATTATGAAATAAGAGATATATTAAAAATATATAATGGTAAAGGTAAACAA
 ATATCTTCCGAAATTTTTTTAAGAACCTTTTTTTCTTCAATGATAAAATAAAAAAAAAA
 AACCAAAATAAAATGATCATTCCAAATCCTGTGATGCAGAAATGTTCTTTGAACAGTTA
 AAAAGGGAAAATTTTGATTTTTTTTGAATTAAATTAAGATGATGAAAATAGTAGAT
 CCTTGAATACGTTTAATATAAATATATCTAAGAAAGAGACGACATATCATATTCTTCT
 TAAATTTGGAAAAAATCAAAGAACAGTCTCAATATGGTAGCATCTGTTGTCGGGGACT
 GAACAATCCCAGAAACTCGAGCACCACCATCACCATCACCATCACTAAGTGATTAAAC
CTCAGGTGCAGGCTGCCTATCAGAAGGTGGTGGCTGGTGTGGCCAATGCCCTGGCTCA
CAAATACCACTGAGATCGATCTTTTTCCCTCTGCCAAAAATTATGGGGACATCATGAA
GCCCCCTTGAGCATCTGACTTCTGGCTAATAAAGGAAATTTATTTTCATTGCAATAGTGT
GTTGGAATTTTTTGTGTCTCTCACTCGGAAGGACATATGGGAGGGCAAATCATTTAAA
ACATCAGAATGAGTATTTGGTTTAGAGTTTGGCAACATATGCCCATATGTAAC TAGCA
TAACCCCTTGGGGCCTCTAAACGGGTCTTGAGGGGTTTTTTGCTGAAAGCATGCGGAG
GAAATTCTCCTTGAAGTTTCCCTGGTGTCAAAGTAAAGGAGTTTGCACCAGACGCAC
CTCTGTTCACTGGTCCGGCGTATTAAACACGATACATTGTTATTAGTACATTTATTAA
GCGCTAGATTCTGTGCGTTGTTGATTTACAGACAATTGTTGTACGTATTTTAATAATTC
ATTAAATTTATAATCTTTAGGGTGGTATGTTAGAGCGAAAATCAAATGATTTTCAGCG
TCTTTATATCTGAATTTAAATATTAAATCCTCAATAGATTTGTAAAATAGGTTTCGATT

AGTTTCAAACAAGGGTTGTTTTTCCGAACCGATGGCTGGACTATCTAATGGATTTTCG
CTCAACGCCACAAAACCTTGCCAAATCTTGTAGCAGCAATCTAGCTTTGTTCGATATTCG
TTTGTGTTTTGTTTTGTAATAAAGGTTTCGACGTCGTTCAAAATATTATGCGCTTTTGTA
TTTCTTTCATCACTGTCGTTAGTGTACAATTGACTCGACGTAAACACGTTAAATAGAG
CTTGACATATTTAACATCGGGCGTGTTAGCTTTATTAGGCCGATTATCGTCGTCGTCC
CAACCCTCGTCGTTAGAAGTTGCTTCCGAAGACGATTTTGCCATAGCCACACGACGCC
TATTAATTGTGTCGGCTAACACGTCCGCGATCAAATTTGTAGTTGAGCTTTTTGGAATT
GCGATCGCATAACTTCGTATAGCATACATTATACGAAGTTATAAGCTCGGAACGCTGC
GCTCGGTGCTTCGGCTGCGGCGAGCGGTATCAGCTCACTCAAAGGCGGTAATACGGTT
ATCCACAGAATCAGGGGATAACGCAGGAAAGAACATGTGAGCAAAAGGCCAGCAAA
AGGCCAGGAACCGTAAAAAGGCCGCGTTGCTGGCGTTTTTCCATAGGCTCCGCCCCCT
GACGAGCATCACAAAATCGACGCTCAAGTCAGAGGTGGCGAAACCCGACAGGACTA
TAAAGATACCAGGCGTTTCCCCCTGGAAGCTCCCTCGTGCGCTCTCCTGTTCCGACCCCT
GCCGCTTACCGGATACCTGTCCGCCTTTCTCCCTTCGGGAAGCGTGGCGCTTTCTCAAT
GCTCACGCTGTAGGTATCTCAGTTCGGTGTAGGTCGTTTCGCTCCAAGCTGGGCTGTGT
GCACGAACCCCCCGTTTCAGCCCGACCGCTGCGCCTTATCCGGTAACTATCGTCTTGAG
TCCAACCCGGTAAGACACGACTTATCGCCACTGGCAGCAGCCACTGGTAACAGGATT
AGCAGAGCGAGGTATGTAGGCGGTGCTACAGAGTTCTTGAAGTGGTGGCCTAACTAC
GGCTACACTAGAAGAACAGTATTTGGTATCTGCGCTCTGCTGAAGCCAGTTACCTTCG
GAAAAAGAGTTGGTAGCTCTTGATCCGGCAAACAAACCACCGCTGGTAGCGGTGGTT
TTTTTGTTTGCAAGCAGCAGATTACGCGCAGAAAAAAGGATCTCAAGAAGATCCTTT
GTTACCAATGCTTAATCAGTGAGGCACCTATCTCAGCGATCTGTCTATTTTCGTTTCATCC
ATAGTTGCCTGACTCCCCGTCGTGTAGATAACTACGATACGGGAGGGCTTACCATCTG
GCCCCAGTGCTGCAATGATACCGCGAGACCCACGCTCACC GGCTCCAGATTTATCAGC
AATAAACCAGCCAGCCGGAAGGGCCGAGCGCAGAAGTGGTCCTGCAACTTTATCCGC
CTCCATCCAGTCTATTAATTGTTGCCGGAAGCTAGAGTAAGTAGTTCGCCAGTTAAT
AGTTTGCGCAACGTTGTTGCCATTGCTACAGGCATCGTGGTGTCACGCTCGTCGTTTG
GTATGGCTTCATTCAGCTCCGGTTCCCAACGATCAAGGCGAGTTACATGATCCCCCAT
GTTGTGCAAAAAAGCGGTTAGCTCCTTCGGTCCCTCCGATCGTTGTCAGAAGTAAGTTG
GCCGCAGTGTTATCACTCATGGTTATGGCAGCACTGCATAATTCTCTTACTGTCATGCC
ATCCGTAAGATGCTTTTTCTGTGACTGGTGAGTACTCAACCAAGTCATTCTGAGAATAG
TGTATGCGGCGACCGAGTTGCTCTTGCCCGGCGTCAATACGGGATAATACCGCGCCAC
ATAGCAGAACTTTAAAAGTGCTCATCATTGGAAAACGTTCTTCGGGGCGAAAACCTCTC
AAGGATCTTACCGCTGTTGAGATCCAGTTCGATGTAACCCACTCGTGACCCAACTGA
TCTTCAGCATCTTTTACTTTACACGCGTTTCTGGGTGAGCAAAAACAGGAAGGCAAA
ATGCCGCAAAAAAGGGAATAAGGGCGACACGGAAATGTTGAATACTCATACTCTTCC
TTTTTCAATATTATTGAAGCATTTATCAGGGTTATTGTCTCATGTCCGCGCGTT 3'

***Pf*B0150c-pTriEx-3 DNA sequence length: 6 480bp**

The cloned functional region of *Pf*PK8 is the underlined segment with the centrally located kinase domain (822bp) denoted by the red bases.

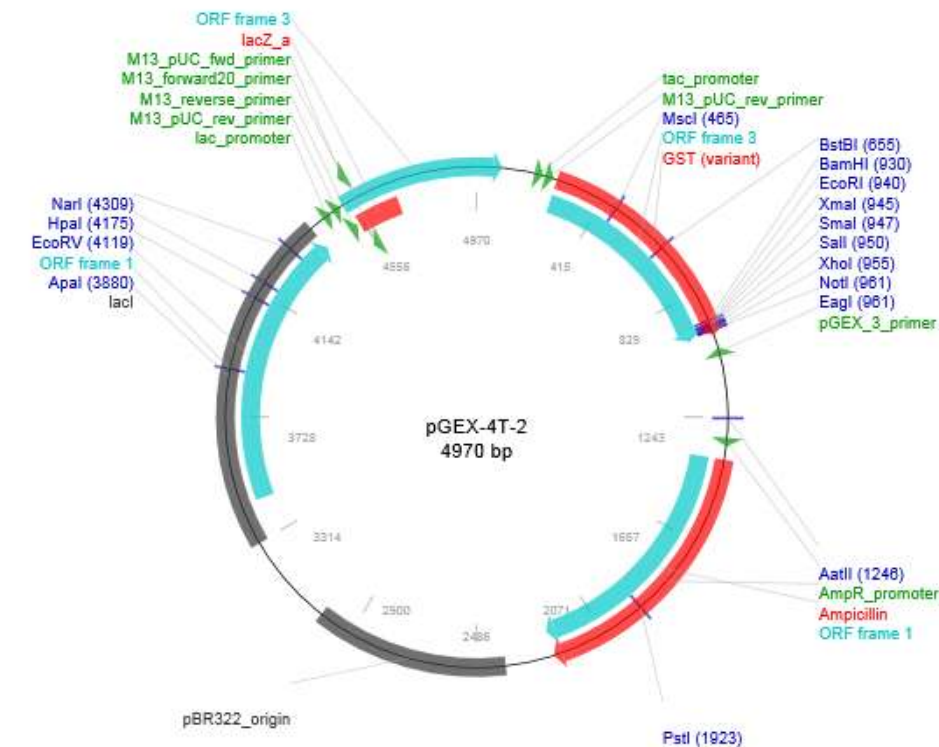
The pTriEx-3 vector sequence is indicated by the green bases.

The Histidine tag (24 bp) is denoted by the blue bases.

7.3.6 Expression vector maps

7.3.6.1 pGEX-4T-2- vector map

Map was obtained from: <http://www.addgene.org/vector-database/2874/>



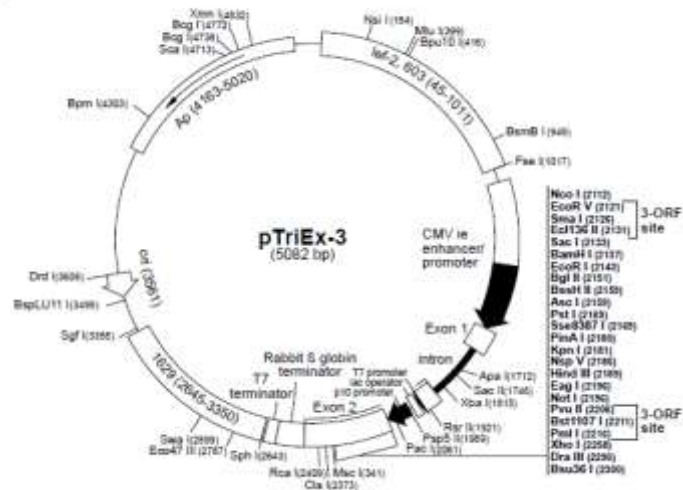
Feature Name	Start	End	ORF	Start	End
tac_promoter	184	212	ORF frame 3	258	974
M13_pUC_rev_primer	224	246	ORF frame 1	1378	2238
GST (variant)	258	978	ORF frame 1	3442	4401
pGEX_3_primer	1042	1020	ORF frame 3	4524	81
AmpR_promoter	1308	1336			
Ampicillin	1378	2238			
pBR322_origin	2393	3012			
lacI	3310	4401			
lac_promoter	4450	4479			
M13_pUC_rev_primer	4493	4515			
M13_reverse_primer	4514	4532			
lacZ_a	4541	4696			
M13_forward20_primer	4560	4544			
M13_pUC_fwd_primer	4575	4553			
			Enzyme Name		Cut
			MscI		465
			BstBI		655
			BamHI		930
			EcoRI		940
			XmaI		945
			SmaI		947
			SalI		950
			XhoI		955
			NotI		961
			EagI		961
			AatII		1246
			PstI		1923
			Apal		3880
			EcoRV		4119
			HpaI		4175
			NarI		4309

7.3.6.2 *Pf*B0150c-pTriEx-3 plasmid vector map

Map was obtained from: http://www.merckmillipore.com.au/life-science-research/vector-table-novagen-ptriex-vector-table/c_8iSb.s1OyKwAAAEhbSsLdcah

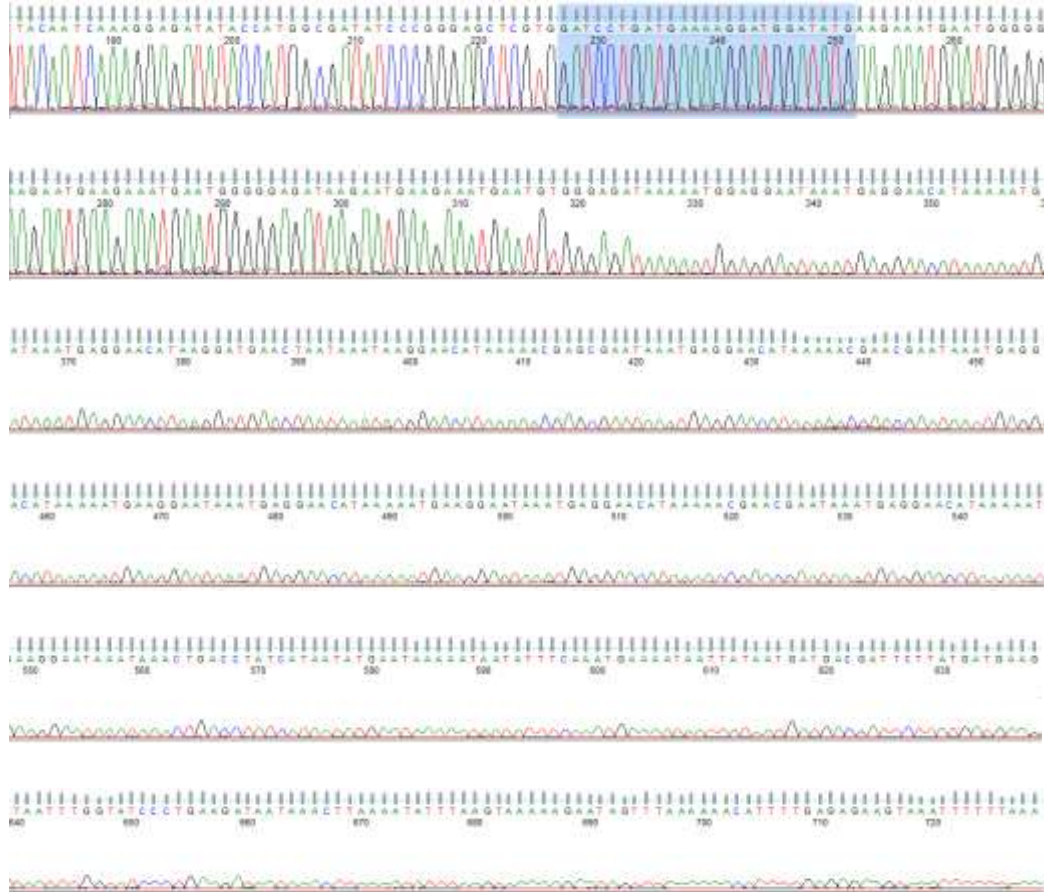
pTriEx-3 sequence landmarks

CMV ie enhancer/promoter	1021-1597
Veterbrate transcription start	1598
T7 promoter	1931-1947
T7 transcription start	1948
<i>lac</i> operator	1952-1972
p10 promoter region	1986-2099
p10 transcription start	2030-2031
Multiple cloning sites (<i>Nco</i> I- <i>Dra</i> III)	2112-2290
HSV-Tag [®] coding sequence	2222-2257
His-Tag [®] coding sequence	2264-2287
Rabbit globin terminator region	2375-2581
T7 terminator	2585-2632
pUC origin	3561
<i>bla</i> coding sequence	4163-5020

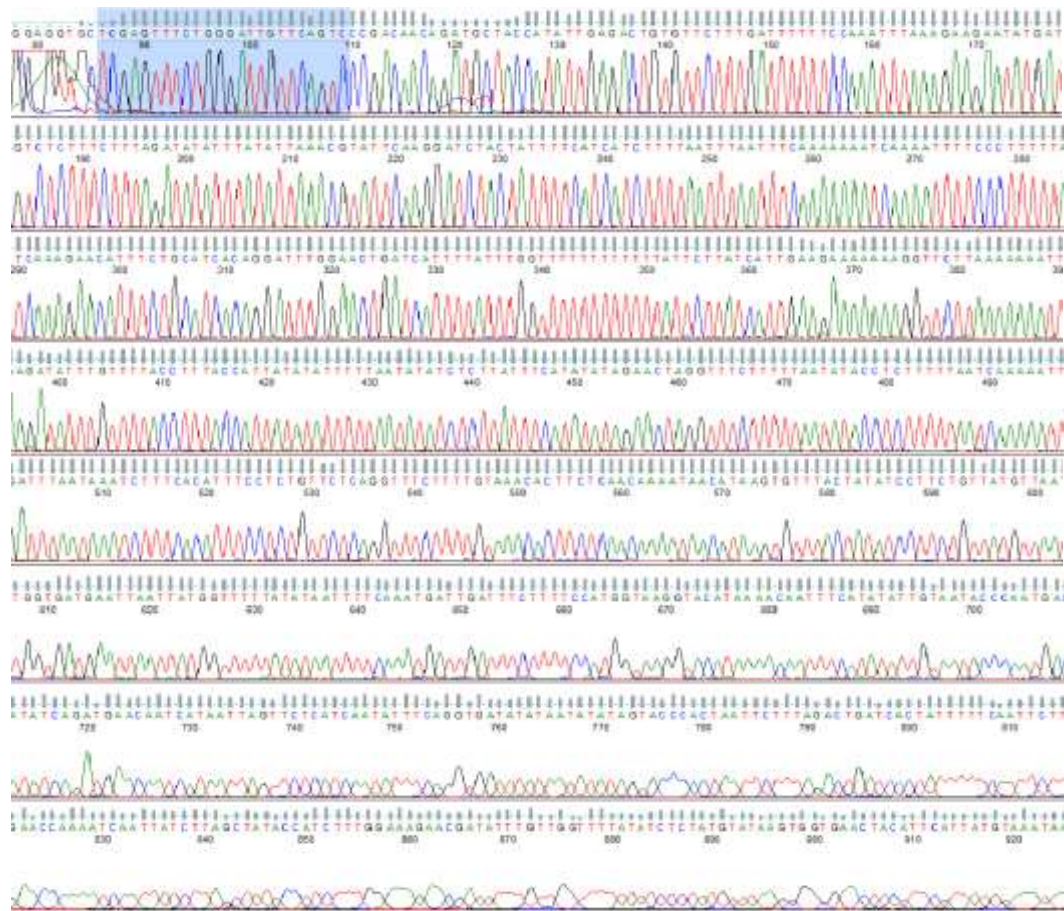


7.3.7 *PfB0150c*-pTriEx-3 sequence chromatograms

Sequence chromatogram obtained using a pTriEx-3 vector-specific forward primer. The *PfB0150c* gene specific forward primer is highlighted in blue.



Sequence chromatogram obtained using a pTriEx-3 vector-specific reverse primer. The *PfB0150c* gene specific reverse primer is highlighted in blue.

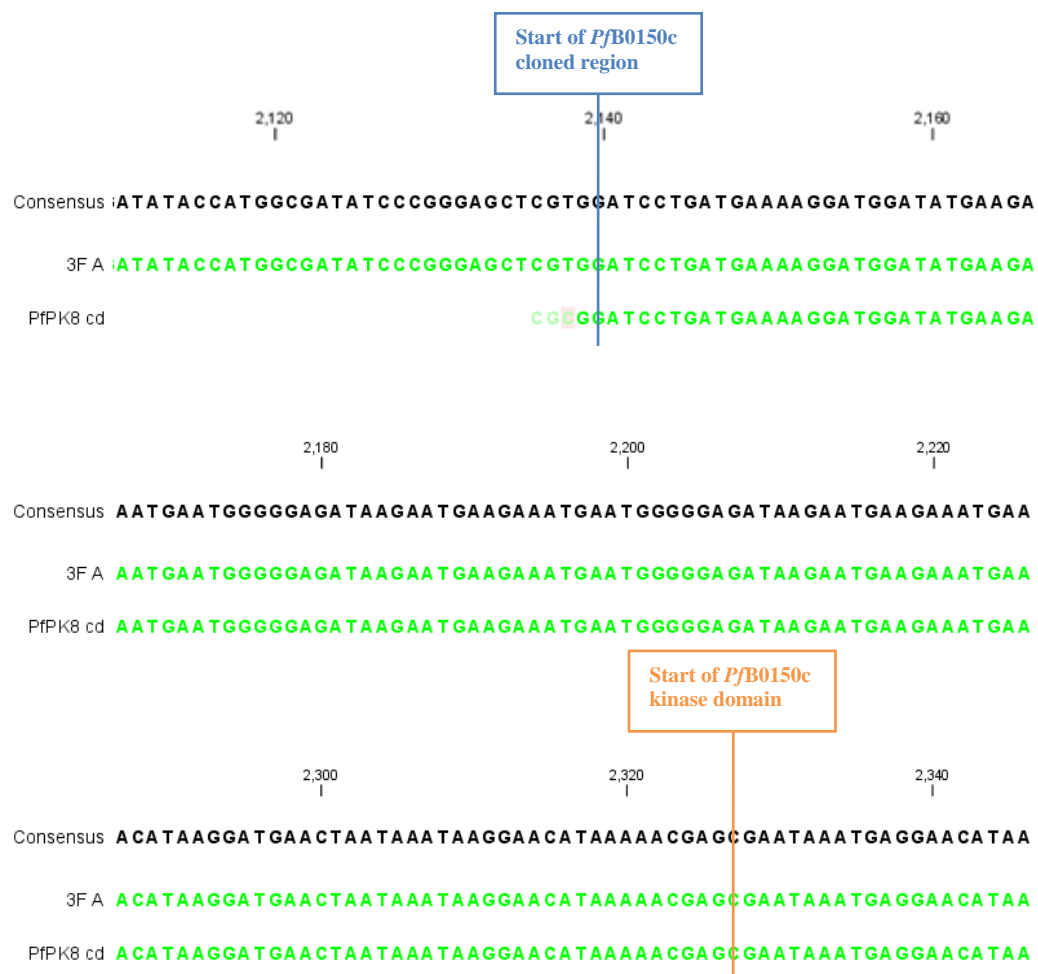


7.3.8 *Pf*B0150c-pTriEx-3 construct 2 DNA sequence alignment

The DNA sequence of the subcloned *Pf*B0150c sequenced using a forward (3F A, green) and reverse (3R A, red) vector-specific primer was aligned with the *Pf*B0150c catalytic domain sequence (*Pf*PK8 cd) (green bases) obtained from the PlasmDB version 8.1 (2011) database. The consensus sequence is indicated in black. A non-alignment is indicated by a conflict-flag in the consensus sequence (black).

The bright green and red bases indicate a good read with distinct high amplitude peaks and a low baseline noise according to the sequence chromatograms. The light green and light red bases indicate a base with a low amplitude peak. These bases were not sequenced with high confidence. Shaded green or red bases do not correspond to any one of the other sequences in the alignment and were not used in the analysis.

A conflict in the consensus sequence was resolved by comparing the conflicting base to the corresponding base in the 3F A or 3R A sequence. If a base in the same position as the conflict base had been sequenced with high confidence (bright green or red) in either the 3F A and/or 3R A sequence and corresponded to the *Pf*B0150c sequence, it was assumed to be correct.



2,360 2,380 2,400
 Consensus **AAACGAACGAATAAATGAGGAACATAAAAAATGAAGGAATAAATGAGGAACATAAAAAATGA**

3F A **AAACGAACGAATAAATGAGGAACATAAAAAATGAAGGAATAAATGAGGAACATAAAAAATGA**

PfPK8 cd **AAACGAACGAATAAATGAGGAACATAAAAAATGAAGGAATAAATGAGGAACATAAAAAATGA**

2,420 2,440 2,460
 Consensus **AGGAATAAATGAGGAACATAAAAAAGAACGAATAAATGAGGAACATAAAAAATGAAGGAAT**

3F A **AGGAATAAATGAGGAACATAAAAAAGAACGAATAAATGAGGAACATAAAAAATGAAGGAAT**

PfPK8 cd **AGGAATAAATGAGGAACATAAAAAAGAACGAATAAATGAGGAACATAAAAAATGAAGGAAT**

3R A **GTGGGGAAACATAA**

2,480 2,500 2,520
 Consensus **AAATAAACTGACCTATCATAATATGAATAAAAAATAATATTTCAAATGAAAATAATTATAA**

3F A **AAATAAACTGACCTATCATAATATGAATAAAAAATAATATTTCAAATGAAAATAATTATAA**

PfPK8 cd **AAATAAACTGACCTATCATAATATGAATAAAAAATAATATTTCAAATGAAAATAATTATAA**

3R A **ACCGATTGATAAATTGGGGAAACATAAACTGAAGATTATACTCCGATCTAATGATAAAAAATA**

2,540 2,560 2,580
 Consensus **TGATGACGATTCTTATGATGAAGATAATTTGGTATCCCTGAAGATAATAAACTTAAAATA**

3F A **TGATGACGATTCTTATGATGAAGATAATTTGGTATCCCTGAAGATAATAAACTTAAAATA**

PfPK8 cd **TGATGACGATTCTTATGATGAAGATAATTTGGTATCCCTGAAGATAATAAACTTAAAATA**

3R A **AATTTTCCATGGAAATAATTATATTGATGCGATTCTATTGATGAAGATAAATGTTTCTGAG**

2,600 2,620 2,640
 Consensus **TTTAAGTAAAAAGAATAGTTTAAAAAACATTTTGAGAGAAGTAAATTTTTTAAAAATGTG**

3F A **TTTAAGTAAAAAGAATAGTTTAAAAAACATTTTGAGAGAAGTAAATTTTTTAAAAATGTG**

PfPK8 cd **TTTAAGTAAAAAGAATAGTTTAAAAAACATTTTGAGAGAAGTAAATTTTTTAAAAATGTG**

3R A **ATAATAAATAAAATATTAGTAAAAGATAGTTTAAAACATTTGAGAGAGTAAATTTTAAAA**

2,660 2,680 2,700
Consensus : **TGAACATCCAAATGTAGTAAAAATATTTTGAATCTTTTTTTGGCCTCCTTGTTATTTAGT**
3F A : **TGAACATCCAAATGTAGTAAAAATATTTTGAATCTTTTTTTGGCCTCCTTGTTATTTAGT**
PfPK8 cd : **TGAACATCCAAATGTAGTAAAAATATTTTGAATCTTTTTTTGGCCTCCTTGTTATTTAGT**
3R A : **TGTTGTGACATCCAAATGTAGTAAAAATATTTTGAATCTTTTTTTGGCTCCCTGTTATTTAGT**

2,720 2,740 2,760
Consensus : **TATTGTGTGTGAATATTTATCAGGAGGAACATTATATGATTTATATAAAAAATTATGGTAG**
3F A : **TATTGTGTGTGAATATTTATCAGGAGGAACATTATATGATTTATATAAAAAATTATGGTAG**
PfPK8 cd : **TATTGTGTGTGAATATTTATCAGGAGGAACATTATATGATTTATATAAAAAATTATGGTAG**
3R A : **TATTGTGTGTGAATATTTATCAGGAGGAACATTATATGATTTATATAAAAAATTATGGTAG**

2,780 2,800 2,820
Consensus : **AATATCAGAAGATCTTTTAGTATATATCTTAGATGATGTATTAAATGGTTTAAATTATTT**
3F A : **AATATCAGAAGATCTTTTAGTATATATCTTAGATGATGTATTAAATGGTTTAAATTATTT**
PfPK8 cd : **AATATCAGAAGATCTTTTAGTATATATCTTAGATGATGTATTAAATGGTTTAAATTATTT**
3R A : **AATATCAGAAGATCTTTTAGTATATATCTTAGATGATGTATTAAATGGTTTAAATTATTT**

2,840 2,860 2,880
Consensus : **ACATAATGAATGTAGTTCACCACTTATACATAGAGATATAAAACCAACAAATATCGTTCT**
3F A : **ACATAATGAATGTAGTTCACCACTTATACATAGAGATATAAAACCAACAAATATCGTTCT**
PfPK8 cd : **ACATAATGAATGTAGTTCACCACTTATACATAGAGATATAAAACCAACAAATATCGTTCT**
3R A : **ACATAATGAATGTAGTTCACCACTTATACATAGAGATATAAAACCAACAAATATCGTTCT**

2,900 2,920 2,940
Consensus : **TTCCAAAGATGGTATAGCTAAGATAATT - GATTTTGG - TTCTTGTGAAGAATTGAAAAA -**
3F A : **TTCCAAAGATGGTATAGCTAAGATAATT - GATTTTGG - TTCTTGTGAAGAATTGAAAAA -**
PfPK8 cd : **TTCCAAAGATGGTATAGCTAAGATAATT - GATTTTGG - TTCTTGTGAAGAATTGAAAAA -**
3R A : **TTCCAAAGATGGTATAGCTAAGATAATT - GATTTTGG - TTCTTGTGAAGAATTGAAAAA -**

Conflict 2,960 Conflict 2,980 Conflict 3,000 Conflict

Consensus TAGTGATCAGTCTAAAGAATTAGTGGGTACTATATATTATATATCACCTGAAATATTGAT

3F A TAGTGATCAGTCTAAAGAATTAGTGGGTACTATATATTATATATCACCTGAAATATTGAT

PfPK8 cd TAGTGATCAGTCTAAAGAATTAGTGGGTACTATATATTATATATCACCTGAAATATTGAT

3R A TAGTGATCAGTCTAAAGAATTAGTGGGTACTATATATTATATATCACCTGAAATATTGAT

3,020 3,040 3,060

Consensus GAGAACTAATTATGATTGTTTCATCTGATATATGGTCATTGGGTATTACAATATATGAAAT

3F A GAGAACTAATTATGATTGTTTCATCTGATATATGGTTCATTGGGTATTACAATATATGAAAT

PfPK8 cd GAGAACTAATTATGATTGTTTCATCTGATATATGGTCATTGGGTATTACAATATATGAAAT

3R A GAGAACTAATTATGATTGTTTCATCTGATATATGGTCATTGGGTATTACAATATATGAAAT

3,080 3,100 3,120

Consensus TGTTTTATGTACCTTACCATGGAAGAAGAAATCAATCATTGGAATAATATATAAAACCAT

3F A ATGTTTTATGTACCTTACCATGGAAGAAGAAATTCATCATTTGAATTATATAAAACCATA

PfPK8 cd TGTTTTATGTACCTTACCATGGAAGAAGAAATCAATCATTGGAATAATATATAAAACCAT

3R A TGTTTTATGTACCTTACCATGGAAGAAGAAATCAATCATTGGAATAATATATAAAACCAT

3,140 3,160 3,180

Consensus AATTAATTCATCACCAAAAATTAACATAACAGAAGGATATAGTAAACACTTATGTTATTT

3F A ACTAATCTCACCGAAAATTAACATACGATGATTATACGCTACCGCTTATGGTTATTTTGG

PfPK8 cd AATTAATTCATCACCAAAAATTAACATAACAGAAGGATATAGTAAACACTTATGTTATTT

3R A AATTAATTCATCACCAAAAATTAACATAACAGAAGGATATAGTAAACACTTATGTTATTT

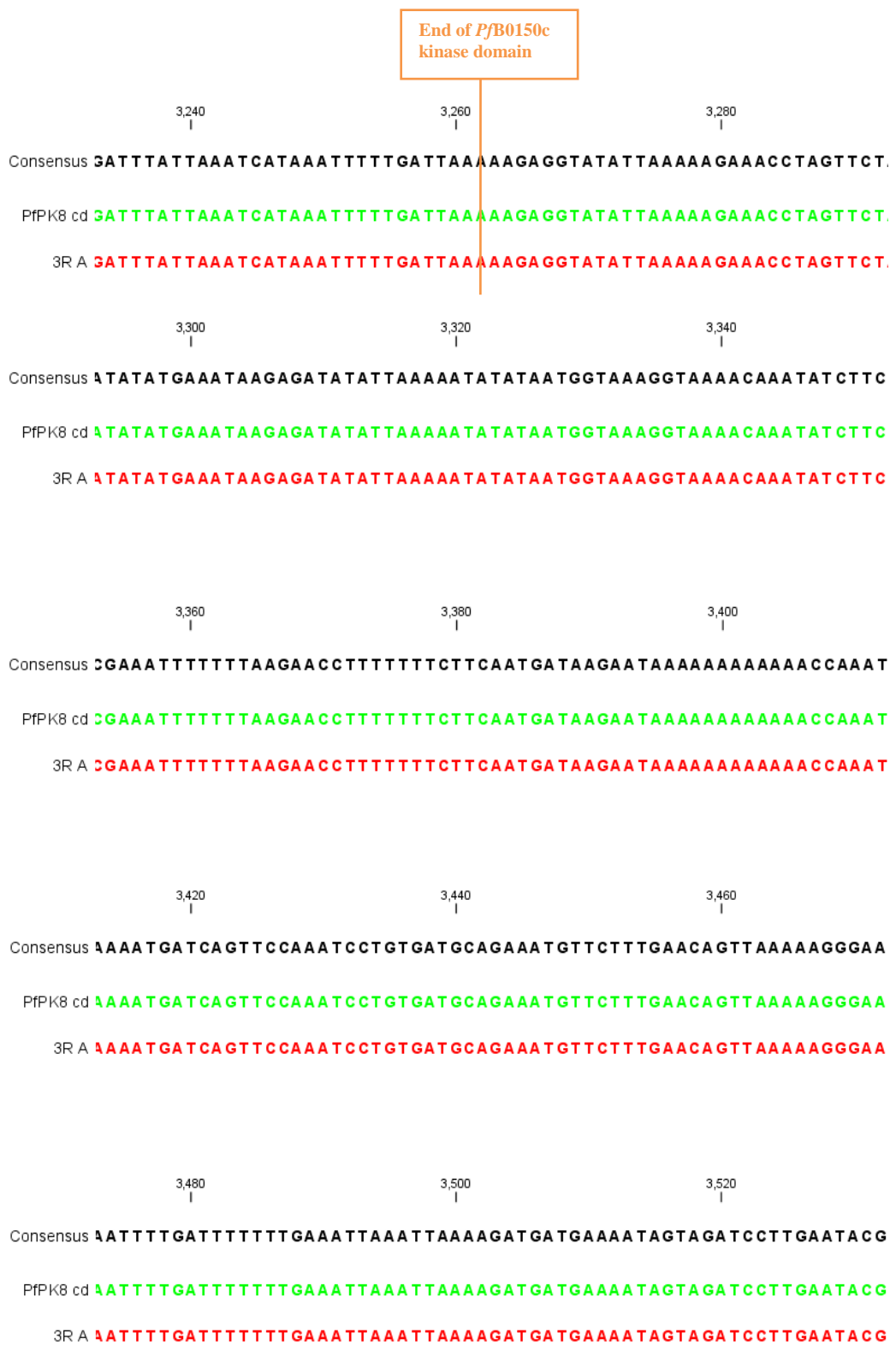
3,200 3,220 3,240

Consensus TGTTGAGAAGTGTTTACAAAAGAAACCTGAGAACAGAGGAAATGTGAAAGATTTATTAA

3F A TTGAGAAAATGGTGCT

PfPK8 cd TGTTGAGAAGTGTTTACAAAAGAAACCTGAGAACAGAGGAAATGTGAAAGATTTATTAA

3R A TGTTGAGAAGTGTTTACAAAAGAAACCTGAGAACAGAGGAAATGTGAAAGATTTATTAA



3,540 3,560 3,580
 Consensus **TTTAATATAAATATATCTAAAGAAAGAGACGACATATCATATTCTTCTTTAAATTTGGAA**

PfPK8 cd **TTTAATATAAATATATCTAAAGAAAGAGACGACATATCATATTCTTCTTTAAATTTGGAA**

3R A **TTTAATATAAATATATCTAAAGAAAGAGACGACATATCATATTCTTCTTTAAATTTGGAA**

3,600 3,620 3,640
 Consensus **AAATCAAAGAACACAGTCTCAATATGGTAGCATCTGTTGTCGGGACTGAACAATCCCAG**

PfPK8 cd **AAATCAAAGAACACAGTCTCAATATGGTAGCATCTGTTGTCGGGACTGAACAATCCCAG**

3R A **AAATCAAAGAACACAGTCTCAATATGGTAGCATCTGTTGTCGGGACTGAACAATCCCAG**

End of *Pf*B0150c
 cloned region
 3,660 3,680 3,700
 Conflict
 Consensus **AAACTCGAGCACCTCCATCACCATCACCATCACTAAGTGATTAACTCAGGTGCAGGCTG**
 PfPK8 cd **AAACTCGAGC**
 3R A **AAACTCGAGCACCTCCATCACCATCACCATCACTAAGTGATTAACTCAGGTGCAGGCTG**

3,720 3,740 3,760
 Consensus **CCTATCAGAAAGGTGGTGGCTGGTGT**
 3R A **CCTATCAGAAAGGTGGTGGCTGGTGT**

7.4 BLAST data of *Pf*PK8 protein sequence

7.4.1 Sequences with significant alignments to the target sequence

Description	Max score	Total score	Query cover	E value	Max ident	Accession
protein kinase, pADKs (Plasmodium falciparum 3D7)-p6AAC271620.1 protein kinase, pADKs (Plasmodium falciparum 3D7)	897	897	100%	0.0	96%	XP_001149544.2
serine/threonine-specific protein kinase (Plasmodium vivax) (aa 8)	488	488	67%	2e-164	68%	GA95086.1
serine/threonine-specific protein kinase (Plasmodium vivax) (aa 11)-p6EDL43236.1 serine/threonine-specific protein kinase, autolysin (Plasmodium vivax)	489	489	67%	2e-162	66%	XP_001512867.1
protein kinase (Plasmodium knowlesi strain 10)-p6DQAG0845.1 protein kinase, autolysin (Plasmodium knowlesi strain 10)	462	462	72%	7e-142	65%	XP_00258993.1
Protein kinase domain-containing protein (Tetrahymena thermophila)-p6EAP80349.1 Protein kinase domain-containing protein (Tetrahymena thermophila) (8)	150	150	41%	7e-37	35%	XP_00181854.1
Phospho domain-containing protein (Drosophila sp. GIM-73.1.001)	149	149	47%	3e-36	38%	EJ80327.1
Serine/threonine protein kinase (Drosophila melanogaster)	150	150	47%	3e-35	35%	EJ99674.1
PREDICTED: serine/threonine protein kinase (Drosophila melanogaster)-p6AF315267.1 MRC2 (Drosophila melanogaster)	145	145	47%	5e-35	36%	XP_003528736.1
GE12125 (Drosophila melanogaster)-p6EDU42206.1 GE12125 (Drosophila melanogaster)	142	142	47%	2e-34	37%	XP_001853845.1
serine/threonine protein kinase MMT4 (Drosophila melanogaster)-p6A821674.1 Zap-17288 protein (Drosophila melanogaster)	142	142	52%	3e-34	35%	XP_001120842.1
MAP kinase kinase (Drosophila melanogaster)	142	142	53%	3e-34	36%	ES015303.1
hypothetical protein BRAP1.DRAFT_230712 (Drosophila melanogaster)-p6ECP64749.1 hypothetical protein BRAP1.DRAFT_230712 (Drosophila melanogaster)	141	141	52%	5e-34	36%	XP_002588717.1
GA18103 (Drosophila melanogaster)-p6EAL77107.2 GA18103 (Drosophila melanogaster)-p6EAL77107.2	143	143	47%	5e-34	37%	XP_001352977.2
serine kinase (Drosophila melanogaster) A44-p6C91122.105K5A (Drosophila melanogaster) Farn-Serine/threonine protein kinase (Drosophila melanogaster) A44-p6C91122.105K5A	142	142	46%	5e-34	37%	XP_0037789.1
OL27268 (Drosophila melanogaster)-p6EDW27965.1 OL27268 (Drosophila melanogaster)	143	143	47%	5e-34	37%	XP_002023292.1
STE kinase protein kinase (Trichomonas vaginalis) GGE-p6EAY02613.1 STE kinase protein kinase (Trichomonas vaginalis) GGE	140	140	48%	8e-34	37%	XP_001215036.1
Serine/threonine protein kinase 24 (Drosophila melanogaster)	141	141	45%	7e-34	38%	EJ915963.1
PREDICTED: serine/threonine protein kinase (Drosophila melanogaster)-p6AF315268.1 MRC2 (Drosophila melanogaster)	141	141	47%	1e-33	36%	XP_003528855.1
predicted protein product (Tetradodon nigropinnatus)	140	140	61%	1e-33	31%	CA93529.1
PREDICTED: serine/threonine protein kinase 24-like (Drosophila melanogaster)	140	140	50%	1e-33	35%	XP_003601873.1
STE301E20Y196 protein kinase (Drosophila melanogaster)-p6ECP29996.1 STE301E20Y196 protein kinase (Drosophila melanogaster)-p6ECP29996.1	141	141	46%	1e-33	37%	XP_002012106.1
Q10528 (Drosophila melanogaster)-p6EDW16475.1 Q10528 (Drosophila melanogaster)	142	142	47%	1e-33	38%	XP_002001014.1
BE36270a (Drosophila melanogaster)	142	142	47%	1e-33	37%	GA91385.1
serine/threonine protein kinase (Drosophila melanogaster)-p6EAF33383.1 serine/threonine protein kinase (Drosophila melanogaster)-p6EAF33383.1	142	142	47%	2e-33	37%	XP_0035999.1
Q621995 (Drosophila melanogaster)-p6EDV48758.1 Q621995 (Drosophila melanogaster)	142	142	47%	2e-33	37%	XP_001919606.1
Q621548 (Drosophila melanogaster)-p6EDV49000.1 Q621548 (Drosophila melanogaster)	142	142	47%	2e-33	37%	XP_001903764.1
Q615280 (Drosophila melanogaster)-p6EDW4780.1 Q615280 (Drosophila melanogaster)	142	142	47%	2e-33	37%	XP_002041152.1
Q624833 (Drosophila melanogaster)-p6EDV99844.1 Q624833 (Drosophila melanogaster)	141	141	47%	2e-33	37%	XP_002087232.1
PREDICTED: serine/threonine protein kinase 24 (Drosophila melanogaster)	139	139	50%	2e-33	36%	XP_003433112.1
PREDICTED: serine/threonine protein kinase 24 (Drosophila melanogaster)	139	139	50%	3e-33	37%	XP_001920586.1
predicted protein (Laccaria bicolor) S238H-H87-p6EDW15100.1 predicted protein (Laccaria bicolor) S238H-H87	137	137	46%	3e-33	37%	XP_001872488.1
PREDICTED: serine/threonine protein kinase (Drosophila melanogaster)-p6EAF33384.1 serine/threonine protein kinase (Drosophila melanogaster)-p6EAF33384.1	140	140	50%	3e-33	38%	XP_003536507.1
DEH42C19872a (Drosophila melanogaster) CB57671-serine/threonine protein kinase (Drosophila melanogaster) CB57671	139	139	61%	4e-33	32%	XP_0036381.2
Chain A, Human MitD Kinase-p6DQAG0845.1 Chain A, Human MitD Kinase-p6DQAG0845.1 Chain B, Human MitD Kinase-p6DQAG0845.1 Chain A, Human MitD Kinase-p6DQAG0845.1	136	136	50%	4e-33	36%	3A7F_A
predicted protein (Drosophila melanogaster) valent, valent	136	136	47%	4e-33	36%	GA99003.1
Serine/threonine protein kinase 50T4 (Drosophila melanogaster)	136	136	52%	4e-33	34%	AC23475.1
STE301E20Y196 protein kinase (Drosophila melanogaster)	137	137	47%	4e-33	35%	XP_001147467.1
STE301E20Y196 protein kinase (Drosophila melanogaster)	137	137	47%	4e-33	35%	EJ99674.1
hypothetical protein ROD1-13813 (Rhopus domain RA-99-888)	139	139	51%	5e-33	34%	EJ88802.1
Serine/threonine protein kinase MMT4 (Drosophila melanogaster)	138	138	52%	5e-33	34%	AC23488.1
PREDICTED: serine/threonine protein kinase 24 (Drosophila melanogaster)	139	139	51%	5e-33	36%	XP_003599534.1
Protein kinase domain-containing protein (Tetrahymena thermophila)-p6EAP80349.1 Protein kinase domain-containing protein (Tetrahymena thermophila) (8)	143	143	41%	5e-33	37%	XP_001818547.1
Chain C, Human MitD (aa241) in Complex With Mc20Ste2-p6DQAG0845.1 Chain D, Human MitD (aa241) in Complex With Mc20Ste2	135	135	54%	6e-33	36%	3A7F_C
PREDICTED: serine/threonine protein kinase 24 (Drosophila melanogaster)	138	138	50%	6e-33	36%	XP_003528828.2
PREDICTED: serine/threonine protein kinase 24-like (Drosophila melanogaster)	138	138	51%	6e-33	36%	XP_003472953.1
Chain A, Crystal Structure Of Ste20-25-Like Kinase 2 (Ste20) In Complex With Shc20Ste20	135	135	54%	6e-33	36%	3A7F_A
serine/threonine kinase 24 (Drosophila melanogaster)-p6EDW16475.1 MRC2 (Drosophila melanogaster)	138	138	51%	7e-33	36%	XP_001085238.1
Chain A, Crystal Structure Of Ste20-25-Like Kinase 2 (Ste20) In Complex With Shc20Ste20	135	135	54%	7e-33	36%	3A7F_A
hypothetical protein Tcs2A2-TC014757 (Tribolium castaneum)	139	139	47%	8e-33	37%	EJ94440.1
PREDICTED: serine/threonine protein kinase 24 (Drosophila melanogaster)	137	137	54%	8e-33	36%	XP_001172703.1
TPA, serine/threonine kinase 25 (Drosophila melanogaster)	137	137	52%	9e-33	36%	GA93845.1
PREDICTED: serine/threonine kinase 24 (Drosophila melanogaster)	138	138	50%	9e-33	36%	XP_002123888.1

serine/threonine-protein kinase 25 (Rat brain) ->AA055285.1 serine/threonine kinase 25 (Rat brain)	137	137	52%	14-32	36%	NP_899966.1
Serine/threonine-protein kinase 24 (Cratichneumon)	137	137	47%	14-32	37%	AF011288.1
MASK (Drosophila)	137	137	47%	14-32	35%	AB022488.1
PREDICTED: serine/threonine-protein kinase 24-like (Pezomachus melanogaster)	137	137	50%	14-32	36%	XP_002714807.1
unannoted protein encoded (Homo sapiens)	135	135	50%	14-32	36%	Q6U19974.1
FAK-related kinase Prk11 (Schistosoma mansoni) contig 972b-1 ->AF214647.1 PRPK11 (Schistosoma mansoni) Full-length serine/threonine-protein kinase prk11 ->ser1	135	135	47%	14-32	34%	NP_584517.1
PREDICTED: serine/threonine-protein kinase 25-like (Heterotis niloticus)	139	139	47%	14-32	36%	XP_003029801.2
hypothetical protein GPPUCRAET_47708 (Daphnia pulex)	138	138	48%	14-32	37%	EF383423.1
serine/threonine-protein kinase 24 (Rat brain) ->AF012029.1 serine/threonine kinase 24 (STE20 homolog, yeast) (Rat brain) ->AA133599.2 STE24 (pro)	137	137	50%	14-32	37%	NP_001082428.1
STE25 protein (Homo sapiens)	137	137	52%	14-32	36%	AAH15793.1
PREDICTED: serine/threonine-protein kinase 25-like (Homo sapiens)	137	137	52%	14-32	36%	XP_001487795.2
hypothetical protein PANDA_002850 (Adiantum melanocephalum)	137	137	50%	14-32	36%	EF326728.1
hypothetical protein E1K_04885 (part) (Mycaraca mulethi)	137	137	52%	14-32	36%	EF421842.1
serine/threonine kinase 25 (Pari trochodactyl)	137	137	52%	14-32	36%	AA027207.1
Ste20-like kinase (Homo sapiens)	137	137	52%	14-32	36%	CA481738.1
TPA, serine/threonine kinase 24 (Rat brain)	137	137	50%	14-32	37%	QAA27591.1
PREDICTED: serine/threonine-protein kinase 25 isoform 1 (Psephodes) ->ref XP_002612134.1 PREDICTED: serine/threonine-protein kinase 25 isoform 2 (Psephodes)	137	137	52%	24-32	36%	XP_002612133.1
serine/threonine-protein kinase 24 (Mycaraca mulethi) ->AF478490.1 serine/threonine-protein kinase 24 isoform b (Mycaraca mulethi) ->AF478492.2 (1, serine)	137	137	50%	24-32	36%	NP_001213788.1
PREDICTED: serine/threonine-protein kinase 24 (Pari trochodactyl)	137	137	52%	24-32	36%	XP_001779172.1
PREDICTED: similar to QA15701-FA17 (obolus caribaeus)	142	142	42%	24-32	39%	XP_049118.2
PREDICTED: serine/threonine-protein kinase 24 (Lusodactyl affinis)	137	137	50%	24-32	37%	NP_001488997.1
serine/threonine kinase 25 (Pari trochodactyl) ->AA27572.1 serine/threonine kinase 25 (Pari trochodactyl)	137	137	52%	24-32	36%	AA018626.1
Deafness, Full-Serine/threonine-protein kinase 25 ->AA044988.1 STE25 protein (Rat brain)	137	137	52%	24-32	36%	Q18974.1
serine/threonine-protein kinase 25 isoform 1 (Homo sapiens) ->ref NP_001258909.1 serine/threonine-protein kinase 25 isoform 1 (Homo sapiens) ->ref NP_001258909.1	137	137	52%	24-32	36%	NP_001350302.2
PREDICTED: serine/threonine-protein kinase 24-like (Heterotis niloticus)	134	134	50%	24-32	36%	XP_002260003.1
PREDICTED: serine/threonine-protein kinase 24 isoform 1 (Nematocys leucodermis)	137	137	50%	24-32	36%	XP_003279268.1
serine/threonine-protein kinase 24 isoform 1 (Homo sapiens) ->ref XP_003014009.1 PREDICTED: serine/threonine-protein kinase 24 isoform 1 (Psephodes)	137	137	50%	24-32	36%	NP_001327497.2
PREDICTED: serine/threonine-protein kinase 25 (Pari trochodactyl)	137	137	52%	24-32	36%	XP_003091359.1
PREDICTED: serine/threonine-protein kinase 25 isoform 2 (Pari trochodactyl)	137	137	52%	24-32	36%	XP_003091310.1
Serine/threonine-protein kinase 25 (part) (Homo sapiens) (partial)	136	136	52%	24-32	36%	EF382258.1
serine/threonine kinase 24 (Drosophila) (contig)	137	137	50%	24-32	36%	AA022573.1
PREDICTED: serine/threonine-protein kinase 24 (Drosophila) (contig)	137	137	50%	24-32	37%	XP_001769023.1
PREDICTED: serine/threonine-protein kinase 25 isoform 2 (Pari trochodactyl)	136	136	52%	24-32	36%	XP_003090926.1
PREDICTED: serine/threonine-protein kinase 25 isoform 1 (Pari trochodactyl)	137	137	52%	24-32	36%	XP_001762208.2
Serine/threonine-protein kinase 24 (Mycaraca mulethi)	137	137	50%	24-32	36%	EF458674.1
STE20-like kinase 3 (Homo sapiens)	137	137	50%	24-32	36%	AA062548.1
Serine/threonine kinase 24 (STE20 homolog, yeast) (Homo sapiens)	137	137	50%	24-32	36%	AAH05203.1
Serine/threonine-protein kinase 24 (Mycaraca mulethi)	137	137	60%	24-32	36%	EF423880.1
serine/threonine-protein kinase 24 isoform a (Homo sapiens) ->ref NP_001258909.1 PREDICTED: serine/threonine-protein kinase 24 isoform 2 (Homo sapiens)	137	137	50%	24-32	36%	NP_001258712.2
PREDICTED: serine/threonine-protein kinase 24 isoform 2 (Pari trochodactyl)	137	137	50%	24-32	36%	XP_003091407.1
PREDICTED: serine/threonine-protein kinase 25 (Drosophila) (contig)	136	136	52%	24-32	36%	XP_004032423.1
Serine/threonine-protein kinase 25 (Heterotis niloticus) (partial)	136	136	52%	24-32	35%	EF381838.1
Phalloidin serine/threonine-protein kinase, partial (Drosophila) (contig)	136	136	52%	24-32	35%	AA041784.1
serine/threonine kinase 1/acidic domain (Drosophila) (contig)	137	137	47%	24-32	35%	EF382753.1
PREDICTED: serine/threonine-protein kinase 25 (Drosophila) (contig)	136	136	52%	24-32	36%	XP_003786387.1
PREDICTED: serine/threonine-protein kinase 24-like (Pari trochodactyl)	138	138	47%	24-32	36%	XP_003090970.1
serine/threonine kinase 24 (STE20 homolog, yeast) (Homo sapiens)	136	136	50%	24-32	37%	EF389988.1
PREDICTED: serine/threonine-protein kinase 24-like (Heterotis niloticus)	137	137	47%	24-32	37%	XP_001216746.1